

Title	The development of an algorithm to track blood pressure accurately based on the pulse transit time method
Authors	McCarthy, Brian M
Publication date	2015
Original Citation	McCarthy, B .M. 2015. The development of an algorithm to track blood pressure accurately based on the pulse transit time method. PhD Thesis, University College Cork.
Type of publication	Doctoral thesis
Rights	© 2015, Brian M McCarthy. - http://creativecommons.org/licenses/by-nc-nd/3.0/
Download date	2024-05-02 18:26:49
Item downloaded from	https://hdl.handle.net/10468/3376

The Development of an Algorithm to Track Blood Pressure Accurately Based on the Pulse Transit Time Method

Brian M McCarthy

B.E M.ENG.SC



NATIONAL UNIVERSITY OF IRELAND, CORK

SCHOOL OF ENGINEERING

ELECTRICAL AND ELECTRONIC ENGINEERING

TYNDALL NATIONAL INSTITUTE

**Thesis submitted for the degree of
Doctor of Philosophy**

July 2015

Head of Department: Prof. Nabeel Riza

Supervisors: Dr Alan Mathewson
Mr Brendan O'Flynn

Advisor: Dr. Carl Vaughan

Research supported by IRCSET, Dublin
Intel Ireland Ltd, Leixlip, Ireland

Contents

Acknowledgements	vii
Abstract	ix
1 Introduction to Non-Invasive Blood Pressure Monitoring	1
1.1 Introduction	1
1.2 Motivation	1
1.2.1 What is Blood Pressure?	3
1.2.2 The Importance of Blood Pressure	4
1.2.3 The Electrocardiogram and its Relationship to BP	5
1.3 Outline of Thesis	7
2 State of the Art of Blood Pressure Measurement Techniques	10
2.1 Introduction	10
2.2 BP Measurement Standards	11
2.3 Auscultatory Techniques	12
2.3.1 Improvements to the Auscultatory Technique	13
2.3.2 Significant Advances	14
2.4 Oscillometric Method	15
2.4.1 Origins of the Oscillometric Method	15
2.4.2 Improvements to the Oscillometric Method	15
2.5 Tonometry	16
2.5.1 Current State of the Art Tonometers	19
2.6 Vascular Unloading Technique	21
2.6.1 Finapres	21
2.6.2 Portapres	22
2.6.3 Other Peñáz Implementations	23
2.7 Pulse Transit Time	24
2.7.1 Chen’s Significant Contribution to the PTT method	28
2.7.2 Significant Advances to the PTT Method	29
2.8 Discussion	34
3 Evaluation of the Pulse Transit Time Method	39
3.1 Introduction	39
3.2 The Tyndall 25mm Development Platform	40
3.3 The Development of a Pulse Transit Time Measurement System	41
3.4 Development of the Physiological Health for Assisted Living Board	41
3.4.1 Design Specification	42
3.4.1.1 Electrocardiograph	42
3.4.1.2 Communications	44
3.4.1.3 Microcontroller Choice	45
3.4.1.4 Activity Monitor	47
3.4.1.5 Other Features	48
3.4.2 Pulse Oximeter Board	48
3.5 Software	50
3.5.1 Embedded C Code	51

3.5.2	Data Recording / LabView	51
3.5.2.1	Data Pre-Processing	53
3.5.3	Post-Processing and Matlab Code Development	54
3.6	Pulse Transit Time Calculation	55
3.6.1	ECG R Wave Detection	55
3.6.2	PPG Wave Characteristic Points Detection	57
3.7	Testing the Pulse Transit Time Method	58
3.7.1	Introduction: Preliminary Testing	58
3.7.2	Sensor Optimisation	58
3.7.2.1	Pulse Oximeter	58
3.7.2.2	ECG Testing - Electrode Placement	59
3.8	Evaluating the PTT Method - Round 1 of Testing	59
3.8.1	Required Improvements for Subsequent Testing	61
3.9	Evaluating the PTT Method - Round 2 of Testing	62
3.10	Evaluating the PTT Method Using Two Different PTT Algorithms - Round 3 of Testing	64
3.10.1	Evaluating Chen's Algorithm	66
3.10.2	Evaluating Poon's Algorithm	72
3.11	Conclusions	77
4	Measuring Stroke Volume and Other Parameters	80
4.1	Introduction	80
4.2	PhysioNet Database	81
4.3	The Impedance Cardiograph	87
4.3.1	Impedance Cardiography Instrumentation	87
4.3.2	Calculation of Stroke Volume	89
4.4	Choice of Acquisition Methodology	91
4.5	Evaluation of Existing Algorithms using the PhysioNet Database	92
4.5.1	Testing Methodology	92
4.5.2	Characteristic Point Extraction Algorithms	93
4.5.3	Systolic & Diastolic BP Determination from the Arterial Blood Pressure Wave	96
4.5.4	Evaluating the Database	97
4.6	Conclusions	105
5	Deriving a Novel Blood Pressure Tracking Algorithm	107
5.1	Introduction	107
5.2	Identifying Parameters of Interest	108
5.2.1	Direct Correlations	109
5.2.2	Semblance Analysis	111
5.3	Multiple Linear Regression	113
5.3.1	Deriving β values and Testing Algorithm 1-x	114
5.3.2	Evaluating Algorithm 1-x	118
5.3.3	Algorithm 2-x	119
5.3.4	Algorithm 3-x	121
5.3.5	Algorithm 4-x	127

5.4	Derivation and Evaluation of a New Algorithm Based on Physiological Parameters	131
5.4.1	Quantifying the Performance	132
5.4.2	Derivation of the New Algorithm	133
5.4.3	Evaluation of the New Algorithm	136
5.4.4	Relative Performance	140
5.5	An Investigation of the Algorithm as Part of a Wearable System	145
5.6	Summary	150
6	Discussion, Conclusions and Future Work	154
6.1	Summary	154
6.2	Discussion and Conclusions	157
6.3	Future Work	162
	Appendices	165
A	The Use of the Poiseuille Equation in the New Algorithm	166
B	An Examination of the European Society of Hypertension Standard for Blood Pressure Monitoring	168
B.1	The Specifics of the Standard	168
B.2	The Exclusion of the ESH standard in the Evaluation of this Work	171
C	Design of an Impedance Cardiograph	172
C.1	Current Injection Hardware	173
C.2	Impedance Measurement Hardware	175
C.2.1	Other Design Features	177
D	Protocol for Recording Data from Volunteers	180
D.1	Round 1 Testing	180
D.2	Round 2 Testing	182
D.3	Round 3 Testing	183

I, Brian M McCarthy, certify that this thesis is my own work and I have not obtained a degree in this university or elsewhere on the basis of the work submitted in this thesis.

Brian M McCarthy

“Stubbornly persist, and you will find that the limits of your stubbornness go well beyond the stubbornness of your limits.” - Robert Brault

Acknowledgements

To my supervisor Alan Mathewson, who has guided me along the way, giving me advice and support wherever I needed it

To my co-supervisor Brendan O’Flynn, who gave me this opportunity and without whom I would never have been able to do this

To my advisor Carl Vaughan for his help in all things medical and his patience with us engineers

Cian Ó Máthúna for his support through some difficult times

John Barton for always being available for a chat and help at any time.

Declan Coogan in the school of Psychology in NUIG, for giving me access to an Impedance Cardiograph and his help during my time there

Michael Cronin for his help with the statistical parts of this work and for taking the time to explain all things statistical very slowly

Intel and IRCSET for funding this PhD

All the members of the WSN group, who have all contributed in some way to this PhD especially Michael Walsh, Javier, John Buckley, Philip and all others through the years

To all my office mates throughout the years who always listened and helped Wassim, Seán, Mark, Donal, Tingcong, Liqiang, and Chong

To all the friends I made in Tydall: Pdraig, Rosemary, Conor, Aidan, Amélie, Seán, Rathnait, Colm McC, Rory, Ian, Evan, Meere, Santosh, Pierre, Cormac, Paudie, Wensi, Nicholas Sassiati, Monika, Nick, Vanessa, Courtney, Jeff and all of NTG

A special thanks to all the volunteers that I used throughout this work. For their patience and willingness to take time out of their own busy schedules and for their ability to remain perfectly motionless and provide good quality signals over the duration of the tests.

I would especially like to thank my parents for their love and support, both financially and emotionally, without whom this would have ended much more abruptly

To my fiancée Claire, whom I met in Tyndall, and who has been there throughout giving me love and support

Abstract

Oscillometric blood pressure (BP) monitors are currently used to diagnose hypertension both in home and clinical settings. These monitors take BP measurements once every 15 minutes over a 24 hour period and provide a reliable and accurate system that is minimally invasive. Although intermittent cuff measurements have proven to be a good indicator of BP, a continuous BP monitor is highly desirable for the diagnosis of hypertension and other cardiac diseases. However, no such devices currently exist.

A novel algorithm has been developed based on the Pulse Transit Time (PTT) method, which would allow non-invasive and continuous BP measurement. PTT is defined as the time it takes the BP wave to propagate from the heart to a specified point on the body. After an initial BP measurement, PTT algorithms can track BP over short periods of time, known as calibration intervals. After this time has elapsed, a new BP measurement is required to recalibrate the algorithm.

Using the PhysioNet database as a basis, the new algorithm was developed and tested using 15 patients, each tested 3 times over a period of 30 minutes. The predicted BP of the algorithm was compared to the arterial BP of each patient. It has been established that this new algorithm is capable of tracking BP over 12 minutes without the need for recalibration, using the BHS standard, a 100% improvement over what has been previously identified.

The algorithm was incorporated into a new system based on its requirements and was tested using three volunteers. The results mirrored those previously observed, providing accurate BP measurements when a 12 minute calibration interval was used. This new system provides a significant improvement to the existing method allowing BP to be monitored continuously and non-invasively, on a beat-to-beat basis over 24 hours, adding major clinical and diagnostic value.

Publications

Patent Application

B. M. McCarthy. A Non-Invasive Blood Pressure Monitoring System and Method. filed to U.K. Patent Office, December 2014. Application No. GB1422667.4

Journals

B. M. McCarthy, C. J. Vaughan, B. O’Flynn, A. Mathewson and C. Ó Mathúna. A Novel Approach to Accurately Track Blood Pressure based on the Pulse Transit Time Method. **Submitted** *IEEE Transactions on Biomedical Engineering*, June 2015.

B. M. McCarthy, C. J. Vaughan, B. O’Flynn, A. Mathewson and C. Ó Mathúna. An Examination of Calibration Intervals Required for Accurately Tracking Blood Pressure Using Pulse Transit Time Algorithms. *J Hum Hypertens*, 27(12):744-750, Dec 2013.

Conferences

B. M. McCarthy, B. O’Flynn and A. Mathewson. An Investigation of Pulse Transit Time as a Non-Invasive Blood Pressure Measurement Method. *Journal of Physics: Conference Series*, 307(1):012060, 2011.

Brian McCarthy, Michael Walsh, Brendan O’Flynn, Alan Mathewson, Tyn-dall Physiological Health Monitoring System, *34th International Microelec-tronics and Packaging IMAPS - CPMT*, 2010.

Glossary

Term	Explanation
AAL	Ambient Assisted Living
AAMI	Association for the Advancement of Medical Instrumentation
ABP	Arterial Blood Pressure
ADC	Analogue to Digital Converter
BCG	Ballistocardiograph
BHS	British Hypertension Society
BP	Blood Pressure
CO	Cardiac Output
CVD	Cardiovascular Disease
CWT	Continuous Wavelet Transform
DABP	Diastolic Arterial Blood Pressure
DAC	Digital to Analogue Converter
DBP	Diastolic Blood Pressure
DDS	Direct Digital Synthesis
ECG	Electrocardiograph
EEPROM	Electrically Erasable Programmable Read Only Memory
ESH	European Society of Hypertension
HFC	High Frequency Component
GMR	Giant Magneto Resonance
IC	Integrated Circuit
ICG	Impedance Cardiograph
ICU	Intensive Care Unit
I^2C	Inter Integrated Circuit
IMU	Inertial Measurement Unit
LED	Light Emitting Diode
LFC	Low Frequency Component
LVET	Left Ventricle Ejection Time
MLR	Multiple Linear Regression
MAP	Mean Arterial (Blood) Pressure
MMSB	Modulated Magnetic Signature of Blood
NIR	Near Infra-Red
PAC	Pulmonary Arterial Catheter
PAT	Pulse Arrival Time
PCB	Printed Circuit Board
PEP	Pre-Ejection Period
PHAL	Physiological Health for Assisted Living
PO	Pulse Oximeter
PPG	Photoplethysmograph
PTT	Pulse Transit Time
SABP	Systolic Arterial Blood Pressure
SBP	Systolic Blood Pressure
SD	Secure Digital
SPI	Serial Peripheral Interface
SV	Stroke Volume
TFI	Thoracic Fluid Index
VEPT	Volume of Electrically Participating Tissue
WSN	Wireless Sensor Network

Chapter 1

Introduction to Non-Invasive Blood Pressure Monitoring

1.1 Introduction

The thesis under investigation in this work was to develop a new algorithm that would continuously track blood pressure (BP) as part of a non-invasive, unobtrusive and comfortable personal monitoring system that is highly accurate and reliable. The first section of this chapter provides the motivation for developing this algorithm, explains why such an algorithm is required and why it is so important. The next section of this chapter introduces some basic concepts including a description of BP and provides an introduction to the electrocardiogram (ECG) trace that is used throughout the thesis as part of one of the measurement systems. Some general terms that are used throughout the thesis will be introduced and the standards that are used to evaluate BP monitors are explained. The final section of this introductory chapter provides an outline of the thesis, introduces the subject of each chapter and describes what will be discussed.

1.2 Motivation

BP is a major indicator of the health of a person and is one of the four primary vital signs. However, unlike other vital signs, abnormal BP can be an indication of a long term illness and can be used as a predictor of Cardiovascular Disease (CVD). CVD is the leading cause of death worldwide and accounted for 32.16%

of all deaths in Ireland in 2013 [1].

There are a number of methods used to measure BP. The most accurate method to do this is by using invasive intra-arterial pressure transducers (catheters). However, invasive BP monitors are not usually found outside of the hospital and rarely outside of the Intensive Care Unit (ICU). Catheters also have many risks associated with their use, including embolism, arrhythmias, heart attacks and even mortality [2, 3]. The more practical BP monitors used outside the ICU are known as non-invasive BP monitors.

The most common non-invasive BP monitor system typically used in a clinical setting is a sphygmomanometer, which also requires a stethoscope and a trained clinician. Although this method is considered to be the gold standard for BP measurement, it has been recognized that there are numerous problems with it [4, 5, 6]. Furthermore, since it relies on an inflatable cuff it is not a continuous measurement. It is commonly acknowledged that a non-invasive and continuous BP measurement device would be preferable to the sphygmomanometer [7] if one could be found that provides the necessary accuracy and reliability.

Even when BP is measured by an expert in a clinical setting, there are other known issues which can cause inaccuracies in the reading. Many of these can be minimised by ensuring that the person who is being tested has not eaten, taken any BP altering drugs (including caffeine or nicotine), or performed any exercise prior to the measurement. However, another source of error comes from white coat hypertension, something which is not easily controllable and which has cast doubt on many measurements. White coat hypertension is a false reading of an elevated BP, due to the presence of a clinician [6, 8]. This occurs because the person that is having their BP read is nervous about having their BP taken and as a consequence their BP increases temporarily. This means that the clinician records an abnormally high BP. If the BP is read outside of a clinical setting i.e. at home or at work, or frequently just by an automated monitor, this effect can be minimised if not avoided.

It is frequently desirable to measure BP outside of the clinical setting. Usually if a clinician would like to diagnose a patient for an abnormal BP, the patient is given an automated BP monitor for 24 hours that takes a measurement once every 15 to 20 minutes throughout the day and night[6]. This method helps to reduce the effect of white coat hypertension and has also been shown to give lower and more accurate readings.

Another area in which home BP readings are becoming more prevalent and useful is in the area of Ambient Assisted Living (AAL), which is an area of growing interest. It is well documented that over the next number of years there will be a demographic shift in the average age of the general population. In fact it is predicted that by 2050 there will be more people over the age of 65 than people between the ages of 18 and 64 [9]. This demographic change is already leading to an increased burden on already strained healthcare systems. In an effort to combat this strain, there has been a considerable amount of research into the area of AAL. AAL technologies allow the continuous monitoring of people in the home and alert healthcare practitioners if the person they are monitoring were to fall ill. This minimises the need for a live-in healthcare practitioner in many cases. As BP is one of the *vital* parameters, being able to measure it continuously is highly desirable in the area of AAL.

Although there are numerous non-invasive methods available for many other AAL monitoring applications such as falls, there are many associated shortcomings with BP monitoring in this area. The most prominent of these is that most automated BP monitors that are in use today recommend the use of an inflatable cuff to measure BP. This is undesirable for two reasons

- When an inflatable cuff is used, there is an associated inflation and deflation time and the measurement is not continuous (due to the time required to inflate and deflate the cuff)
- The inflatable cuff used to prevent flow through the brachial artery and the BP monitor can be quite uncomfortable to use, especially over extended periods of time

For these reasons, the need for a continuous, non-invasive, unobtrusive and comfortable system that is accurate and reliable becomes more apparent. The specifics of each BP monitoring system and their benefits and shortcomings will be discussed at length in Chapter 2.

1.2.1 What is Blood Pressure?

Blood pressure is a measurement of the force applied to the walls of the arteries as the heart pumps blood through the body. This pressure is determined by the force and amount of blood pumped, as well as the size and flexibility of the arteries. A contraction of the heart pumps blood into the vascular system which

leads to an increased BP around the rest of the body. This high pressure is known as the Systolic Blood Pressure (SBP). While the heart is refilling with blood, the blood pressure around the body drops to a low pressure known as the Diastolic Blood Pressure (DBP). The connection between the BP and heart activity is shown in Figure 1.1.

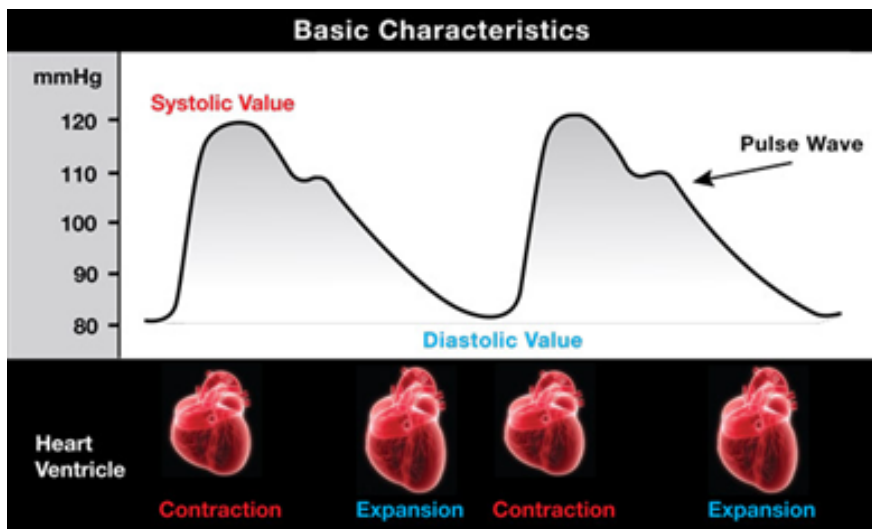


Figure 1.1: The BP in comparison to the activity of the ventricle of the heart. Image taken from Braun [10]

1.2.2 The Importance of Blood Pressure

Blood pressure is one of the primary vital signs which indicate the health of a person. Other primary vital signs include:

- Heart Rate
- Respiration Rate
- Temperature

These vital signs are measured and monitored to determine an individual's level of physical health. A normal BP is given as 120/80 mmHg, where the numerator is the systolic BP and the denominator is the diastolic value. However, along with the other vital signs, this varies with age, sex, weight, exercise tolerance and condition. Like the other vital signs above, an abnormal blood pressure can be a good indicator that there is something physically wrong with an individual. Although low BP is also of concern, the vast majority of people who have an abnormal BP are concerned with high blood pressure or hypertension.

High BP increases the risk of getting heart disease and/or kidney disease, and/or having a stroke. Anyone, regardless of age, sex and race can have high BP. Once high BP develops, it usually lasts a lifetime although it can be prevented and controlled. This is why over a third (36%) of people who are receiving long term medical treatment in the EU, are doing so because of hypertension.

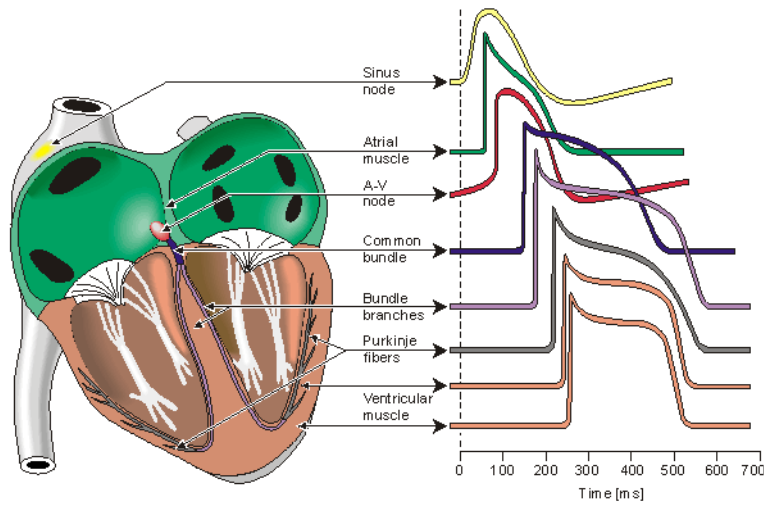
- High BP (hypertension) killed 54,186 people in the United States in 2004. It was listed as a primary or contributing cause of death in about 277,000 U.S. deaths in 2004 [9].
- 28% of people with high BP don't know they have it [9].
- Of all people with high BP, 71.8% are aware of their condition, 61.4% are under treatment, 35.1% have it under control and 64.9% do not have it controlled [9].
- The cause of 90-95% of the cases of high BP is unknown; however, high BP is easily detected and is usually controllable using drug treatment and exercise [9].

1.2.3 The Electrocardiogram and its Relationship to BP

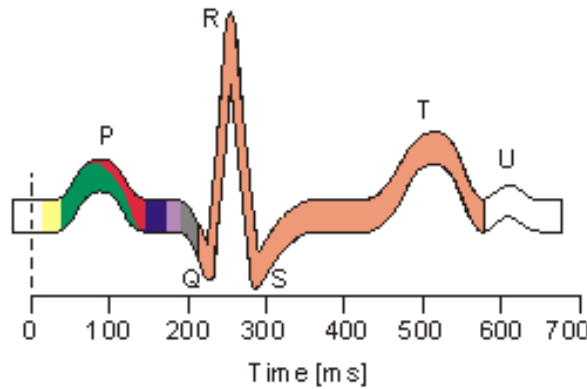
An electrocardiogram (ECG) is a device that measures the electrical activity of the heart. Frequently there is confusion over the meaning of each part of the graph. The most important point to note is that the ECG measures the *electrical activity* of the heart. Most of the components of this electrical activity have a corresponding physiological or mechanical effect, but some components have no direct mechanical meaning.

The cardiac cycle of the heart is illustrated in Figure 1.2a, where each sequential contribution is shown separately. The cycle begins with the depolarisation of the *sinoatrial* (SA) node. Once the electrical signal leaves the SA node, the atria are activated and blood flows into them. This wave of depolarisation passing through the atrial muscle corresponds to the P wave, shown in Figure 1.2b. When the atria become full of blood, the electrical activity spreads to the left and right atria, which then contract and push blood into the ventricles.

As blood flows into the ventricles, the electrical activity occurs at the Atrio-Ventricular (AV) Node. Once the signal passes through the AV node, it continues to the Bundle of HIS, and separates to the bundle branches. The electrical signal then flows to Purkinje fibres which corresponds to the Q wave of the ECG signal.



(a) The components of each electrical signal in the ECG waveform



(b) The sum of each of the components provide the total signal recorded from an ECG

Figure 1.2: An explanation of the ECG signal. Image taken from [11]

From the Purkinje fibres the electrical signal flows to the ventricle walls. This causes the ventricle walls to contract, indicated by the large electrical impulse represented by the R wave. The signal then relaxes as the blood is ejected from the ventricles around the body, creating a BP wave and the SBP while the electrical signal falls to the S point. From this point, ventricular re-polarisation begins and terminates at the T point. A further wave, the U wave is then noted as the Purkinje fibres re-polarise, however this point is not always observed in people that have been measured [11, 12, 13].

The most important component of the characteristic ECG wave from the perspective of this project, i.e. the measurement of Blood Pressure, is the start of the R wave or the point at which blood is ejected from the heart and circulated

around the body.

1.3 Outline of Thesis

The chapters of this thesis have been divided as follows.

Chapter 2 begins with an introduction to the BP measurement standards that are used to evaluate each of the methodologies discussed within this thesis. The State of the Art for BP measurement techniques, starting with the sphygmomanometer and progressing through to the Pulse Transit Time (PTT) method will then be described. The significance and shortcomings of each of these methods are outlined and discussed in detail. This chapter highlights the need for an improvement to all existing methods and identifies the PTT method as the area where a potential improvement could be made.

In Chapter 3, the PTT methodology is discussed in more detail and evaluated. The chapter begins with the development of the hardware that was required to measure PTT in conjunction with a description of each component that was included in the design, as well as the software and middleware that were required to capture the data. The various rounds of testing where volunteers were used to record the required signals and the subsequent evaluation of the PTT methods using algorithms to derive BP from the PTT measurements from both Chen [14] and Poon [15], who are two of the most referenced authors in the area, are also described. Using the results of these tests, the specific shortcomings of the method were clearly identified. This is something which had not previously been identified in the literature, and, furthermore, potential ways to improve the system in practice are suggested.

The inclusion of extra parameters that could be included into the PTT method so that a new and improved algorithm could be developed is described in Chapter 4. The focus of this chapter is investigating how Stroke Volume (SV) among other physiological signals can be examined for the development of a new algorithm. Two methods were investigated which would allow the examination of these signals. One method used a hardware implementation known as an Impedance Cardiograph which would require the measurement of data from volunteers. The second method was to use the PhysioNet Resource, which is a database that contained the required signals that had been previously captured through invasive techniques. The identification of the most suitable source of validating data as

well as the test protocol and algorithm evaluation based on results from Chapter 3 will be discussed.

Methods with which a new algorithm could be developed that could include both the PTT, SV as well as other parameters are discussed in Chapter 5. In this chapter, the importance of each physiological parameter is identified and Multiple Linear Regression is investigated as a tool for the development of a new algorithm. One potential solution identified by this method provided very good results. However due to some concerns arising from the statistical basis of the work used in the derivation of this algorithm, an alternative method was sought. This alternative method used the lessons learned from the equations developed using Multiple Linear Regression, and helped to derive an algorithm using a combination of existing equations and physical and physiological relationships. This new algorithm yielded even better, more universally applicable results. The new algorithm and its results are also compared to current state of the art algorithms to emphasise its quality, with the results showing a 100% increase in the calibration intervals provided by Chen's and Poon's algorithms. Furthermore, a description of how the new algorithm could be implemented and integrated into technology that is currently available to provide a minimally intrusive 24 hour continuous BP monitor, is described. A preliminary validation of this system was investigated using a number of volunteers from the test outlined in Chapter 3. The results recorded in this test matched those found when the PhysioNet database was used and has validated both the system and the algorithm concepts. Although these results appear to only double the calibration intervals of the existing PTT algorithms of Poon and Chen, the implications of the validation of the system and algorithm have much more long term consequences. Although the test contained only three people and a non-invasive BP monitor was used as a reference, these results indicate that it is now possible to measure BP on a continuous basis, by non-invasive methods over calibration intervals that are twice that of previously investigated algorithms, making them practical from the perspective of both clinicians and users.

The importance of this new algorithm and why its results make the PTT method useful in a practical sense is described in Chapter 6. Prior to the development of this algorithm, none of the state of the art algorithms were useful in a practical setting. However, this new approach has addressed these shortcomings, and this new algorithm and method provide a valid practical alternative and significant improvement on existing technologies. Furthermore, this system is the first reported non-invasive and continuous BP monitoring system that does not require

a continuously inflated or inflating cuff as is required with other state of the art BP monitors. Instead this novel system only requires one cuff measurement every 12 minutes. This chapter also outlines the next steps that are required for the continuation of this work, including clinical trials, so that its value can be confirmed in accordance with international standards.

Chapter 2

State of the Art of Blood Pressure Measurement Techniques

2.1 Introduction

As discussed, there are many ways by which Blood Pressure (BP) can be measured, the most accurate being by invasive methods. However, the focus of this thesis is measurement of BP by non-invasive methods only and an attempt is being made to replicate the accuracy of the invasive methods through the use of non-invasive techniques. In order to facilitate this explanation, it is necessary to provide a baseline and identify the currently used non-invasive BP measurement approaches, as well as their respective characteristics and identify ways to improve on these. In this chapter each method will be examined, starting with the oldest (and still most accurate) method and progressing through the evolution of this method to incorporate technology. Similarly, other less well known and implemented technologies and methods are examined and the advantages and disadvantages of these methods are highlighted, in terms of accuracy and reliability, as well as ease of use and practicality from the user and clinician perspectives. The chapter begins with an introduction to the various BP measurement standards that are used to evaluate each methodology. The objective of this chapter is to identify the research opportunity which would allow a continuous BP monitor to be developed.

2.2 BP Measurement Standards

There are currently three standards used for evaluating BP monitors. These are the Association for the Advancement of Medical Instrumentation (AAMI) Standard (SP-10) [16], the British Hypertension Society (BHS) standard [17] and the European Society for Hypertension (ESH) protocol [18].

Of these, the AAMI standard is the most straightforward. Using this standard, 85 subjects should be examined and the error between the BP of the measurement device under test and the gold standard sphygmomanometer should not differ by a mean of ± 5 mmHg or should not have a standard deviation greater than 8 mmHg. There are few instances in the literature when adherence to the requirement of 85 subjects is satisfied, due to the practical implementations of such a test. Essentially this means that if any of these test results were actually submitted to the AAMI, they would fail. However, applying the standard to any tests with fewer subjects can give a good indication of performance.

The BHS standard is a little more complex and grades results in terms of their accuracy. This is presented in Table 2.1. In this standard both a grade A or grade B is considered a pass while a grade C or D is a fail. For a device to achieve a grade A, 60% of its measurements, when compared to the gold standard, have to have a mean error of less than 5 mmHg, 85% of the measurements have to have an error less than 10 mmHg and 95% of its measurements have to have an error less than 15mmHg, and so on.

Table 2.1: A summary of the British Hypertension Society (BHS) standard which uses percentages of total error of values falling within 5, 10 and 15 mmHg, based on the system for assessing BP measurement accuracy, a rating of “B” is deemed acceptable, while a rating of “C” is deemed a fail.

Grading	% < 5 mmHg	% < 10 mmHg	% < 15 mmHg
A	60 %	85 %	95%
B	50 %	75 %	90%
C	40 %	65 %	85%
D	Worse than C		

The final standard is the European Society of Hypertension (ESH) International Protocol for validation of BP measuring devices. This is the most complex of the three standards and uses lessons learned from the BHS and AAMI standards. The aim when creating this standard was to make it more practical for smaller companies to be able to validate their devices because both the BHS and AAMI

standards require a large data set to be tested with a large variance of BP across all the subjects. This makes any new device very expensive to validate.

The ESH standard is very detailed on how the validation should be carried out. The ESH standard uses a categorisation system similar to the BHS standard to evaluate the device. However, it is far more detailed about procedures and thus more complex.

Each of the standards described in this section were developed with intermittent or cuff measurements in mind and this presents some problems when trying to evaluate a continuous beat to beat system. Although the AAMI standard and BHS standard can be applied to a continuous monitoring system, it was felt that due to the limitations in the ESH standard with regard to its measurement methodology, and its explicit descriptions of procedure with regard to observers and subjects, it would not be appropriate for this suite of tests. It should be noted that Appendix C of the ESH standard [18] recommends that continuous or beat to beat devices should be compared to intra-arterial measurements but states that it is not appropriate to use this standard when a new device is being compared to intra-arterial BP measurements, something which is undertaken in Chapter 5. A full explanation of the ESH standard is available in Appendix B. However, it should be noted that the ESH standard was not applied in any of the tests in this project for reasons also outlined in Appendix B.

2.3 Auscultatory Techniques

In 1905, Nikolai Korotkoff published his thesis regarding measuring BP in animals using a sphygmomanometer, a stethoscope and a Riva-Rocci sleeve [5] and this method became known as the “Auscultatory Technique”. This method formed the basis of a BP monitoring technique that is still used worldwide today and is considered by many to be the “gold standard” for non-invasive BP measurement [8]. The technique involves inflating a pressure cuff placed on the brachial artery to ≈ 30 mmHg above systolic BP, so that the brachial artery becomes occluded. While the pressure cuff is slowly deflated at a rate of 2 - 3 mmHg per heartbeat [5], the operator uses a stethoscope to listen to arterial sounds as the pulsatile blood flow is re-established. The sounds associated with this measurement have been classified in one of five phases based on their intensity as follows:

- Phase I: Appearance of clear tapping sounds corresponding to a clear pal-

pable pulse

- Phase II: Sounds become softer and longer
- Phase III: Sounds become crisper and louder
- Phase IV: Sounds become muffled and softer
- Phase V: Sounds disappear completely.

Phase I corresponds to systolic pressure and the pressure at which Phase V occurs is said to be the diastolic pressure. There is agreement that the systolic pressure as measured by this method generally underestimates the pressure when compared to a direct intra-arterial measurement, while the diastolic pressure given by the “Korotkoff sounds” is generally higher than that of a direct measurement [19]. These phases and the related cuff pressure measurement is shown in Figure 2.1.

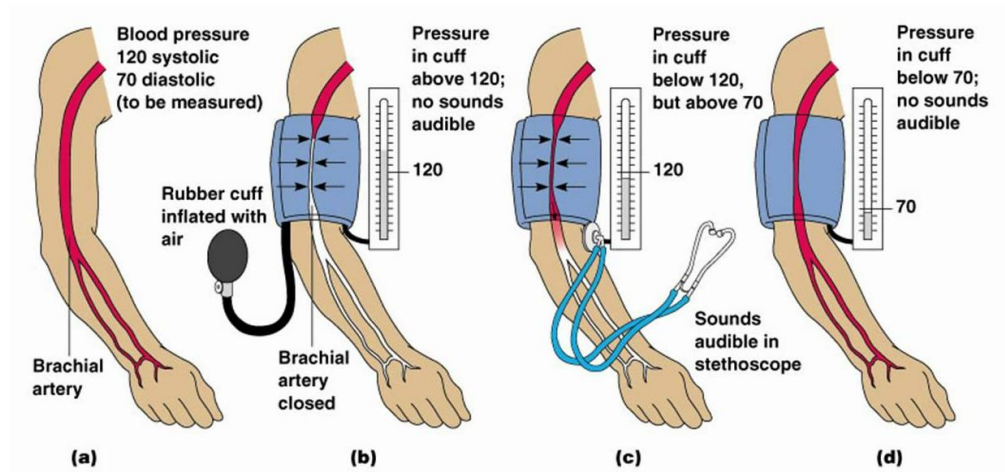


Figure 2.1: A graphical representation of the arm while listening for Korotkoff Sounds using an inflatable cuff [20]

2.3.1 Improvements to the Auscultatory Technique

There have not been any major changes to the Korotkoff principal since its first proposal in 1905 or in its first use on humans in 1932 by von Bonsdorff. In 1911 the sounds were characterised into the five phases as described above by Goodman and Howell [21]. However, the sphygmomanometer has been improved since its first use along with the techniques used for analysis. Mercury sphygmomanometers have always been considered the “gold standard” for BP measurement and have changed very little in the past 50 years, the major difference being that those now in use are less likely to spill mercury if dropped. An example of a

typical mercury sphygmomanometer is shown in Figure 2.2. One of the major advantages of the mercury sphygmomanometers is that they are of a simple design and so are less prone to faults. Furthermore, there is negligible difference in the accuracy between different brands [5].



Figure 2.2: A “gold standard” mercury sphygmomanometer [22].

Other improvements have been implemented since its first use. Among these are a set of guidelines as to how measurements should be taken [5]. These guidelines include what size the cuff should be in relation to the arm, where the cuff should be placed, how the stethoscope should be held and perhaps most significantly the phase at which the diastolic pressure is measured. Prior to 1988, it had been recommended that Phase IV sounds should be adopted for the measurement of diastolic BP. However, since Phase V is more easily identifiable, this is what is usually used and accepted in literature as the gold standard [6].

Aneroid sphygmomanometers are an alternative to mercury ones; however, they must be calibrated frequently to avoid errors. Aneroid sphygmomanometers use a mechanical system of metal bellows that expand as the cuff pressure increases to register the pressure.

2.3.2 Significant Advances

Electronic sphygmomanometers have been used in some cases. These new machines use microphones to hear the sounds disappear or an oscilloscope which senses motion from the occluded artery in order to record BP [23]. These electronic sphygmomanometers are usually inflated and deflated automatically and went some way to address the concerns that using a sphygmomanometer with a

stethoscope is a subjective measurement because it relies on the operator “hearing sounds” [4] and can vary from clinician to clinician.

2.4 Oscillometric Method

In 1876, a French physiologist, Etienne Jules Marey, first used the oscillometric method for non-invasive BP measurement. This method uses the amplitude of cuff pressure oscillations to measure BP [24].

2.4.1 Origins of the Oscillometric Method

In a similar way to the “Auscultatory method”, the cuff is first inflated to such a pressure that the artery becomes occluded. As the pressure in the cuff is deflated, a sensor registers the onset of oscillations that originate from the blood starting to flow through the arm again. The amplitude of these oscillations increase steadily until they reach a maximum, when the cuff pressure equals the Mean Intra-Arterial Pressure. The oscillations begin well above systolic pressure and continue to well below diastolic pressure so these pressures can only be determined using specific fractions of the maximum oscillation amplitude and the cuff pressure. These fractions are known as characteristic ratios. The characteristic ratios vary between manufacturers and the algorithms used to calculate BP are not divulged by any of the manufacturers. This causes significant differences in reading between equipment from different manufacturers [6].

2.4.2 Improvements to the Oscillometric Method

Since the oscillometric technique does not rely on the detection of Korotkoff sounds, it is much simpler to use this technique to measure BP than the auscultatory method. For this reason, the oscillometric method is the favoured one among ambulatory and home BP measurement systems. Furthermore, the readings are taken automatically and do not require subjective judgement or perceptions from an observer. These home and ambulatory BP measurement systems generally show good agreement with the auscultatory methods and many have been shown to adhere to the standards provided by the AAMI and BHS. A comprehensive list of these systems is available at Dabl Educational [25]. Figure 2.3 shows one of

the most highly recommended oscillometric BP Monitors from the Dabl database, the Omron M6.



Figure 2.3: The Omron M6 Oscillometric BP Monitor [26].

2.5 Tonometry

Tonometry is an alternative method for measuring BP compared to the two previous techniques. Historically, tonometry has been used to measure intra-ocular pressure. In this application, a sensor is placed on the eye, and the intra-ocular pressure is determined by the force that is required to flatten a given area or a measurement of the corneal indentation produced by a given weight loaded rod [27]. Figure 2.4 shows an example of this type of system where the end of a small handheld probe is pressed against the eye. The tip of the probe carries a pressure-sensitive area approximately 1 mm across. If the eye is momentarily flattened to beyond this sensitive area, the only pressure that will be recorded is the intra-ocular pressure of the eye [27].

When tonometry is used in the area of BP measurement, it is usually known as applanation tonometry, radial tonometry or arterial tonometry. Applanation tonometry has the desirable characteristic of not having an occluding cuff but does have an inflatable component. In this application, the tonometer comprises of a small cylinder with an opening on one end. This is the part that will be in contact with the skin. This opening is covered by a flexible diaphragm and inside the cylinder there is a saline solution [28]. The diaphragm is then placed in contact with the skin typically over the radial artery as shown in Figure 2.5.

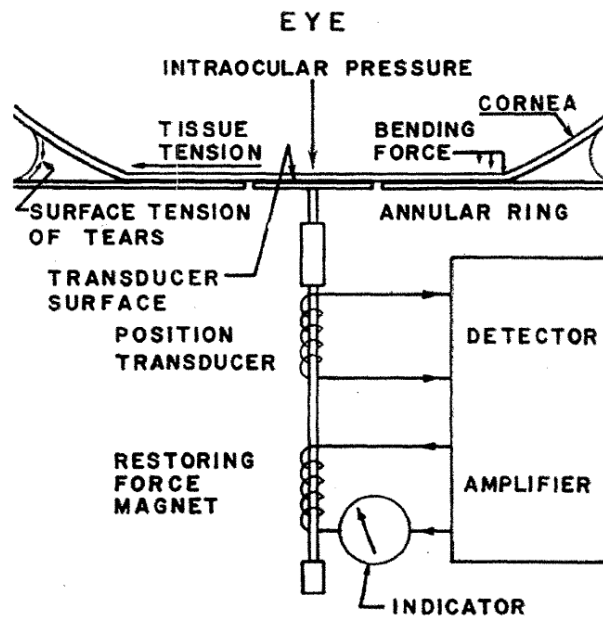


Figure 2.4: A simplified diagram of the tonometer [27].

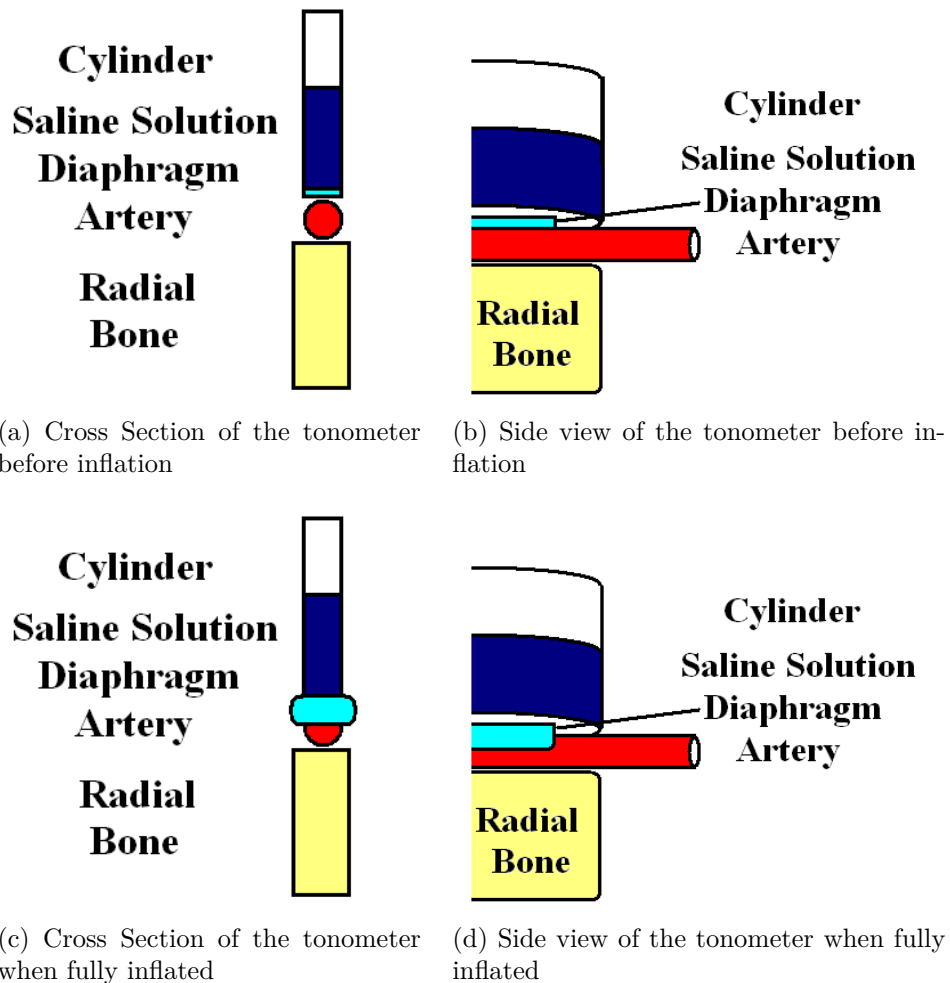


Figure 2.5: A cross section a side view of the tonometer before and during occlusion of the artery

The amount of saline fluid in the cylinder can be controlled using a syringe or other automated method. The cylinder is divided into small compartments, each compartment running from the top of the cylinder to the diaphragm and each compartment has an electrode pair. The volume of saline in the cylinder is measured by an impedance plethysmograph, which injects a small current between the electrode pair in that compartment and into the liquid and depending on the resistance measured, can determine its volume. Since the volume changes with the deflection in the diaphragm when it is placed over an artery, the volume change in the artery is reflected in the volume change in the compartment. A pressure sensor is also present in each compartment to measure the pressure exerted by the artery on the diaphragm [29].

Once the device is in place, the volume of saline in the cylinder is increased by injecting more saline into the cylinder, thus compressing the radial artery over the radial bone to reduce the effects of intervening tissue, damping effects and arterial wall stress. This is the equivalent of compressing the eye with the flattened surface of the transducer as shown in Figure 2.4 and this procedure is known as an applanation sweep and is illustrated in Figure 2.6. Just as in oscillometric cuff measurement, in tonometry the maximum arterial compliance occurs at zero transmural pressure. This level of artery compression results in maximum pulse pressure at mean arterial BP. When additional pressure is exerted, the artery begins to occlude and the signal amplitude is reduced. Since many factors impact the maximum pressure, this pressure needs to be identified using multiple measurements [30].

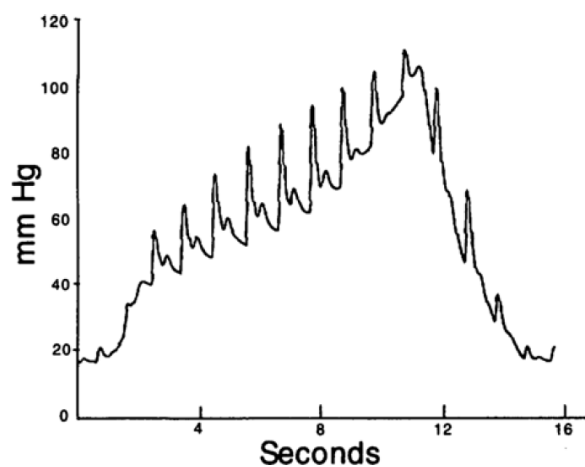


Figure 2.6: A representation of the applanation sweep used to detect the arterial waveform for BP measurement [31].

2.5.1 Current State of the Art Tonometers

One persistent feature and shortcoming of tonometers that has been observed is that it can be quite difficult to align the sensor exactly with the artery when using only a single transducer. Therefore, multiple compartments are used in an attempt to guarantee that at least one of the transducers will be positioned correctly [32].

In general, tonometers have shown good agreement to arterial BP. Kemmotsu et al [32], with support from Colin Electronics Company, used an intra-arterial line and compared the results from this to the Colin CBM-3000 tonometer using 28 patients under anaesthesia. The results showed good results and good correlations between the two devices for systolic ($r = 0.78$, $r^2 = 0.61$), mean ($r = 0.81$, $r^2 = 0.66$) and diastolic pressures ($r = 0.70$, $r^2 = 0.49$), although there is no mention of compliance with standards in their publication.

Nair et al [33] tested 89 subjects in line with the ESH, and AAMI standards, outlined in section 2.2. The tonometer used was a HealthSTATS BPro and the readings from this was compared with a sphygmomanometer and an oscillometric cuff, (the HealthSTATS MC3000), in line with the ESH standard. The results showed that this device met the accuracy criteria for both the ESH and AAMI standards.

Dueck et al [30] investigated the TL-200, a third generation tonometer from Tensys using 19 subjects. The TL-200 has the advantage of being able to automatically adjust its pressure sensor to the optimal position to achieve maximal pulsation. The recorded data was then compared to measurements taken by an intra-arterial catheter. The results showed good correlation between the two devices with Systolic BP ($r = 0.93$, $r^2 = 0.86$), Mean BP ($r = 0.93$, $r^2 = 0.86$) and Diastolic BP ($r = 0.89$, $r^2 = 0.80$). This study also showed that the TL200 would pass the AAMI standard for each of systolic (2.3 ± 7.8 mmHg), diastolic (1.7 ± 6.2 mmHg) and mean (2.3 ± 5.9 mmHg) BPs, when the AAMI standard was applied, but that it continuously failed the BHS standard for all three analysed BPs. Dueck noted that the number of subjects that they used needed to be increased in line with the standards, vasoactive drugs should be introduced to the study and a greater range of pressures need to be examined. However, he states that the device can be recommended as a non-invasive beat-to-beat device for hemodynamically unstable patients during general anaesthesia and surgery based on the results obtained in this study. However, Dueck does state in the “conflict of

interest” section of this paper that he had received funding from Tensys Medical Inc for this study.

Weiss et al [34] found considerably different results when comparing the Colin SA-250 tonometer to a radial artery catheter using 22 high risk surgical patients. During the same investigation an oscillometric BP monitor, BP-508, was also compared to the catheter. The results showed a good correlation between both the catheter and tonometer and catheter and cuff, but the correlations for the cuff were found to be better than the tonometer. Using the oscillometer the following correlations were found: Systolic BP $r = 0.83$ ($r^2 = 0.69$), Diastolic BP $r = 0.90$ ($r^2 = 0.81$), Mean BP $r = 0.92$ ($r^2 = 0.85$). Using the tonometer the following correlations were found: Systolic BP ($r = 0.80$, $r^2 = 0.64$), Diastolic BP ($r = 0.77$, $r^2 = 0.59$), Mean BP ($r = 0.84$, $r^2 = 0.71$). The conclusions of this study were that, compared to a catheter, intermittent measurements using a oscillometric BP meter provided more accurate arterial pressure monitoring measurements, whereas the tonometer offered a reliable trend indicator of pressure. It should be noted that the subjects in this study were high risk surgical patients and this may have affected the results.

The Vasotrac system is a modified tonometer and does not require the frequent calibrations needed by other tonometers. However, it does not provide beat to beat BP with arterial waveform display. It has been compared with both a non-invasive (oscillometric) meter and an arterial catheter with good results. In their paper Belani et al [31] tested the Vasotrac system using these devices to analyse the accuracy of the device using 54 volunteers. Out of these 54, 11 were given vasoactive drugs to alter their BP to test the accuracy and ability of the device to track induced BP changes. In the 43 volunteers who were not given drugs, the results showed that the Vasotrac measurements were highly correlated with the Systolic BP ($r = 0.94$, $r^2 = 0.89$), Diastolic BP ($r = 0.94$, $r^2 = 0.88$) and Mean BP ($r = 0.97$, $r^2 = 0.94$). These results also showed that 90% of the recorded errors were less than 5mmHg. In the remaining 11 volunteers similar results were found compared to the other 43 volunteers with high correlations again of Systolic BP ($r = 0.91$, $r^2 = 0.82$), Diastolic BP ($r = 0.94$, $r^2 = 0.89$) and Mean BP ($r = 0.98$, $r^2 = 0.96$).

2.6 Vascular Unloading Technique

The vascular unloading method is another method that has evolved from Marey's work in 1876 [2]. This method was first specified by Shirer [35] and can be explained as follows: changes in the volume of blood vessels that arise due to intra-arterial pressure can be countered by an external pressure to maintain a constant pressure in an unloaded state. This can occur because tissue can be assumed to be essentially incompressible and therefore an externally applied pressure is transmitted directly onto the underlying vessels where it results in an altered transmural (external minus internal) pressure. If the external pressure exceeds the internal pressure, the vessel collapses. When the external pressure equals the internal pressure, the vessel is said to be in an unloaded state. This allows the indirect measurement of the intra-arterial pressure [36].

Using this concept in 1973, Jan Peñáz, a Czech physiologist proposed a non-invasive BP monitoring method [37]. His technique involved the use of a transparent finger cuff, a photoelectric plethysmogram and pressure controller. The photoelectric plethysmogram (PPG) measures blood volume changes in the finger. As the BP increases, the volume of blood in the finger increases and therefore the output of the PPG also increases linearly. The PPG controls the pressure controller at the base of the finger using a measurement and feedback system. As the volume of blood in the finger increases, the PPG responds by increasing the external pressure to counter these volume changes through adjustments of the pressure controller. By repeating this procedure rapidly at a rate of 40-60Hz, the vessels are kept in a constantly unloaded state and the pressure measured in the cuff corresponds directly to the intra-arterial pressure.

2.6.1 Finapres

In 1985, van Wesseling first commercialised the Peñáz method using the name Finapres (FINger Arterial PRESSure) [38]. The value of this system was quickly recognised because it was the first system to provide a reliable measurement of the beat-to-beat BP measurement in a non-invasive manner [39]. The major changes implemented from the original Peñáz method were: the Finapres PPG light sensor was mounted directly onto the skin, whereas the Peñáz method had the light sensor mounted in such a way that the light had to pass through the inflatable cuff as well as the skin. This resulted in the motion artifacts being

greatly reduced.

The original design also had an electro-pneumatic transducer which consisted of an electrically controlled valve which controlled the amount of air shunted to the finger cuff. This was a severely restricting factor in the operation of the instrument because it limited the speed with which the cuff could be inflated. The Finapres used a dynamic compressor which consisted of an air bellows controlled by a linear motor. This allows pressure changes to be introduced by an order of magnitude faster than the original. As the Finapres became increasingly accepted, a substantial number of studies were carried out in an attempt to verify its accuracy and precision. One of the first of these studies was by Kurki in 1987 [40] who studied 50 men during surgical operations and found that the device had a high accuracy when compared to intra-arterial methods. These studies continued and by 1998 the accuracy of the Finapres was broadly acknowledged [41].

The Finapres, has subsequently been replaced by a newer device known as the Finometer. The differences between the two include: the signal from the Finometer is digitally filtered, to reconstruct the brachial artery waveform and; a correction algorithm is applied to compensate for the pressure gradient along the arm arteries [42]. Although very accurate and reliable, the Finometer differs from other BP monitors described in this chapter, as it is quite big and is more comparable to a bedside monitor rather than the smaller devices that have been previously discussed. However, the Finometer's sister product, the Portapres, shares both the technology and reliability of the Finometer, but is a portable and more appropriate device for comparison.

2.6.2 Portapres

The Portapres was introduced to the market in 1991 as a portable version of the successful Finapres product, described above. Additional functionality was added to enable the device to become portable. Systems were added to record signals on tape, a second finger cuff and additional circuitry was added to correct for the hydrostatic height of the hand. The Portapres is also operated from a battery [43]. The second finger cuff, which is shown in Figure 2.7, is an attempt to reduce venous congestion and the two cuffs are used alternately for 30 minute periods throughout the measurement time.

The Portapres has been shown to be valuable since its introduction due to its



Figure 2.7: The Portapres device from Finapres with the associated finger cuffs, their servo controller and 5kg belt. Image taken from [44]

portability and has been used in many studies to monitor sleep apnoea. It has also been compared favourably with the Finapres and has shown good results when compared with an intra-arterial BP monitor. The Portapres is also recommended for 24 hour BP monitoring [45]; however, it has been observed to be quite heavy, weighing 5 kg and cumbersome, as shown in Figure 2.7. Given its size, the Portapres is unsuitable for most home monitoring and AAL situations but is a very useful research tool.

2.6.3 Other Peñáz Implementations

The Nexfin monitor [46] is another system which implements the Peñáz method to measure BP and bears a lot of similarities to the Finometer line of devices. It has been suggested that the Nexfin is an evolution of the Finometer; however, the Nexfin monitor does not require a cuff monitor for recalibration [46]. The Nexfin has also been widely recognised as being accurate and numerous tests have shown that the monitor has an acceptable error [47] and is within the standards across various implementations [48, 49, 50]. It should be noted however, that although Schattenkerk et al [49] claim that the Nexfin monitor is within the standards in their paper, the results that are presented in the paper indicate that, without some adjustments, the Nexfin monitor is outside the AAMI standards. Although these required adjustments are clearly detailed within the paper, all presented data within the paper that do not have these adjustments exceed that AAMI standard. However, in the other studies outlined here, it has been shown that the Nexfin monitor is within the AAMI standards, although it has been shown

not to pass the ESH standards in a pregnant population [51].

Tatara [52] has also developed an “in ear” Peñáz based BP measurement system. The ear was chosen as the arterial location for two reasons:

- The height above the heart remains relatively constant, especially in contrast to the arms where the height is unpredictable and is the typical location of the sensor
- The temperature in the ear reflects changes in the core body temperature more closely than the arms

Evaluating the device on 7 test subjects it was found that the mean error and standard deviation was 3.4 ± 9.9 mmHg which is outside the AAMI standard.

2.7 Pulse Transit Time

Since the beginning of the 20th century, there have been many attempts to relate the pulse to blood pressure. During cardiac systole, blood is pumped into the circulatory system and a pressure wave is propagated away from the heart. The velocity of the propagation is dependent on numerous factors, one of which is the arterial wall stiffness which affects the speed of the wave. Pulse Transit Time (PTT) is defined as the time it takes the wave to propagate from the heart to a specified point on the body, typically the finger. This time is related to the propagation velocity of the pulse wave [53]. PTT is also sometimes referred to as Pulse Arrival Time (PAT), but these are different parameters which are unfortunately used interchangeably, depending on whose work is being reported. The difference between the two parameters is the PAT takes account of the Pre-Ejection Period (PEP), which represents the isovolumetric contraction time of the heart, i.e. the time it takes for the myocardium to raise enough pressure to open the aortic valve and start pushing blood out of the ventricle [54]. Conversely, PTT generally does not account for the PEP or anything else which may affect the signal.

There have been many investigations that attempt to relate PTT directly to BP [55, 56, 57, 58], and many authors have found that there is a relatively high correlation between PTT and BP, usually $r > 0.7$ although this can vary by a significant amount depending on how PTT is defined, as shown by Hennig’s PTT review, where a difference in correlation coefficients of up to $\Delta r = 0.23$

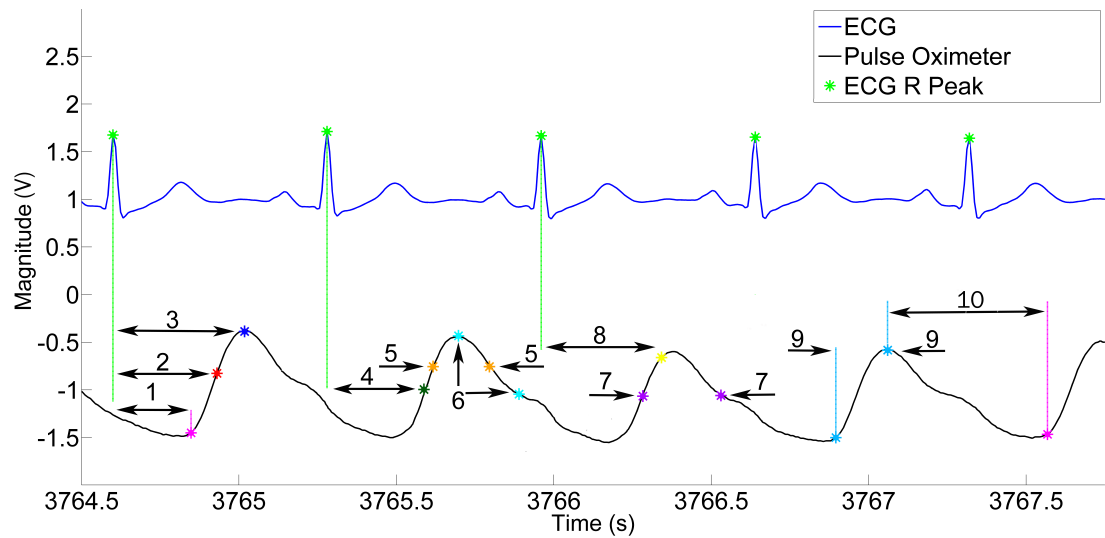


Figure 2.8: The various PTT definitions and other characteristic points defined in this review.

Table 2.2: A brief explanation of the characteristic points shown in Figure 2.8

Point of Interest	Name
1	Foot / Onset of Wave
2	Point of Inflection
3	Peak
4	50% of Peak
5	$\frac{2}{3}$ Pulse Width
6	Relative Amplitude Second Peak
7	Width of $\frac{1}{2}$ Pulse Width
8	Point of Maximum Inclination
9	Systolic Upstroke Time
10	Diastolic Time

has been reported between authors [53]. The general definition states the PTT as the time for the pulse wave to reach a second arterial location i.e. the finger. However, how/when this arrival is defined is the subject of a considerable amount of debate. When the finger, ear or toe is used as the second arterial location, the photoplethysmograph is normally used to detect the arrival of the pulse wave. Table 2.2 provides the name for each of these points and Table 2.4 provides a full explanation of each point and a summary of some the authors, discussed here, who use each. Perhaps the easiest location in this signal to use is the peak (Point 3 in Figure 2.8), because it is the most easily defined. Another favoured part of the curve is the foot of the PPG wave (Point 1 in Figure 2.8). Many authors have reported that using this provides a better correlation between PTT and BP [57]. Other points that are used are the point of maximum inflection [56] (Point 2), the systolic time and diastolic time [56, 59] (Points 9 and 10), the point of maximal slope, derived from a continuous wavelet transform, [58]

(Point 8) and various widths of the wave [60, 56, 59], all of which provide varying levels of success and correlations. During these studies it was also common for both systolic and diastolic BPs to be investigated and each value correlated to PTT and these studies have established that SBP and DBP each show strong correlations to different locations on the PPG wave.

Masé [61] used a linear regression technique on each individual studied to relate BP to PTT. Using this technique Masé found inverse correlation values of $r^2 = 0.89$ and 0.78 for systolic and diastolic BP respectively using 33 different individuals. The period of the test lasted 30 minutes and included 5 minutes of rest followed by 3 minutes of cycling followed by two minutes of rest, repeated 4 times, followed by 5 minutes of rest. PTT was recorded during the two minute rest periods, while the subject sat on the exercise bike.

Hassan [62] also used a linear regression technique on 10 individuals, each test lasting 45 seconds across 3 different conditions: rest, exercise and recovery. Hassan found the maximum recorded value for the mean and standard deviation between the cuff and PTT method was 5.72 ± 8.90 mmHg from these 10 individuals. However, most individuals provided lower valued means and standard deviations than these maximum values. Although this result is quite promising, more subjects need to be recorded with a wider range of BPs for the technique to be confirmed according to the standards.

Although the specific definition of PTT is open to debate, a related parameter, Pulse Wave Velocity (PWV), measured in m/s, is better defined and it forms the basis for all PTT methods, regardless of how the PTT is actually measured. Moens and Korteweg in 1878 [21, 63] first derived a mathematical equation which related PWV to the elasticity of the artery E (Young's modulus) [$m^{-1}kgs^{-2}$], its diameter d [m], the thickness of the wall t [m] and the density of the blood ρ [kg/m^3], given below by equation 2.1.

$$PWV = \sqrt{\frac{tE}{\rho d}} \quad (2.1)$$

Using some simplification, substitution and manipulation, as can be found in Sorvoja [21], PWV can be expressed as:

$$PWV = \frac{K}{PTT} = \sqrt{\frac{tE_0 e^{\gamma P}}{\rho d}} \quad (2.2)$$

Where E_0 is the elastic modulus of the artery at zero pressure [$m^{-1}kgs^{-2}$], P is the BP (mmHg), γ is a coefficient ranging from 1.6×10^{-2} to 1.8×10^{-2} [$mmHg^{-1}$] and K is a proportionality coefficient [m], indicating the specific distance for the pulse wave to transit within time t [s] at velocity v [m/s], according to Chen [14].

This equation is the basis for all work that has been performed with regard to PTT or PWV in respect of BP. Most authors who have developed PTT based algorithms have manipulated this equation further and these modified equations and the reasons for using each of them will be outlined in the next section.

Shriram et al [64] used the Moens Korteweg equation directly as presented in equation 2.2 in their investigation into the use of the PTT method to monitor BP. They found a correlation of $r = 0.983$ between the PTT method and both the automatic BP measurement machine that they used (which was not specified) and the sphygmomanometer, measured from 23 healthy volunteers. The mean and standard deviation between the PTT method and the automatic machine was found to be 0.52 ± 3.3 mmHg, which is well inside the AAMI standard. However, it is unclear whether the use of calibration intervals was investigated and the duration of these examinations is not specified either.

More recently, there has been a considerable investigation into the measurement of PTT via ECG and Modulated Magnetic Signature of Blood (MMSB) which is detected using Giant Magneto Resonance (GMR) sensors. MMSB is the term applied to the method of blood pulse and flow monitoring where a uniform magnetic field is applied to the skin in close proximity to a major blood vessel. The uniform magnetic field from a permanent magnet will create a magnetic field that encompasses skin, fabric and blood vessels. If there is no change in any of these parameters, a DC magnetic field will be received by the nearby GMR sensor. However, due to the pulsatile nature of the blood flow in the arteries, the uniform magnetic field is disturbed which is then detected by the GMR sensor [65]. This waveform can be then used, in conjunction with an ECG sensor, to measure PTT, in place of a regular PPG sensor [66]. The advantage of this system is that it is a planar device and thus can be placed near any major blood vessel. Phua has investigated using the MMSB system in place of a PPG sensor to measure PTT for BP acquisition [67]. BP was recorded from 10 individuals and then compared to the estimated BP derived from the system and an adaptation of Fung's algorithm [58]. The exact procedure that is followed is unclear but Phua claims that the measurement of MAP provided by their system has errors of less than 8% when compared to a traditional oscillometric BP monitor.

Another device, known as a Ballistocardiograph (BCG), has also been investigated to be used as part of a PTT system. A BCG measures the body's mechanical reaction to the blood ejected during the systole and can be measured using either a low friction bed [68] or an accelerometer placed on the head [69]. Using a BCG with an ECG, it has been suggested that it is possible to measure PEP [70], however most studies have investigated using the BCG and PPG to measure PTT [71, 72]. Chen's paper in 2013 [72] uses a BCG and PPG to measure PTT and, by developing a linear regression model, have produced an algorithm which allows measurement of DBP within the AAMI standards. However, using this technique, the SBP was outside the AAMI standard. It is also unclear how many volunteers were used, but these results seem to be based on five measurements.

2.7.1 Chen's Significant Contribution to the PTT method

Since the original concept by Moens-Korteweg, many researchers have investigated both the relationship between pulse wave velocity, human arterial extensibility and the relationship between PWV and BP. During the period between the 1960's and the 1980's, researchers found statistically significant relationships between PTT and either systolic BP, diastolic BP or Mean Arterial Pressure (MAP) [73]. However, the breakthrough came in 2000, when Chen [14] et al proposed a method based on measuring the beat-to-beat time interval between the QRS apex in the ECG signal and the onset of photoplethysmogram in an oximeter sensor placed on the finger tip.

Chen simplified the relationship between BP and PTT to the following:

$$P_e = P_b - \frac{2}{\gamma PTT_b} \Delta PTT \quad (2.3)$$

Where P_e is the estimated BP, P_b [mmHg] is the base BP measured at the beginning of the measurement and PTT_b [s] is the value of the PTT at the beginning of the measurement and ΔPTT [s] is the change in the PTT. This can then be further simplified and explained as:

$$P_e = P_b + \Delta P \quad (2.4)$$

If the changes in the wall thickness (t) and the diameter of the vessel with respect to BP are negligible, and if the change in the arterial wall tonus (E_0) is slow

enough, the first term on the right hand side above can be regarded as constant as long as the change in vessel elasticity is negligible, over a short period. This means that over a short period of time, PTT can be linearly related to the change in BP. Where P_b is the base BP level, and ΔP is the change over the base level.

Using this theory as a basis for their method, Chen developed his algorithm, which uses two components, a High Frequency Component (HFC) and a Low Frequency Component (LFC). During testing, Chen found that a linear relationship existed between SBP and PTT if the data was filtered using a bandpass filter between 5.3×10^{-4} Hz and 4×10^{-3} Hz, varying with the calibration interval that is used. Therefore, when a PTT measurement is recorded it is filtered and is known as the high-frequency component. It should be noted that no other authors reviewed have reported this relationship to be true and neither its derivation nor the motivation for using it was explained in the original work. The lower-frequency component (LFC) is derived from BP cuff measurements. The time between these measurements was also the calibration interval. Using a linear lookup table these measurements were interpolated at 1 Hz to form the LFC. At each calibration point, the estimation was corrected and between the calibration points, a combination of the higher-frequency component and LFC were used to track changes in BP. Using this method, Chen obtained an accuracy of 0.97 ± 0.02 mmHg for SBP using 5 min calibration intervals. This result indicated that BP changes could be tracked using PTT as long as the calibration measurements were performed regularly and the elasticity of the vessels remained constant.

2.7.2 Significant Advances to the PTT Method

Since the initial work by Chen, the team of Zhang from the Chinese University of Hong Kong has explored the topic extensively [59, 74, 75, 76]. Others outside of this group have also worked on calculating BP from the PWV/PTT methods and calculations, but Zhang's group have followed Chen's original work more closely. Since Chen's original paper, many researchers have examined the use of PTT in an attempt to further his concepts. However, there are many inconsistencies in the studies in this area. The most prominent of these is how to define and measure PTT itself, as previously discussed.

There are also ongoing debates about whether the Pre-Ejection Period (PEP) should be included as part of a PTT measurement. Payne et al [77] have reported that the inclusion of PEP in the measurement of PTT makes the BP measurement

unreliable; however, others have found good correlations by including PEP in the measurement of PTT [57].

Ahlstrom [57] used an ECG, a PPG and a phonocardiogram to measure three different transit times associated with the heart: PEP, VTT (time from first heart sound to onset of peripheral pulse) and PTT. In this study, PTT was measured from the peak of the ECG R-wave to the foot of the PPG signal. BP was recorded using either an oscillometric cuff or via a catheter. Partial correlation analysis was used to clarify the correlation between the transit times and BP. The best correlation coefficients were found between SBP and PTT with $r = 0.80 \pm 0.06$. Although Ahlstrom used a phonocardiogram in an attempt to measure PEP, he warned that it may not have been accurate because of the difficulty associated with detecting the signal.

While basing her work on that of Chen, Poon [75], used an alternative method to calculate SBP [mmHg] and DBP [mmHg]. Poon used a slightly different perspective when using Young's modulus. Poon equated the rate of change of stress to the difference between SBP and DBP in the arterial system. Substituting this definition into the Moens-Korteweg equation shows that the difference in SBP and DBP is inversely proportional to the square of PTT. Poon stated that mean BP is often approximated as a third of SBP plus two thirds of DBP [78], SBP and DBP can be estimated as:

$$DBP = \frac{SBP_0}{3} + \frac{2DBP_0}{3} + A \ln \frac{PTT_{W_0}}{PTT_W} - \frac{(SBP_0 - DBP_0) PTT_{W_0}^2}{3 PTT_W^2} \quad (2.5)$$

$$SBP = DBP + (SBP_0 - DBP_0) \frac{PTT_{W_0}^2}{PTT_W^2} \quad (2.6)$$

This approach led to an accuracy of 0.6 ± 9.8 mmHg for SBP and 0.9 ± 5.6 mmHg for DBP. The BP measurements were recorded using a Colin BP-8800, which adheres to the AAMI requirements for BP measurements. The standard deviation of the SBP in this review is slightly outside the recommended AAMI requirement (8mmHg) but the standard deviation of the DBP of 5mmHg is better than the AAMI requirement. In order to improve these results, it was suggested that the equations should incorporate other factors which affect BP recordings while using PTT, such as ambient temperature, contact force between the sensor and the skin and arterial vascular properties. It should be noted that neither the measurement

nor definition of PTT is included in the paper.

In 2008, Poon [74], investigated how the relationship between BP and PTT changes over time, in particular the number of heartbeats where the BP-PTT relationship with constant A (Equation 2.8) and B (Equation 2.9) will hold on a subject. The investigation was based on the equation derived by Chen from the Moens-Korteweg equation:

$$BP = A \ln(PTT) + B = A \cdot PTT_{\ln} + B \quad (2.7)$$

Where A and B are subject dependent coefficients (both measured in [mmHg]) namely:

$$A = \frac{-2}{\gamma} \quad (2.8)$$

and

$$B = \frac{1}{\gamma} \left[\ln\left(\frac{\rho d K^2}{t E_0}\right) \right] \quad (2.9)$$

The results of Poon's study showed that beat to beat logarithmic PTT values (PTT_{\ln}) and SBP were highly correlated over a short period but the correlation coefficient decreased as the number of heart beats increased. In fact, for the data collected, it was found that this method needs to be recalibrated as often as every 60 beats in order for 95 % of the cases to have a standard deviation within 9.4mmHg, if the optimum pair of A and B coefficients can be obtained for each subject.

In the work of Yoon [56], ECG, PPG and BP was recorded from five subjects. Eighteen seconds of data at the middle of the 60 second measurement were analysed in order to match the actual BP measurement time. These measurements were recorded simultaneously with the subjects in a seated position after they had rested for at least 5 minutes. Immediately after 100 step-climbing exercise (each step was 21 cm high), more measurements were recorded as post-exercise data in the same seated position. This measurement trial was repeated three times during the same day. Each trial had at least 20 minutes rest to avoid the exhaustion of the subject. The experiments were repeated for 5 days with the same subjects. Five different parameters were measured from the ECG and PPG signals. These were PTT from the ECG R peak to the PPG wave onset

(PTT_foot), PTT from the ECG R peak to the maximum derivative point of the PPG wave (PTT_dp), systolic upstroke time, diastolic time and the width of 2/3 pulse amplitude (Points 1, 2, 8, 9 and 6 respectively of Figure 2.8). Linear regression analysis was set up for the systolic and diastolic BP. The results of this work shows that the PTT to a maximum first derivative point (PTT_dp) is highly correlated with SBP (-0.712) and that the diastolic time had the highest correlation with DBP (-0.764).

Gu et al [76] (who are part of the same group as Poon above) have also examined the PTT / BP relationship. In their research study, they measured PTT during rest periods and after periods of exercise and included a new parameter known as the Relative Amplitude of Secondary peak of PPG (RAS), Points 5 of Figure 2.8. As with many of the other studies described in this review, the duration of the examinations was not specified exactly but the method was shown to be accurate, even after exercise with a mean error and standard deviation of -0.4 ± 5.3 mmHg.

McCombie [79] used a modified version of the PTT system that has been presented previously. In this system, Peripheral PTT was examined. In Peripheral PTT the system consisted of two PPG sensors; one placed on the wrist; the other placed on the little finger, thus giving the two arterial locations required for PTT measurements. By examining hydrostatic pressure (defined to be the height at which the pressure is measured relative to the heart [80]) along with PTT, McCombie developed a novel calibration method using the hydrostatic measurement and an adaptive signal processing algorithm. Although only 7 subjects were used in this investigation, the calibration constant derived using the hydrostatic pressure almost matched that derived from the Finapres which was used as a gold standard in his experiments.

Teng [59] examined four features of the PPG wave in an attempt to further the PTT-BP relationship using 15 subjects. Teng however had some difficulty identifying the foot of the PPG wave and thus used a Continuous Wave Transform (CWT) on the PPG wave to clarify this position. Using the results of this, Teng examined the use of the width of $\frac{2}{3}$ pulse amplitude, the width of $\frac{1}{2}$ pulse amplitude, systolic upstroke time and diastolic time (Points 4, 6, 8 and 9 respectively of Figure 2.8). Correlation analysis was then performed and it was found that the highest correlation was achieved when the diastolic time was used. Using this feature, the PTT was calculated giving a prediction of 0.21 ± 7.32 mmHg for SBP and 0.02 ± 4.39 mmHg for DBP.

Lin et al [60] investigated the use of 3 different measurements based on the PPG waveform as an alternative to the more usual PTT definition. The three measurements were the duration from the ECG R wave to 50% of the PPG wave, $T_{R_50}(i)$, the pulse width $T_W(i)$ (Points 2 and 6 respectively of Figure 2.8) and the normalised pulse width $\frac{T_W(i)}{T_{R_50}(i)}$. Using these measurements to calculate PTT, Lin used linear regression on each PTT measurement and intra-arterial BP on 9 subjects and found the correlation between the results, each providing a mean correlation value in excess of $r = 0.73$. A combination of these parameters and the correlation results were then combined to create a new parameter $SBP_{combining}$. This was found to be a good predictor of SBP when compared to the intra-arterial measurement with a correlation $r = 0.82$. However, as noted in his paper, the regression coefficients are needed and since these were calculated using the Arterial BP, this means that this method cannot be classified as a non-invasive BP measurement in its present form.

Muehlsteff et al [81] examined 18 volunteers in their 2006 paper which described their investigations into the inclusion of PEP in the PTT measurement. PEP was measured with a NICCOMO patient monitor and BP was measured using an oscillometric monitor. Posture was also recorded using a 3 axis accelerometer. PAT was measured from the peak of the ECG R wave and the foot of the PPG wave (which was determined using a tangent to the uprising pulse) and PTT was defined as $PTT = PAT - PEP$. Each subject was tested at rest, during exercise and during recovery after exercise and the Moens-Korteweg equation was used to relate PTT/PAT to BP. The results showed that when the SBP changes due to exercise, the PEP has a higher influence on PAT measurements than PTT. This shows the importance of PEP and how it dominates PTT in short term stress tests. However, because of the Moens-Korteweg derivation and its associated assumptions PEP cannot be excluded from the measurement. Furthermore, because the true PWV is not available, a linear calibration function was designed (based on the PWV) which gave a good estimation of SBP. This calibration function included the length of the subjects arm and is defined as:

$$SBP = A \cdot \frac{L}{PAT} + B \quad (2.10)$$

measured in mmHg and where A and B are defined in the Moens-Korteweg equation and L is the length of the subjects arm. When A and B are calibrated for each individual, a mean RMS error of 3.9mmHg was found whereas if A was averaged over all subjects and B was individually calibrated, an RMS error of

6.9 mmHg was found. In the first case, it was found that it was possible to achieve a better (lower) RMS error of 2.7 mmHg if a quadratic equation was used, but this involved a more complex calibration procedure and was therefore not implemented.

In 2008, Muehlsteff et al [82] repeated their experiment with a focus on the effect that posture has on changes on PAT. Left Ventricle Ejection Time was also monitored in this test, which complemented the measurement of PEP. A further test outside of the lab was also performed using a wireless body sensor network system, but in this test no BP was recorded. Results from these tests show that posture changes have a significant subject-dependent effect on PAT even at constant SBP and DBP. Specifically, it was found that if subjects rose from lying to sitting or standing, their PTT increased and vice versa. It is noted that for any PAT based BP measurement system, the effect of posture must be taken into account. During stationary lab tests, each test subject should have the same posture. It is also noted that hydrostatic effects should be accounted for in any BP measurements.

2.8 Discussion

A variety of non-invasive BP measurement techniques has been presented in this chapter. Although each technique has its advantages, three techniques provide results which are superior to the others for long term 24 hour BP monitoring. These are the Peñáz / Vascular Unloading method, the tonometric method and the PTT method. These techniques are favoured due to their ability to monitor BP without the need for an inflatable arm/wrist cuff. This feature is particularly desirable in the area of BP monitoring for ambient assisted living, because an unobtrusive nature and comfort to the subject have a major impact on the usefulness of any given system. Another valuable trait is that each of these systems can be used to monitor short term changes in BP, something which the other techniques cannot do [83].

Although the tonometric method also has the highly desirable feature of providing an arterial waveform, it has been noted that it is critical to the successful measurement that the sensor is placed precisely over the radial artery. A few steps have been taken to improve this, namely the use of multiple compartments and the automatic adjustment of the sensors. However, this method is very susceptible to movement artifacts. The Tensys TL200 [30] is capable of eliminating

many of these issues. However, in an attempt to compensate for these, the sensor has become quite large and could be considered obtrusive, as can be seen in Figure 2.9.



Figure 2.9: The TL200 tonometric BP monitor is capable of optimising the signal quality but at the cost of its size and bulkiness. Image taken from [30].

While the vascular unloading method has been shown to be very accurate and reliable and its comfort is much greater than previous methods, a number of disadvantages remain associated with its use in AAL. The most obvious of these is the size associated with the products that are most well known, used and proven to be reliable i.e. the Finometer/Portapres. It is worth noting that the Portapres name indicates portability rather than that the system is wearable. In fact from Figure 2.10 it becomes apparent that the system is far from wearable and could only be considered portable by the young and not by an ageing population. Pickering et al [6] noted that the Portapres is “not suited to clinical use because of its cost, inconvenience, and relative inaccuracy for measuring absolute values of BP” and that “its greatest value is for research studies” Another concern when using either the Finometer or Portapres is misapplication of the cuff, which can lead to underestimation of MAP in the case of tight finger cuffs, or overestimation in the case of loose finger cuffs [84]. Again, although both devices are known for their reliability and accuracy, even the Portapres, shown in Figure 2.10, is quite obtrusive and heavy and not practical for many applications where such monitors are required i.e. in the area of ambulatory monitoring.

Shaltis et al are working on a system, based on the Peñáz method that can be implemented and worn on the finger similar to a ring [86]. This ring sensor, and indeed the Peñáz method in general, still requires an inflatable pressure cuff to be worn on the finger. Although this ring based system would be much more comfortable than previous implementations, the use of a pressure cuff, no matter



Figure 2.10: The Portapres Device being worn during an exercise test with the associated finger cuffs, their servo controller and 5kg belt. Image taken from Finapres website [85].

how small, is undesirable. Another concern is that an inflatable cuff on the finger may cause other medical problems if the cuff is worn over a long period.

It thus becomes evident that the most suitable BP monitoring technique is that of the PTT method. Using this method, no inflatable cuff is required. In a similar way to the work of Shaltis, the PTT system can be implemented on a ring type sensor and an ECG worn on the chest. The PPG sensor can also be redesigned to work at other arterial locations such as the ear. It is also possible to use peripheral PTT measurements so that an ECG does not have to be worn.

Table 2.3, based on Peter's paper [87], gives a good summary of the characteristics of each of the BP measurement methods discussed in this chapter. Most of this table is self-explanatory, but some points need to be expanded. The first of these is with regards to the auscultatory method. This is described as being not wearable, the reason being that although the sensor is wearable, since a doctor or clinician is still required, it is not suitable as a wearable system when no doctor or clinician is present. The wearability of the Peñáz method in this table is also described as being questionable. The basis for this is that the system is quite large and bulky as has been previously described and as is shown in Figure 2.10. There are also questions about the accuracy and wearability of the tonometer in this table. The inaccuracy is highlighted in Peter's paper, where it has been noted that as the duration of use of the tonometer increases, its accuracy decreases. In a similar way, it is questionable if the tonometer can be described as being wearable because it is prone to motion artifacts, potentially making it unsuitable as a wearable device. Finally, it can be seen that the PTT method ticks the most

boxes in this table, meaning it has the most potential to be the most suitable BP measurement method. The only question marks that remain concern its accuracy. Thus far, some PTT methods and algorithms have been found to be accurate but these have not been independently validated. However, if it were possible to either prove these methods to be accurate or if a new method was developed, that was proven to be accurate, the PTT method would provide the best BP monitoring solution. This table also highlights why the oscillometric method is currently the most desirable and why it is the most used technique method by doctors and clinicians.

Table 2.3: A summary of all the BP monitoring methods discussed in this chapter

Technique	Continuous	Accurate	Wearable	Cheap
Auscultatory		✓		✓
Oscillometric		✓	✓	✓
Peñáz	✓	✓	?	
Tonometry	✓	?	?	✓
Pulse Transit Time	✓	?	✓	✓

The PTT method is still in its infancy though and there are a number of outstanding issues associated with it. Among these issues is the major problem of determining exactly how the PTT is measured and what the start and end points of the PTT are. Throughout this review, a number of different approaches have been used to define the PTT, including the distance between the peak of the R wave and the peak of the PPG wave [88] and the R wave to the foot of the PPG wave [89] among others summarised in Table 2.4 and Figure 2.8. There has also been discussion as to whether or not the PEP should be included in the measurement of PTT, with various authors saying it should [81] and others arguing against it [77]. Another characteristic of the PTT method is that regular calibration is required, as reported by Poon [74]. Ma [90] has also noted that “PTT is influenced by multi-factors, such as Cardiac Output...and other cardiovascular variables”. Regardless, BP as measured by PTT shows the most promise as a non invasive, unobtrusive BP monitoring technique given the results published thus far.

Although there have been many investigations into using the PTT method and indeed, many authors have derived their own algorithms, most authors have not stated the calibration intervals that are required. Furthermore, in some cases neither the duration of the tests nor the duration of the recording of PTT was provided. This makes comparisons between reported results difficult to perform and evaluations of the practicalities such as those that have been examined here,

Table 2.4: A summary of all the PTT definitions and other characteristic points, that have been reported in this chapter

Point of Interest	Name	r_{SBP}	r_{DBP}	Author
1	Trough	0.88	0.77	[57]
		0.65	0.25	[56] [54], [89], [59]
2	Point of Inflection	0.71	0.42	[56] [76], [61], [54], [74]
3	Peak			[14], [62], [54], [63]
4	50% of Peak	0.79		[60]
5	$\frac{2}{3}$ Pulse Width	0.32	0.38	[56]
				[59]
6	Relative Amplitude Second Peak			[76]
7	Width of $\frac{1}{2}$ Pulse Width	0.73		[60]
				[59]
8	Point of Maximum Inclination			[58]
9	Systolic Upstroke Time	0.60	0.66	[56]
				[59]
10	Diastolic Time	0.60	0.76	[56]
				[59]

also are quite difficult. However, since most authors admit that the PTT method is only accurate over short periods, a similar outcome to that of this thesis can be expected and it is suggested that other cardiac parameters may need to be included to extend the calibration intervals that would allow for accurate tracking of BP over extended periods of time.

Chapter 3

Evaluation of the Pulse Transit Time Method

3.1 Introduction

In this chapter the evaluation of the Pulse Transit Time (PTT) method and how it has been implemented in this work is discussed. The chapter begins with a discussion of the Tyndall 25mm Development Platform. This platform was used as a basis of the system that was required to make PTT measurements, starting with the hardware and then progressing from there to the middle-ware and software for data acquisition.

The next section discusses the development of the PTT acquisition algorithm and the steps that were necessary to implement it. This begins with an analysis of the electrocardiograph (ECG) waveform and the relevant characteristic points of each of its components for this project. These points were extracted and incorporated into the PTT calculation as necessary. A similar approach was taken with respect to the PPG waveform and using this, the PTT was measured.

The third section details the novel evaluation of the PTT method which would establish the maximum calibration interval that was required for the PTT method to remain accurate. Previous examinations of various algorithms typically only tested the PTT method after certain short periods e.g 1 minute. However, this examination evaluated the PTT methods across numerous intervals in an attempt to evaluate the maximum period for which the PTT remained accurate or, in other words, what was the maximum calibration interval possible from each algorithm

that would allow that algorithm to remain accurate. First an evaluation of the Moens-Korteweg equation is described followed by an evaluation of the two state of the art PTT algorithms that are used to estimate Blood Pressure (BP), which have been previously described. These algorithms were examined in an attempt to identify the key parameters and the relationships which were most important in relating BP and PTT which could later be used to establish a new algorithm.

Finally, the last section of this chapter identifies the shortcomings and limitations of the algorithms that have been developed by other authors, from both theoretical and practical perspectives.

3.2 The Tyndall 25mm Development Platform

Much of the hardware and middle-ware developed in this project are based on the Tyndall 25mm development platform [91, 92]. This platform has been designed for use as part of a Wireless Sensor Network (WSN) prototyping system and has been used in a variety of different applications, from environmental monitoring [93] to energy harvesting [94] and healthcare management [95]. An important feature of this platform is its modular design which allows the rapid development of specific systems for new application areas or research topics. Each node of this platform generally consists of a wireless communicating layer, a microcontroller, an energy source and a sensor, which are stacked on top of each other. Each layer is designed as a 25mm \times 25mm printed circuit board and layers are connected via high density connectors. Therefore, if a new research topic is being investigated, the design of only one such layer is usually required as the sensing layer.

Another benefit of the modular nature of the platform is that an extensive software library is available along with the wide range of sensors. When a new layer is designed, this software library can be modified, if necessary, to accommodate the features of the new layer. However, due to the large number of devices that have already been implemented, only minor modifications of code are usually needed when a new system is designed and this allows rapid turnaround of the prototype system. Once a prototype system has been implemented and evaluated using the modular development protocol, a custom miniaturised and optimised planar system can be developed for each specific application.

3.3 The Development of a Pulse Transit Time Measurement System

The following sections describe the system that was developed and used in the measurement of PTT in this work. The hardware developed comprises of two main components: the Physiological Health for Assisted Living (PHAL) board (which contributes the ECG system) and the Pulse Oximeter, which was used to detect the arrival of the pressure wave at the secondary location. The PHAL board was developed as part of this project and has a number of sensors, most importantly, from the perspective of this work, an ECG, to measure the initiation of the PTT measurement. The Pulse Oximeter was a part of a system developed in the WSN group and was part of the Tyndall 25mm platform family of sensor systems, and both of the BP Monitors used in this work were commercial off the shelf sensors which were purchased for this project for calibration and validation of the tests that were carried out.

3.4 Development of the Physiological Health for Assisted Living Board

The “Physiological Health for Assisted Living Board” or “PHAL Board” was designed to be used as a system dedicated to monitoring the ECG signals that were required for this project but would also allow it to be used as part of a BP monitoring system. One requirement of the system was that it should be as small as possible so that it could be worn unobtrusively. There are two reasons for this

- **Comfort** If a device is uncomfortable, a user will not wear it
- **Social Perception** It is important that any system which monitors someone’s health should be invisible and seen by the user as an enabler of well being. Otherwise, it can be perceived as an identifier of someone who is frail or sick [96].

Since this had been an issue with other previous assisted living systems, it was also desirable that the system be wireless and have a long lasting battery life. Although long battery life was a concern and it was necessary to pick the most power efficient components possible, it was felt that the biggest gains for long battery life could be achieved via duty cycling and other optimisations at a later

stage if necessary.

3.4.1 Design Specification

Although the primary focus of this board was to be used in a PTT detection system, an activity monitor was also included in the design which could also be used to identify motion artifacts. The choices for an ECG system in this type of application are discussed in detail in section 3.4.1.1. Two other components were also crucial to the build and these were the communications interface and the on board data storage facility. The requirement for communications is clear: once the data has been recorded it is important that it be transmitted so those monitoring the subject in an assisted living setting know that the subject is safe and well. The second component is the on board storage facility. This is also important in the case where live transmission of data is not possible and by having a data storage facility, no data is lost.

3.4.1.1 Electrocardiograph

The ECG sensor was identified as the key component of the PHAL board. Due to the wearable and unobtrusive requirements of the application, the minimum number of electrodes that could be used for the ECG system that would retain the accuracy and reliability would be the most desirable. The most accurate systems, which allow a clinician to diagnose cardiac problems from ECG waveforms are the twelve lead systems that are employed in hospitals. Although there are a number of systems which employ a two electrode ECG approach, it has been found that many authors recommend a three electrode system, because this allows greater accuracy. The original design of the ECG circuitry, which is shown in Figure 3.1, was based on the Tyndall designs outlined by O'Donoghue [97] and datasheets such as the Analog Devices AD620 [98], which is an instrumentation amplifier, which is commonly used as a basis for ECG systems.

One other specification that was identified by clinicians advising the project was the specification of the physical dimensions of the board. Due to the wearable nature of the board it was desirable that the board be as small as possible. Using an existing ECG system, it was found that it was possible to record an ECG signal if the patches were placed in the usual configuration, as specified by Einthoven's Triangle [12] and each electrode was at least 50 mm from each other. It was

therefore decided that the minimum dimensions of the board should be at least 50 mm × 50 mm. This would allow each electrode to be directly attached to the board and satisfy the 50mm requirement. The reason for this was that it had been noted that other ECG systems had been designed as a single patch/bandage type system. If it were possible to attach each of the three electrodes to the board and manufacture the board with a flexible PCB, a similar system to that of IMEC's [99] could be presented. It was found that by increasing the size of the board to a 50 mm × 80 mm, or a credit card sized board, the three electrodes could be attached to the board without interfering with each other, as shown in Figure 3.2, with the studs/attachments of the electrodes being placed 5mm in from the edge of the board.

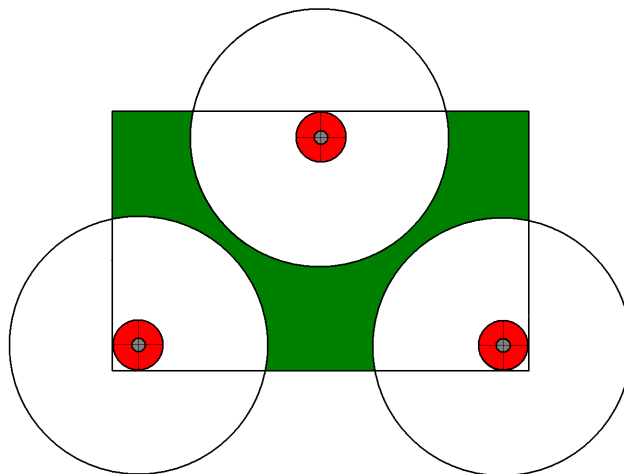


Figure 3.2: By increasing the board to 50 mm × 80 mm, the three electrodes (in white) could be attached to the board (green), using the studs on the electrodes (grey) without interfering with each other or need for modification

3.4.1.2 Communications

There are many choices when it comes to implementing wireless communications for this type of application. One of the most frequently used systems are the Zigbee or IEEE 802.15.4 based systems, because of their low power consumption and high data rate of communication. These have been used extensively for various applications developed using Tyndall 25mm system and are the most frequently used in similar body area network projects. Each of these systems is available in the library and each one exists as a stand-alone layer. By using these existing layers, design time and space required in the new system could be minimised. Other choices for communication are Bluetooth, which shares the

Table 3.1: Some of the Bluetooth options that were considered for this board

	CSR Bluecore 5	RN 21/22	RN 41	WML C46 [102]	LMX 9838 [103]
Version	v3.0	v2.1	v2.1	v2.0	v2.0
Data Rate		300Kbps	3Mbps	1.3Mbps	704kbps
Range			100m	100m	
Min. Supply Voltage	1.5V	3.0V	3.0V	2.8V	1.8V
UART Interface	✓	✓	✓	✓	✓
USB Interface	✓	✓	✓	X	X
SPI Interface	✓	X	X	X	X
I ² C Interface	✓	X	X	X	X
Transmission Current	45mA	65mA	65mA	70mA	65mA
Receive Current	45mA	35mA	35mA	70mA	65mA
Module	X	✓	✓	✓	✓

same frequency as Zigbee and IEEE 802.15.4 or another lower frequency, such as 433MHz or 868MHz, which would have greater range and be less susceptible to detrimental RF effects associated with the body. The trade off of using a lower frequency is that the data rate is much less.

However, the major advantage of using Bluetooth in this system is that it would allow it to communicate directly to a mobile phone, most of which are now Bluetooth enabled. The primary advantage of this is that it would allow the system to indirectly broadcast its data to a GP or send an alert in times of emergency. With some modification, it could also potentially allow any signal manipulation i.e. filtering, to be performed on the phone instead of onboard the system. With this in mind a number of Bluetooth chips were considered as shown in Table 3.1.

It is clear from this table that the best system would be the CSR Bluecore 5 because it had the latest version of Bluetooth at the time and provided the lowest transmission current. However, since it was not available as a module, it is far less desirable, because this would require the design and manufacture of an additional, custom antenna. The alternatives then were either the RN-21 [100] or RN-41 [101] because these provided the newer Bluetooth versions, had the next lowest transmission current consumption, the lowest overall receive current consumptions as well as an antenna built in to the module. Therefore, it was decided that the newer of the chips would be chosen i.e. the Roving Networks RN-41 Bluetooth module.

3.4.1.3 Microcontroller Choice

The choice for the Microcontroller followed much the same procedure as that of the Bluetooth module. Four microcontrollers were shortlisted after an extensive review as can be seen in Table 3.2. Two microcontrollers, the Atmel Mega 128 [104] and 1281 [105] were considered because they had been previously imple-

3. EVALUATION OF THE PULSE TRANSIT TIME METHOD

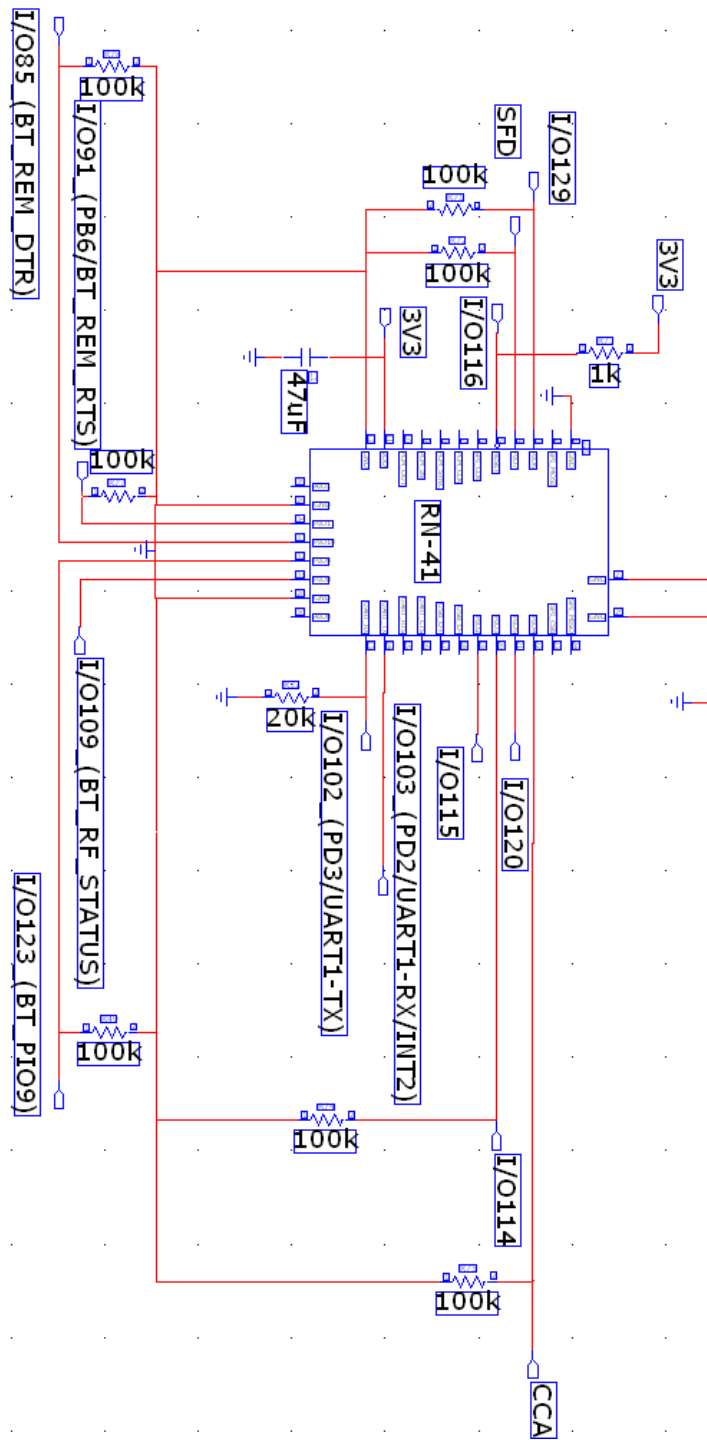


Figure 3.3: The Schematic for the Bluetooth module in the PHAL Board.

Table 3.2: Some of the Microcontroller options that were considered for this board

	Atmel 128	Atmel 1281	MSP430 [109]	XMega A1 [110]
Pin Count	64	64	100	100
Flash	128KB	128KB	128KB	128KB
ADC Resolution	10 bit	10bit	12 bit	12 bit
Min. Supply Voltage	2.7V	1.8V	1.8V	1.6V
Sleep Current	2.5 μ A	0.1 μ A	1.7 μ A	0.1 μ A
Operating Current	50 μ A	10 μ A	200 μ A	50 μ A
Size	16mm \times 16mm	16mm \times 16mm	16mm \times 16mm	16mm \times 16mm
Available Libraries	✓	✓	✗	✗

mented in designs using the Tyndall platform, the 1281 being an updated version of the 128. The other two microcontrollers were considered because they were two of the best microcontrollers that were used in similar systems and other embedded systems that had been researched [106, 107, 108]. Each of the microcontrollers had similar basic specifications although the XMega had many more features than the others. However, in a similar manner to the Bluetooth choice, it was decided that the Mega 1281 should be used for ease of compatibility with other layers in the Tyndall 25mm collection of motes and since the software libraries had already been developed and verified.

3.4.1.4 Activity Monitor

The original specification of the PHALs board was to include an activity monitor to allow the system to be incorporated into an ambient assisted living systems. This activity monitor could then be used as an activity monitor, a falls monitor and could also be used to identify any potential motion artifacts. From reading Noury [111] and Bourke [112] it became apparent that at the very least a three axis accelerometer and a three axis gyroscope would be necessary to accurately identify a fall. Therefore, an Inertial Measurement Unit (IMU) was incorporated into the design that satisfied the specifications of Noury and Bourke, but also that were in accordance to other work that was also concurrent in the group [113]. Using these three sources an accelerometer from Analog Devices (the ADXL345 [114]), two gyroscopes from Invensense (the IDG650 [115] and the ISZ650 [116]) and a tri-axis digital magnetometer from Honeywell (the HMC5843 [117]) were implemented in the design, to be used as an activity monitor.

3.4.1.5 Other Features

The PHAL Board has also incorporated the connectors available on the Tyndall mote, which would allow additional sensors and communication layers to be attached. Using the extra modules provided by the Tyndall Mote, the system is also capable of transmitting data wirelessly and incorporating different sensors depending on a given application. This allows a variety of possible wireless transceiver systems (operating in the 433MHz, 868/915MHz and 2.4GHz ISM Band) with embedded protocol software, depending on the requirements of the user.

Peripheral components

- **Storage** There were two main options for storage of the data: either an SD card or flash storage. Although flash storage has a number of advantages with respect to size and power consumption it was decided that a Secure Digital (SD) card would be preferable, because it is easier to read data from it, without needing specialised equipment.
- **Analogue to Digital Converter (ADC)** The requirements for the Analogue to Digital Converter were: at least 12 bits of resolution, 7 inputs (for the gyroscope's outputs: 3 for the 2000 deg/s outputs, 3 for the 440 deg/s and 1 for the temperature sensor output [115, 116]) and 1Mbps throughput rate to follow the previous configurations. The ADC (AD7490) [118] from Analog Devices was selected for use in the project. When all the necessary connections had been made, it was found that there were an additional 5 ADC pins that were not required for any onboard sensors. It was therefore decided to connect these extra pins to holes at the edge of the board that could be used to add new sensors at a later stage if required.
- **EEPROM** An EEPROM was added in order to separately calibrate each part of the IMU and store the corresponding calibration data. The 24AA128 from Microchip [119] was selected for this purpose because it exhibits low power consumption, has a broad voltage range and comes in a variety of package types. The chip communicates via an I^2C interface.

3.4.2 Pulse Oximeter Board

The Pulse Oximeter used in this project had originally been developed for the National Access Program [97]. The design of the Pulse Oximeter is well docu-

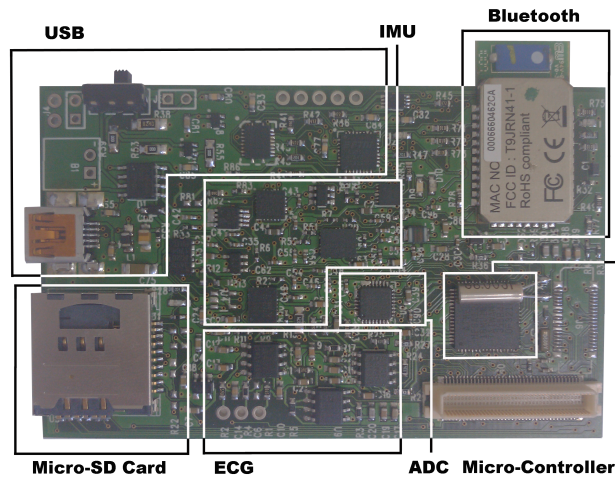


Figure 3.4: The Manufactured PHAL Board.

mented, as outlined by Allen [120]. A Pulse Oximeter is used to measure the amount of saturated oxygen in the blood. In general, two Light Emitting Diodes (LED's) are mounted within a finger cuff, one a Red LED with a wavelength about 660nm and the other a Near Infra-Red (NIR) LED with a wavelength of 940nm. Depending on the design, a photodiode can either be mounted on the same side as the LEDs (Reflective Design) or on the opposite side of the LEDs (Refractive Design). These wavelengths were chosen because *deoxygenated* hemoglobin exhibits higher absorption at 660 nm, whereas *oxygenated* hemoglobin exhibits a peak absorption at 940 nm. Once the absorption levels are detected from each, it is possible to determine the ratio of the absorption between the deoxygenated and oxygenated hemoglobin.

There are two components to this measurement: the DC component and the AC component. The DC component is comprised of the absorbance due to the tissue and bone and non-pulsatile arterial blood which remain constant. It is only the change of the amount of blood in the finger that contributes to the AC component and thus the amplitude of the signal will indicate the amount of blood within the finger. The waveform is gathered from both frequencies for both the AC and DC components and the ratio is defined as follows:

$$R = \frac{\left(\frac{AC_{RED}}{DC_{RED}}\right)}{\left(\frac{AC_{NIR}}{DC_{NIR}}\right)} \quad (3.1)$$

This ratio is then used in a calibration curve based on studies of healthy individuals to determine the SpO₂.

3. EVALUATION OF THE PULSE TRANSIT TIME METHOD

In this particular application though, it is not necessary to measure the ratio, as the sensor is only being used to detect when the BP wave arrives at the finger. Therefore, the system could be simplified and only one LED was necessary. From a practical point of view it was decided that the Red LED would be used, since it would be easier to ensure that this LED was operational during testing of individuals.



Figure 3.5: The Pulse Oximeter which had been developed as part of the Tyndall system .

3.5 Software

The software section of this chapter discusses all the software used in this project. Here the term “software” is employed in its most general sense and is used in a wide encompassing manner. The first part of this section discusses the embedded C code that is used to enable and control the hardware as described in the previous section. The next part describes the software that was used to enable the recording of the data. The software used for this data recording is National Instruments LabView [121] which was written specifically for this application so that the data could be recorded reliably without loss, while enabling the highest data rate possible. The final section discusses how the data was then exported to the data analysis software and why Matlab [122] was chosen as the post-processing tool.

3.5.1 Embedded C Code

As outlined in section 3.2, much of the code and the software libraries were part of the Tyndall WSN modular system. However, there was still some development work required to get all the sensors in this implementation to work coherently. This began by mapping all the pins of the microcontroller to each of its respective connections and writing an initialisation protocol for the board and each pin. This procedure ensured that the minimum power was used and sensors were only enabled as they were needed. From this, the enabling software for each sensor was developed and optimised so the data from each sensor could be recorded individually or all the data from every sensor data could be recorded simultaneously at a high enough sampling rate to ensure the quality of the data was not affected.

3.5.2 Data Recording / LabView

A preliminary investigation was undertaken to measure the PTT and to derive the BP from this signal. This initial investigation used data recorded from both the ECG board and Pulse Oximeter board via an oscilloscope. Given the nature of this setup, it was only possible to record the signals over a period of 20 seconds but the principle was shown to work well.

All the signals that were recorded by the oscilloscope at a 1 kHz sampling rate were saved to a *.csv* file which was then exported to an Excel spreadsheet for processing. The results of this process can be seen in Figure 3.6. Once the principle had been proven with the oscilloscope method, it was necessary to devise a more practical method of recording the data.

The initial setup included adding a Zigbee layer, from the Tyndall suite of motes, to both the PHAL board and the Pulse Oximeter board and transmitting the data recorded by both of these devices to a third Zigbee device which would act as a base station. The reason for using Zigbee, rather than Bluetooth, was that existing protocols and libraries existed for transmitting data from two nodes to a base station using Zigbee, whereas this had not been previously done using Bluetooth within the WSN Team and this setup was more complex to implement using Bluetooth.

However, there were concerns that by using wireless communications of any kind, the data could be susceptible to small delays due to synchronisation errors. Given the small times associated with the PTT measurement of approximately 150 -

3. EVALUATION OF THE PULSE TRANSIT TIME METHOD

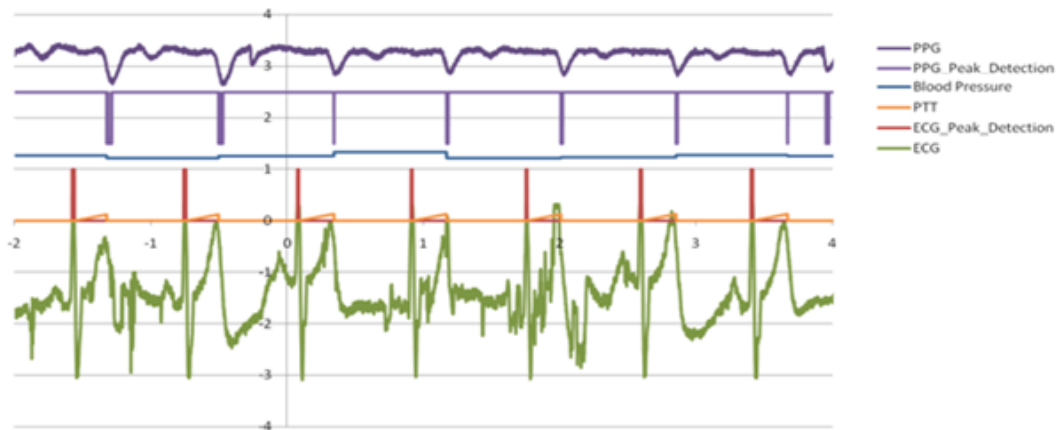


Figure 3.6: The data recorded from the oscilloscope was analysed and plotted using Excel.

200 ms, and the possible effect that slight delays could have on the outcome, this could have a significant impact on the results. Since this investigation was focused on evaluating the PTT method and its associated algorithms, rather than the evaluation of the PTT method as part of a WSN, it was felt that any potential sources of error, from anything other than the algorithms should be removed and so a wired serial communication method was used as it is the most reliable and accurate communications method for this type of application. To enable this methodology, a wire was connected from the output of the Pulse Oximeter to one of the extra ADC inputs of the AD7490 that was used on the PHAL board. Since the ECG was also sampled using this ADC, this meant both signals were digitized in exactly the same way, removing any possible delay errors. The PHAL board was then connected directly to a PC via a USB cable. Although this ensured no loss of data due to synchronisation errors, there were still a number of issues to be addressed for reliable data recording, as will be explained in the next section.

The next step in the process was to decide how the data would be recorded into a file that could be used to process the data at a later stage. One possible solution was to use LabView to record the data. Due to the serial connection between the sensors and the PC it would also be possible to display the data as it was being recorded, ensuring any errors could be flagged and addressed immediately. LabView can also be used to record data into Microsoft Excel files with relative ease and since some preliminary work had already been done in Excel including some post-processing of data, it was decided to record the data to an Excel file while maintaining a high sampling rate.

3.5.2.1 Data Pre-Processing

Once it had been established that LabView could be used to write data to Excel sheets, the data from both ECG and PPG sensors were written to an Excel sheet and reconstructed for post processing. During this post-processing it was observed that parts of the signals seemed to be missing when the signals were reconstructed. In an attempt to verify that data was actually missing, a counter was implemented on the micro-controller that would continuously count up and down for the duration of the test. The result of this count function was then plotted and, provided no data was being lost, a perfectly periodic triangular wave should appear. If data was lost, it would then be obvious and easy to identify where this loss took place. An analysis of these triangular waveforms revealed that data was indeed being lost, even when only two minutes of data was being recorded. Figure 3.7 shows an example of this. At every point where there is a sudden jump in data values, if there is a gap or if there is any place on the graph that does not show an evenly rising or falling line, data has been lost.

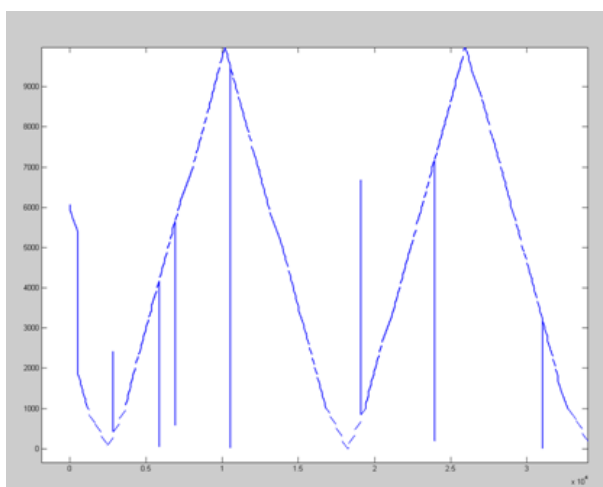


Figure 3.7: A counter was used to identify locations of data loss in the recorded signals. Anywhere that the graph is uneven or if there are gaps in the data, some data has been lost.

After examining the data, it was found that the data was being lost in a semi-periodic manner. The hardware was investigated first and data was transmitted to a PC, without using LabView and plotted but no data loss was observed. It was therefore evident that the problem was associated with LabView and its recording process. Investigations showed that this was a known issue when trying to write large amounts of data at a high sampling rate. Due to the high sampling rate of the hardware, it was found that the buffer in LabView which was used to

write the data to a spreadsheet, would periodically fill up, and dump the excess data and then start recording fresh data again.

The solution of this was to write to a *.csv* file (a comma separated value file), since it contained less overhead than an Excel file, but the same issue was found. Alternative formats were examined and it was established that if data was recorded to a binary file, no data loss occurred and it was also possible to record at an even higher sampling rate of up to 650 samples per second from each of the two sensors, although it had been estimated a sampling rate of 400 samples per second would have been adequate. Once all the data had been recorded to a binary file, a second LabView program translated the data from the binary format and wrote the data to a *.csv* for data processing.

3.5.3 Post-Processing and Matlab Code Development

From the literature it is evident that much of the signal quality attributed to ECGs are due to the incorporation of hardware [123] and software filters. By using tools such as Matlab [122] and Mathematica [124], it is possible to achieve a similar signal quality as those found in commercial solutions. Using either of these tools, the data that was required for this application could be processed much faster than the tools available in Excel. It was also found that both tools had extensive filters that could be used to smooth the signals in an adaptive manner rather than by using predetermined filters in an hardware application. An example of a moving average filter defined in Matlab can be seen in Figure 3.8. Of these tools, it was found that Matlab was generally faster and seemed to have a lot more useful functions and was therefore chosen as the tool that would be used for all post-processing. It was also discovered at a much later date that Matlab could have been used to directly record the data. However, since so much data had been recorded using the LabView method and the subsequent testing of this data had taken place and was published, there was a concern about consistency of test protocols. It was felt that by changing the testing procedures, subsequent tests may have some influence on the data and this new data could not be directly compared to those previous tests.

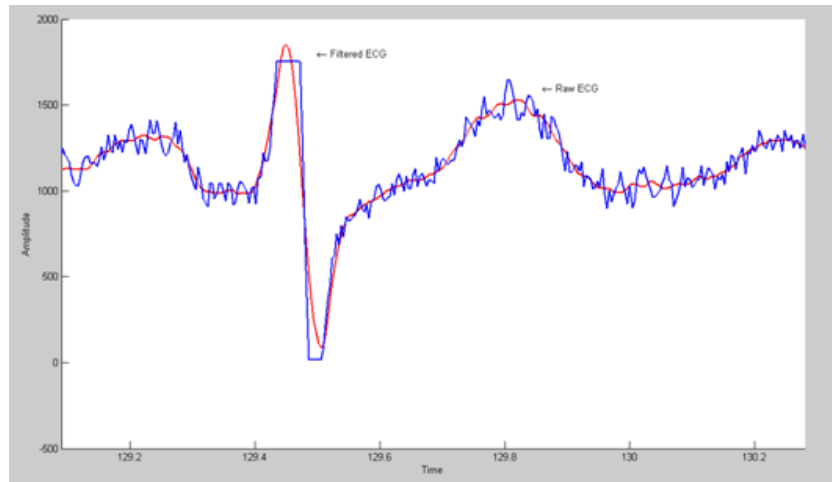


Figure 3.8: A Moving Average Filter of 31 terms (red) implemented in Matlab on a noisy ECG Signal (blue)

3.6 Pulse Transit Time Calculation

As reported in Chapter 2, many authors have reported different methods for measuring and defining PTT. However, there is a general consensus that the peak of the R wave of the ECG should be used as the initiation point for the measurement. The difference in the definition of PTT relates to the PPG wave. Most authors have defined the PTT as being measured from one of three locations on the PPG wave: the peak, the onset of the PPG wave, or the point of maximum inflection. The following subsections describe the steps necessary to identify each of these locations, using code written and developed using Matlab.

3.6.1 ECG R Wave Detection

One of the most critical points that needs to be identified as part of a PTT measurement is the peak of the R wave. The first stage in detecting R waves from the ECG signal is to implement a DC rejection filter as can be seen in Figure 3.9. This DC rejection filter removes the baseline wander (a known occurrence where a DC component is introduced to the ECG signal over time) and some other artifacts that are of an ECG signal. Although baseline wander is responsible for some of the distortion of the ECG signal, much of the amplitude variation of the QRS waves in Figure 3.9 is compounded by motion artifacts from the volunteer (seen here as saturation of the signal). The filtered signal removes and minimises the effect of both but also causes a reduction in the amplitude of the signal.

3. EVALUATION OF THE PULSE TRANSIT TIME METHOD

As is apparent from Figure 3.9, a simple threshold based algorithm would not be sufficient to detect R waves, even if a DC rejection filter has already been implemented. The red line here represents the minimum height that would be required to detect all R peaks in this window. If this threshold was used, many other peaks in the ECG signal could also be misidentified as being R peaks. Therefore a more detailed algorithm is required to detect the R peaks.

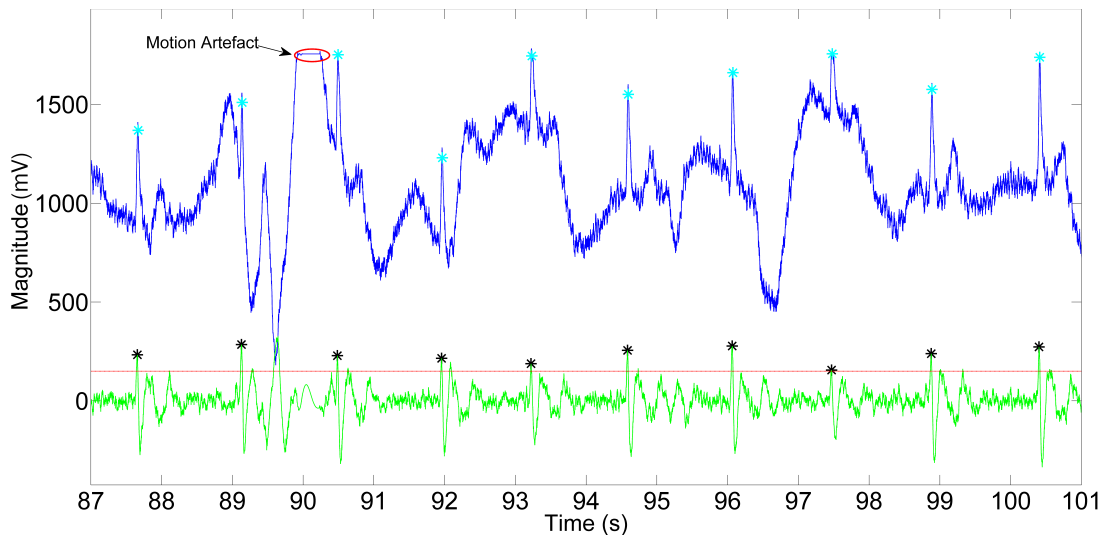


Figure 3.9: The result of a DC rejection filter (in green) on the raw ECG signal seen in blue. It is also apparent that a simple threshold based algorithm would not be sufficient to detect R peaks.

One of the characteristics of the ECG R wave is that, following the R wave, the signal has a quick transition from its value to the S peak, milliseconds later. This characteristic is rarely observed elsewhere in the signal even in the presence of motion artifacts as illustrated by Figure 3.10 which focuses on the filtered signal from Figure 3.9. To detect an R wave the following procedure was applied

- All peaks above a certain threshold (green line) were identified and characterised as being potential R peaks (green stars)
- All troughs below a certain threshold (blue line) were identified and characterised as being potential S “peaks” (blue stars)
- If there was a rapid enough transition between a potential R peak and a potential S “peak”, the potential R peak was determined to be an R peak (black stars)
- Once an R peak had been identified, all other potential R peaks were ignored over a certain window, or exclusion zone, to ensure artifacts could not be misidentified as being R peaks

The window/exclusion zone described above is shown in Figure 3.10 as the black dotted line, and was identified by assuming no volunteers had a resting heart rate higher than 150 beats per minute or one beat every $\frac{60}{150} = 0.40$ seconds. Therefore, once an R wave had been identified, no other peaks were examined for the next 0.40 seconds i.e. in Figure 3.10, none of the potential R (or S) peaks in the 89-90 second exclusion zone were examined once the R wave had been identified. Using this procedure, the motion artefact in Figure 3.10 is not identified as an R peak because, although it is outside the exclusion window, the transition from potential R peak to S peak is too large.

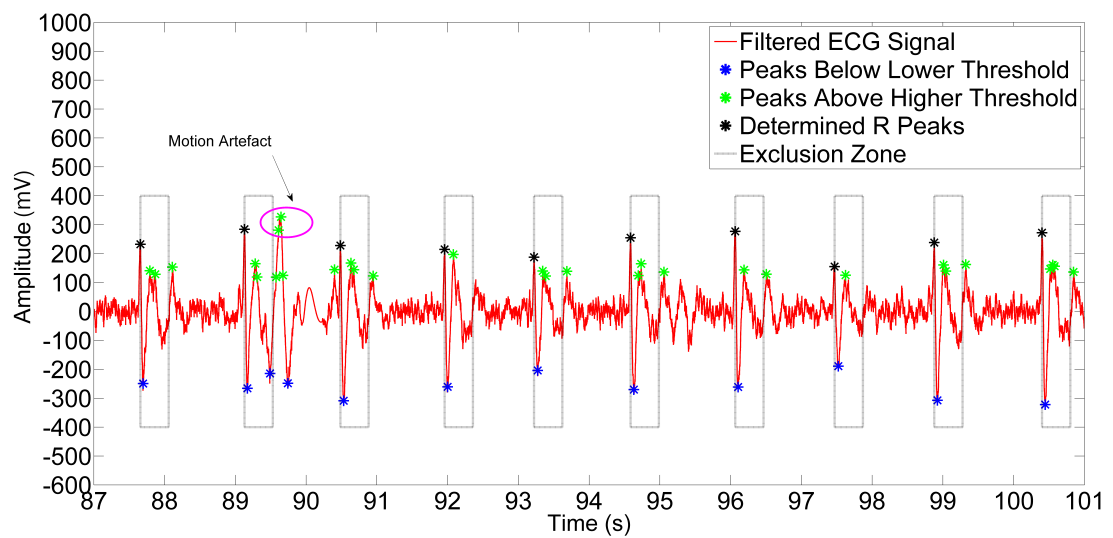


Figure 3.10: The various thresholds, windows and other components used to detect an ECG R wave.

3.6.2 PPG Wave Characteristic Points Detection

For the evaluation of the PTT methods, PTT was measured from the peak of the ECG R Wave to the peak of the PPG signal, because it was found to be the easiest to identify and provided the most reliable measurement, especially in the presence of noise and artifacts. It was found that by using a threshold based system of the PPG signal, the peak of the PPG signals could be correctly identified and therefore used as in the measurement of PTT. This threshold based system used a percentage of the maximum height to identify all major peaks of the signal (since no baseline drift was observed in this signal) and the same minimum distance between peaks that had been used in the ECG R detection algorithms was specified so only the peaks of PPG signals would be used in the PTT measurement, in a way that is similar to the exclusion zone seen in Figure

3.10 in relation to the ECG wave and R peak detection. An example of this can be seen in Figure 3.11.

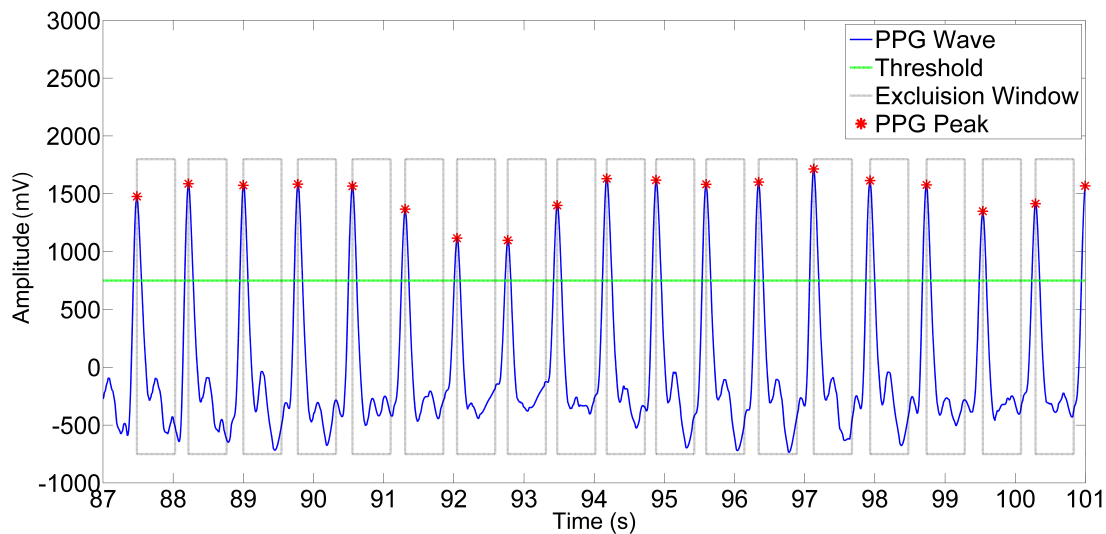


Figure 3.11: The use of a minimum threshold and an exclusion window was found to be sufficient to detect a PPG Peak.

3.7 Testing the Pulse Transit Time Method

3.7.1 Introduction: Preliminary Testing

Prior to the commencement of the evaluation tests of the PTT method, it was necessary to ensure that all the signals were sufficiently noise - and artefact - free and the characteristic points of all signals were easily identifiable. This would ensure that the methodology would provide representative results and give an accurate evaluation of the technique. The first part of this process was to ensure that both the ECG and Pulse Oximeter sensors gave signals of sufficient quality across a number of individuals. Three individuals agreed to provide 5 minutes of sample data each before the full test would be undertaken.

3.7.2 Sensor Optimisation

3.7.2.1 Pulse Oximeter

During the preliminary research for this round of testing, it was found that a number of precautions were identified as being necessary to acquire a good signal

from the Pulse Oximeter/PPG sensor. One of the most critical of these was to ensure that no one who was being tested was wearing nail polish during the test as it would distort the signal and introduce errors due to distortion of the reflected signal. It was also noted that the PPG sensor is very susceptible to motion and light artifacts. Therefore, it was important that all people under test would keep their hand still throughout the test and that there was no chance of light shining into the sensor during measurement

3.7.2.2 ECG Testing - Electrode Placement

While testing the ECG system during the preliminary testing it was found that in some volunteers, using the traditional electrode placement i.e. Einthoven's Triangle, as outlined by Bernston [12], gave a signal, where the T wave was much larger than the R wave. After consulting with the clinical advisory team, it was found that this was not an unknown or unusual problem, the solution to which was to move the electrodes. After some experimentation it was found that by moving one of the electrodes it was possible to recover the typical ECG signal as can be seen in figure 3.12. This is also known as Modified Central Lead (MCL_1) [125].

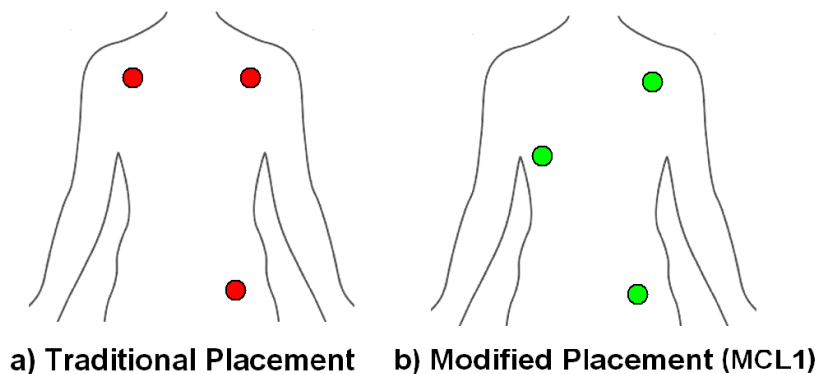


Figure 3.12: An example of the traditional and modified ECG electrode placement used throughout testing

3.8 Evaluating the PTT Method - Round 1 of Testing

Once the experimental set up as described in the previous sections had been put in place, it was possible to begin the first round of testing and evaluating the PTT

method. This round of testing was an attempt to recreate some of the results that had been seen in literature and to test the validity of the concept using a simple BP monitor: the Sanitas SBM30. The testing methodology was defined using Pickerings recommendations [6] as a basis for BP measurement. The exact procedure that was followed for this test and all subsequent tests is outlined in Appendix D. Six volunteers were chosen for the test. This was validated by the advisory team who recommended using four male and two female subjects. Each volunteer was then subjected to the same test, under the same conditions where possible. The test setup and procedure was as follows:

- Each subject rested for 5 minutes prior to each test
- The ECG electrodes were placed in accordance with Einthoven's Triangle where possible: One under each collarbone and one on the right hand side as seen in Figure 3.12a)
- The Pulse Oximeter was placed on the middle finger of the left hand
- The inflatable cuff was placed on the upper left arm, 2 -3 cm above the bend in the elbow
- A BP measurement from the Sanitas device was taken every 5 minutes (this was the minimum allowed time from its manual)
- This BP reading was used as an initiation point or a calibration point for the PTT method
- The ECG and PPG was continuously recorded for the duration of the test which was 15 minutes.

Due to assumptions made by Moens-Korteweg in relating PTT to BP, the relationship is only said to be valid over short periods of time, after which a recalibration is required i.e. a new cuff measurement has to be taken to realign or recalibrate the PTT method. This was discussed as being one of the major limitations of the state of the art. One of the most critical features, therefore, that should be examined when evaluating the PTT method is the calibration interval which is defined as the time between the initial BP measurement (defined as SBP_0 or DBP_0 by Poon [75] or P_b by Chen [14]) and the subsequent BP measurement that is required to recalibrate the PTT method. In this case, because of the limitation of the BP monitor the minimum calibration interval was 5 minutes i.e. an initial BP cuff measurement was taken, the PTT was used to track changes of BP for 5 minutes, after which another BP cuff measurement

was used to recalibrate the PTT and continue this cycle. However, if the method was found to be accurate, a longer calibration interval could be used, meaning less cuff measurements would be required. Therefore, the usefulness of the PTT method should not only be defined by the ability of the method to track BP but how long is required between subsequent BP measurements that allow the method to remain accurate.

Although six volunteers were initially measured, only five managed to complete the test, as one had a panic attack during their test. It was also discovered that one of the other volunteers was a diabetic and hypotensive, although this did not adversely affect the results for this volunteer. Finally, one other patient was found to have a high T-wave which caused some problems for the algorithm to distinguish between it and the R wave of this patient. Upon inspection of the data files for each volunteer, it was found that the algorithm that had been developed had failed to detect a number of ECG and PPG peaks which resulted in poor results. Also due to the small number of tests performed it was difficult to draw any definitive conclusions with regards the value of the PTT method. However, each of these highlighted issues identified valuable information that would be required for future testing.

3.8.1 Required Improvements for Subsequent Testing

A number of lessons were learned from the testing in “Round 1” which meant optimisation of the experimental protocol were required for “Round 2”. A more detailed list of the required improvements is discussed in Appendix D.

The first change was to choose 6 Volunteers who would be able to complete the testing and they should undergo an initial trial to test for any ECG signal abnormalities. Under this process, one volunteer was eliminated due to the fact that they had a very small R wave. The testing procedure was adjusted so that a second female was added to the group.

Further changes included each volunteer being tested for half an hour and each of the sensors was also packaged prior to the testing. Most importantly, the Sanitas BP Monitor was replaced by a top of the range BP monitor, the Omron M6. This is shown in Figure 3.13 and was used because of its compliance with the standards [126] and could be considered a gold standard for comparative purposes.



Figure 3.13: The Omron M6 Oscillometric BP Monitor [26].

3.9 Evaluating the PTT Method - Round 2 of Testing

During this round of testing, PTT was directly evaluated using Chen's interpretation of the Moens-Korteweg equations to relate PTT directly to BP only. Six volunteers were chosen for this test, four males and two females all between 24 and 28 years old. ECG data was recorded from the PHAL board and Pulse Oximeter data was recorded from the device directly to the PC, as described in section 3.4.2. PTT was defined as the time between the ECG R wave and the peak of the Pulse Oximeter wave. Each test was recorded for 30 minutes between the times of 2.00 PM and 4.30PM in a quiet environment at 20°C. The volunteers were asked to refrain from smoking and ingesting caffeine or any other BP altering drugs in the hours prior to the test, as per the recommendations for all BP measurements [6]. The Omron M6 was worn on the upper left arm and was used to recalibrate the estimated BP at five minute intervals. The Pulse Oximeter was worn on the index finger of the right hand, so as to be unaffected by the inflation and deflation of the cuff. The data was then post-processed using Matlab, which filtered and extracted the points and data of interest according to the algorithms developed and described in section 3.6.

The results of this test can be seen in Table 3.3 [127]. The PTT method was evaluated using the AAMI standard. When using a 5 minute calibration interval i.e. one BP reading every 5 minutes with each measurement also being used to evaluate the prediction, the PTT method was found to be accurate for every volunteer and adhered to the AAMI standards. As can be seen in Table 3.3, it

Table 3.3: The results of “Round 2” testing to evaluate the PTT method

Volunteer	Estimated Error of Systolic BP (mmHg)
1	1.81 ± 4.39
2	-0.82 ± 3.69
3	-1.34 ± 7.93
4	-1.44 ± 5.71
5	-2.57 ± 6.23
6	-0.53 ± 3.70

is apparent that some volunteers provided a lower mean and standard deviation than others, indicating that the PTT suits some people more than others. The reason for this seemed obvious for at least one volunteer, volunteer 3 who had been found to be diabetic and hypotensive in “Round 1”, who was included to provide a greater range of people tested. It was also noted that Volunteers 4 and 5 had a noisy signal with respect to the results recorded from the Pulse Oximeter due to motion artifacts. By using Matlab it was possible to remove some of these artifacts but it was not possible to remove them entirely. Therefore, given the similar age, fitness and general health of the remaining volunteers it was unclear what were the reasons for the discrepancies of the results between individuals, although the low number of volunteers could be the problem. However, since there are so many factors which can affect blood pressure, there are only so many precautions that can be undertaken prior to a BP reading being recorded, especially when volunteers are being used, rather than patients who can be controlled or people who are being paid. For example, although the tests were recorded in a noise free and temperature controlled environment, it is not possible to evaluate a person’s mental state during these tests.

Although, each of the volunteers claimed good general health and that they had refrained from blood pressure altering activities prior to the tests but none of these claims could be substantiated without employing a more rigorous controlled environment, something which was not feasible for these tests.

Although these results were promising because they all adhered to the AAMI standards having a mean less than 5 mmHg and standard deviation less than 8 mmHg, it was clear that a more thorough investigation was required. The first decision was that in order to minimise the impact of the variability of the subjects a larger number of subjects should be examined. Also each subject should be tested numerous times and perhaps each test should have a longer duration. Furthermore, the granularity of the investigation should be increased by measuring the BP more frequently to find the point at which the PTT first

failed or exceeded the AAMI standards. It was also decided that instead of solely examining the PTT, other algorithms which related PTT to BP should be studied. These algorithms are described in literature and have been widely published but the calibration intervals that are required for them to remain accurate or their ability to track BP has never been established to date. Although many authors report that their methods and algorithms show a strong relationship between BP and PTT, most have only been evaluated over very short periods of time, typically less than 2 minute intervals and frequently with a few minutes between PTT measurements. In these cases, a break in testing occurred so the patient could exercise before the test resumed and the impact of exercise on BP and PTT could be observed [56, 61, 62]. Although well intentioned and valuable to a degree, it meant that a non-continuous measurement of PTT and BP was recorded and the duration of accuracy or the role of the calibration interval was never investigated. Therefore, it was decided to test two of the most cited algorithms, to evaluate which provided the best results, in terms of tracking BP and also for which algorithm allowed for the longest calibration interval.

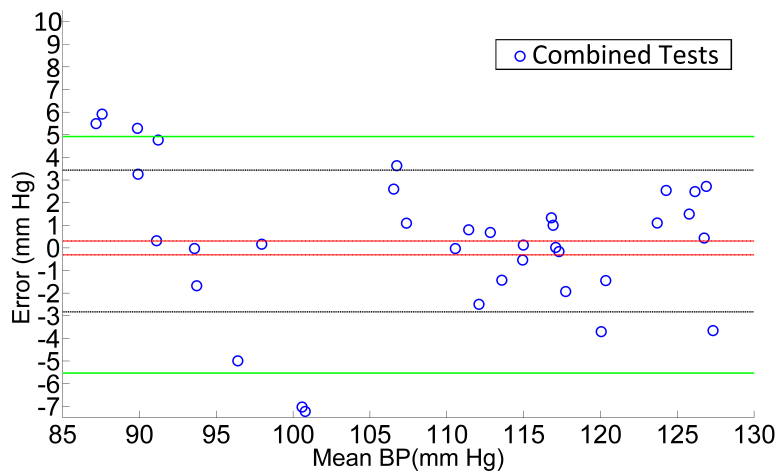
3.10 Evaluating the PTT Method Using Two Different PTT Algorithms - Round 3 of Testing

From section 3.9, it became apparent that a larger number of volunteers was required for testing the PTT method so as to ensure that any results would be statistically significant. The number of volunteers was originally increased from six to ten (this was subsequently further increased to fifteen based on the recommendations of the reviewers of the paper that was published based on the results of these tests [128]). Two algorithms were identified in the literature as discussed in section 2.7, namely Chen's algorithm [14] and Poon's algorithm [75], for an evaluation of the PTT method rather than examining the Moens-Korteweg equation. These two algorithms were chosen because they are two of the most cited works in the PTT area. Finally, it was decided that each algorithm would be evaluated at two minute intervals, so that a more precise calibration interval could be determined. The figure of two minutes was chosen as a function of the Omron M6 BP monitor, which under normal circumstances would take 45 seconds to take a measurement, but occasionally would need a second inflation which could

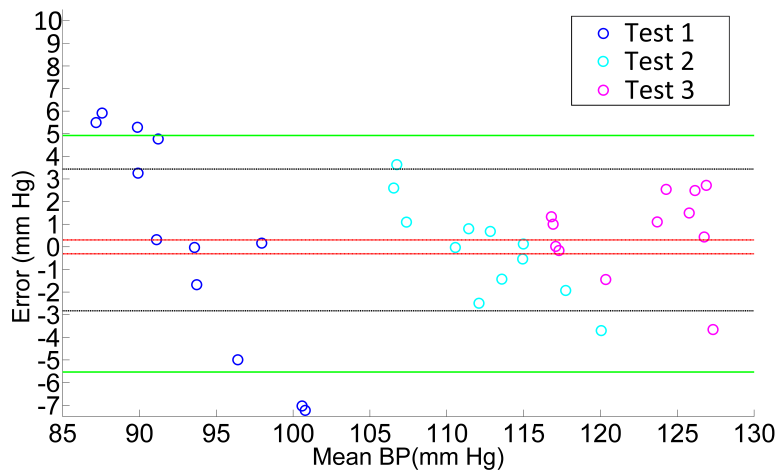
double the measurement time to one and a half minutes. The occurrence of these incidents is rare, however, since a test to identify the calibration intervals over which various PTT algorithms remain accurate had never been previously investigated, testing using one BP measurement every two minutes over the 30 minute test was deemed to be satisfactory, even if it was found to cause some discomfort for some of the volunteers at this interval due to the constant inflation and deflation of the cuff. The second part of evaluation of these algorithms was to investigate how well each one was able to track the BP i.e. if a large change in BP was found during the tests, would either algorithm be able to track this change. Both of these criteria will be discussed in the following sections.

Another statistical analysis tool was also used in this round of testing, the Bland Altman graph [129], which presents results in a graphical manner and allows the data to be presented in line with other works in the area. A Bland Altman graph is used to compare the measurement and accuracy of experimental measurements from the two methods, neither of which are the gold standard. This graphing technique is common in the area of BP monitor evaluations. In a Bland Altman graph the difference, or error, between the two methods is plotted against the mean result obtained of the two methods. An example of a Bland Altman graph used to assess the BP derived from PTT algorithms against a BP monitor is shown in Figure 3.14a and shows good agreement between the two methods. The red lines of this graph show the mean error, the black lines show the error \pm the standard deviation and the green lines show the 90% confidence intervals. The close agreement between the two methods can be determined in Figure 3.14a because the error is small when compared to the mean. More specifically, for the area of BP monitoring, the good agreement can be seen since most of the errors are less than 5 mmHg, a key figure in both the AAMI standard and BHS standard. The standard deviation in this graph is also seen to be less than 4 mmHg, which is well within the 8 mmHg specified by the AAMI standard. Finally, all the errors displayed here are less than 10 mmHg indicating a very good agreement from the perspective of the BHS standard. This is emphasised by the 95% confidence intervals being less than 8 mmHg, but these lines are not always displayed. Although there is a large spread of values across the *x-axis*, this is due to the fact that the results from three different individuals are shown in this example, each individual having a different mean BP. The individual breakdown can be seen in Figure 3.14b.

3. EVALUATION OF THE PULSE TRANSIT TIME METHOD



(a) The Bland Altman Graph of three different individuals, without being distinguished



(b) The Bland Altman Graph specifying which data points are from each individual

Figure 3.14: An example of the Bland Altman Graph used in the analysis of the accuracy of the PTT method

3.10.1 Evaluating Chen’s Algorithm

Chen’s method was evaluated using the system described in section 3.3 to confirm his findings and to establish the maximum calibration interval that could be used for his method to remain reliable and accurate.

Table 3.4 shows the results of using Chen’s algorithm to track BP over each calibration interval, presented in the format used in the AAMI standard. This determines that the test “device” (PTT) must not differ from the standard (the Omron M6) by a mean difference of less than 5 mmHg or a standard deviation greater than or equal to 8 mmHg. The last row presents the accumulated results

Table 3.4: A summary of the results from testing Chen’s algorithm from each volunteer. Each result represents the mean error \pm the standard deviation of error between the Estimated BP, given by the PTT method, and Measured BP given by the Omron M6

<i>Volunteer</i>	<i>2 Minute Interval</i>	<i>4 Minute Interval</i>	<i>6 Minute Interval</i>	<i>8 Minute Interval</i>	<i>10 Minute Interval</i>	<i>12 Minute Interval</i>
1	0.59 \pm 0.89	0.03 \pm 0.09	1.13 \pm 0.78	6.79 \pm 3.94	4.19 \pm 9.88	-47.32 \pm 9.31
2	0.62 \pm 0.73	0.02 \pm 0.02	1.02 \pm 0.55	6.73 \pm 4.15	5.99 \pm 6.14	-46.09 \pm 13.08
3	1.02 \pm 2.16	0.04 \pm 0.07	1.05 \pm 1.01	5.39 \pm 4.93	5.54 \pm 10.06	-31.92 \pm 26.24
4	0.68 \pm 1.83	0.03 \pm 0.05	0.06 \pm 0.92	4.88 \pm 6.25	10.25 \pm 7.96	-3.47 \pm 35.02
5	0.69 \pm 2.26	0.04 \pm 0.14	0.89 \pm 1.21	3.61 \pm 4.84	2.08 \pm 17.07	-20.24 \pm 32.07
6	0.51 \pm 0.64	0.04 \pm 0.05	0.85 \pm 0.82	5.41 \pm 3.64	5.14 \pm 10.24	-34.18 \pm 31.86
7	0.79 \pm 0.16	0.05 \pm 0.11	1.19 \pm 1.13	5.48 \pm 4.95	-0.87 \pm 20.65	-33.97 \pm 20.99
8	0.94 \pm 2.68	0.04 \pm 0.09	2.17 \pm 8.31	7.30 \pm 10.64	4.59 \pm 11.28	-26.04 \pm 25.21
9	0.40 \pm 0.27	0.02 \pm 0.02	0.92 \pm 0.39	6.74 \pm 3.07	7.29 \pm 4.27	-45.96 \pm 6.38
10	0.31 \pm 0.58	0.03 \pm 0.04	0.68 \pm 1.78	4.60 \pm 5.74	8.88 \pm 4.12	-16.33 \pm 40.61
11	0.54 \pm 0.54	0.03 \pm 0.03	1.03 \pm 1.12	8.97 \pm 11.49	11.77 \pm 7.99	-34.68 \pm 30.43
12	0.45 \pm 0.45	0.02 \pm 0.02	0.82 \pm 0.38	5.85 \pm 4.92	9.17 \pm 4.58	-35.50 \pm 18.23
13	0.38 \pm 0.44	0.03 \pm 0.04	0.51 \pm 0.66	5.61 \pm 4.05	12.97 \pm 10.78	-10.27 \pm 36.92
14	0.68 \pm 1.55	0.03 \pm 0.07	0.94 \pm 0.76	6.72 \pm 6.71	8.79 \pm 8.44	-43.05 \pm 22.29
15	1.03 \pm 3.02	0.04 \pm 0.07	1.10 \pm 0.87	6.31 \pm 4.14	5.19 \pm 9.77	-45.48 \pm 13.65
Overall	0.64 \pm 1.55	0.03 \pm 0.07	0.99 \pm 2.35	6.02 \pm 6.12	6.81 \pm 10.85	-3.42 \pm 29.22

across all volunteers.

Table 3.4 shows the results of using Chen’s algorithm to track BP over each calibration interval, presented in the format used in the AAMI standard. This determines that the test “device” (PTT) must not differ from the standard (the Omron M6) by a mean difference of less than 5 mmHg or a standard deviation greater than or equal to 8 mmHg. The last row presents the accumulated results across all volunteers.

Examining the last row of Table 3.4 it can be seen the algorithm exceeds the standard after the 6 minute calibration interval. Looking at the calibration intervals greater than 8 minutes it can be seen that the results degrade rapidly after this point. The reason for this degradation lies with the filter associated with High Frequency Component (HFC) of Chen’s method, which employs a bandpass filter (between 5.3×10^{-4} Hz and 4×10^{-3} Hz, using a 5 minute calibration interval, but the lower value (F_L) varies depending on what calibration interval that is used, defined by $F_L = \frac{1}{2\pi} \times (CalibrationInterval)$) on all the PTT data recorded.

In Chen’s paper, a 5 minute calibration interval is used. Chen found that when the filter that is described in his paper is applied to the PTT using this calibration interval, there is a direct linear relationship between this filtered PTT and BP. However, the origin of this filter is unclear. In Table 3.4 it can be seen that when a 4 minute calibration interval is applied, the algorithm performs exceedingly well.

One possible reason for this performance is that the filter is tuned specifically for performance at 5 minutes and as the calibration interval approaches 5 minutes, its performance is enhanced.

Over the first two/three intervals, the effect of the bandpass filter has a minor role in the results and the Low Frequency Component (LFC) was the major contributor to the results. When the PTT data is filtered, the resulting HFC component becomes what is essentially a straight, horizontal line with a variation of less than 3mmHg over the course of the test. In the case of the 4 minute interval, this variation is even further reduced to approximately 0.15 mmHg, because of its proximity to the linear relationship that had been established using a 5 minute calibration interval. However, as the calibration interval grows and the appropriate changes were accordingly made to the filter i.e as F_L was updated per calibration interval, the effect of the filter on the data changed significantly. At the times when the calibration interval was shorter, the filter caused the data to change only by 1 - 3 mmHg over the interval, up to and including when the 6 minute calibration interval is applied.

When a calibration interval of greater than 6 minutes is used, the filter causes an even greater change over the course of the test and this is reflected in the results in Table 3.4 and in the Bland Altman graphs Figure 3.15, d) - f). A similar degradation can be seen in the data from examining the BHS standard in Table 3.5. Using the BHS standard, it is in many ways easier to see how the effect of the filter changes, with 100% of the results being less than 5mmHg when using a 2 minute calibration interval, while in the 8 minute calibration interval, this has fallen to 29.04%. During the 6 minute calibration, where Chen's algorithm passes both standards, a linear relationship has been found with $r = 0.96$ and an $r^2 = 0.98$.

Although these results show that Chen's method is very good at tracking BP up to 6 minutes, there are some concerns with relation to this method. These are explained as follows:

It has been noted when using Chen's method, that due to the filtering, the estimated BP doesn't change much from the initial BP measurement, when using a small calibration interval, (i.e. when a calibration interval of less than 6 minutes is used), the filtered PTT data (or the HFC) is essentially a straight, horizontal line. Indeed, it can be seen that no matter what change is recorded using the cuff, the shape of the Chen's estimation remains constant, as illustrated in Figure 3.16a where a six minute calibration interval is used. In this figure the

3.10 Evaluating the PTT Method Using Two Different PTT Algorithms - Round 3 of Testing

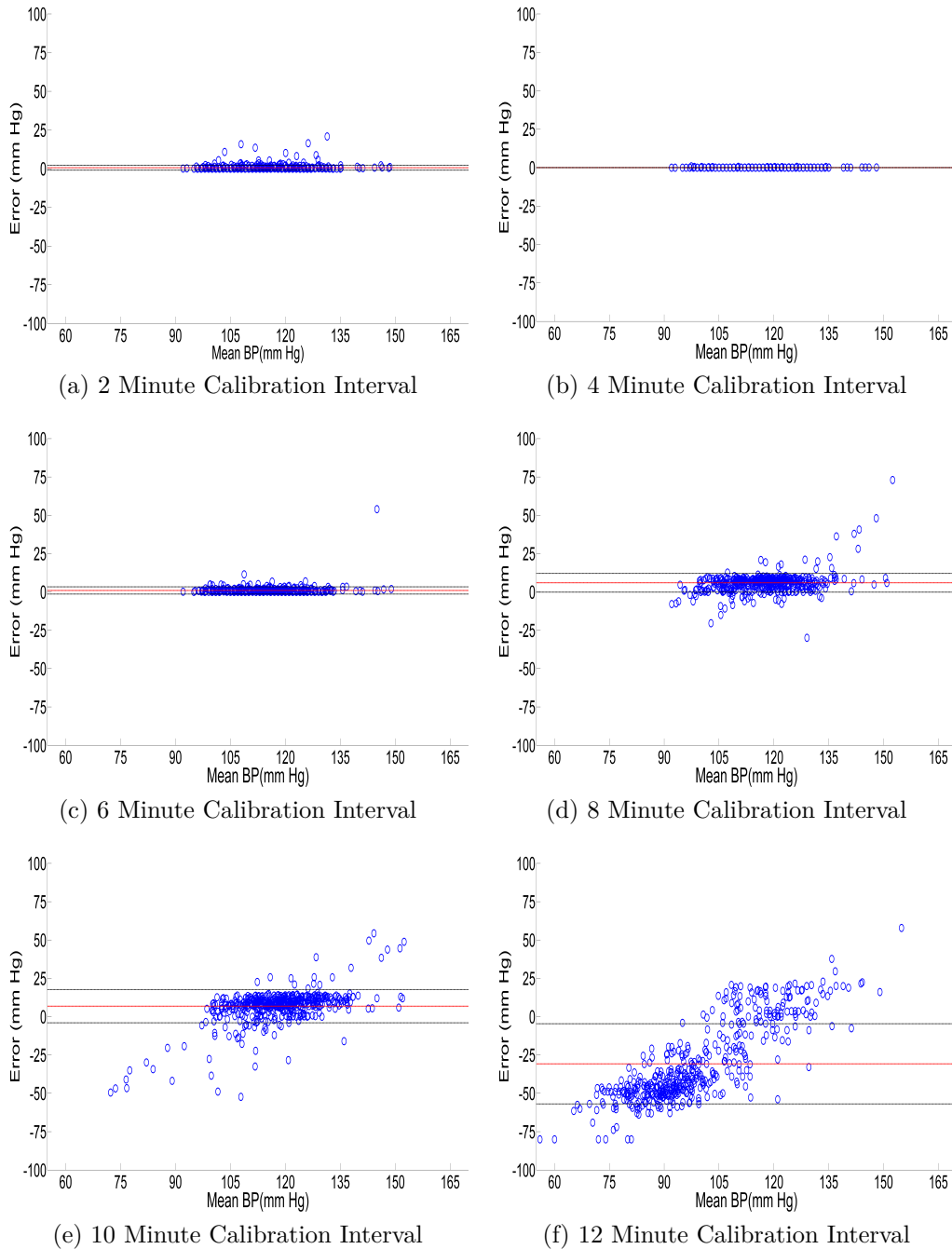


Figure 3.15: Using the Bland Altman graphs and Table 3.4 to analyse Chen's algorithm, a deterioration of the results in each subsequent calibration interval can be seen by the growing error and standard deviation (black).

3. EVALUATION OF THE PULSE TRANSIT TIME METHOD

Table 3.5: A summary of the results using percentage predicted values falling within 5, 10 and 15 mmHg, based on the BHS system for assessing BP measurement accuracy. Each calibration interval is assessed using this method and the associated BHS standard is provided in the last column. A rating of “B” is deemed acceptable, while a rating of “C” is deemed a fail.

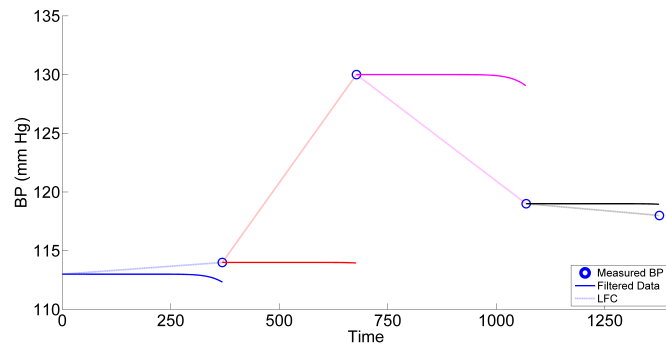
Volunteer	2 Minute Interval				4 Minute Interval				6 Minute Interval			
	5 mmHg	10 mmHg	15 mmHg	Grade	5 mmHg	10 mmHg	15 mmHg	Grade	5 mmHg	10 mmHg	15 mmHg	Grade
1	97.67 %	100 %	100 %	A	100 %	100 %	100 %	A	97.30 %	100 %	100 %	A
2	100 %	100 %	100 %	A	100 %	100 %	100 %	A	100 %	100 %	100 %	A
3	93.75 %	97.92 %	100 %	A	100 %	100 %	100 %	A	97.62 %	100 %	100 %	A
4	95.83 %	97.92 %	100 %	A	100 %	100 %	100 %	A	100 %	100 %	100 %	A
5	97.92 %	97.92 %	97.92 %	A	100 %	100 %	100 %	A	100 %	100 %	100 %	A
6	100 %	100 %	100 %	A	100 %	100 %	100 %	A	100 %	100 %	100 %	A
7	97.73 %	100 %	100 %	A	100 %	100 %	100 %	A	100 %	100 %	100 %	A
8	95.83 %	97.92 %	97.92 %	A	100 %	100 %	100 %	A	95.24 %	97.62 %	97.62 %	A
9	100 %	100 %	100 %	A	100 %	100 %	100 %	A	100 %	100 %	100 %	A
10	100 %	100 %	100 %	A	100 %	100 %	100 %	A	100 %	100 %	100 %	A
11	100 %	100 %	100 %	A	100 %	100 %	100 %	A	97.62 %	97.62 %	100 %	A
12	100 %	100 %	100 %	A	100 %	100 %	100 %	A	97.62 %	100 %	100 %	A
13	100 %	100 %	100 %	A	100 %	100 %	100 %	A	100 %	100 %	100 %	A
14	97.92 %	97.92 %	100 %	A	100 %	100 %	100 %	A	100 %	100 %	100 %	A
15	97.87 %	97.87 %	97.87 %	A	100 %	100 %	100 %	A	100 %	100 %	100 %	A
All	98.31 %	99.15 %	99.58 %	A	100 %	100 %	100 %	A	99.03 %	99.68 %	99.84 %	A

Volunteer	8 Minute Interval				10 Minute Interval				12 Minute Interval			
	5 mmHg	10 mmHg	15 mmHg	Grade	5 mmHg	10 mmHg	15 mmHg	Grade	5 mmHg	10 mmHg	15 mmHg	Grade
1	3.03 %	100 %	100 %	D	6.45 %	83.87 %	96.77 %	D	3.57 %	3.57 %	3.57 %	D
2	5.00 %	97.50 %	100 %	D	11.11 %	72.22 %	100 %	D	0.00 %	3.03 %	3.03 %	D
3	23.08 %	97.44 %	97.44 %	D	19.44 %	50.00 %	91.67 %	D	0.00 %	9.09 %	18.18 %	D
4	58.97 %	97.44 %	97.44 %	D	8.33 %	27.78 %	94.44 %	D	30.30 %	33.33 %	51.52 %	D
5	46.15 %	100 %	100 %	C	11.11 %	66.67 %	88.89 %	D	3.03 %	3.03 %	15.15 %	D
6	35.90 %	94.87 %	97.44 %	D	27.78 %	55.56 %	91.67 %	D	15.15 %	18.18 %	21.21 %	D
7	34.29 %	94.29 %	97.14 %	D	25.00 %	43.75 %	78.13 %	D	17.24 %	20.69 %	20.69 %	D
8	46.15 %	87.18 %	89.74 %	C	47.22 %	75.00 %	94.44 %	C	36.36 %	42.42 %	42.42 %	D
9	12.82 %	100 %	100 %	D	22.22 %	72.22 %	100 %	D	0.00 %	0.00 %	0.00 %	D
10	48.72 %	94.87 %	94.87 %	C	13.89 %	36.11 %	86.11 %	D	12.12 %	21.21 %	27.27 %	D
11	58.97 %	97.44 %	97.44 %	B	22.22 %	52.78 %	97.22 %	D	3.03 %	6.06 %	21.21 %	D
12	20.51 %	84.62 %	89.74 %	D	5.56 %	50.00 %	88.89 %	D	6.06 %	12.12 %	15.15 %	D
13	15.38 %	97.44 %	97.44 %	D	2.78 %	61.11 %	100 %	D	12.12 %	18.18 %	21.21 %	D
14	10.26 %	87.18 %	94.87 %	D	2.78 %	61.11 %	86.11 %	D	0.00 %	6.06 %	9.09 %	D
15	13.16 %	97.37 %	100 %	D	17.14 %	77.14 %	97.14 %	D	0.00 %	0.00 %	3.13 %	D
All	29.04 %	95.13 %	96.87 %	D	16.23 %	58.87 %	92.83 %	D	9.28 %	13.20 %	18.35 %	D

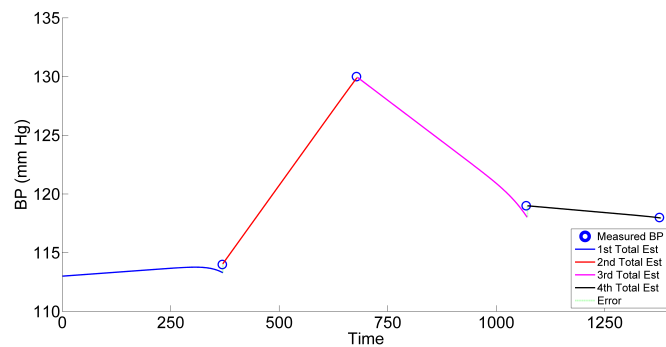
solid line shows the PTT data after it has been filtered i.e. by the HFC. Despite large changes being observed in the cuff measurements (the circular points), the shape of HFC remains almost exactly the same. The LFC interpolates the values between the cuff measurements and a combination of the LFC and HFC is used as the final estimation of Chen’s algorithm. This is presented in Figure 3.16b.

Since use of the filter results in only small changes in the data and the LFC essentially connects one cuff measurement to the other, the overall estimation is very accurate and the effect is that the errors, if any, are minute. From what has been observed, it seems that the filter is tuned such that if a 5 minute calibration interval had been examined, the HFC or filtered PTT, would be reduced to a perfectly straight, horizontal line. The results of the 4 minute calibration interval support this, since the variation at this interval have been observed to be less than 0.15 mmHg. By combining an almost perfectly straight, horizontal line at 4 minutes, with a variation of less than 0.15 mmHg provided by the HFC and a

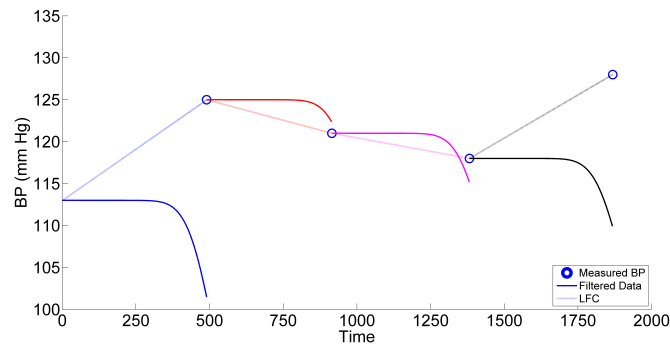
3.10 Evaluating the PTT Method Using Two Different PTT Algorithms - Round 3 of Testing



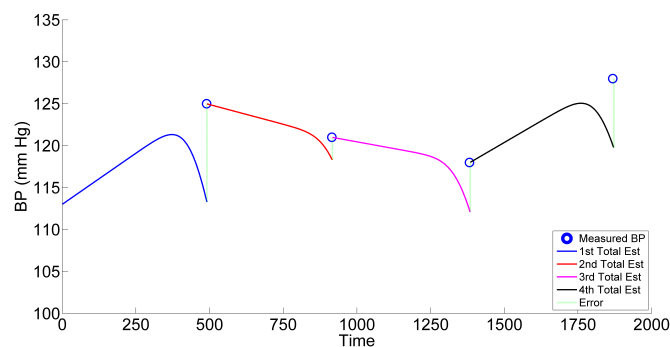
(a) The filtered PTT and the LFC, shown separately at the 6 minute calibration interval



(b) Chen's prediction at the 6 minute calibration interval when the two components are added



(c) The filtered PTT and the LFC, shown separately at the 8 minute calibration interval



(d) Chen's prediction at the 8 minute calibration interval when the two components are added

Figure 3.16: The shortcoming of Chen's algorithm can be seen by comparing the filtered PTT in the 6 minute calibration to the 8 minute calibration interval

linear interpolation between the initial BP measurement and test or calibration BP measurement, it is no surprise that the associated error is so low, since the only variation from the test point is due to the variation of the HFC. In line with other filters, it has been found that the algorithm performs much better at intervals less than the 5 minute interval, the algorithm improves as it approaches 5 minutes and then degrades once the calibration interval exceeds this.

Furthermore, because a healthy person's BP at rest doesn't vary substantially over short intervals, by keeping the amplitude of the estimation (the HFC) low, the estimate can remain within the 5mmHg limit that is defined by the AAMI and BHS standards

Therefore, since Chen's HFC provides a straight line that doesn't vary by more than $\approx 3\text{mmHg}$ throughout the entire 6 minutes of the test and relies on the LFC to correct any errors, it complies with the standards. Due to the requirement for the LFC to correct the errors, the data is also not provided in real time but with a lag period which is equal to the duration of the calibration interval. However, as outlined previously, at 8 minutes the filter introduces a large change in the data over the calibration interval and becomes the dominant factor in the results, as can be seen in Figure 3.16c. In this case, the amplitude of the HFC is much larger (usually in the order of greater than 5mmHg), so when the LFC and the HFC are added together, the LFC component becomes incapable of compensating by a large enough degree. This is as shown in Figure 3.16d and thus causing the failure of the algorithm to meet the standards.

3.10.2 Evaluating Poon's Algorithm

Tables 3.6 and 3.7 present the results of evaluating Poon's algorithm described in 2.7. While analysing this algorithm, it was noted that, on occasion, large spikes in BP occurred during some tests. These spikes exceeded 1000 mmHg and as a consequence adversely affect the standard deviation of the data. These values, clearly being errors, were removed and were replaced by a value that was a mean of the previous ten results. A total of fourteen of these anomalous points occur in this data set. These spikes are due to motion artifacts in the data where the patient either moved their body causing a motion artefact in the ECG signal or moved their hand or finger causing a motion artefact in the PPG signal. These motion artifacts caused the peak detection algorithms to misidentify them as points of interest meaning that the changes in PTT were excessively short, and

Table 3.6: Evaluation of Poon’s algorithm with respect to the AAMI standard. Each result represents the mean error \pm the standard deviation of error between the Estimated BP, given by the PTT method, and Measured BP, given by the Omron M6.

<i>Volunteer</i>	<i>2 Minute Interval</i>	<i>4 Minute Interval</i>	<i>6 Minute Interval</i>	<i>8 Minute Interval</i>	<i>10 Minute Interval</i>	<i>12 Minute Interval</i>
1	1.16 \pm 7.34	1.16 \pm 6.45	0.58 \pm 8.40	-0.79 \pm 6.38	-0.56 \pm 8.16	0.34 \pm 6.72
2	0.01 \pm 6.48	-0.23 \pm 6.80	0.08 \pm 8.02	0.45 \pm 6.98	-0.13 \pm 7.65	0.01 \pm 8.07
3	0.75 \pm 11.11	0.37 \pm 8.34	0.47 \pm 10.25	-1.06 \pm 8.85	-0.48 \pm 9.96	-0.68 \pm 8.00
4	2.39 \pm 13.05	1.26 \pm 12.34	3.41 \pm 14.24	1.89 \pm 13.20	2.13 \pm 12.75	1.07 \pm 13.13
5	0.21 \pm 5.50	0.11 \pm 5.30	0.07 \pm 6.48	-0.37 \pm 6.68	-0.20 \pm 5.76	-0.86 \pm 6.27
6	0.30 \pm 8.25	-0.50 \pm 9.52	-0.35 \pm 9.36	-0.51 \pm 9.35	0.59 \pm 8.48	-0.14 \pm 10.62
7	-0.88 \pm 9.80	-1.39 \pm 10.08	-1.77 \pm 9.66	-1.41 \pm 10.74	-1.53 \pm 11.04	-0.94 \pm 9.56
8	4.44 \pm 10.41	4.44 \pm 10.80	4.91 \pm 8.91	4.65 \pm 9.75	5.38 \pm 10.35	5.33 \pm 8.46
9	0.18 \pm 6.70	0.21 \pm 7.07	-0.46 \pm 8.30	0.04 \pm 7.74	0.57 \pm 6.56	1.38 \pm 6.53
10	4.36 \pm 12.35	6.17 \pm 13.39	6.34 \pm 10.14	4.95 \pm 10.58	4.07 \pm 11.12	5.43 \pm 11.07
11	2.25 \pm 11.85	1.39 \pm 11.20	0.82 \pm 12.16	1.10 \pm 11.86	0.22 \pm 9.82	0.10 \pm 10.73
12	0.33 \pm 7.43	-0.13 \pm 6.88	-0.72 \pm 5.91	-0.72 \pm 7.18	-0.41 \pm 6.34	0.68 \pm 7.49
13	9.65 \pm 15.97	6.09 \pm 17.46	6.78 \pm 15.59	5.71 \pm 10.62	5.23 \pm 12.98	4.62 \pm 13.22
14	1.21 \pm 11.49	1.20 \pm 10.03	0.34 \pm 10.69	0.00 \pm 10.64	-0.12 \pm 10.67	0.05 \pm 9.50
15	0.23 \pm 10.35	0.07 \pm 11.32	-1.45 \pm 11.47	-0.49 \pm 9.16	0.16 \pm 9.49	0.01 \pm 8.97
Overall	1.79 \pm 10.50	1.40 \pm 10.48	1.40 \pm 10.59	1.08 \pm 9.74	1.15 \pm 9.84	1.24 \pm 9.74

because of the inverse relationship between PTT_W and BP in Poon’s algorithm, a small error in the measurement of PTT will result in a large error in BP. The Bland Altman graphs in Figure 3.17, a - f, show a slight deterioration of results and the cluster also grows slightly from the 2 minute calibration interval to the 12 minute calibration interval, and the number of outliers also increases. The reason for the similarities and only slight deterioration is because each of the tests fail by a similar amount when each standard is applied regardless of the calibration interval. There are also a large number of outliers (errors) that can be found in each of the Bland Altman graphs, and these are the primary reason for the large standard deviation and consequent poor performance of the algorithm. Examining the Bland Altman graphs also reveal that there is a range of 100 mmHg to 135 mmHg where the algorithm is accurate. Below 100 mmHg, it appears that the algorithm underestimates the actual BP whereas above 135 mmHg the algorithm overestimates the actual BP. Therefore, it could be said that Poon’s algorithm is accurate for people whose BP is within this range and if the tests were repeated and volunteers were chosen whose BP was within this range, the algorithm could have much better performance.

The reason for this linear relationship in the Bland Altman graphs i.e. the underestimation of low BPs, the accuracy of the “middle” range, and the overestimation of higher BPs, is unclear. One observation that could be made is that there are very few BP measurements in excess of 130 mmHg and more data would be re-

3. EVALUATION OF THE PULSE TRANSIT TIME METHOD

Table 3.7: A summary of the results of Poon’s algorithm when the BHS standard is applied.

Volunteer	2 Minute Interval				4 Minute Interval				6 Minute Interval			
	5 mmHg	10 mmHg	15 mmHg	Grade	5 mmHg	10 mmHg	15 mmHg	Grade	5 mmHg	10 mmHg	15 mmHg	Grade
1	53.33 %	86.67 %	93.33 %	B	61.90 %	85.71 %	97.62 %	A	56.41 %	79.49 %	89.74 %	C
2	62.50 %	89.58 %	97.92 %	A	53.33 %	84.44 %	97.78 %	B	50.00 %	76.19 %	90.48 %	B
3	47.92 %	70.83 %	83.33 %	D	46.67 %	77.78 %	93.33 %	C	28.57 %	73.81 %	92.86 %	D
4	33.33 %	64.58 %	77.08 %	D	26.67 %	60.00 %	82.22 %	D	23.81 %	54.76 %	73.81 %	D
5	68.75 %	91.67 %	97.92 %	A	62.22 %	93.33 %	100 %	A	54.76 %	85.71 %	97.62 %	B
6	45.83 %	81.25 %	89.58 %	C	35.56 %	77.78 %	86.67 %	D	40.48 %	69.05 %	92.86 %	C
7	45.45 %	77.27 %	88.64 %	C	36.59 %	63.41 %	92.68 %	D	39.47 %	71.05 %	89.47 %	D
8	37.50 %	64.58 %	81.25 %	D	31.11 %	55.56 %	84.44 %	D	42.86 %	69.05 %	80.95 %	D
9	60.42 %	87.50 %	95.83 %	A	51.11 %	91.11 %	95.56 %	B	59.52 %	85.71 %	95.24 %	B
10	37.50 %	52.08 %	58.33 %	D	35.42 %	47.92 %	60.42 %	D	39.58 %	56.25 %	72.92 %	D
11	50.00 %	70.83 %	81.25 %	C	35.42 %	60.42 %	77.08 %	D	50.00 %	70.83 %	83.33 %	D
12	35.42 %	60.42 %	77.08 %	D	39.58 %	60.42 %	81.25 %	D	45.83 %	58.33 %	77.08 %	D
13	58.33 %	87.50 %	97.92 %	B	56.25 %	83.33 %	95.83 %	B	62.50 %	89.58 %	100 %	A
14	47.92 %	81.25 %	89.58 %	C	56.25 %	75.00 %	87.50 %	C	50.00 %	79.17 %	87.50 %	C
15	42.55 %	70.21 %	89.36 %	C	40.43 %	68.09 %	85.11 %	C	38.30 %	63.83 %	82.98 %	D
All	48.46 %	75.70 %	86.52 %	C	44.53 %	72.12 %	87.59 %	C	45.59 %	72.04 %	86.93 %	C

Volunteer	8 Minute Interval				10 Minute Interval				12 Minute Interval			
	5 mmHg	10 mmHg	15 mmHg	Grade	5 mmHg	10 mmHg	15 mmHg	Grade	5 mmHg	10 mmHg	15 mmHg	Grade
1	72.22 %	91.67 %	97.22 %	A	60.61 %	81.82 %	90.91 %	B	70.00 %	90.00 %	96.67 %	A
2	64.10 %	87.18 %	97.44 %	A	61.11 %	83.33 %	88.89 %	C	48.48 %	75.76 %	90.91 %	C
3	33.33 %	66.67 %	97.44 %	D	38.89 %	72.22 %	91.67 %	D	45.45 %	78.79 %	93.94 %	C
4	28.21 %	51.28 %	71.79 %	D	33.33 %	66.67 %	77.78 %	D	24.24 %	63.64 %	84.85 %	D
5	43.59 %	89.74 %	97.44 %	C	52.78 %	94.44 %	100 %	B	42.42 %	93.94 %	100 %	C
6	46.15 %	71.79 %	92.31 %	C	44.44 %	77.78 %	88.89 %	C	51.52 %	81.82 %	87.88 %	C
7	51.43 %	71.43 %	80.00 %	D	43.75 %	65.63 %	87.50 %	C	48.28 %	68.97 %	89.66 %	C
8	38.46 %	74.36 %	87.18 %	D	30.56 %	63.89 %	80.56 %	D	45.45 %	72.73 %	84.85 %	D
9	61.54 %	94.87 %	94.87 %	A	47.22 %	91.67 %	97.22 %	C	63.64 %	90.91 %	96.97 %	A
10	41.67 %	60.42 %	77.08 %	D	50.00 %	62.50 %	75.00 %	D	58.33 %	62.50 %	68.75 %	D
11	52.08 %	64.58 %	79.17 %	D	54.17 %	68.75 %	79.17 %	D	54.17 %	72.92 %	81.25 %	D
12	43.75 %	64.58 %	79.17 %	D	52.08 %	75.00 %	89.58 %	C	47.92 %	66.67 %	81.25 %	D
13	60.42 %	87.50 %	93.75 %	A	66.67 %	87.50 %	95.83 %	A	75.00 %	81.25 %	91.67 %	B
14	56.25 %	81.25 %	89.58 %	C	52.08 %	72.92 %	89.58 %	C	56.25 %	81.25 %	91.67 %	B
15	57.45 %	76.60 %	85.11 %	C	55.32 %	78.72 %	87.23 %	C	53.19 %	82.98 %	93.62 %	B
All	50.08 %	75.28 %	87.64 %	C	50.17 %	75.99 %	87.75 %	C	53.03 %	77.12 %	88.21 %	C

quired in this range to confirm that the algorithm always overestimates BPs in this range. This may just be a feature of one particular volunteer, to whom the algorithm is not suited. A similar argument could also be made for the range of measurements below 100 mmHg. Analysing the Bland Altman graphs provided by Poon in her paper would support this to some degree since no linear relationship is observed in these graphs, and a much larger number of BP measurements in excess of 135 mmHg are available.

Using Poon’s algorithm, it was found that calibration is required before the two minute calibration interval, even when the large artifacts are removed. The majority of mean errors recorded were within the acceptable limits i.e. 5mmHg, but the standard deviation is always greater than 8mmHg.

Poon’s algorithm showed a failure even when using a 2 minute calibration interval against the standards. This is in line with the results that Poon reported. However, on examination of the algorithm, it appears that it tracks the changes in BP over some intervals e.g. over the first three intervals Poon’s algorithm is capable of tracking the large decrease and increase in BP given by the cuff, as

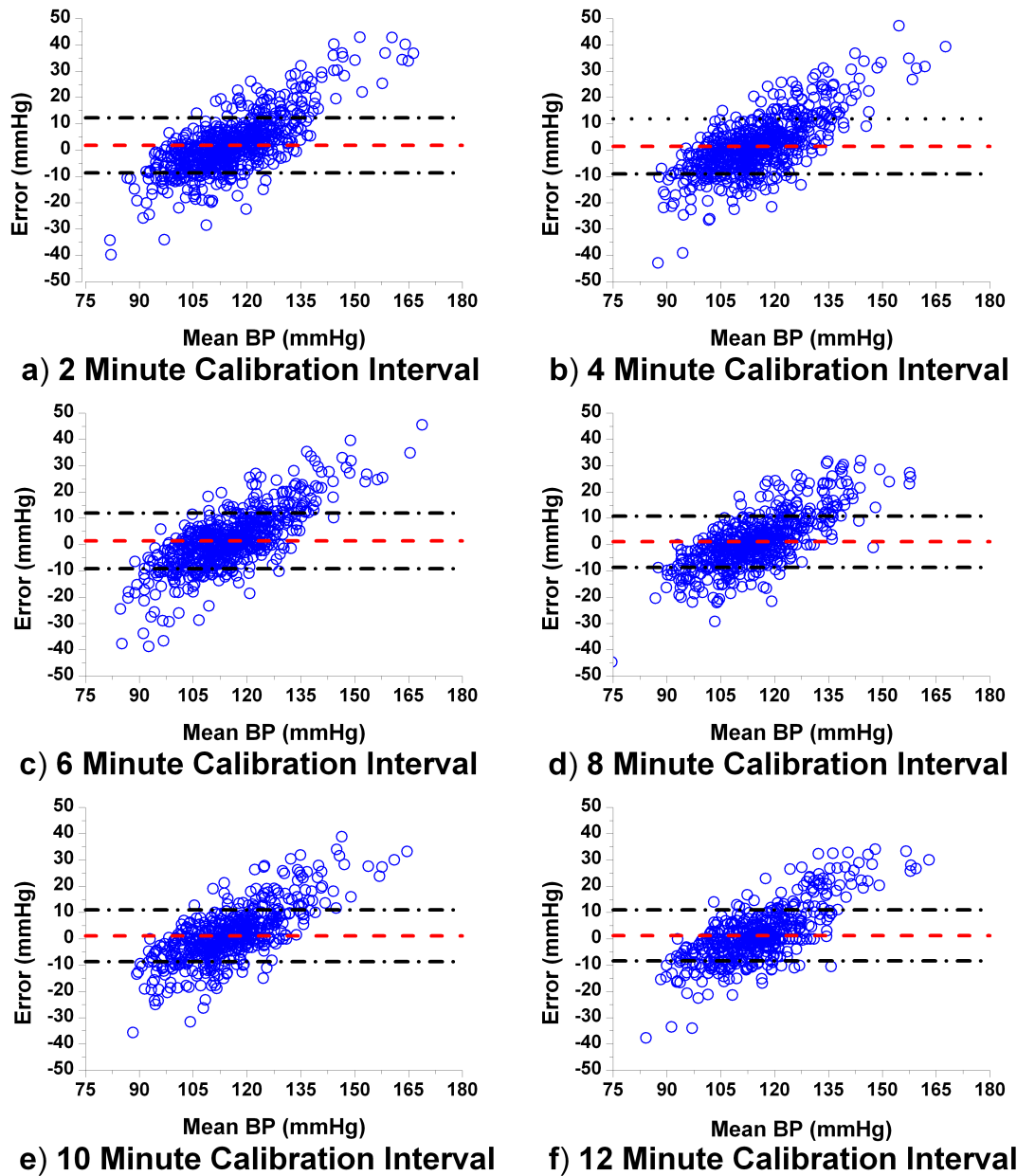


Figure 3.17: The Bland Altman graphs of Poon’s algorithm for each of the six intervals (a - f). These Bland Altman graphs represent a visualisation of the last row of Table 3.6, and show the mean error (red) and the mean \pm the standard deviation (black) of the results.

3. EVALUATION OF THE PULSE TRANSIT TIME METHOD

can be seen in Figure 3.18. The ability to track changes in BP is also apparent over the fifth to seventh intervals and again over the tenth to fourteenth intervals. Although this is not sufficient or satisfactory, and a drastic improvement is clearly required, it does indicate that the PTT could be used to track changes in BP if an improvement could be made. Although it was necessary to remove some spikes due to motion artifacts, Poon's algorithm seems to be much better at tracking BP than Chen's method. However, this can be quite difficult to qualify because of the high magnitude of "noise" associated with it. If this "noise" could be eliminated or diminished, Poon's algorithm would be the better method of the two to use for tracking BP.

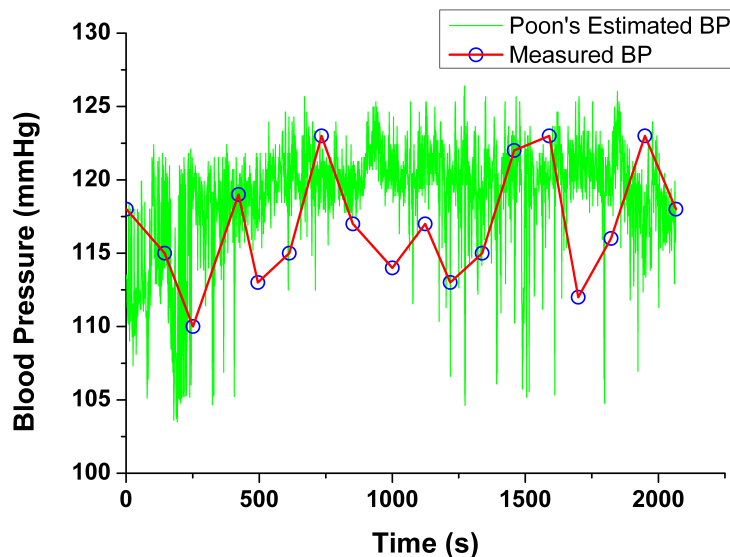


Figure 3.18: Poon's algorithm (in green) and its ability to track measured BP (in red)

3.11 Conclusions

The purpose of the work described in this chapter was to evaluate the state of the art of the PTT algorithms that have been published in the last few years. In order to perform this evaluation, a number of steps were required so the PTT could first be measured.

The first section of this was the development of the PHALs Board, which would provide an ECG wave to measure the initiation of the PTT. A Bluetooth module was also included to allow wireless communication and allow maximum compatibility with other electronic devices which may be common in peoples' households, although it was not used during the subsequent tests.

The hardware component that was necessary to measure PTT consisted of the Pulse Oximeter device which measures the arrival of the pulse wave at the secondary location. However, for the evaluation of the PTT method, some modification was required to allow both devices to record data at a high sampling rate to Excel via LabView without loss of data.

Once the data was recorded to a satisfactory standard, the use of post-processing of the data to improve signal quality and extract the various characteristic points was investigated. The extraction of the characteristic points to measure PTT is explained in section 3.6 which enabled the evaluation of the various PTT algorithms.

The first evaluation of the PTT method ,“Round 1 of testing”, used the Moens - Korteweg equation as a basis for an investigation into the usefulness of the PTT method, and the calibration intervals required for accurate tracking of BP. This test used a Sanitas SMB30 BP monitor and 5 minute calibration intervals and data was recorded from 5 volunteers for 15 minutes each. The results of this test showed that a number of refinements were necessary, including a requirement for a better BP monitor for testing and that it would be better to test each of the volunteers over a longer duration.

“Round 2” testing was undertaken with the lessons learned in “Round 1” being taken into account. The most important difference between the two rounds was the new BP monitor. The tests used 6 volunteers, 4 males and 2 females, each tested over 30 minutes and using 5 minute calibration intervals. The PTT method was evaluated using the Moens-Kortewegg equation as a basis. The results of this test showed that a 5 minute calibration interval was necessary, with

longer calibration intervals failing the AAMI standard [127]. To identify a more precise calibration interval, it was decided that another round of testing should be undertaken, using a more frequent calibration interval of 2 minutes and using more volunteers. It was also decided to evaluate the state of the art algorithms for their ability to calculate BP from PTT in this test.

The final test, “Round 3 Testing”, described in this chapter was the evaluation of the state of the art algorithms to track BP using PTT. The two algorithms that were tested were the two most cited works in the area: Chen’s and Poon’s algorithms. For these tests 15 volunteers were examined, 30 minutes of data was recorded per sitting, with three sittings per volunteer i.e. each volunteer provided a total of 90 minutes of data. BP was once again measured using the Omron M6 cuff at two minute intervals.

Chen’s algorithm was found to be statistically accurate when using a 6 minute calibration interval, which was a slight improvement over Round 2 testing which only used the Moens-Korteweg equation. However, throughout this work there were significant concerns raised over the usefulness of the method due to the use of the LFC and the filter. It was found that at short calibration intervals the LFC kept the method accurate. For longer calibration intervals the filter was found to have a much larger effect and the effect of the LFC was reduced.

Poon’s algorithm provided contrasting results, failing even when a two minute calibration interval was used. The standard deviation of 11mmHg that was achieved was far greater than the allowed 8mmHg from the AAMI standard. This was primarily due to large spikes in the data which affected the mean and standard deviation. However, an examination of the estimation of the BP provided by Poon’s algorithm showed that it was capable of tracking changes in BP to some extent rather than Chen’s algorithm whose prediction was dominated by the filter, and thus bore no resemblance to either changes in PTT or BP.

Although Chen’s algorithm was shown to be accurate when using a 6 minute calibration interval, neither of the two algorithms tested were deemed good enough for practical or clinical use. These results indicate that the PTT alone may not be sufficient to track BP non-invasively and this conclusion along with these results was published in the Journal of Human Hypertension [128]. Other authors have also concluded that other parameters, the most prevalent of which is Pre-Ejection Period or the time it takes the valve on the ventricle to open completely after the R wave may need to be included in any such estimation in the future. Other parameters that have been suggested include heart rate, stroke volume and a

product of the two, Cardiac Output. The measurement of these parameters and subsequent data recording will be discussed in the next chapter.

Chapter 4

Measuring Stroke Volume and Other Parameters

4.1 Introduction

As discussed in the previous chapter, there is a clear need for improvement in the existing PTT algorithms, so that the PTT method can have a useful and practical calibration interval as part of a continuous BP monitoring system. By examining the results provided by these existing algorithms and studying the literature, a number of parameters have been identified that could provide an improvement to these algorithms if they were to be included in the calculation. The most critical of these parameters include, but are not limited to, Cardiac Output (CO) [7, 81], Stroke Volume (SV) and Pre-Ejection Period (PEP) [130].

In this chapter the methodology that was used to acquire these important parameters is discussed. Two methods were identified by which these parameters could be acquired, either by using an Impedance Cardiograph (ICG) [131] or by using the PhysioNet Resource. Each method has its own advantages and disadvantages and a two pronged approach was taken to investigate which method would be most beneficial. Once the advantages and disadvantages were identified for the PhysioNet Resource, they were also established for the ICG.

The first section discusses the use of the PhysioNet Resource [132], which is one potential method that could be used to acquire the required parameters. This is a large database of medical signals that have been measured from patients that have been treated or have been in hospitals over extended periods of time, for a variety

of reasons and who have had direct measurements of the parameters performed through invasive means. The use of this database has its own difficulties, such as identifying appropriate data, but also it eased some other concerns with reference to clinical approval.

The next section discusses the evaluation of the ICG; this is a system that has been used in the past to measure SV and CO, but is not a widely used technique. However, due to the number of parameters that can be measured by this system, which also include PEP, it is the ideal tool to use because it could also be incorporated into an existing PTT device, because both are wearable systems. However, due to the limited information about the system, the lack of reference material and design notes available, the issues associated with constructing such a system were soon established.

Section 4.4 summarises the benefits and shortcomings of each method. The PhysioNet Resource was chosen as the tool to acquire the parameters of interest. The main disadvantage of using the PhysioNet Resource was that it was not possible to measure PEP, but this database had one major advantage, namely the inclusion of Arterial BP (ABP) data. Unlike the intermittent cuff measurements that were used to evaluate the PTT algorithms in the previous chapter, the use of ABP allowed a much better evaluation on a beat to beat and continuous basis of these algorithms and any other that would be derived.

Finally, in section 4.5 Chen [14] and Poon [75] are re-examined using the PhysioNet database, both as confirmation of the results of the previous chapter and as an assurance of the value of the database.

4.2 PhysioNet Database

The PhysioNet Resource [132] is intended to stimulate current research and new investigations in the study of complex biomedical and physiological signals. It has three closely interdependent components:

- **PhysioBank** is a large archive and collection of 50 databases containing biological and physiological signals for use by the biomedical community. Some of the records within these databases are signals taken from healthy people as well as from people suffering from a number of conditions including, but not limited to, congestive heart failure, sleep apnoea and ageing.

- **PhysioToolkit** is a growing collection of software applications for physiological signal processing, detection of various events and analysis of signals.
- **PhysioNet** is the name of the resource and also the name of the website. The website exists so that the signals and software available on it can be freely distributed to allow the exchange of open source software and evaluation of new algorithms.

The data within PhysioBank was the primary interest for this project. PhysioBank itself contains 50 databases and among these databases 36,000 records of annotated and digitized signals and time series data. Many of the databases were developed in MIT and at Boston's Beth Israel Hospital (now the Beth Israel Deaconess Medical Center). Each of these records can be downloaded using the software provided by PhysioToolkit. Further software from this resource is also available to convert the downloaded records into a usable format that could be interpreted by Matlab.

Depending on which database is used, any number of physiological signals may be available. These are divided into two major categories described as being continuous and non-continuous. For example in the Apnoea-ECG database, the primary continuous signals monitored are various ECG signals and respiratory signals whereas in the MIMIC II database, continuous signals recorded include ECG Lead I, ECG Lead II, ECG Lead III, ECG Lead IV, ECG Lead V, Respiratory, Plethysmography, Arterial BP and Pulmonary Arterial Pressure, among others. Non-continuous measurements include systolic, diastolic, and mean blood pressures, non-invasive arterial BP, cardiac output, carbon dioxide and heart rate, among others. Throughout this database, "continuous" refers to signals that have been sampled at a relatively high sampling rate (typically 125 Hz), whereas "non-continuous" data is typically sampled only at approximately 1 Hz. A typical example of the continuous signals available from the PhysioNet website can be seen in Figure 4.1

It should be noted that regardless of the database, some records may only have a selection of these signals whereas other records may contain all of them. For this application the signals required were:

- An ECG signal that contained an easily recognisable R wave
- A plethysmograph (PPG) signal
- A BP measurement, preferably Arterial Blood Pressure (ABP)



Figure 4.1: A typical chart of signals available from the PhysioNet website. [133].

- A Cardiac Output (CO) measurement

Both ECG and PPG signals are required to measure PTT. Since ABP seemed to be almost as common as ECG in the records that also contained the PPG signal, it was chosen to be another crucial signal. By including ABP as opposed to a non-invasive or non-continuous BP measurement, it would be possible to compare the prediction from the new algorithm to the actual BP on a beat-to-beat basis, eliminating any errors that may occur due to point measurements from the non-invasive BP measurement that may be a misrepresentation of the actual data (i.e. a BP measurement taken during an artefact). This was particularly important because many of the records were from patients with various ailments that may include cardiac arrhythmias for example, although information of this kind was not always available.

The final critical signal was CO. Although it had been initially hoped that a continuous CO or SV signal would be available, the only CO measurements available were non-continuous ones, typically taken at intervals of 1 minute. It was found

that there were a number of different methods that could be used to derive CO and SV from non-continuous records and the use of an ABP signal. All of these methods are summarised and evaluated in the work of Sun [134]. The results of this paper showed that the Liljestrand non-linear compliance method proved to be the best at predicting CO on a beat to beat basis as opposed to the other methods evaluated. The PhysioNet Resource also recommends this paper as the best way to estimate CO from non-continuous measurements.

Although nearly every record examined had an associated ECG signal, finding records that contained each of the four signals needed proved to be more difficult. In fact, the most limiting signal was that of CO. Of the 50 databases that were available, only 3 were found to have CO. One of these databases, the MIMIC II database had to be omitted because while measuring the PTT, it was noted that the PTT had a periodic repetitiveness, as can be seen in Figure 4.2. This meant the PTT was found to have an almost sinusoidal waveform in this particular database, something which had not been observed in any previous tests or in other databases on the PhysioNet Resource. In an attempt to overcome this issue, various different PTT definitions were used:

- Measuring the PTT as the time from the ECG R Wave to the peak of the PPG wave
- Measuring the PTT as the time from the ECG R Wave to the foot of the PPG wave
- Measuring the PTT as the time from the ECG R Wave to the point of maximum inflection of the PPG wave

Examining the signal more closely, it was found that, regardless of which definition was used, the periodic nature of the wave was apparent throughout, as can be seen in Figure 4.2. It was also found that the sinusoidal nature of the waveform corresponded to the sampling frequency and so it was felt, because of concerns with regard to data reliability that this particular database should be ignored.

The two remaining databases, which contained all the required signals, were the MIMIC database [135] and the database from the 2009 Challenge [136], as described below.

The MIMIC database has 72 complete records, most of which contain both ECG and PPG records but only 38 were found to contain CO measurements. Of these

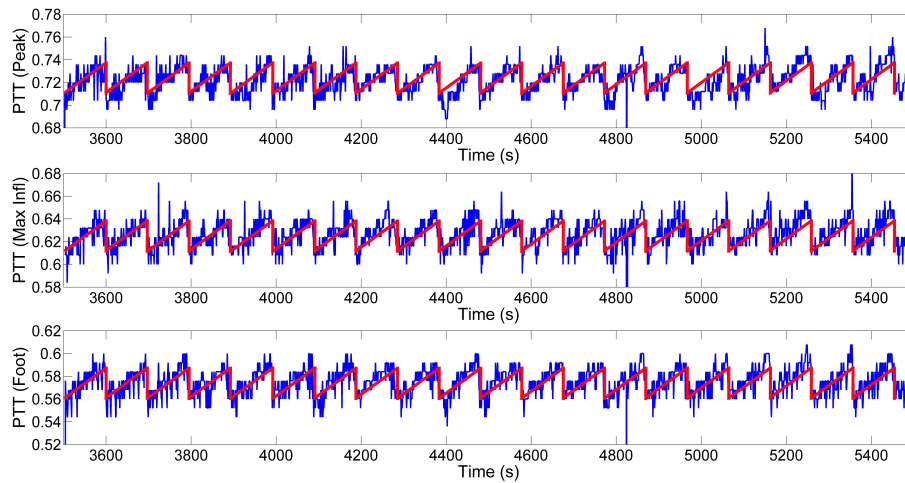


Figure 4.2: The Periodic nature of the PTT measurement was apparent no matter which of the three definitions were used.

38, only 14 records contained each of the four necessary signals.

The other database was the Challenge Set A and B from 2009. PhysioNet annually hosts a challenge, inviting participants to tackle clinically interesting problems. In 2009, the goal of the challenge was to predict which patients in the challenge dataset would experience an acute hypotensive episode beginning within a certain forecast window. Each participant to the challenge is given access to a limited number of records from an otherwise restricted database. These databases are known as the challenge set databases and are used to create and test any algorithm that the user can derive to predict, which patient would experience this episode. Once each of the participants has submitted their algorithm, their algorithms would be then tested on another database to check their effectiveness. Using two of these Challenge Sets, Challenge Sets A and B, 27 of the records from these databases reportedly had CO measurements; however, only 2 were found to have CO, PPG, ABP and ECG signals.

A further limitation can be seen when Figure 4.3 is examined and compared to its description in the database. In this database, CVP is listed as being available throughout but in this particular window of 10 seconds, the signal is not present. Unfortunately, this feature can be seen throughout all of the databases. In many cases, signals may be available only for a matter of seconds or minutes. However, in some records these signals may not be present at all. In the more typical case, where the data becomes unavailable for a small period of time, this becomes a large limitation when either developing or analysing algorithms. Ideally, each

4. MEASURING STROKE VOLUME AND OTHER PARAMETERS

signal should be present for a matter of hours, over each record. This would allow any algorithm that was developed to be analysed over the same timeline. However, if there is a break in any of the signals, even for a few seconds, a beat to beat analysis, such as the one being developed in this work, is not possible in that window. Figure 4.3 shows the ABP signal disappearing and not reappearing in this particular window (of 1 minute) as an example.



Figure 4.3: An example showing the ABP signal disappearing during a measurement. It reappears a few minutes later [137]. It is also worth noting that although being listed as available, CVP is not available in the window shown

There are many possible reasons why these gaps appear. Three suggested reasons for this behaviour are:

- The patient was disconnected from the monitor for some period (perhaps for a scan or to replace electrodes)
- The data collection system or the network over which the data was transmitted crashed
- The data that was collected was corrupted and conversion was not possible

It was also not unusual for only one of the four signals to disappear for a few seconds before reappearing.

4.3 The Impedance Cardiograph

Impedance Cardiography, Transthoracic Bioimpedance or Impedance Plethysmography is a non-invasive tool used for the measurement of Stroke Volume (SV) and Cardiac Output (CO). Other cardiac parameters such as PEP and Left Ventricle Ejection Time (LVET), which are important parameters for the diagnosis of cardiac illnesses can also be derived from the use of an ICG. The concept of ICG was first developed by Kubicek in 1966 [138] for NASA, which resulted in the Minnesota Impedance Cardiograph [139]. Since then, there have been a number of commercially available devices developed, but the invasive method of thermodilution remains the gold standard in Cardiac Output estimation. Thermodilution uses a Pulmonary Artery Catheter (PAC) to estimate cardiac output but has associated risks such as infection, sepsis and mortality and it is therefore only used for critically ill patients [140]. The main attraction of ICG is that it is non-invasive, easy to use, inexpensive and provides real-time data [141]. However, its main disadvantage is that it is very susceptible to motion artifacts.

4.3.1 Impedance Cardiography Instrumentation

The ICG method involves the application of an alternating current of less than 4mA at a frequency of 20 - 100kHz into the body through a set of outer thoracic electrodes and recording the associated voltage drop across another inner set of electrodes as shown in Figure 4.5. Although direct current could present a medical hazard, the 4 mA alternating current in the frequency range of 20 - 100kHz does not [131]. If no inductive or capacitive elements are contained in the system, the impedance measured is equal to the resistance. Human tissue is known to be mainly resistive in this frequency range [142]. Due to Ohms Law, the recorded voltage will vary inversely with the resistivity of the thoracic current path. The body components with the lowest resistivity are blood and plasma, so the measured thoracic impedance is highly sensitive to changes in the cardiac and aortic distribution and flow of blood in the cardiac cycle [143].

The electrode placement shown in Figure 4.4 is the most common arrangement and most widely accepted [144]. The inner (red) set of electrodes shown in the diagram, are used to record the impedance changes within the thorax [12]. This measured signal is known as the impedance or ΔZ waveform but contains no information and is not directly used to calculate any of the parameters. The

4. MEASURING STROKE VOLUME AND OTHER PARAMETERS

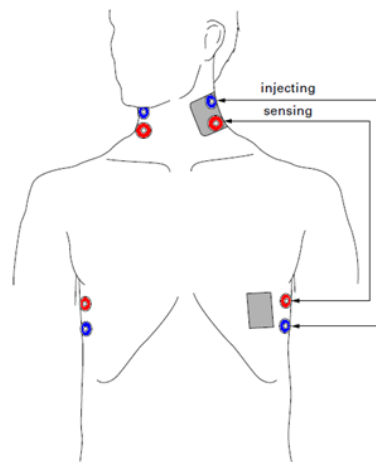


Figure 4.4: A representation of a typical ICG electrode system, the blue dots representing the current injection strip electrodes and the red dots representing the impedance measurement strip electrodes.

important waveform is that of $\frac{dZ}{dt}$ from which the systolic times and SV can be calculated.

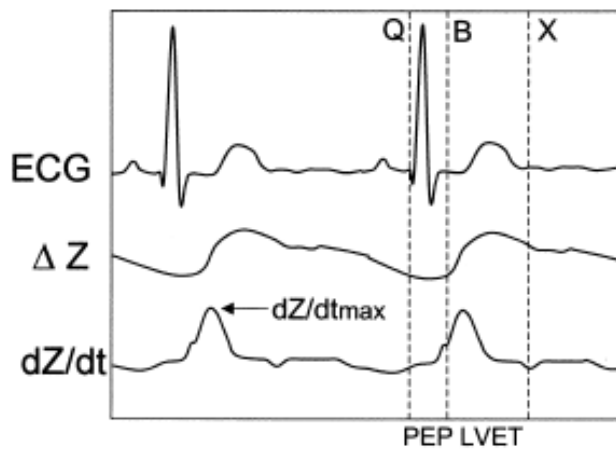


Figure 4.5: The waveforms measured and recorded from an ICG system [12].

Three variables measured from the impedance waveform are used to calculate SV.

- The baseline impedance of the thorax Z_0 , also known as the Thoracic Fluid Index (TFI)
- The maximum rate of change occurring in the ΔZ waveform, $\left(\frac{dZ}{dt}\right)_{max}$, identified as the peak value in the $\frac{dZ}{dt}$ signal.
- The Left Ventricle Ejection Time (LVET)

The relevant waveforms that are extracted from ICG measurements are shown in Figure 4.5. ECG is also required as part of the ICG system to calculate the Heart Rate (HR) but more importantly it is also used to identify the onset of electromechanical systole, which is required to measure Pre-Ejection Period. This onset occurs at the Q point of the ECG waveform. It can be difficult to identify the Q wave and so the R-wave can be used as an approximation of the onset of the electromechanical systole.

The B point is used to indicate the onset of the rapid up slope of the $\frac{dZ}{dt}$ as it rises to the peak value $\left(\frac{dZ}{dt}\right)_{max}$. The B point is used to indicate the time of onset of LVET and the end of the PEP. Finally the X point represents the lowest point in the $\frac{dZ}{dt}$ waveform. It is seen as the sharp notch which represents the closure of the aortic valve at the end of the left ventricle ejection.

4.3.2 Calculation of Stroke Volume

As mentioned in section 4.3, Kubicek presented the original ICG in 1966 [138] and presented the results of correlation with other invasive methods using the formula:

$$SV = \rho_b \frac{L^2}{Z_0^2} \Delta Z \quad (4.1)$$

measured in [ml] and where ρ_b is the resistivity of the blood [Ω/cm], L is the distance between the electrodes [m], Z_0 is the basal impedance (or impedance of the body between the electrodes) [Ω] and ΔZ [Ω] is the impedance change as a function of time. In 1974, this formula was modified using the first derivative of the impedance signal and incorporating LVET [s].

$$SV = \rho_b \frac{L^2}{Z_0^2} LVET \left(\frac{dZ}{dt}\right)_{max} \quad (4.2)$$

Since impedance Z_0 of a uniform volume conductor, is directly proportional to ρ_b and L and inversely proportional to the cross sectional area A [cm^2].

$$Z_0 = \rho_b \frac{L}{A} \quad (4.3)$$

Rearranging and incorporating (4.3) into (4.2):

$$SV = \frac{Z_0 \times A}{L} \cdot \frac{L^2}{Z_0^2} LVET \left(\frac{dZ}{dt} \right)_{max} \quad (4.4)$$

$$SV = A \times L \times LVET \frac{\left(\frac{dZ}{dt} \right)_{max}}{Z_0} \quad (4.5)$$

$$SV = VEPT \times LVET \frac{\left(\frac{dZ}{dt} \right)_{max}}{Z_0} \quad (4.6)$$

Where *VEPT* is the Volume of Electrically Participating Tissue of the thorax [m^3]. Absolute values of SV depend on a good estimation of VEPT and this is the primary difference between existing formulae [145]. Sramek and Bernstein estimate VEPT by modeling the thorax as a cylinder [146] and that the circumference C [m] of the lower part of the body at the xiphoid is roughly three times the measured linear distance between the electrodes regardless of age and sex [147].

$$C = 3L = 2\pi r \quad (4.7)$$

$$r = \frac{3L}{2\pi} \quad (4.8)$$

$$VEPT = r^2 \times \pi \times L \quad (4.9)$$

$$VEPT = \left(\frac{3L}{2\pi} \right)^2 \pi L = \frac{9L^3}{4\pi} \approx \frac{L^3}{1.4} \quad (4.10)$$

$$SV = \frac{L^3}{1.4} \times LVET \frac{\left(\frac{dZ}{dt} \right)_{max}}{Z_0} \quad (4.11)$$

Sramek reported that SV is overestimated in (4.11), and therefore changed the cylindrical model to that of a frustum and determined this volume to be one third of the cylinder.

$$SV = \frac{1}{3} \times \frac{L^3}{1.4} \times LVET \frac{\left(\frac{dZ}{dt} \right)_{max}}{Z_0} \quad (4.12)$$

$$SV = \frac{L^3}{4.2} \times LVET \frac{\left(\frac{dZ}{dt}\right)_{max}}{Z_0} \quad (4.13)$$

Finally Sramek determined that in a large normal adult population, the distance between electrodes L should be 17% of body height H [m].

$$SV = \frac{(0.17H)^3}{4.2} \times LVET \frac{\left(\frac{dZ}{dt}\right)_{max}}{Z_0} \quad (4.14)$$

In 1986 Bernstein [148] modified (4.14) by introducing the term δ (the actual weight divided by the ideal weight) which accounted for deviations from ideal body weight as established by Metropolitan Life insurance tables. The reason for this was to more accurately determine the volume of the thorax [139]. This resulted in the equation for SV :

$$SV = \frac{\delta \times (0.17H)^3}{4.2} \times LVET \frac{\left(\frac{dZ}{dt}\right)_{max}}{Z_0} \quad (4.15)$$

Once SV has been determined, the calculation of CO [l/min] can be performed easily by comparison and is given by:

$$CO = SV \times HR \quad (4.16)$$

4.4 Choice of Acquisition Methodology

The ICG is, in theory, the ideal system to be used for this application. Each of the relevant parts of the ICG has been identified and designed as described in Appendix C, as part of this project, while the investigation of the PhysioNet database was taking place. However, during the design process the complexity of the system became apparent. It also became evident that the implementation of such a system was outside the scope of the project, which was to develop an algorithm to enable a continuous BP monitoring system, rather than developing a full system to do the same. Once the algorithm was developed, it was clear that the ICG was the system that could be used to measure the required parameters as part of a non-invasive and wearable continuous BP monitor, but the algorithm was the primary focus of the work described in this thesis.

Since the PhysioNet Database had been shown to contain all the required parameters, it was considered to be a valid alternative to the use of the ICG system. Although using the PhysioNet Resource meant that PEP could not be included in the evaluation and development of a new algorithm, the major advantage of the PhysioNet Resource was that it contained beat to beat invasive measurements of ABP. This parameter is of significant importance when evaluating beat to beat and continuous based algorithms and when designing or deriving new algorithms, this parameter would also be of vital importance.

Therefore, the PhysioNet Resource was chosen as the tool to acquire all the parameters of interest for this application. Once the algorithm had been developed, it would then be possible to return to the ICG board to continue the development and implementation that were required for it to become operational and the entire system (the ICG and PTT systems) could be further tested on volunteers as the wearable system that was original envisaged.

To verify the database and identify its usefulness, it was decided that the algorithms discussed in Chapter 3 i.e. Chen and Poon, should be re-evaluated using the PhysioNet data. An added benefit of doing this would be that it would further emphasise the usefulness and accuracy of the algorithms used to convert PTT to BP using the existing algorithms.

4.5 Evaluation of Existing Algorithms using the PhysioNet Database

4.5.1 Testing Methodology

As discussed in Chapter 3, various authors have reported the benefits of the PTT method and there is no consensus as to which approach is best. Following the results discussed in chapter 3, a better understanding of the strengths and weaknesses of two of the existing algorithms i.e. those of Chen's and Poon's algorithms had been established. Since this new data resource was available, it was possible to re-examine these algorithms using a more comprehensive database to verify the results obtained previously. To this end, 15 subjects/records were chosen to examine this relationship and these algorithms. Three tests, each having a duration of 30 minutes were taken from each record, in a similar fashion to the original tests [128].

Although it was originally hoped that 15 records could be chosen at random (once the record had the required signals), it was quickly discovered that some records did not have sufficient signal quality, due to artifacts or noise. From the 16 complete records that were available, 15 records were found to have sufficient signal quality and continuous data over the 30 minutes required for the same analysis that had been performed in the original test.

4.5.2 Characteristic Point Extraction Algorithms

Although the specifics for extracting the characteristic points from each of the signals had been previously developed, new code and algorithms had to be developed so that the various peaks and points of interest could be extracted because of the change of quality of the signals. Most of the peak extraction algorithms that had been previously developed were equally applicable here i.e. the ECG R wave identification algorithm worked very well for this database, as it had when used on the original data. However, the most significant change was required when extracting data from the PPG signal.

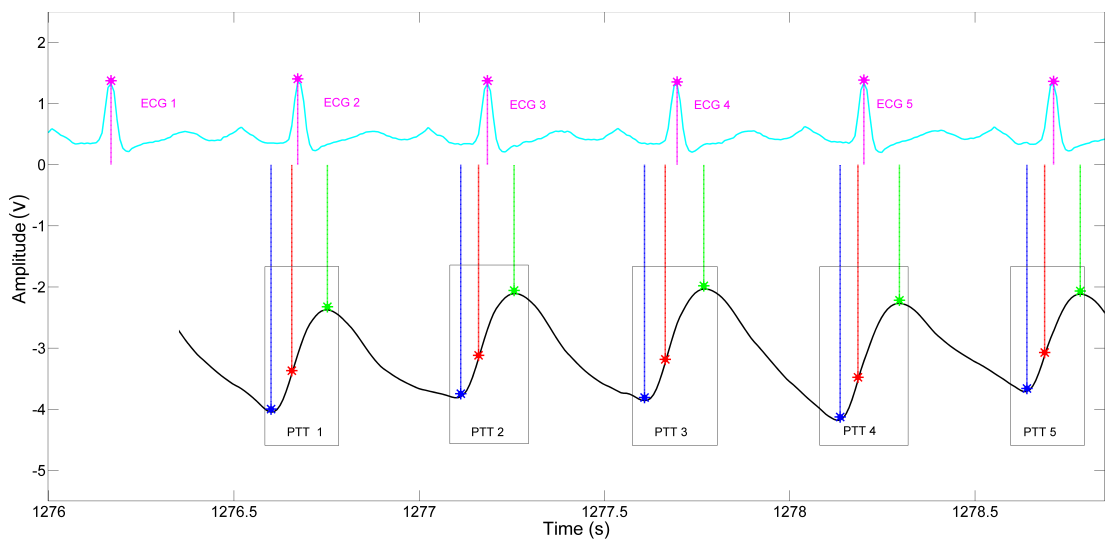


Figure 4.6: When the peak of the PPG wave was used to measure the PTT of some patients in this test, it was found that the peak occurred after the R wave of next cardiac cycle.

Upon initial investigation, it became apparent that using the peak of the PPG data was no longer valid as it was found that in some cases the PPG peak occurred after the subsequent ECG peak, as illustrated in Figure 4.6. In this figure, it is evident that the peak point of the PPG wave occurs after the ECG R wave of the next cardiac cycle. Due to the lack of information available for each

patient, it could not be established exactly why this was but from the records that were available, the only significant commonality was that the patients from the database were significantly older than the volunteers that had been tested in-house in Tyndall, which may have been a factor. However, in order to overcome this from an analytical perspective, various other characteristic points of the PPG wave were examined as alternatives to measure PTT. It has been previously established that other points of the PPG wave can be used to measure PTT and there is some debate as to which point is best. The points normally used to define the PTT are:

- The peak of the PPG wave
- The point of maximum inflection
- The onset of the PPG wave

The point of maximum inflection of the PPG wave is found by taking the first derivative of the PPG wave. The peak of this wave is the point of maximum inflection of the PPG wave. The peak (of the first derivative wave) was detected in a similar fashion to that described in the description of peak PPG wave detection, discussed previously in chapter 3 i.e. by using a combination of a threshold based technique and a minimum specific distance between points, as shown in Figure 4.7

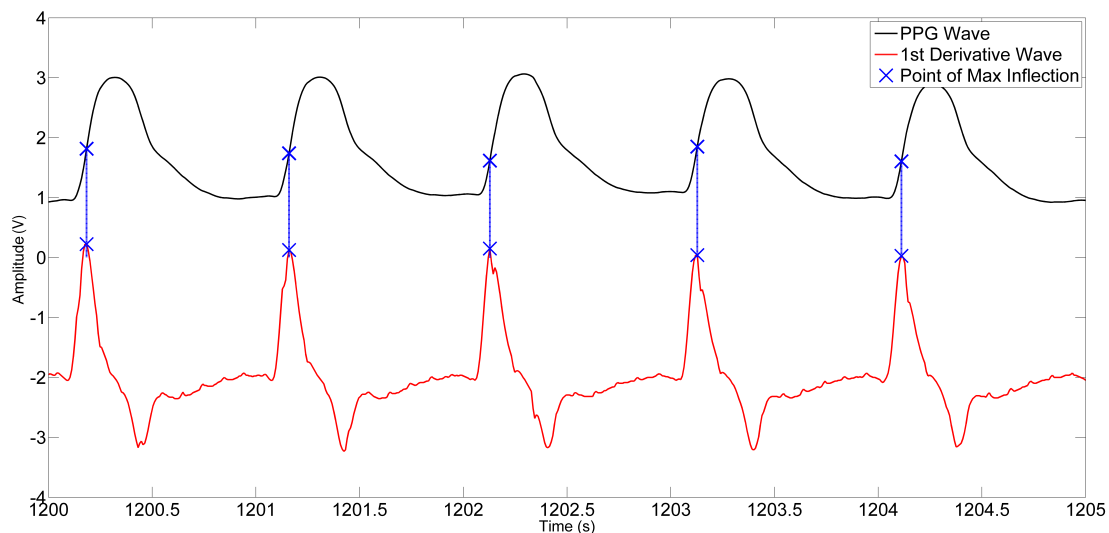


Figure 4.7: The use of the first derivative of the PPG wave to find the point of maximum inflection.

The onset of the PPG wave was detected using the second derivative of the PPG wave. However, it was found that the 2nd derivative of this wave was quite noisy,

as can be seen in green in Figure 4.8. So, the second derivative was filtered using a 30 point Moving Average Filter, and this helped to reduce noise and artifacts. It was found that the filtered 2nd derivative waveform, plotted in magenta in Figure 4.8, had similar characteristics to that of the ECG wave. In this signal there are numerous other peaks that could be misinterpreted as the point of interest which a thresholding based system could not differentiate from the point of interest. Similar to the ECG R peak, in this signal there was a sudden drop in amplitude after the peak of interest, similar to the S wave in the ECG signal, marked by a red star in Figure 4.8. It was decided that this characteristic "S" wave could be used to identify the point of interest and was identified by using a modified version of the ECG R wave detection algorithm, using a combination of a threshold and minimum distance approach to the inverted, second derivative filtered waveform.

The peak of this second derivative wave, which marked the onset point (blue star) was then identified by using the minimum distance and threshold approach, as well as specifying a maximum distance between it and the characteristic "S" point. Using all of these characteristics the location of the onset point of the PPG wave was identified, marked by a blue star in Figure 4.8 .

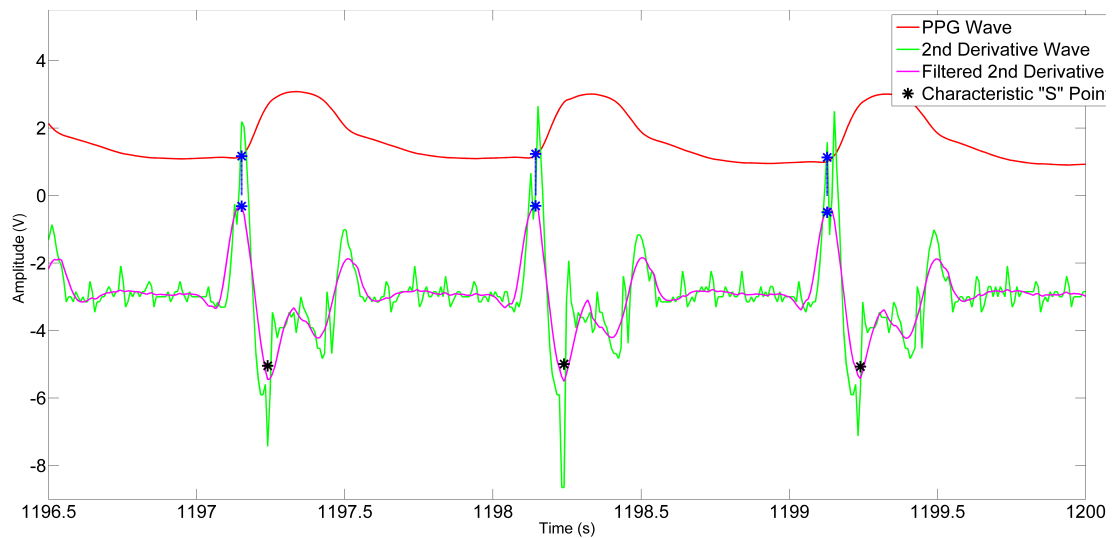


Figure 4.8: The characteristic points and waveforms used to identify the onset of the PPG wave.

It was noted that the quality of the signals was generally better than those that had been recorded from volunteers in the previous tests. The reason for the improvement in signal quality was because these new signals were recorded in a clinical setting, from much more expensive and precise pieces of equipment. This type of equipment generally employs various filters and technology that are not

generally available. However, some motion artifacts were still present throughout the test data. These artifacts were primarily with regard to either the ECG or the PPG sensor but the previously developed peak detection algorithms managed to deal with the minor artifacts. All other artifacts were found to be either too large to compensate for or the data quality around them was too poor to be of any use; an example of a large artefact can be seen in Figure 4.9. In this figure, a large artefact can be seen on the PPG signal, which affects the signal and foot detection algorithm for a few seconds before returning to a more typical signal. There is also a minor artefact present in the ECG signal; however, this does not adversely affect the peak detection algorithm.

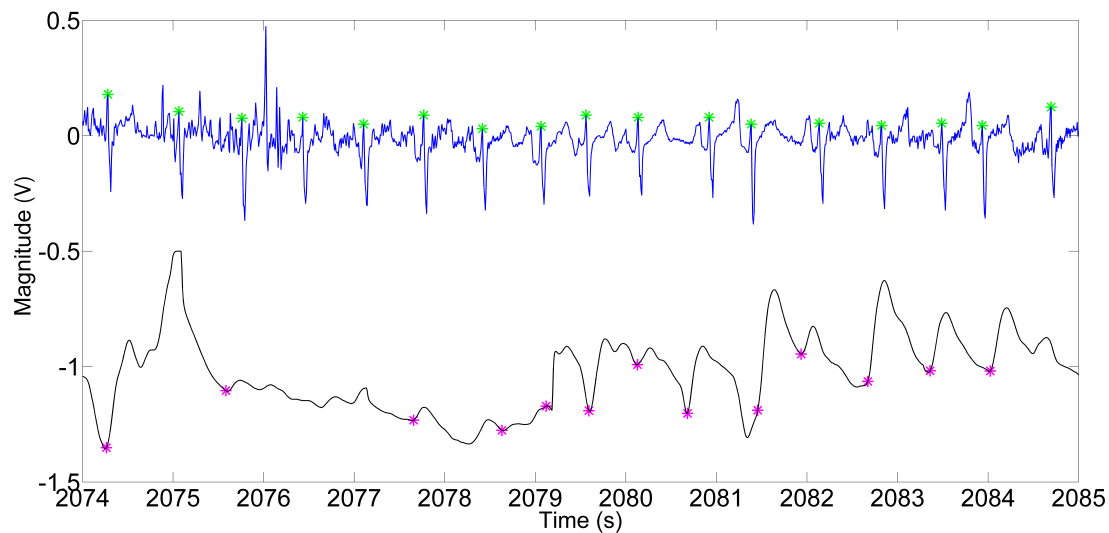


Figure 4.9: An example of both large artifacts (PPG signal in black with foot points in magenta) and minor artifacts (ECG signal in blue with R peaks in green) that were occasionally present among patients from the PhysioNet Database.

4.5.3 Systolic & Diastolic BP Determination from the Arterial Blood Pressure Wave

Both the Diastolic BP (DBP) and the Systolic BP (SBP) were derived from the Arterial BP (ABP) wave, the peak of the wave being the SBP and the trough being the DBP. The SBP was determined using the threshold and minimum distance based algorithm described earlier. The DBP was found in the same manner, but by using the inverse of the ABP wave. The method that had been developed for R peak detection was also found to be effective for extracting both of these values.

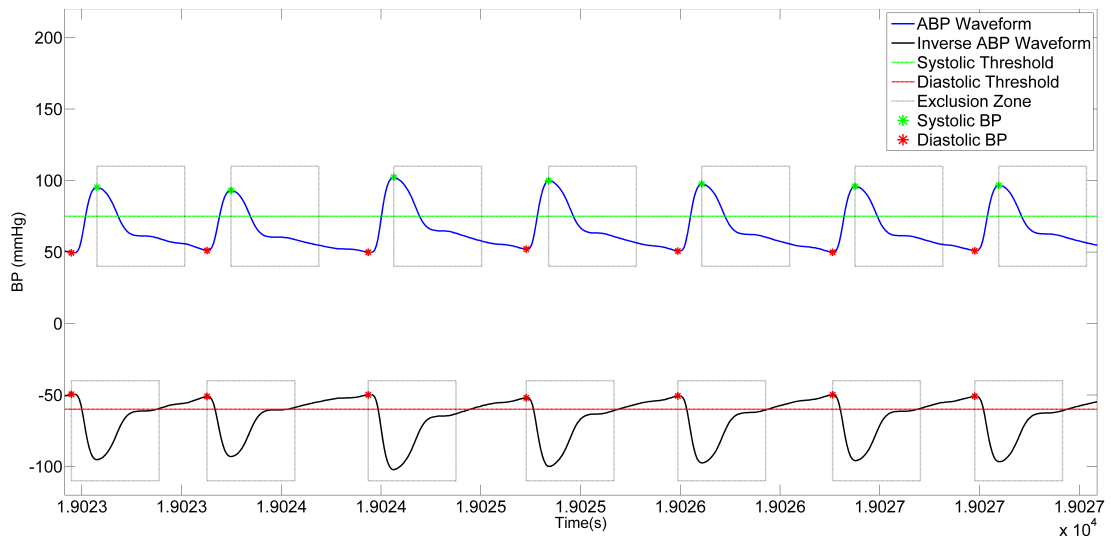


Figure 4.10: The steps required for calculating ABP.

4.5.4 Evaluating the Database

Table 4.1 shows the results of using Chen’s algorithm to track BP over each calibration interval, presented in the format used in the AAMI standard and Table 4.2 uses the BHS standard to evaluate Chen’s algorithm.

On examination of both Table 4.1 and Table 4.2, the point at which the filter becomes dominant is obvious. Up to and including the 6 minute calibration interval, a combination of the low frequency component and the filter that Chen uses, which seems to be tuned to a 5 minute interval, ensures the error always remains low and the effect of the filter is seen by the fact that all the errors occur in one direction only in Figure 4.11a and Figure 4.11b. However, the longer the calibration interval, the more dominant the filter becomes and the error becomes greater. This is further emphasised using the Bland Altman graphs (explained previously in section 3.10), Figure 4.11, where the standard deviation steadily increases over the 2 - 6 minute calibration intervals before dramatically increasing after each subsequent calibration interval.

In all of these graph, from Figure 4.11a through to Figure 4.11f, the number of outliers only slightly increases as the calibration interval grows. The reason for the growth in outliers is strongly linked with the growth of the error that is due to the characteristics of the HFC and the LFC in Chen’s algorithm. If there is a large change in BPs between measurements, the LFC is capable of accounting for these changes at lower calibration intervals. However, at higher calibration intervals, the error is completely dependent on the effect of the filter.

4. MEASURING STROKE VOLUME AND OTHER PARAMETERS

Table 4.1: A summary of the results overall and from each volunteer. Each result represents the mean error \pm the standard deviation of error between the Estimated BP, given by the PTT method, and Measured BP given by the ABP

<i>Volunteer</i>	<i>2 Minute Interval</i>	<i>4 Minute Interval</i>	<i>6 Minute Interval</i>	<i>8 Minute Interval</i>	<i>10 Minute Interval</i>	<i>12 Minute Interval</i>
pat 1	0.01 \pm 0.02	0.01 \pm 0.01	0.43 \pm 0.40	10.90 \pm 11.77	19.91 \pm 2.84	-27.43 \pm 5.96
pat 2	0.02 \pm 0.04	0.02 \pm 0.02	0.30 \pm 0.07	6.04 \pm 2.25	17.54 \pm 4.58	-22.56 \pm 11.13
pat 3	0.00 \pm 0.01	0.00 \pm 0.01	0.32 \pm 0.75	6.64 \pm 14.10	11.28 \pm 8.38	-5.20 \pm 19.80
pat 4	0.04 \pm 0.06	0.02 \pm 0.03	0.32 \pm 0.06	7.21 \pm 0.91	18.83 \pm 2.16	-30.39 \pm 5.54
pat 5	0.01 \pm 0.02	0.01 \pm 0.01	0.35 \pm 0.02	7.70 \pm 0.25	18.54 \pm 0.53	-34.63 \pm 1.18
pat 6	0.01 \pm 0.03	0.01 \pm 0.02	0.42 \pm 0.49	7.58 \pm 0.36	18.94 \pm 1.04	-33.45 \pm 2.15
pat 7	0.02 \pm 0.03	0.01 \pm 0.02	0.26 \pm 0.09	5.92 \pm 2.09	17.94 \pm 3.28	-21.76 \pm 16.58
pat 8	0.01 \pm 0.02	0.01 \pm 0.01	0.23 \pm 0.02	5.48 \pm 0.32	15.13 \pm 0.48	-23.90 \pm 2.20
pat 9	0.04 \pm 0.06	0.03 \pm 0.04	0.35 \pm 0.17	7.93 \pm 4.57	22.27 \pm 13.82	-30.27 \pm 3.84
pat 10	0.03 \pm 0.05	0.02 \pm 0.03	0.26 \pm 0.07	6.15 \pm 1.25	19.51 \pm 2.28	-13.55 \pm 15.58
pat 11	0.01 \pm 0.02	0.01 \pm 0.01	0.35 \pm 0.02	7.67 \pm 0.22	18.62 \pm 0.30	-34.37 \pm 1.16
pat 12	0.03 \pm 0.04	0.02 \pm 0.02	0.35 \pm 0.05	7.56 \pm 0.69	19.02 \pm 1.25	-32.44 \pm 4.74
pat 13	0.03 \pm 0.04	0.01 \pm 0.02	0.29 \pm 0.07	6.73 \pm 1.14	19.23 \pm 2.25	-27.38 \pm 8.33
pat 14	0.01 \pm 0.01	0.01 \pm 0.01	0.36 \pm 0.52	6.08 \pm 1.00	19.72 \pm 1.35	-21.34 \pm 8.74
pat 15	0.01 \pm 0.02	0.01 \pm 0.01	0.30 \pm 0.04	6.95 \pm 0.58	19.11 \pm 0.66	-28.24 \pm 6.60
All	-0.02 \pm 0.04	-0.01 \pm 0.02	-0.33 \pm 0.30	-7.08 \pm 5.10	-18.26 \pm 4.62	25.65 \pm 12.27

Table 4.2: A summary of the results using percentage predicted values falling within 5, 10 and 15 mmHg, based on the system for assessing BP measurement accuracy. Each calibration interval is assessed using this method and the associated BHS standard is provided in the last column. A rating of “B” is deemed acceptable, while a rating of “C” or “D” is deemed a fail.

<i>Volunteer</i>	<i>2 Minute Interval</i>				<i>4 Minute Interval</i>				<i>6 Minute Interval</i>			
	5 mmHg	10 mmHg	15 mmHg	Grade	5 mmHg	10 mmHg	15 mmHg	Grade	5 mmHg	10 mmHg	15 mmHg	Grade
pat 1	100%	100%	100%	A	100%	100%	100%	A	100%	100%	100%	A
pat 2	100%	100%	100%	A	100%	100%	100%	A	100%	100%	100%	A
pat 3	100%	100%	100%	A	100%	100%	100%	A	100%	100%	100%	A
pat 4	100%	100%	100%	A	100%	100%	100%	A	100%	100%	100%	A
pat 5	100%	100%	100%	A	100%	100%	100%	A	100%	100%	100%	A
pat 6	100%	100%	100%	A	100%	100%	100%	A	100%	100%	100%	A
pat 7	100%	100%	100%	A	100%	100%	100%	A	100%	100%	100%	A
pat 8	100%	100%	100%	A	100%	100%	100%	A	100%	100%	100%	A
pat 9	100%	100%	100%	A	100%	100%	100%	A	100%	100%	100%	A
pat 10	100%	100%	100%	A	100%	100%	100%	A	100%	100%	100%	A
pat 11	100%	100%	100%	A	100%	100%	100%	A	100%	100%	100%	A
pat 12	100%	100%	100%	A	100%	100%	100%	A	100%	100%	100%	A
pat 13	100%	100%	100%	A	100%	100%	100%	A	100%	100%	100%	A
pat 14	100%	100%	100%	A	100%	100%	100%	A	100%	100%	100%	A
pat 15	100%	100%	100%	A	100%	100%	100%	A	100%	100%	100%	A
All	100%	100%	100%	A	100%	100%	100%	A	100%	100%	100%	A

<i>Volunteer</i>	<i>8 Minute Interval</i>				<i>10 Minute Interval</i>				<i>12 Minute Interval</i>			
	5 mmHg	10 mmHg	15 mmHg	Grade	5 mmHg	10 mmHg	15 mmHg	Grade	5 mmHg	10 mmHg	15 mmHg	Grade
pat 1	0.00 %	84.62%	89.74 %	D	0.00 %	0.00 %	0.00 %	D	0.00 %	0.00 %	0.00 %	D
pat 2	12.82%	100 %	100 %	D	5.56 %	11.11%	11.11 %	D	15.15%	15.15 %	15.15 %	A
pat 3	74.36%	89.74 %	89.74 %	C	33.33 %	33.33 %	50.00 %	D	48.48 %	57.58%	66.67 %	D
pat 4	2.56 %	97.44 %	100 %	D	0.00 %	0.00 %	2.78 %	D	0.00 %	0.00 %	0.00 %	D
pat 5	0.00 %	100 %	100 %	D	0.00 %	0.00 %	0.00 %	D	0.00 %	0.00 %	0.00 %	D
pat 6	0.00 %	100 %	100 %	D	0.00 %	0.00 %	0.00 %	D	0.00 %	0.00 %	0.00 %	D
pat 7	25.64 %	100 %	100 %	D	2.78 %	2.78 %	8.33 %	D	6.06 %	6.06 %	9.09 %	D
pat 8	10.26 %	100 %	100 %	D	0.00 %	0.00 %	0.00 %	D	0.00 %	0.00 %	0.00 %	D
pat 9	0.00 %	95.83 %	95.83 %	D	0.00%	0.00%	0.00 %	D	0.00 %	0.00 %	0.00 %	D
pat 10	23.08 %	100 %	100 %	D	0.00 %	0.00 %	2.78 %	D	0.00 %	6.06 %	33.33 %	D
pat 11	0.00 %	100%	100 %	D	0.00 %	0.00 %	0.00 %	D	0.00 %	0.00 %	0.00 %	D
pat 12	0.00 %	97.44 %	100 %	D	0.00 %	0.00 %	0.00 %	D	0.00 %	0.00 %	0.00 %	D
pat 13	10.26 %	100 %	100 %	D	0.00 %	0.00 %	2.78 %	D	3.03 %	6.06 %	12.12 %	D
pat 14	17.95 %	97.44 %	97.44 %	D	0.00 %	0.00 %	0.00 %	D	0.00 %	6.06 %	24.24 %	D
pat 15	0.00 %	100 %	100 %	D	0.00 %	0.00 %	0.00 %	D	3.03 %	3.03 %	3.03 %	D
All	12.11 %	97.72 %	98.42 %	D	2.86 %	3.24 %	8.19 %	D	5.21 %	6.88 %	11.25 %	D

Although the general shape of the HFC is always the same, it has been observed that sometimes the magnitude of the change due to the HFC can be dramatically different. This can be seen in Figure 3.16a where there is very little change due to the HFC in the second interval (in red), while the change is much greater during the third interval (in magenta) and in Figure 3.16c where the change in magnitude of the HFC in the first interval (in blue) is much greater than the second interval (in red). It is these large changes that occur even within the same tests that are responsible for the outliers. As can be seen from Figure 3.16a and Figure 3.16c, the magnitude of the change, increases with the calibration interval. When there is a particularly large (inter-test) change in magnitude due to the HFC in the larger calibration intervals, the outlier is more prominent. For example, in Figure 4.11d the maximum outlier has an error of -60 mmHg, whereas in Figure 4.11f, the maximum outlier has an error of 120 mmHg.

Conversely, the results from Poon show a slight, albeit insignificant, improvement in results. In Chapter 3, it was established that Poon failed even when using the lowest calibration interval of 2 minutes. This was found to be the case again when the AAMI standard is used. However, when using this new database and the BHS standard, the results showed a slight improvement since the algorithm passes when a two minute calibration interval is used, but fails when a four minute calibration interval is applied. In the original test, one of the primary criticisms of Poon's algorithm was that it was quite noisy compared to the cuff measurements that were being used to evaluate it. In this test, the arterial systolic BP was available on a beat-to-beat basis and a more detailed analysis was possible. Comparing Poon's prediction to the ABP on a beat to beat analysis, it was found that the algorithm was capable of tracking BP to a much higher degree than the original results would suggest. Comparing Poon's algorithm to Chen's it can be seen that Poon's algorithm actually tracks changes in BP quite well, as shown in Figure 4.12.

The use of the foot of the PPG wave to define PTT, rather than using the peak of the PPG wave, as was the case in the previous chapter made no difference, because Poon's algorithm divides the beat to beat PTT value by its base value i.e. a normalised PTT value is used.

Tables 4.3 and 4.4 present the results of using Poon's algorithm on the data from the PhysioNet Resource. A noteworthy set of results was obtained from patients 1 and 4 where the standard deviations were found to be quite high throughout. This is highlighted by examining both Table 4.3 and Table 4.4, even at the lower

4. MEASURING STROKE VOLUME AND OTHER PARAMETERS

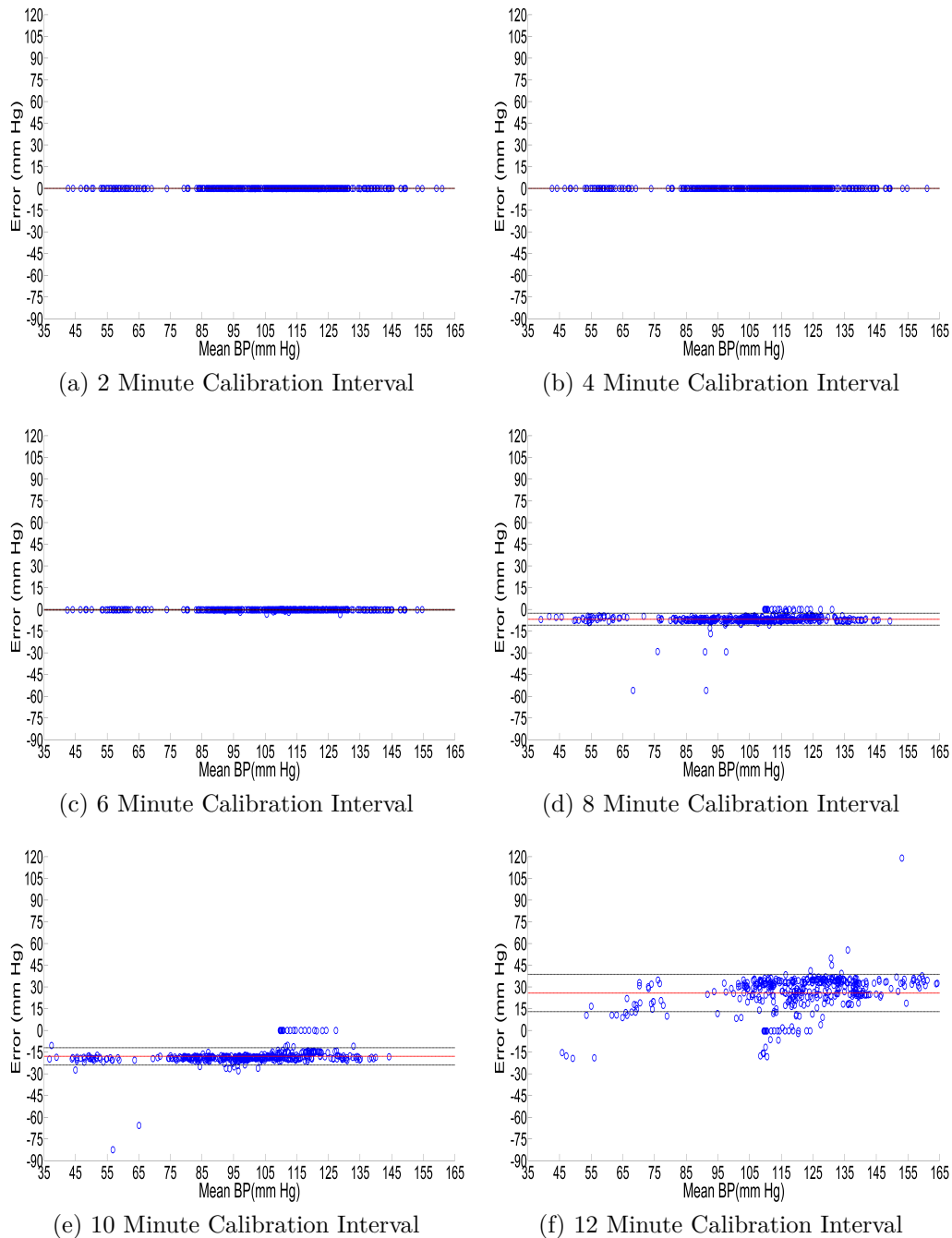


Figure 4.11: The Bland Altman graphs for Chen’s algorithm accumulated across 13 individuals for the six intervals (a - f). The deterioration of the results is seen by the increase in magnitude of the outliers and the growing errors at each interval.

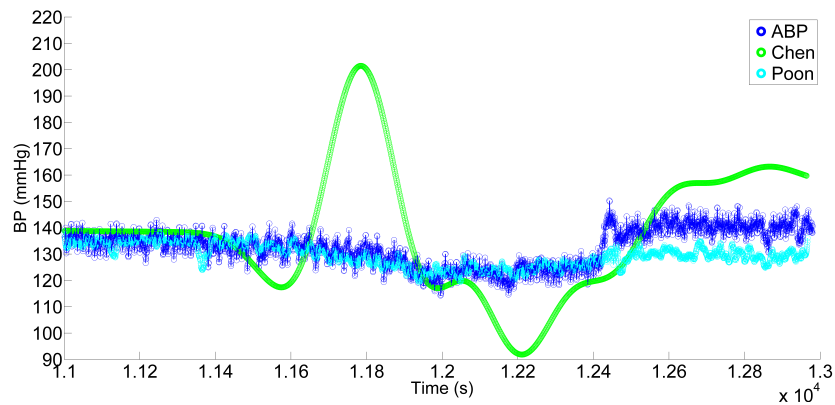


Figure 4.12: Poon’s algorithm (in cyan) is able to track the actual changes in ABP (blue) quite well, especially when compared to Chen’s prediction (in green)

Table 4.3: Evaluation of Poon’s algorithm with respect to the AAMI standard. Each result represents the mean error \pm the standard deviation of error between the Estimated BP, given by the PTT method, and Measured BP, given by the ABP.

Volunteer	2 Minute Interval	4 Minute Interval	6 Minute Interval	8 Minute Interval	10 Minute Interval	12 Minute Interval
pat 1	3.78 \pm 17.02	2.39 \pm 16.98	3.82 \pm 16.09	6.32 \pm 14.23	-0.15 \pm 14.34	-2.67 \pm 14.10
pat 2	0.32 \pm 6.65	0.82 \pm 8.64	1.17 \pm 9.70	2.25 \pm 11.54	2.68 \pm 12.53	4.15 \pm 11.29
pat 3	3.11 \pm 8.77	2.08 \pm 8.64	2.01 \pm 8.52	1.73 \pm 9.74	1.76 \pm 9.17	0.26 \pm 7.99
pat 4	-0.98 \pm 12.62	-0.68 \pm 11.78	-0.35 \pm 12.31	-1.27 \pm 12.76	-2.31 \pm 13.47	0.16 \pm 15.12
pat 5	-0.37 \pm 4.64	-0.75 \pm 5.03	-0.84 \pm 5.85	-1.43 \pm 6.19	-2.28 \pm 5.69	-2.28 \pm 6.05
pat 6	0.81 \pm 10.22	1.42 \pm 9.35	1.55 \pm 9.73	1.40 \pm 11.27	0.88 \pm 10.10	3.12 \pm 10.10
pat 7	-0.53 \pm 10.02	-1.07 \pm 11.18	0.16 \pm 11.67	0.19 \pm 9.95	0.00 \pm 7.05	1.78 \pm 8.57
pat 8	0.37 \pm 3.37	0.74 \pm 3.81	0.81 \pm 4.11	0.97 \pm 4.33	1.71 \pm 4.70	2.27 \pm 5.08
pat 9	0.48 \pm 9.60	1.40 \pm 14.42	2.71 \pm 16.18	4.04 \pm 16.25	2.93 \pm 14.59	1.05 \pm 12.77
pat 10	-1.34 \pm 8.01	-1.51 \pm 8.46	-1.87 \pm 6.78	-1.78 \pm 8.53	-1.92 \pm 8.62	-2.30 \pm 8.37
pat 11	-0.75 \pm 3.93	-1.09 \pm 6.04	-0.88 \pm 6.25	-0.57 \pm 6.22	-0.60 \pm 6.16	-0.70 \pm 5.99
pat 12	-0.34 \pm 10.11	-0.36 \pm 11.86	0.18 \pm 10.44	0.25 \pm 9.93	0.59 \pm 10.80	1.42 \pm 10.54
pat 13	-0.61 \pm 9.79	-0.66 \pm 9.03	-1.09 \pm 9.97	-1.98 \pm 11.95	-1.87 \pm 12.40	-1.67 \pm 9.81
pat 14	1.13 \pm 7.93	0.46 \pm 8.70	0.31 \pm 9.65	0.89 \pm 6.75	0.38 \pm 7.57	0.86 \pm 8.21
pat 15	0.43 \pm 3.23	0.72 \pm 3.77	0.93 \pm 4.28	1.25 \pm 4.75	0.94 \pm 4.04	1.10 \pm 6.68
All	-0.36 \pm 9.14	-0.24 \pm 9.69	-0.52 \pm 9.88	-0.73 \pm 10.09	-0.10 \pm 9.85	-0.42 \pm 9.77

calibration intervals. The reasons for this are unclear for *Patient 4*, but a possible explanation exists for *Patient 1* and this will be expanded below.

Examining Figure 4.13, a slight growth of outliers and growth of the standard deviation can be seen. Examining the “All” values of Table 4.4, in particular for the 4 minute calibration interval, it can be seen that the level of failure is very slight, the key number being the third percentages. A “B” rating or pass is awarded if the third percentage is greater than 90%. In the 4 minute calibration interval the algorithm fails by 0.61%. This shows the level of failure is quite slight and so observing this failure is not practical, especially by comparing the 2 and 4 minute calibration intervals, shown in Figure 4.13a and Figure 4.13b. The

4. MEASURING STROKE VOLUME AND OTHER PARAMETERS

Table 4.4: A summary of the results of Poon’s algorithm using the BHS standard. A rating of “B” is deemed acceptable, while a rating of “C” is deemed a fail.

Volunteer	2 Minute Interval				4 Minute Interval				6 Minute Interval			
	5 mmHg	10 mmHg	15 mmHg	Grade	5 mmHg	10 mmHg	15 mmHg	Grade	5 mmHg	10 mmHg	15 mmHg	Grade
pat 1	50.00%	66.67%	68.75%	C	31.11%	62.22 %	71.11 %	D	47.62%	71.43%	73.81 %	C
pat 2	70.83%	87.50%	95.83%	A	53.33%	84.44 %	93.33%	B	50.00%	76.19%	88.10%	C
pat 3	83.33%	87.50%	87.50%	C	84.44%	88.89 %	88.89 %	C	76.19%	88.10%	88.10 %	C
pat 4	25.00%	56.25 %	75.00 %	D	20.00%	64.44 %	75.56 %	D	28.57%	54.76%	78.57 %	D
pat 5	81.25%	95.83%	97.92%	A	73.33%	93.33 %	100 %	A	69.05%	90.48%	97.62 %	A
pat 6	58.33%	79.17 %	89.58%	C	46.67%	84.44 %	91.11 %	C	54.76%	80.95%	92.86 %	B
pat 7	58.33%	79.17 %	87.50%	C	46.67%	71.11 %	80.00 %	C	40.48%	69.05%	76.19%	B
pat 8	87.50%	100%	100%	A	84.44%	97.78 %	100 %	A	78.57%	97.62%	100%	A
pat 9	66.67%	78.79%	90.91%	A	43.33%	66.67 %	76.67 %	D	37.04%	55.56%	62.96%	D
pat 10	50.00%	75.00%	93.75%	A	51.11%	71.11 %	91.11 %	A	50.00%	80.95%	100%	A
pat 11	89.58%	95.83 %	100%	C	68.89%	88.89 %	95.56%	A	71.43%	92.86%	95.24%	D
pat 12	50.00%	77.08%	85.42%	C	48.89%	71.11 %	86.67 %	C	33.33%	71.43%	85.71%	C
pat 13	43.75%	79.17%	91.67%	B	55.56%	77.78%	91.11 %	B	52.38%	83.33%	92.86%	B
pat 14	66.67%	93.75 %	95.83%	A	71.11%	91.11 %	95.56 %	A	64.29%	88.10%	92.86%	A
pat 15	89.58%	100%	100 %	A	84.44%	100 %	100 %	A	80.95%	97.62%	100%	A
All	64.68%	83.55%	90.64%	B	57.88%	81.21%	89.39 %	C	56.10%	80.49 %	88.94%	C

Volunteer	8 Minute Interval				10 Minute Interval				12 Minute Interval			
	5 mmHg	10 mmHg	15 mmHg	Grade	5 mmHg	10 mmHg	15 mmHg	Grade	5 mmHg	10 mmHg	15 mmHg	Grade
pat 1	23.08 %	51.28%	71.79%	D	41.67%	58.33%	75.00%	D	27.27 %	54.55%	75.76%	D
pat 2	43.59 %	74.36%	82.05%	D	38.89%	63.89%	80.56%	D	39.39 %	66.67%	75.76%	D
pat 3	58.97 %	82.05%	84.62%	C	58.33%	83.33%	83.33%	C	60.61 %	87.88%	87.88%	C
pat 4	35.90 %	64.10%	79.49%	D	22.22%	52.78%	63.89%	D	30.30 %	51.52%	69.70%	D
pat 5	53.85 %	92.31%	94.87%	B	66.67%	83.33%	100 %	B	54.55%	87.88%	96.97%	B
pat 6	43.59 %	71.79%	84.62%	C	44.44%	75.00%	88.89%	C	54.55 %	75.76%	87.88%	C
pat 7	41.03 %	82.05%	87.18%	C	50.00%	86.11%	97.22%	C	39.39 %	81.82%	93.94%	C
pat 8	74.36%	97.44%	100 %	A	80.56%	91.67%	100 %	A	66.67 %	90.91%	100 %	A
pat 9	25.00%	50.00%	58.33%	D	33.33%	47.62%	76.19%	D	27.78 %	55.56%	77.78%	C
pat 10	33.33%	74.36%	94.87 %	A	44.44%	75.00%	86.11%	A	42.42 %	72.73%	87.88 %	A
pat 11	66.67%	87.18%	97.44%	D	69.44%	86.11%	97.22%	D	69.70 %	87.88%	100%	D
pat 12	41.03%	64.10%	82.05%	B	38.89%	66.67%	83.33%	B	33.33 %	72.73%	84.85%	D
pat 13	58.97%	84.62%	94.87%	D	44.44%	75.00%	91.67%	C	36.36 %	69.70%	84.85%	C
pat 14	69.23%	92.31%	97.44%	A	61.11%	91.67%	97.22%	A	60.61 %	87.88%	96.97%	B
pat 15	74.36%	94.87%	97.44%	A	77.78%	97.22%	100 %	A	78.79 %	93.94%	96.97%	A
All	50.18%	78.25%	87.89%	C	52.00%	76.38%	88.38%	C	48.75 %	76.46%	88.13%	C

expansion of the cluster is more apparent in Figure 4.13e and Figure 4.13f, as are the growing number of outliers, but part of this is due to fewer data points being recorded for these intervals.

Examining both the AAMI and BHS evaluation tables, it can be seen that if Patients 1 and 4 were omitted from the examination a clear improvement in Poon’s results would be observed. Although the SV recorded from Patient 1 is quite high, which could be an indicator of some other illness which may affect these results, there is no other information available about their health nor is there any information available from Patient 4, whose physiological signals are well within the normal distribution. Therefore, without a reasonable explanation, neither of these patients and their associated results can be nor should be omitted from the tests and thus the results must be included.

In the original examination of Poon’s algorithm, described in Chapter 3, the greatest criticism of Poon’s algorithm was that it provided a very “noisy” estimation when compared to the intermittent cuff measurements. However, when Poon’s estimation is compared to ABP, it can be seen that it frequently does not track changes in the BP by a large enough degree. An example of this can be

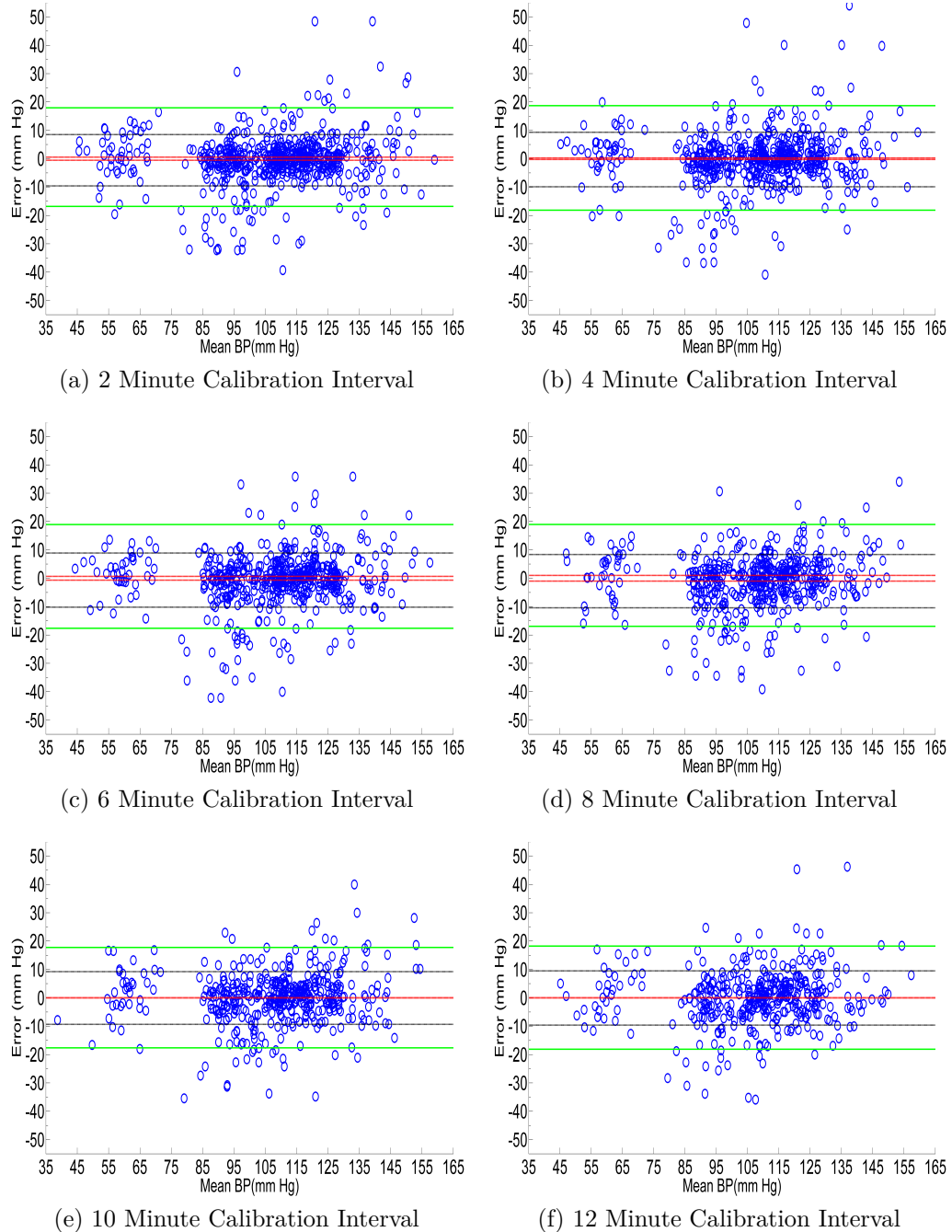


Figure 4.13: The Bland Altman graphs for Poon’s algorithm accumulated across 13 patients for the six intervals (a - f). The deterioration at the 4 minute calibration interval is practically unobservable but is more apparent for longer calibration intervals

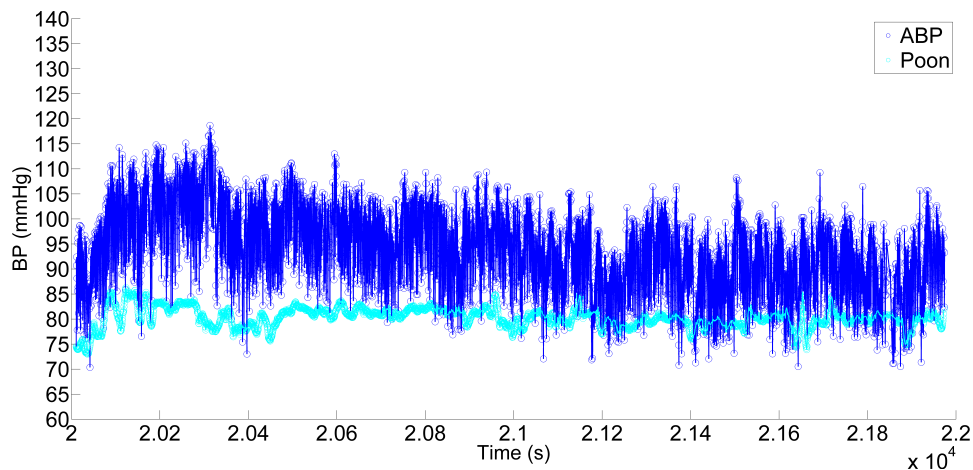


Figure 4.14: Poon's algorithm (in cyan) and its ability to track the measured ABP (in blue). The problem of Poon's algorithm occasionally not tracking changes in BP by a large enough amplitude

seen in Figure 4.15 where although Poon's algorithm increases and decreases as the BP does, the amplitude of the prediction is only a fraction of the amplitude of the actual change in BP.

Unfortunately, this is not the only criticism of the algorithm. It has been noticed that there is frequently a poor initial estimation that is greater than 5 mmHg, a critical value in both standards, as can be seen in Figure 4.14. This estimation is usually corrected after the calibration interval has elapsed. When the calibration interval is short, these errors, due to poor initial estimations, are not very noticeable because there are a lot of other data points that are within the standards i.e. when using a 2 minute calibration interval for each patient, 15 measurements are taken over 30 minutes and a poor initial estimation could mean only one of the 15 measurements is outside the standards. However, as the calibration interval increases, the error due to a poor initial estimation becomes more significant and noticeable because fewer data points are being measured i.e. at a 12 minute calibration interval, only 10 intervals can be examined (i.e. 0 - 12 minutes, 2 - 14 minutes, 4 - 16 minutes, 6 - 18 minutes, 8 - 20 minutes, 10 - 22 minutes, 12 - 24 minutes, 14 - 26 minutes 16 - 28 minutes and 18 - 30 minutes), and a large error due to a poor initial estimation has a much greater influence on the results.

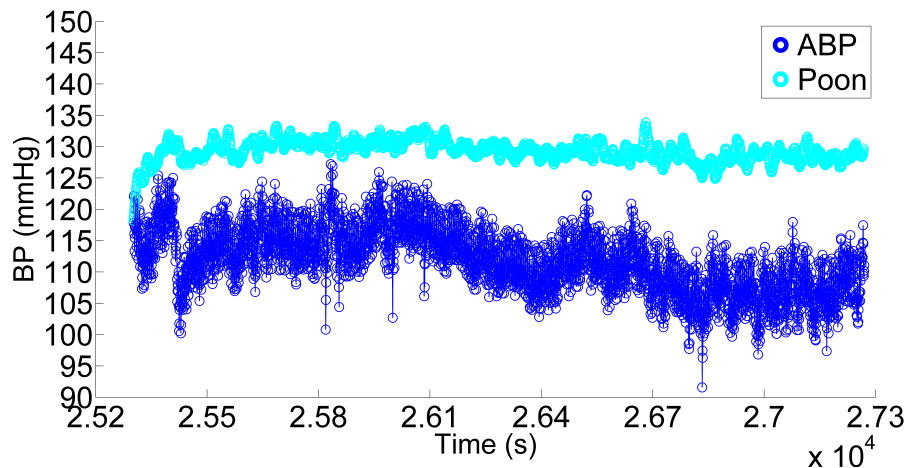


Figure 4.15: Poon’s algorithm (in cyan) and the large offset that is prominent in many of its predictions of ABP (in blue).

4.6 Conclusions

The purpose of the work described in this chapter was to find a method to measure Stroke Volume and associated parameters so that they could be included in a new algorithm that would improve the existing PTT algorithms. Two methods of doing this were investigated, the use of an ICG and the use of the PhysioNet Resource.

The PhysioNet Resource and its associated database provided most of the physiological signals that were required for this investigation. Using selected databases of all those that were available, namely the MIMIC database and the Challenge Sets from 2009, it was possible to find 15 records with all the required signals, over the required duration, that would allow PTT along with SV and all associated parameters to be measured.

Although the objective of this project is to develop an algorithm, an important feature is that any algorithm that is developed must originate from calculating signals that can be recorded using a non-invasive method and ideally that could be part of a wearable system. One technique that would allow this would be through the use of an ICG because it can measure all the relevant parameters and it only requires an extra few electrodes. However, during the design of the ICG system outlined in Appendix C, it became apparent that the implementation of the ICG board was outside the scope of the project and it was far more important to develop the algorithm. In this regard, the PhysioNet Resource has more benefits for investigating and developing a new algorithm. The primary advantage of the PhysioNet Resource was that the ABP was readily available. This ensured that

any algorithm that was evaluated could be studied on a beat to beat basis, rather than the intermittent cuff measurements that would need to be used if the ICG and PTT systems were used.

In an attempt to confirm the value of the database, the tests from Chapter 3 were re-run using this database. Although the results from Chen's algorithm were almost identical to those that had been found previously, the results from Poon's algorithm were significantly different. In a similar fashion to the original test where Poon's algorithm failed even when using the shortest calibration interval of 2 minutes, when using the PhysioNet database the algorithm was found to also fail using a 2 minute calibration interval.

In the original test, Poon's algorithm was compared to cuff measurements of BP once every two minutes. In this database, continuous ABP was available and a beat to beat comparison could be made between Poon and the actual changes in BP. It was noted in Chapter 3 that when compared to the cuff measurements, Poon's prediction was quite noisy but showed some potential. When it was compared to ABP though, it was found that in many cases the prediction was actually quite good. However, as good as the improvement was in some cases, there were still a number of problems among the other tests and records. Two common and frequent problems were identified where either the prediction gave a large offset or its amplitude didn't change enough when compared to changes in the actual BP. Depending on the severity of either of these, it is possible that Poon's algorithm could have been deemed to be acceptable, but since these problems arose frequently and since the algorithm performed poorly for two patients in particular, the maximum calibration was found to be only 2 minutes. This further emphasises the case that neither Poon's nor Chen's algorithms could be deemed to be useful or practical for clinical use or any other practical applications.

Although there has been a slight change in the results due to the use of direct beat to beat measurements, especially with Poon's calibration interval increasing from 0 to 2 minutes, the overall findings of Chapter 3 remain valid and neither of these algorithms are capable of tracking BP for enough time to be usable in a practical setting. This suggests that an improvement in the PTT method is still required. Now that the PhysioNet database has been shown to be even more useful than originally hoped, due to its access to ABP and the fact that it can provide SV along with other parameters of interest, it is possible to develop and test a new algorithm that can improve on the PTT method through the inclusion of new parameters which could ultimately be measured by ICG.

Chapter 5

Deriving a Novel Blood Pressure Tracking Algorithm

5.1 Introduction

The various approaches that were adopted during the development of an algorithm that would improve on the existing PTT algorithms that are needed to track BP are discussed in this chapter. The goal of this thesis was clear: to improve on the state of the art in blood pressure monitoring through the development of a new algorithm. The algorithm developed in this work is based on the premise that the inclusion of additional parameters into existing equations would allow better tracking of BP, for a longer duration, so that it would make the algorithm practically and clinically useful.

Using the PhysioNet database, a number of new parameters was available and had been identified from the outset and the first section deals with identifying which of the available parameters would have the greatest significance. The interaction between these parameters was identified by using a combination of a number of different methods: Correlations, Draftsman Graphs and Semblance Analysis. Each of these had certain advantages, which are discussed in section 5.2.

Section 5.3 describes how Multiple Linear Regression was used in an attempt to initially derive the algorithm. Multiple Linear Regression (MLR) uses a constant set of variables and a corresponding set of weights to predict a known output. By examining multiple sets of inputs and outputs and the weights associated with them, a general set of weights can be derived that would provide an algorithm

for a good prediction of BP, regardless of the inputs. This will be explained in more detail during this section. The evolution of the MLR equations, starting with the most general equation and then using the results from this evaluation, along with the results from the first section to narrow down the variables and get better results, is also discussed. Although this method proved to be ultimately unsuccessful, due to statistical and mathematical concerns, it was an important part of the development process. Each of the MLR algorithms that performed well was found to have two parameters in common, and despite the mathematical concerns due to the derivation of an algorithm using MLR, the identification of these critical parameters via MLR allowed alternative methods of derivation to focus on the inclusion of these parameters in one algorithm.

The final derivation of the new BP monitoring algorithm is described in Section 5.4. Due to concerns and limitations with regard to the MLR derived equations, it was felt that a more universally applicable algorithm should be possible. By examining existing PTT equations, the variables that were identified via the use of the MLR and through other statistical methods from the previous sections, a new algorithm was derived by the use of some fundamental fluid dynamics relationships. This new algorithm was then evaluated and compared to the other approaches, all of which are discussed in detail in this chapter.

5.2 Identifying Parameters of Interest

The first step in deriving a new algorithm is to identify the most relevant variables that should be included. Although a number of parameters that should be investigated [90, 149, 150] had been identified in the literature, these were only suggestions and it was not clear if any previous work had been carried out to see if including these parameters would make an improvement. Therefore, it was necessary to investigate each variable and examine its relationship to BP.

The most fundamental way to identify the relationship is to plot the variable of interest e.g. PTT over a certain period side-by-side against the desired outcome e.g. Systolic BP. Figure 5.1 shows two examples of such a plot, comparing PTT and measured BP from two different patients. In Figure 5.1a, the relationship between this patient's BP and PTT is not immediately apparent, whereas in Figure 5.1b, it is clear there is an inverse relationship between the parameters. This is confirmed in the literature [57]. Although this method is easy to implement, its limitations are quite obvious when Figure 5.1a is examined for a relation-

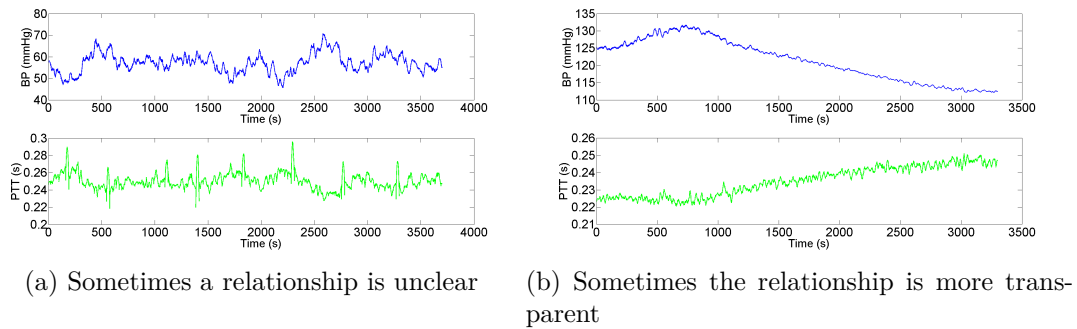


Figure 5.1: Identifying relationships between variables is not always apparent

ship. Furthermore, identifying relationships by eye is not a scientifically sound approach and it has no underlying mathematical rigour associated with it and so a more scientific method was sought.

5.2.1 Direct Correlations

A more mathematical approach was taken to examine the correlation between the two variables. One way to do this is to sample each of the continuous signals at certain intervals e.g. once a minute over 30 minutes, and plot the results against each other. Then, by finding the line of best fit between them, it is possible to find the correlation between the two variables. This is a very simple method and provides an easily identifiable quantification factor, so that the relationships between factors are very easily established.

To this end, an expansion of the correlation graphs was implemented using what is known as a Draftsman's Chart [151]. Figure 5.2 shows one of these Draftsman's Charts for one particular patient. In this example, five parameters were investigated to determine the relationships between them, and to identify which parameters show the strongest relationship with the other parameters. In a Draftsman Chart each parameter is plotted against each other in an $n \times n$ matrix. Therefore, the centre spine of the graph plots the first variable versus itself, the second variable versus itself etc. The correlation of each graph is then also plotted in a matrix and using this method it is easy to get a summary of the relationships between the selected variables. This tool is frequently used with Principle Component Analysis [151], and, as long as representative data is used and analysed, it can quickly be used to identify the strongest relationships of the variables being examined.

5. DERIVING A NOVEL BLOOD PRESSURE TRACKING ALGORITHM

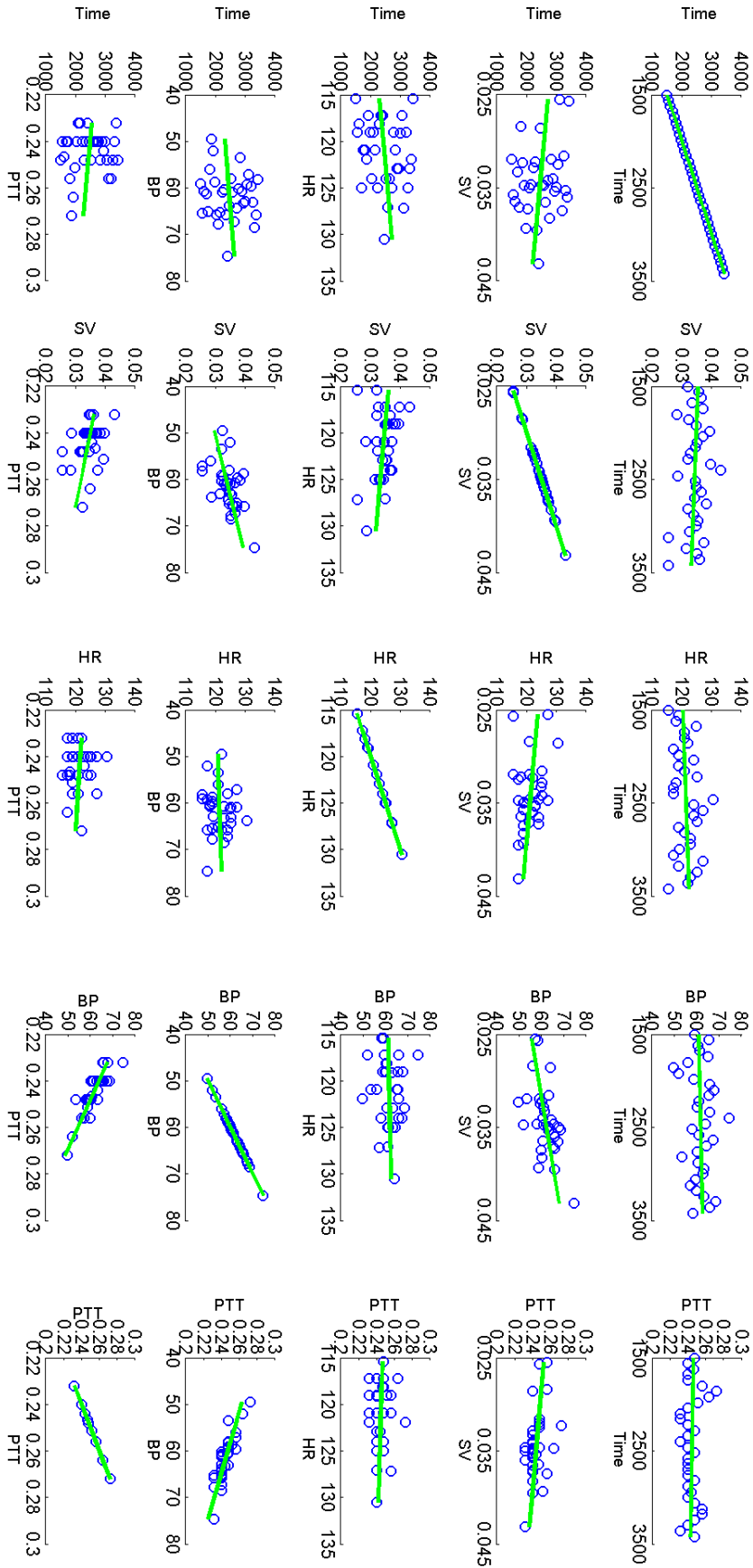


Figure 5.2: An example of a Draftsman's Graph for one patient examining Time, BP, SV, HR and PTT.

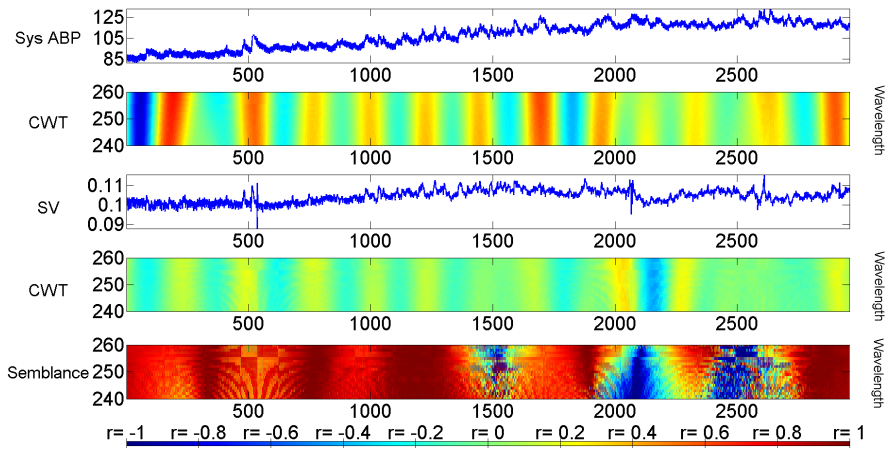
5.2.2 Semblance Analysis

Although using Draftsman Charts can provide a good indication of expected values and relationships, it relies on sampled data and, because of this, it can be difficult to ensure that all the data being examined is representative in that the sampled data does not contain outliers or motion artifacts for example. Therefore, other approaches were also investigated to find a quantification method that would work for continuous data, rather than sampled data, and would allow a rapid identification of well or badly correlated relationships (where continuous refers to the “continuous signals” taken from the PhysioNet database).

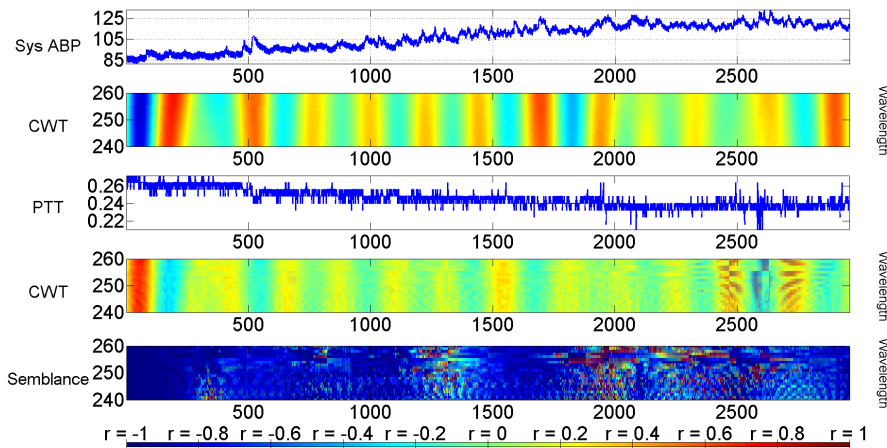
One way to do this is by using semblance analysis. Semblance analysis is primarily used for the analysis and study of seismic data, but has recently been adapted to examine the correlation between two time series signals, which do not need to be measured using the same units [152]. With this adaptation, semblance analysis can now be used as a graphical tool that examines the correlation between two continuous signals. Each continuous signal is transformed using a Continuous Wavelet Transform (CWT), a mathematical tool. Then, a correlation analysis is performed between the two transformed signals, the results being plotted using coloured graphs where red indicates a strong correlation ($r=1$), blue indicates a strong negative correlation ($r=-1$) and green indicates no correlation ($r=0$). It is important that when examining the graphs, the correct scale/wavelength is examined, as determined by the sampling rate of the signals.

From Figure 5.3, the relationships between different signals can be immediately identified. Many of these relationships had been identified previously using the sampled data in the Draftsman charts, but by using semblance analysis it is possible to confirm that these relationships are also valid on a continuous basis. Examining 5.3b, it is also evident that semblance analysis is relatively noise resistant in so far as there is a little noise associated with both signals but the anti-correlation is still evident, not only in the time series graph, but also and more importantly in the semblance graph. Figure 5.3a however, shows the limits of the noise tolerance, where an artefact is apparent in the SV data at around 2100 seconds. At this point in the semblance graph, there is a sudden anti-correlation which is not representative of the data on either side of the artefact. Figure 5.3c, shows the final scenario where there is no consistency with regard to the semblance analysis. This is also representative of previously examined HR analysis, that had been recorded when direct correlations had been examined using Draftsman Charts, where correlations seemed to vary from patient to patient.

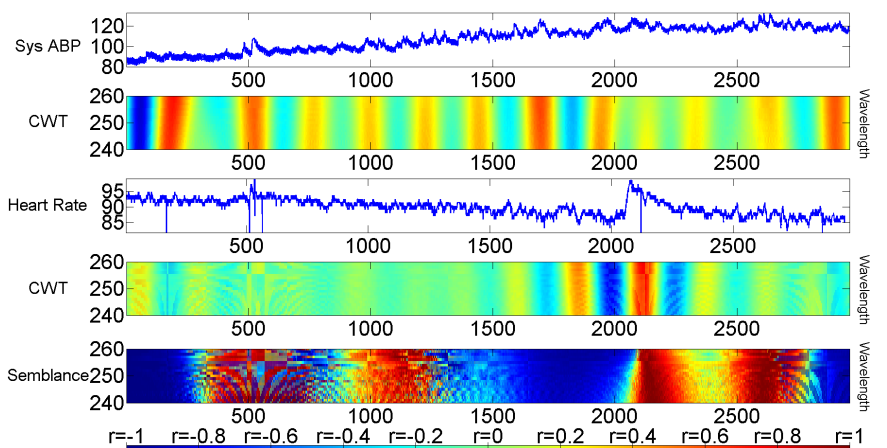
5. DERIVING A NOVEL BLOOD PRESSURE TRACKING ALGORITHM



(a) Semblance Analysis of SV vs. BP with a strong positive correlation



(b) Semblance Analysis of PTT vs. BP with a strong anti-correlation



(c) Semblance Analysis of HR vs. BP. A mixed correlation is seen throughout and is repetition of what was seen previously

Figure 5.3: Examining the semblance analysis of various parameters. A quick glance is enough to reveal what type of relationship exists between signals

Table 5.1: A summary of the results from the semblance analysis comparing various parameters and combinations of them to BP.

Parameter Under Test	$r \approx 1$	$r \approx -1$	Mostly Strong	Mostly Weak	More Analysis
PTT		✓			Yes
SV	✓				Yes
HR			✓		Yes
CO				✓	No
SV × PTT			✓		Yes
$\frac{SV}{PTT}$	✓				Yes
SV ² × PTT				✓	No
$\frac{SV^2}{PTT}$			✓		Yes
SV × PTT ²				✓	No
$\frac{SV}{PTT^2}$	✓				Yes
(SV × PTT) ²			✓		Yes
$(\frac{SV}{PTT})^2$	✓				Yes

Using this technique it was possible to investigate multiple parameters across each of the patients and each of the respective 45 tests very quickly. Each parameter was compared to BP and if a semblance graph was found to be mostly red or mostly blue, the parameter under test was classified as being of potential use and a parameter of interest to the extent that more analysis should be carried out. These parameters and combinations thereof were investigated and depending on their results, were categorised as outlined in table 5.1.

5.3 Multiple Linear Regression

In Multiple Linear Regression (MLR), the objective is to build a probabilistic model that relates a dependant variable Y to more than one independent or predictor variables [153]. If k is the number of independent variables, and x represents these variables, the general expression is

$$Y = \beta_0 + \beta_1 x_1 + \beta_2 x_2 + \beta_3 x_3 + \dots + \beta_k x_k + \epsilon \quad (5.1)$$

Where ϵ is the error term of the prediction and has an important role when using MLR for certain situations in statistics e.g. finding which of the input variables has most influence in the outcome of a prediction. In most situations, ϵ must also adhere to certain assumptions, such as having a normal distribution, but due to the particular application described in this work, ϵ does not have a major

statistical impact or role in the following sections. In this application MLR is only being used to derive an algorithm rather than identify or infer statistical meanings or relationships.

For the most general and simple application in this work, Y would be the BP, x_1 would be PTT, x_2 would be SV, x_3 would be HR etc. Using Matlab [122] or similar, it is possible to calculate β for each respective x value. β_0 provides what is essentially an offset and each subsequent β value represents a weighting factor which determines which variables are most strongly related to BP and which can be used to predict the BP at any particular point. From section 5.2, it is expected that certain parameters will dominate any MLR equation that is derived and certain combinations of those parameters, especially those identified in Table 5.1, should also provide good predictors for BP. A description of how the β values were derived is firstly discussed and applied, while the following subsections describe the evolution of the MLR algorithm starting with its most basic form as seen in equation 5.1 and proceeding to its most complex form, based on the parameters identified previously, such as SV, PTT and to a lesser extent HR.

5.3.1 Deriving β values and Testing Algorithm 1-x

The first equation that was analysed was

$$BP = \beta_0 + \beta_1 \times PTT + \beta_2 \times SV + \beta_3 \times HR + \epsilon \quad (5.2)$$

Since this was the first attempt at deriving an algorithm, it was called *Algorithm 1*. It was realised at this stage that this first attempt would not be the solution to relate BP to the various other parameters being investigated and a few iterations would be necessary to find such a solution. For this reason, it was decided that each different algorithm would be named using the following convention:

A major change to the method by which the algorithm was derived would be denoted by an increase of the letter M in *Algorithm M*, whereas minor changes would be denoted by a change in the letter x in *Algorithm M - x*. An example of a minor change in the algorithm can be seen across equations 5.2 to equation 5.4, where the inverse of each of the parameters is sequentially chosen and each equation is investigated as a potential solution i.e.

$$BP = \beta_0 + \beta_1 \times \frac{1}{PTT} + \beta_2 \times SV + \beta_3 \times HR + \epsilon \quad (5.3)$$

was denoted Alg. 1-2,

$$BP = \beta_0 + \beta_1 \times PTT + \beta_2 \times \frac{1}{SV} + \beta_3 \times HR + \epsilon \quad (5.4)$$

was denoted Alg 1-3, and so on. As the tests progressed, the number of different “x” tests were reduced since a pattern emerged on which configurations of parameters worked best. When the correlation tests and semblance tests from the previous section were considered as part of the evolution of the MLR tests, the reason for these patterns became obvious. It was found that any algorithm which contained the parameters with the strongest linear relationship to BP performed the best, i.e. any algorithm that contained $BP = \dots + \frac{1}{PTT} \dots$ or $BP = \dots + SV \dots$ was shown to perform much better than algorithms that did not have these parameters, in this configuration.

If there was any major change to the form of the algorithm, the Algorithm number increased e.g. from Algorithm 1, to Algorithm 2. An example of a major change would be an elimination of one of the parameters of interest or another change which would have a major impact on how the algorithm was derived or applied.

From the most fundamental point of view, the β values of equation 5.2 were derived by using Matlab or a similar type of program from the independent variables. As described in Chapter 4, all of the data described was taken from 15 patients over three half hour periods, which were known as tests, taken from each patient. The independent variables, as previously discussed, were HR, SV and PTT, and were derived from the continuous beat to beat data, from each of the 45 tests.

Each MLR equation that was derived would provide different β values, each one providing very specific β values for each of the 45 tests. An important point to note is that because of the variance of the parameters from each test, it was necessary to find a way that a general β could be derived and applied in such a way that would satisfy every test. The most obvious way to do this would be to take an average β for each of the independent variables, i.e an average β_0 , an average β_1 for PTT, an average β_2 for SV etc. The problem with this was that, due to the nature of physiological signals, the BP's and other parameters of each patient could be vastly different and if, for example, one patient had a

particularly low BP, by only taking an average value of β_0 , the resulting β_0 could be skewed by that one patient (with a low BP). Therefore the median of each β value was also calculated. The median is the centre value of all available data points and is used to compensate for outliers. For completeness, the mode of each β value was also examined. This extracts the most commonly used value; however, after a brief investigation the mode value was omitted because it was found that, in general, the β values were rarely repeated.

Two other values were also examined. From examining the median values, it was found that the median value was quite often not the centre value. The reason for this was not clear but one possible reason was that in most tests, at least one large outlier was observed. While Excel would include this outlier when calculating the median value, it was found that by omitting it, a more accurate median value could be calculated. In an attempt to determine the actual centre value two new values were examined. These values were derived by creating a histogram of all the available data points, divided into twenty groups or bins, going from the minimum value to the maximum value in equal jumps, shown in Figure 5.4. A second histogram was then created which focused on the centre of the first histogram, or the values of the first histogram that would give a normal distribution, if the outliers were ignored, in this scenario -10 to 215 . This histogram was divided into ten bins, as shown in Figure 5.5. Finally, the three or four bins with the most data points were then examined and all values that fell into these three or four bins were examined for the median and average values, i.e. all values between -10 and 65 . These two values were simply known as the *histogram_average* and the *histogram_median*. In the example shown here, the median calculated by Excel was found to be 32.65 but the *histogram_median* was found to be 1.34 .

During this initial test, one final β derivation was investigated via the use of standardisation, also known as calculating the standard scores or the z scores of the variables. The z score of a variable x is calculated by:

$$z = \frac{x - \mu}{\sigma} \quad (5.5)$$

where μ is the average of all the x values and σ is the standard deviation of the x values.

In this test, each of the variables was standardised before the β values were derived. This was investigated to determine which variables were the most dominant

<i>Bin</i>	<i>Value</i>
1	-10
2	65
3	140
4	215
5	290
6	365
7	440
8	515
9	590
10	665
11	740
12	815
13	890
14	965
15	1040
16	1115
17	1190
18	1265
19	1340
20	1415

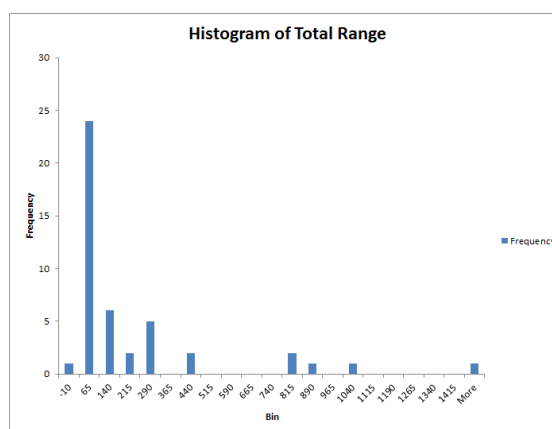


Figure 5.4: A histogram of all the β_1 values calculated for one of the first tests.

<i>Bin</i>	<i>Value</i>
1	-10
2	15
3	40
4	65
5	90
6	115
7	140
8	165
9	190
10	215

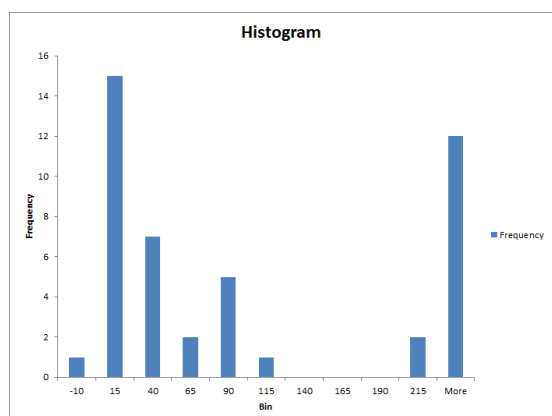


Figure 5.5: A more focused histogram concentrating on the centre values of the β_1 values that had been calculated for the same tests.

when correctly predicting changes in BP. These “ β ” values were denoted with a z to differentiate them from the non-standardised derived values. i.e. β_z .

Therefore, β_0 , β_1 , β_2 and β_3 values were derived from the 45 tests. Each respective β value varied depending on the equation from which it was derived i.e. β_1 derived from Test 1 and Equation 5.2 would be different to β_1 derived from Test 1 and Equation 5.3. To find a set of β values that would form a general equation that would equally describe each of the 45 tests, the following eight calculations were applied to each respective β value

- The average β_{av}

- The median β_{med}
- The histogram average $\beta_{hist-av}$
- The histogram median $\beta_{hist-med}$
- The average of the standardised tests β_{z-av}
- The median of the standardised tests β_{z-med}
- The histogram average of the standardised tests $\beta_{z-hist-av}$
- The histogram median of the standardised tests $\beta_{z-hist-med}$

Therefore, when Equation 5.2 was being examined, 45 β_0 's, 45 β_1 's, 45 β_2 's and 45 β_3 's were derived, i.e. one set of β values from each test. Instead of taking one set of β values, that had been derived from one test and applying it to the other 44 tests (and repeating), the average β_0 , β_1 , β_2 and β_3 values were calculated from the 45 tests, and then applied and evaluated for each of the 45 tests. Once the average had been evaluated, the median was then calculated and evaluated and so on until each of the eight β values had been tested. Once each of the eight had been calculated and evaluated for Equation 5.2, the β values for Equation 5.3 were calculated and the procedure repeated.

5.3.2 Evaluating Algorithm 1-x

After testing various algorithms such as equations 5.2 - 5.4, using the procedure outlined in Section 5.3.1, it became evident that including HR was having a detrimental effect on the results from the algorithms. The reason for this was that, for some patients, there was a positive correlation between HR and BP but for others there was a negative correlation. No matter which type of correlation existed, the correlation was also found to be weak in the majority of cases. This is highlighted in Figure 5.6. This had been identified previously in Section 5.2, in particular in Table 5.1 but HR was included to examine the effect for the first round of testing of the MLR derivations.

Therefore, it was decided that HR should be omitted from subsequent equations and a new set of algorithms, denoted *Algorithm 2 -x* was derived.

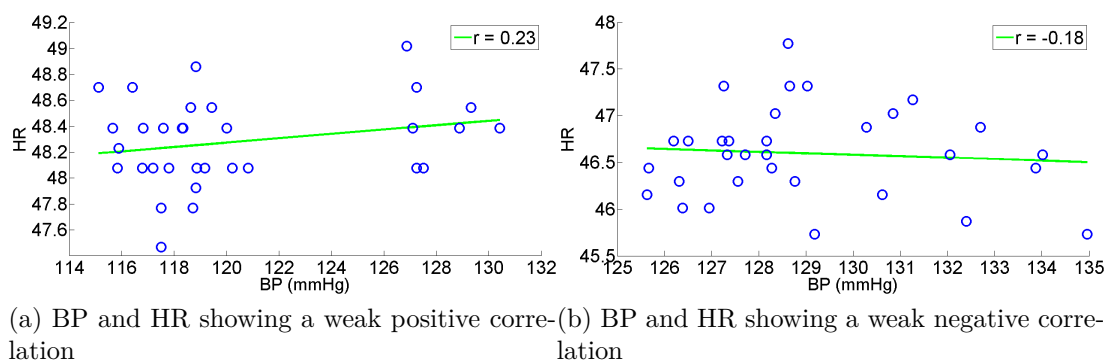


Figure 5.6: The variability of the relationship between BP and HR

5.3.3 Algorithm 2-x

The weighting factors i.e. the β values, were derived and applied for each of the "new" algorithms, based on equation 5.6, using all the knowledge that had been discussed in previous sections.

$$BP = \beta_0 + \beta_1 \times PTT + \beta_2 \times SV + \epsilon \quad (5.6)$$

Each time an algorithm performed well i.e. tracked a number of tests well and provided a low error for the majority of tests, extra time was spent examining the β values in an attempt to maximise the effectiveness and minimise the error of the algorithm. This was primarily done, by investigating the use of median β s, mode β s and histogram derived β s. For example, if it was found that $\beta_{average}$ performed well when applied to some of the 45 tests, but an offset existed for other tests, the use β_{median} was examined to see if an improvement could be observed. However, it was found that if one set of β values performed well, on a set of M tests and poorly on the other N tests, examining a different set of β values would mean that an improvement would be noted on the N tests, but the original M tests would then perform less well.

An example of this can be seen in Figure 5.7. In Figure 5.7a, one particular algorithm *Algorithm 2-g* is being tested on the first half hour test extracted from patient 2 i.e. *Pat 2a*. In Figure 5.7b, *Algorithm 2-g* is also being tested on *Pat 3a*. When *Algorithm 2-g* is applied to *Pat 3a*, it can be seen that there is a low offset and the prediction (in red) tracks the actual BP (in blue) quite well. However, *Algorithm 2-g* does not suit *Pat 2a* where there is quite a large offset, even though the tracking still seems to be quite good. By applying a different

5. DERIVING A NOVEL BLOOD PRESSURE TRACKING ALGORITHM

algorithm, *Algorithm 2-h*, as seen in 5.7c, a large improvement is evident for *Pat 2a*; however *Algorithm 2-h* has negatively affected *Pat 3a*, which now has a large negative offset between the predicted and actual BP shown in Figure 5.7d.

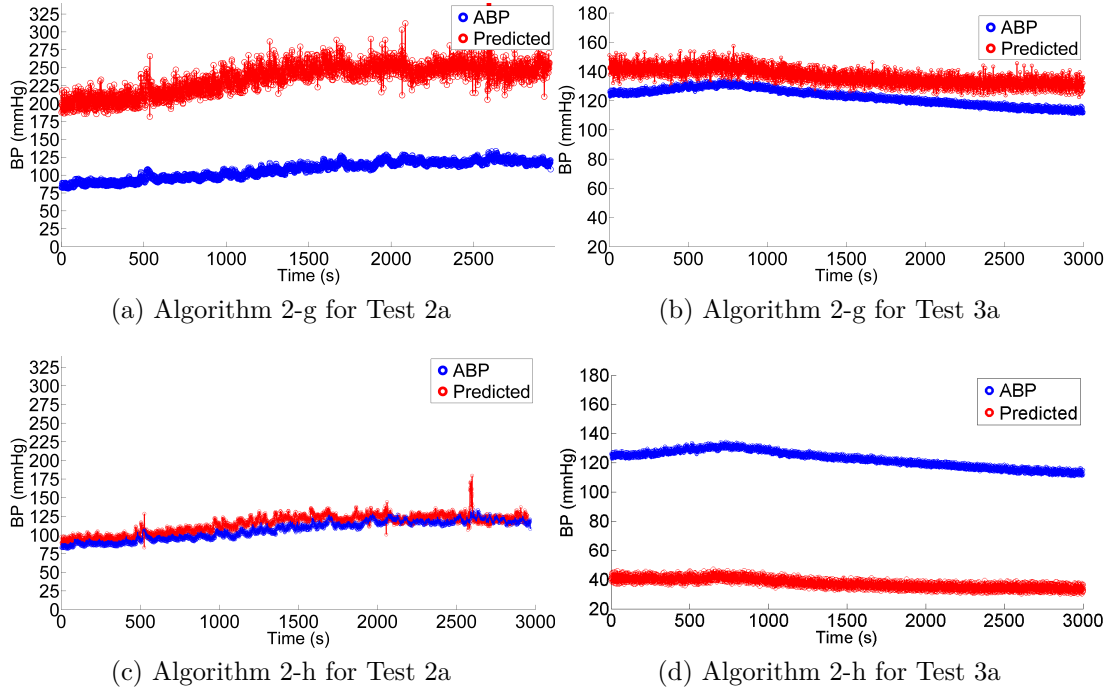


Figure 5.7: The variability of the algorithms; Improvements in one test usually meant another became worse

The reason for the differences between *Algorithm 2-g* and *Algorithm 2-h* can be explained by examining the β values in Table 5.2. The first eight rows of this table show the result of deriving the β values for one particular equation. The final two rows of the table show the Mean and Median β values of this data, either of these could be used to form the general application that would be applied to all tests. Taking β_0 as an example and using the mean value of β_0 , there is a chance that test *Pat 17a* could give good results, but the other tests would not. If the median value was used, tests *Pat 3b*, *Pat 6a* and *Pat 13c* could potentially give good results, whereas the remaining tests would not.

Although Table 5.2 only shows β derived results for one algorithm, the same trend appeared no matter which algorithm, parameters or combinations of parameters were being examined. If some β values suited a number of tests, they were also unsuited to other tests. This was due to the variability of each parameter that was being examined i.e. some patients had a high BP whereas others had a low BP. However, taking this type of variability into account is important when developing an algorithm, so that any algorithm that is developed can be as robust

Table 5.2: A sample of the β values calculated for one of the MLR tests. Even in this example, a large variance between tests can be observed

Test	β_0	β_1	β_2
Pat 1a	100.7082	0.213505	-0.0451
Pat 2a	196.5665	235.3745	-1.46948
Pat 3b	69.9847	984.3945	0.259159
Pat 6a	69.64046	0.202034	0.632133
Pat 6b	-198.077	-0.00714	2.897617
Pat 6c	-56.7137	38.85773	1.67875
Pat 13c	65.95029	777.5987	0.291707
Pat 17a	44.30602	828.9337	0.002577
Mean	36.54568	358.1959	0.53092
Median	67.79538	137.1161	0.275433
Standard Deviation	117.4775919	429.5013481	1.291324619

and universally applicable as possible. However, from the perspective of MLR based algorithms, it was clear that this approach would not yield an equation that was sufficiently general for all tests, and therefore, for our purposes, a new approach was required.

5.3.4 Algorithm 3-x

One solution that could accommodate the variability of the parameters was to implement a categorisation process. For example, if the weighting factor of PTT (β_1), had been derived for a particularly low PTT value, using the categorisation process, this β_1 value would only be applied to other similarly low PTT values. By using this method and by implementing a number of different categories, each respective β value would then only be applied to an appropriate PTT or SV value.

To implement this, a two minute sample of PTT and SV was taken from the beat to beat data from each of the 45 tests. The mean of this sample was then calculated for SV and PTT and was tabulated as shown in Table 5.3, along with the respective β_1 and β_2 values that had been derived for each test in section 5.3.3.

Initially, it had been hoped that specific bounds would exist for each variable and their corresponding β value and clear categories could be observed e.g. all PTT between 200ms and 250ms would have a β_1 value between 1.5 and 2.0. On examination of Table 5.3, it can be seen that in some cases there are clear bounds and thus categories could be observed. For example, examining *Pat 5a* in Table

5.3 shows a mean PTT of 195.6 ms, with a corresponding β_1 value of 1.06. Tests *Pat 5b* and *Pat 5c* also show similar mean and β values, so grouping these values into one category, indicated in blue, makes sense. Applying the same logic to Pat 6, it can be observed that all mean PTT values and β_1 for this patient have similar and unique values and so belong in a new category of their own, marked orange.

For the remaining PTT and associated β_1 values in Table 5.3, it can be seen that the categories aren't as clear or well defined as those of Patients 5 and 6. At first, a similar categorisation process, as that applied to Patients 5 and 6 was strictly followed, but too many categories were created, and most categories only contained one or two tests. Therefore, for the remaining tests, it was necessary to create categories based primarily on the mean PTT. Although the associated β_1 values were considered in each case, they were of less importance. Examining the category indicated in purple, it can be seen that all PTT values are between 215ms and 226ms. However, the associated β_1 values are between 1.09 and 1.84. Examining other β_1 values in the table, it can be seen that many other β_1 values are between these two bounds, but the associated PTT are greater or less than those defined here.

This process was repeated for the SV and the associated β_2 values. Again, some categories were clear and well defined; for example it can be seen that Pat 5a, 5b, 5c and Pat 7b all have similar β_2 values and similar SV values and therefore belong in the same (brown) category. As was the case with the purple category when PTT values were considered, the green category is primarily based on the SV value, with the β_2 value being of less importance in the categorisation procedure. Although all SV values are between 38 and 47 ml, most β_2 values are greater than 18,000. However, since Pat 12c and Pat 13a, also have a SV value within the specified SV range, their β_2 values of approximately 12,000 are also included into this category.

Once the categories had been defined, the mean values of all the β values in that category were calculated e.g. from Table 5.3, for the purple PTT based category, the mean of all the associated β_1 values in this category was found. Therefore, when the algorithm was being applied to data, if the mean PTT value over the 2 minute sampling period was found to be in the range of the purple category, a β_1 value of 1.44 (the mean of all the purple β_1 values) was applied.

During the initial testing of the categorisation, it was noted that no major improvement was apparent, when the averaged β values of the categorisation process

Table 5.3: An example from selected tests of the categorisation process for Algorithm 3-x. Each colour represents a different category as defined by either the mean SV or mean PTT value and its associated β value.

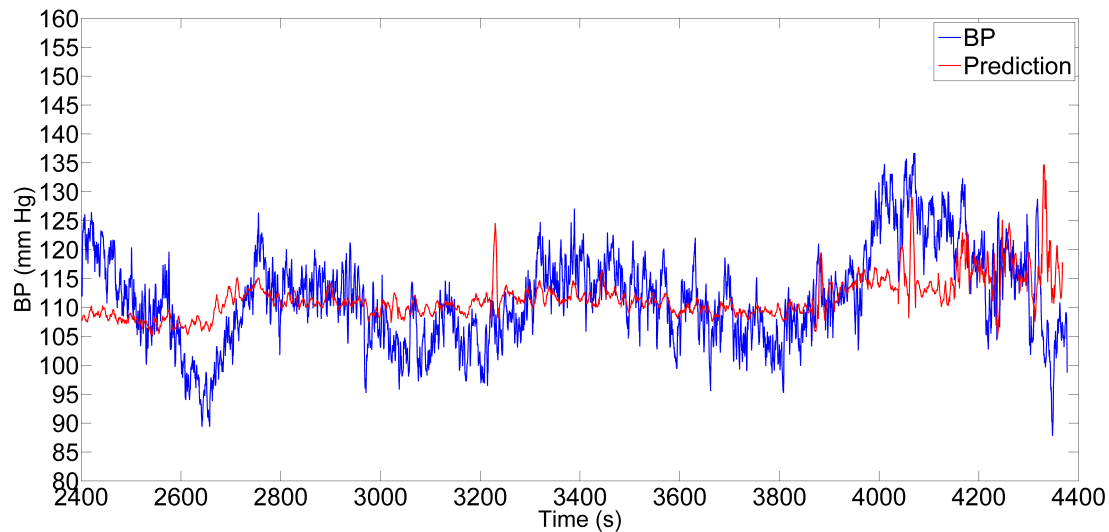
Test	Mean PTT (ms)	Mean SV (ml)	β_1	β_2
pat 3a	225	46.8	1.84	11989.01
pat 3b	266	43.5	1.43	21739.36
pat 3c	275.2	44.4	1.52	18915.61
pat 4a	184.4	40	1.21	20343.56
pat 4b	188.5	38.9	0.81	22937.39
pat 4c	203.4	34.2	0.81	24271.42
pat 5a	195.6	61.1	1.06	9262.23
pat 5b	198	61.8	1.07	7136.96
pat 5c	191.9	63	1.02	7100.5
pat 6a	140.7	42.7	0.68	23000.22
pat 6b	145.5	40	0.56	19505.31
pat 6c	141.6	39.3	0.68	24202.56
pat 7b	694.2	67.1	2.62	7663.25
pat 9b	246.2	46.8	1.14	11715.76
pat 9c	257.4	51.8	2.07	133.4
pat 12a	226	45.1	1.11	7370.87
pat 12b	215.2	40.9	1.09	19601.59
pat 12c	220.1	43.2	1.66	12831.74
pat 13a	216.5	43.4	1.5	12618.3
pat 13b	256.3	39.6	1.14	20258.14
pat 13c	234.4	42.6	1.05	18646.66

were applied to each of the tests. After a detailed investigation, it was frequently found that by using a large β_0 value, the remaining parameter contributions of the algorithm could not provide a large enough reaction, if the BP changed suddenly during any given test. Figure 5.8 shows an example of the effect of having a large β_0 . In this example, the algorithm being applied is

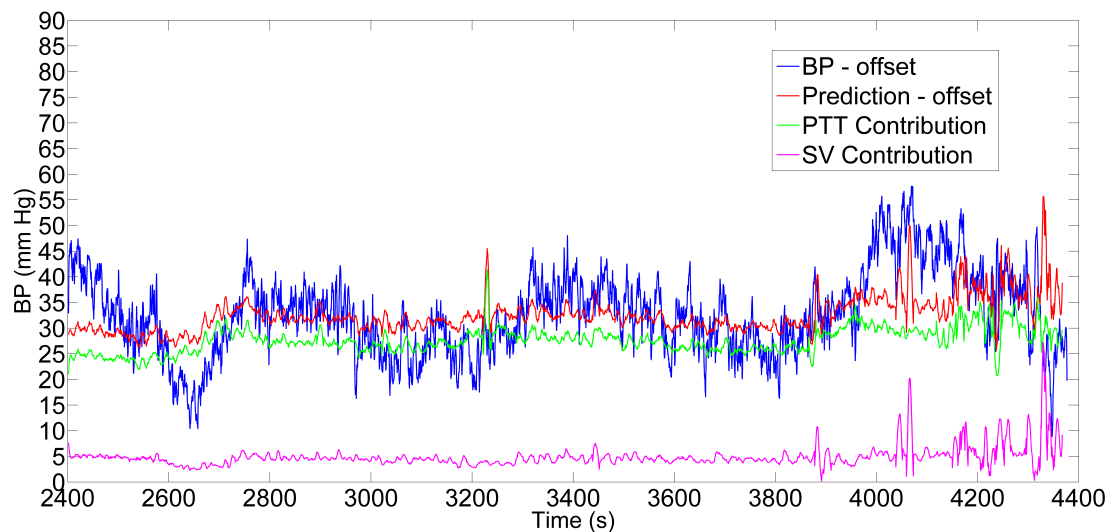
$$BP = 78.99 + 1.146 \times \frac{1}{PTT^2} + 3801.19 \times SV^2 + \epsilon \quad (5.7)$$

where, $\beta_0 = 78.99$, $\beta_1 = 1.146$ and $\beta_2 = 3801.19$. Figure 5.8a shows the prediction provided by Equation 5.7 when compared to the actual BP. To highlight the effect of β_0 , its value was subtracted from the actual BP in Figure 5.8b, i.e. 78.99 was subtracted from the actual BP in this figure. In this figure, the PTT component i.e. $1.146 \times \frac{1}{PTT^2}$ (green) and SV component ($3801.19 \times SV^2$, magenta) are shown individually. The sum of the PTT component and the SV component is shown in red. Although, the BP here does not change dramatically, because β_0

has been relied on to provide such a large offset, the PTT and SV components are not capable of tracking large changes in BP throughout the test.



(a) Predicted BP in red generated from Equation 5.7 vs the Actual BP in blue



(b) The PTT component (green) and the SV component (magenta) when added (red) are not capable of tracking the changes of BP when the offset of β_0 is subtracted

Figure 5.8: Once the offset provided by β_0 is subtracted, it can be seen that the PTT and SV components are not large enough to compensate for large changes in BP

For this reason, it was decided that instead of deriving a value for β_0 , it should be fixed to a percentage of the first BP measurement. Using this method, a constant offset was still being applied and the PTT and SV contributions should be able to track larger changes in the actual BP. Figure 5.9 shows an example of this methodology and the values in Table 5.3 were derived using this premise. The algorithm thus becomes:

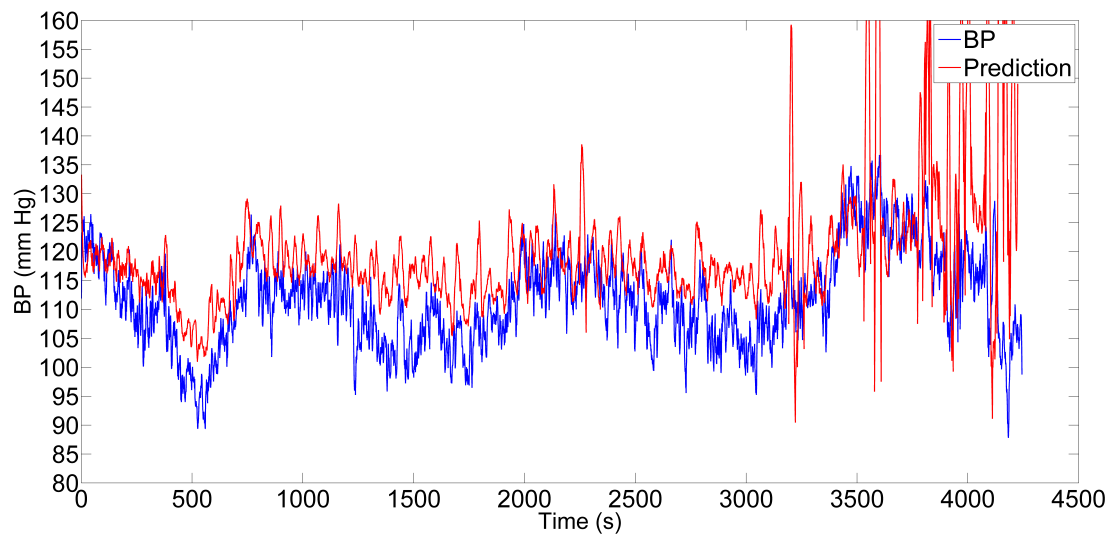
$$BP = 0.6 \times BP(1) + 0.81 \times \frac{1}{PTT^2} + 24271.42 \times SV^2 + \epsilon \quad (5.8)$$

where 0.6 is the percentage chosen for this derivation, 0.81 is β_1 and 24271.42 is β_2 . In Figure 5.9a, there is a clear improvement in the algorithm's ability to track BP over the course of the measurement. Figure 5.9b shows the components of the algorithm. For most of the test duration, the tracking is quite good, especially when compared to Figure 5.8b. However, towards the end of test, large spikes can be seen, the source of which originates from the SV contribution. The magnitude of these spikes is quite large and exceed 200 mmHg, but are not shown so that a more detailed comparison of the tracking ability of the new algorithm can be made.

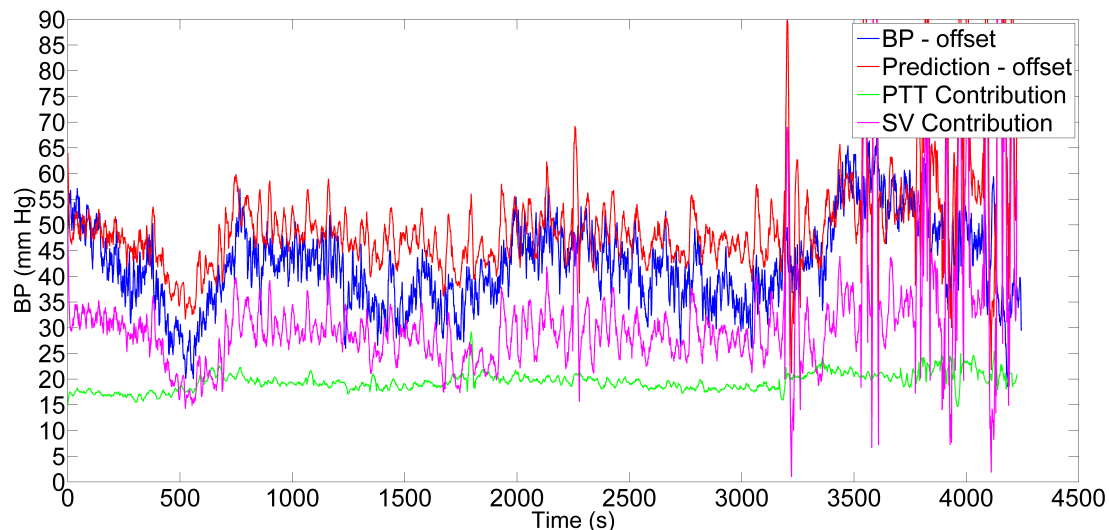
Overall, the various algorithms investigated using this method provided a significant improvement over the MLR procedure studied, since the β values applied to any given test were usually much closer to the β values that would optimise that test. However, as can be seen in Table 5.3, in particular *Pat 4a*, not all categorisation suited every test. In these cases, graphs such as those shown in Figure 5.7 were not uncommon. However, the frequency of the occurrence of these types of offset was dramatically reduced compared to the previously implemented algorithms.

Although this categorisation method made a significant improvement over the previously implemented algorithm, one of the most common problems with regard to this type of categorisation was that due to averaging there were some occasions where one of either the PTT or SV contributions was much larger than the other (as has already been illustrated in Figure 5.9b). Usually, this would cause a slightly larger offset than was desired, but when there was one variable that was dominant, it was not a major issue, since the overall offset (or error) would remain low (demonstrated by Figure 5.9a). However, the problem was amplified, if both the SV and PTT contributions became very large or very small due to the averaging process. For example, in the case of Figure 5.9a, the β_2 value is quite large and therefore the SV contribution is also quite large. However, the β_1 value is quite small and as a consequence the resulting PTT contribution is also quite small. When the two are added together, even though the SV contribution dominates that of PTT, the final prediction is acceptable. However, if a case existed where both β values were quite large, each of the contributions would also be quite large and therefore the sum of each would result in a large offset.

5. DERIVING A NOVEL BLOOD PRESSURE TRACKING ALGORITHM



(a) Predicted BP in red generated from Equation 5.8 vs the Actual BP in blue



(b) The PTT component (green) and the SV component (magenta) when added (red) are now capable of tracking the changes of BP when the offset of β_0 is subtracted

Figure 5.9: Once the offset provided by β_0 is subtracted, it can be seen that the PTT and SV components are now large enough to compensate for large changes in BP

From an analysis of these results, it became obvious that for a categorisation method to be effective, the numerical value of both the SV and PTT contributions had to be taken into account. This would help to ensure that one contribution wouldn't erroneously dominate the other and two large β values would not be applied to the same test and create an error. This led to the implementation of Algorithm 4-x.

5.3.5 Algorithm 4-x

Despite the progress made over the previous number of algorithms, the statistical justification, from what had been studied to date, was questionable. Perhaps the biggest problem was the use of a constant in the MLR calculation, instead of calculating β_0 . Although it is possible to perform regression without calculating β_0 (or the intercept, as it is also known) and this can be justified in some cases, the use of a constant times the base BP has no statistical or physical basis. However, it has been established that MLR components can be calculated without the need to calculate β_0 in certain circumstances, in particular:

“In rare cases you may wish to exclude the constant from the model... Usually, this will be done only if (i) it is possible to imagine the independent variables all assuming the value zero simultaneously, and you feel that in this case it should logically follow that the dependent variable will also be equal to zero; or else (ii) the constant is redundant with the set of independent variables you wish to use. An example of case (i) would be a model in which all variables—dependent and independent—represented first differences of other time series e.g. if you are regressing $\text{DIFF}(Y)$ on $\text{DIFF}(X)$, you are essentially predicting changes in Y as a linear function of changes in X . In this case it might be reasonable to assume that Y should be unchanged, on the average, whenever X is unchanged i.e., that Y should not have an upward or downward trend in the absence of any change in the level of X [154]”

Furthermore, it is said that β_0 can only be omitted if all the independent variables are zero when the dependant variable is zero [155], i.e. if the PTT and SV are zero, then the BP must also be zero, because the heart would not be pumping. Therefore in an attempt to create a better model, the premise of omitting the constant/intercept was investigated. All regression coefficients were recalculated and a general model was generated.

As discussed in Section 5.3.4, it has been shown that much better results were attained by categorising each of the parameters. However, this approach was not without its flaws, the biggest of which are those occasions when one contribution erroneously dominates the other due to the categorisation process. It was thus decided that both SV and PTT contributions should be considered before the respective β values were applied to each. Therefore, an average of SV and PTT

Table 5.4: The β values for both the PTT and SV contributions of Algorithm 4-x. .

Ratio	β_1	β_2
ratio < 3.0	3.285	3371.315
$3.0 \leq \text{ratio} < 3.3$	3.615	5000.845
$3.3 \leq \text{ratio} < 4.0$	3.5	6405.413
$4.0 \leq \text{ratio} < 5.0$	3.765	13726.9
$5.0 \leq \text{ratio} < 5.5$	3.695	16287.79
$5.5 \leq \text{ratio} < 7.0$	4.35	17847.27
$7.0 \leq \text{ratio} < 10$	3.2	5266.515
ratio > 10	3.615	500.845

was initially calculated and then the PTT:SV ($\frac{ms}{ml}$) ratio was found. Depending on the results of this ratio, different β values could then be applied to each contribution.

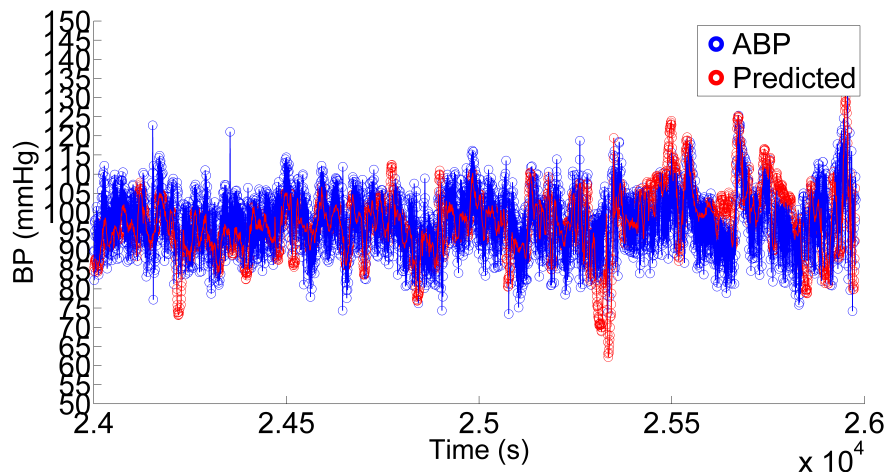
Although not previously discussed, there were a few “outliers” among the dataset. These “outliers” occurred in some tests or, sometimes across every test of a patient, who had excessively high or low PTT and SV values respectively i.e. a PTT of 0.54 s or a SV of 106 ml. Examining each of these tests manually, it was found that these values were real measurements and not errors due to, for example, peaks not being correctly identified or motion artifacts. Up until this algorithm, these “outliers” were not considered to be major factors, because there were only 13 cases of them out of 45 tests and although they did adversely affect the results, the results were never significant enough for them to matter or they had all been categorised together and would not affect the results. However, now that the ratio between PTT and SV was being considered, these outliers were now frequently in the same category as other tests and had to be separated. For this reason, two tables of ratio values are shown here: one for the “normal” tests (Table 5.4) and another for these “outliers” (Table 5.5). These tables were derived from the algorithm described by equation 5.9

$$BP = \beta_1 \times \frac{1}{PTT^2} + \beta_2 \times SV^2 + \epsilon \quad (5.9)$$

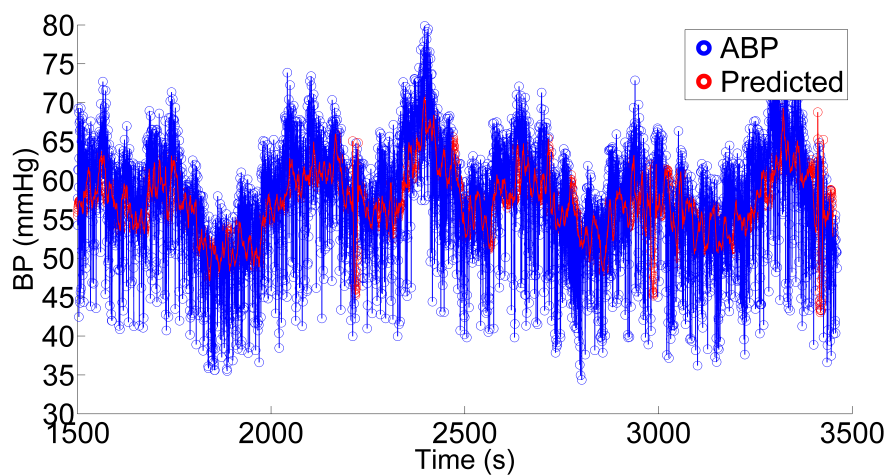
This method provided good results with an improvement over the previous algorithm and examples of this are shown in Figure 5.10. Using this technique, the algorithm tracked BP very well over each test. However, in many of the tests, the prediction had quite a large offset, meaning there was still a significant error associated with this approach.

Table 5.5: The β values for both the PTT and SV contributions for the outliers of Algorithm 4-x. An outlier was defined as being less than 0.16 s or greater than 0.5 s for PTT and less than 20 ml and greater than 80 ml

Ratio	β_1	β_2
ratio < 2.9	5.25	1736.16
$2.9 \leq \text{ratio} < 3.0$	8.31	1207.25
$3.0 \leq \text{ratio} < 5.5$	1.09	47041.82
$5.5 \leq \text{ratio} < 10.0$	23.835	5530.87
$10.0 \leq \text{ratio} < 15.0$	1.24	27105.74
ratio > 15	21.14	27135.22



(a) An example of Algorithm 4-x applied to Pat 14b



(b) An example of Algorithm 4-x applied to Pat 17a

Figure 5.10: Algorithm 4-x proved to be very effective for certain tests as shown here

Upon detailed analysis, it was decided that two patients should be excluded since one was found to have a highly variable BP and was found to be suffering from sepsis and thus was an unsuitable patient for this kind of test. Another patient was found to have a CO of 9.5 l/min, approximately twice the normal. Thus of the remaining 39 tests, 15 of the predictions were found to track the BP well and have a low and acceptable error, for an interval in excess of 10 minutes. The remaining tests either had a large or small offset associated with them due to a poor initial estimation. This remained throughout the test and ultimately resulted in a poor overall estimate.

Even though this algorithm only performs well over the stated period in 15 of the 39 tests, this result was considerably better than either of the Chen or Poon offerings, and also better than the previous algorithms. When repeating the tests that had been performed for Chen and Poon [128], this algorithm was found to be inside the BHS standard when using a 10 minute calibration interval, a significant improvement over those previously reported. Unfortunately, the algorithm failed the AAMI standard when using a 4 minute calibration interval by having a standard deviation greater than 8 mmHg; however, the standard deviation never exceeded 9 mmHg. This result was repeated for all subsequent calibration intervals up to and including a 10 minute calibration interval. Considering how close this algorithm is to passing the AAMI standard and how convincingly it passes the BHS standard, it is clear that this algorithm is an improvement over both the Chen and Poon algorithms.

Although this algorithm provides better results than those previously seen in this work as well as the work of others there are still a few concerns. The first of these is the use of categorisation for applying the MLR results. Although not expanded on in this section, a similar procedure as outlined in section 5.3.4 was followed i.e. the β values were examined in conjunction with the ratio and the categories were thus decided. Categorisation can be used in some cases, if there is a strong justification and clear definition of the categories. Given the process defined here, it is possible that the use of categorisation could be reasonable. However, using a posteriori knowledge to create the categories clearly cannot be justified, especially since there is no clear definition or reasonable explanation between one category and another i.e. what is the reason for a different category between a ratio of 3.2 and that of 3.5 as is apparent from Table 5.4?

The other major concern was that although the algorithm gave good results, it had no real obvious physiological meaning. In the case of Chen and Poon, each

algorithm corresponded to a physiological event and was derived from cardiological knowledge. In this derivation, the algorithm was derived mathematically, with knowledge of correlations but with no concern for physiological or biological parameters. Initially, it had been envisaged that the final algorithm would be a combination of parameters that could also be derived from physiologically known equations and would be universally applicable. In this algorithm, there was no known explanation for the categories or the β values and no indication of how the β values could be derived.

Therefore, it was decided that an alternative algorithm should be created that could be derived from known physiological parameters or equations and that would be universally applicable. From the work described in sections 5.2 through to section 5.2.2, a number of key parameters had been identified. When these key parameters had been applied using the various MLR algorithms, PTT and SV were found to provide the algorithms which performed the best at tracking the ABP, regardless of which variation of MLR was under investigation. Therefore, although MLR is not used in the derivation of the final algorithm, the use of MLR has allowed SV to be identified as the additional, critical parameter that should be incorporated into PTT algorithms to allow them surpass their current limits.

5.4 Derivation and Evaluation of a New Algorithm Based on Physiological Parameters

A considerable amount was learned from the process that was undertaken during the development of the preceding algorithms described in section 5.3. One of the most important outcomes was that, no matter what equation was derived, HR should not be a feature because it was so variable between patients and would adversely affect the results from some patients at the very least. It also emphasised how effective PTT and SV were at tracking BP. However, after examining the results and findings from Chapter 3, it was clear that any future equations should include both PTT *and* SV. Therefore the key to the development of a new algorithm was how SV could be integrated into the existing PTT equations.

It should be noted that many equations, physical and physiological laws, theories and combinations of these were investigated before the solution outlined here was found. This included examining various combinations of existing PTT equations

such as the Bramwell-Hill equation [156] and Moens-Korteweg equation [157], to investigating the Navier-Stokes equations [158], the Darcy-Weisbach equation [159], the Bernoulli equation [160], the Reynolds Number [161] among others.

5.4.1 Quantifying the Performance

One of the most important points in evaluating a new algorithm is its quantification process. Elements of this have already been outlined in Chapter 3 where the performance of Chen and Poon were quantified using the BHS and AAMI standards. However, Chapter 4 revealed a shortcoming in this quantification process when Poon was compared to Arterial BP instead of intermittent cuff measurements. Whereas in Chapter 3, Poon's algorithm had been found to be noisy when compared to these point representations of BP, when Poon's estimation was compared to continuous beat to beat ABP it was found to perform considerably better although it frequently didn't have a great enough amplitude to track the BP accurately.

Throughout the examination of various MLR based algorithms, it had been noted that the Systolic Arterial BP could be considered as being quite noisy, with a variation of 10 mmHg not being unusual over 3 - 4 beats. Therefore when evaluating a new algorithm, it was necessary to average the Arterial BP over at least 3 -4 beats so that a representative Arterial BP would be compared against the predicted value of the new algorithm.

In essence, this type of sampling could be seen as applying a moving average filter. As has been highlighted by Chen's use of a bandpass filter, it is vital that the choice of filter is analysed carefully so that it doesn't dramatically change either the value or shape of the signal. If a moving average filter is applied, the window size is the most important factor to examine. If the window is too small, it will not have any effect but if it is too large it will remove all the valuable information. Therefore, in this type of application, the filter should remove any artifacts and follow the trend line of the signal, but not destroy any information the signal contains.

It was found that a Savitzky-Golay FIR filter [162] would provide the necessary filtering without destroying any information. This filter is widely used, especially in the area of ECG signal filtering [163], but also in other biomedical filtering applications [164] because it is known for preserving peaks and other points of interest while also smoothing and removing noise from data. Both the PTT and

SV signals were filtered using this technique before any algorithm was applied.

5.4.2 Derivation of the New Algorithm

As has been previously outlined, the main focus of the new algorithm was to incorporate SV into the PTT equations. Naturally, the Moens-Korteweg equation [157], seen in equation 5.10, is at the core of this derivation as it has proven to be the most important equation for each of the previously investigated PTT equations:

$$PWV = \frac{K}{PTT} = \sqrt{\frac{tE_0e^{\gamma P}}{\rho d}} \quad (5.10)$$

where PWV is the Pulse Wave Velocity [m/s], K is the length of the blood vessel [m], t is the thickness of the vessel wall [m], E_0 is the elasticity at time zero [$m^{-1}kgs^{-2}$], γ is a derived constant [$mmHg^{-1}$], ρ is the density of blood [kg/m^3], d is the diameter of the blood vessel [m] and P is the blood pressure [mmHg].

An alternative equation, that has been used in the development of other PTT equations is known as the Bramwell-Hill equation [156], seen in equation 5.11, which is also related to the Moens-Korteweg equation

$$PWV = \sqrt{\frac{V \times \Delta P}{\rho \times \Delta V}} \quad (5.11)$$

where V is the volume [m^3], ΔP is the change in Pressure [mmHg], and ΔV is the change in volume [m^3].

While investigating various principles of fluid dynamics and equations concerning the flow of fluids through a pipe, the following relation was identified:

$$\Delta P = Q \times R \quad (5.12)$$

where Q is the flow of blood [l/s] and R is the resistance to the flow of blood.

This is a simplification of another equation, known as the Poiseuille equation [165], which explicitly states the origin of the resistance to the flow of blood, as shown in Equation 5.13.

$$\Delta P = Q \times \frac{8\mu K}{\pi r^4} \quad (5.13)$$

where μ is the viscosity of blood [kg/sm] and r is the radius of the blood vessel [m].

However, it should be noted that when the Poiseuille equation is applied to arteries, where pulsatile flow exists, the value of the resistance is more complex and more factors must be taken into account to calculate its exact value. Specifically, the Womersley Equation [166, 167] is more appropriate, which can be seen in equation 5.14.

$$Q = P \times \frac{\pi r^4}{\mu} \times \frac{M'_{10}(\alpha)}{\alpha^2} \times \sin[\omega t - \phi + \epsilon'_{10}(\alpha)] \quad (5.14)$$

where μ is the coefficient of viscosity [kg/sm], α is a non-dimensional parameter $r\sqrt{\frac{\omega}{\nu}}$, where $\omega = 2\pi \times \text{frequency}$ and $M'_{10}(\alpha)$ and $\epsilon'_{10}(\alpha)$ are functions of α tabulated by Womersley for $\alpha = 0$ to 10 . It should be noted that this equation is per unit length.

Comparing equation 5.14 to Poiseuille equation 5.13, a clear relationship is evident, the difference coming from the α related parameters.

Therefore, the primary difference between both equations is due to the complex relationship derived by Womersley, that defines the actual resistance to flow through the artery. However, in the algorithm that has been derived, the specific value of the resistance is not used and from Womersley's tables the difference becomes a matter of a scaling factor. Since it provides a good estimation of the resistance and for the sake of simplicity, the Poiseuille equation was used as a substitute. Combining Equation 5.11 and 5.13 gives:

$$PWV = \sqrt{\frac{V \times \frac{8\mu K Q}{\pi r^4}}{\rho \times \Delta V}} = \sqrt{\frac{8\mu Q K V}{\rho \pi r^4 \Delta V}} \quad (5.15)$$

Equating 5.10 and 5.15

$$\sqrt{\frac{t E_0 e^{\gamma P}}{\rho d}} = \sqrt{\frac{8\mu Q K V}{\rho \pi r^4 \Delta V}} \quad (5.16)$$

It is well known that

$$Q = \frac{\Delta V}{\Delta t}; \quad d = 2r \quad (5.17)$$

and so using these basic substitutions

$$\frac{tE_0 e^{\gamma P}}{\rho 2r} = \frac{8\mu KV \Delta V}{\rho \pi r^4 \Delta V \Delta t} \quad (5.18)$$

Re-arranging

$$e^{\gamma P} = \frac{16\mu KV}{tE_0 \pi r^3 \Delta t} \quad (5.19)$$

Taking the natural log of both sides yields:

$$P = \frac{1}{\gamma} \left[\ln \left(\frac{16\mu K}{tE_0 \pi r^3} \right) + \ln \left(\frac{V}{\Delta t} \right) \right] \quad (5.20)$$

where V is the Stroke Volume and Δt is the Pulse Transit Time

$$P = \frac{1}{\gamma} \left[\ln \left(\frac{16\mu K}{tE_0 \pi r^3} \right) + \ln \left(\frac{SV}{PTT} \right) \right] \quad (5.21)$$

using the natural log theorems, this can be re-written as

$$P = \frac{1}{\gamma} \left[\ln \left(\frac{16\mu K}{tE_0 \pi r^3} \right) + \ln(SV) - \ln(PTT) \right] \quad (5.22)$$

Using partial differentiation on both sides with respect to PTT and SV

$$\frac{\partial(P)}{\partial(PTT)\partial(SV)} = \frac{1}{\gamma} \frac{\partial}{\partial(PTT)\partial(SV)} \left[\left(\ln \left(\frac{16\mu K}{tE_0 \pi r^3} \right) \right) + (\ln(SV) - \ln(PTT)) \right] \quad (5.23)$$

which yields

$$\frac{\partial}{\partial(PTT)\partial(SV)} (P) = \frac{1}{\gamma} \left[\frac{1}{SV} - \frac{1}{PTT} \right] \quad (5.24)$$

rearranging and updating the notation:

$$\Delta P = \frac{1}{\gamma} \left[\frac{\Delta(SV)}{SV} - \frac{\Delta(PTT)}{PTT} \right] \quad (5.25)$$

Equation 5.25 will track changes in BP, much in a similar fashion way that Chen's basic equation would. Therefore

$$P_E = P_B + \frac{1}{\gamma} \left[\frac{SV}{SV_B} - \frac{PTT}{PTT_B} \right] \quad (5.26)$$

will provide a BP [mmHg] estimate at any given time (P_E), once a base or initial BP (P_B) has been provided and SV and PTT has been monitored continuously since the initial measurement.

This derivation bears some similarities to the procedure followed by Chen. However the main and important differences are that a bandpass filter, as described by Chen, is not applied and this equation incorporates SV as well. This equation is also significantly different to those derived from the various MLR equations that had been previously examined. The following sections evaluate and quantify the performance of this new algorithm when compared to both the existing equations and the standards.

5.4.3 Evaluation of the New Algorithm

Overall, this new algorithm performs very well, especially in comparison to the algorithms described in this work and all previously examined algorithms, including Chen and Poon. One of the most instantly identifiable features of the new algorithm is that the tracking ability of this new algorithm exceeds that of the MLR algorithms and it is universally applicable, with at least one test from each patient performing very well.

The new algorithm provided a very low error for 24 of the 45 tests over short periods. More specifically, the algorithm provided an acceptable error for 20 of the 45 tests over half an hour, without the need for recalibration, an example of which is shown in Figure 5.11. This is a stark difference to that found from examining Chen and Poon, who could typically only manage 6 minutes before a recalibration was required. Furthermore, 9 tests were able to track BP for 45 minutes without the need for calibration. It should be noted the biggest limitation with regard to these tests was identifying tests which had 45 minutes of continuous data that was of sufficiently high quality for tracking, rather than the quality of the algorithm.

In terms of standards, the algorithm was found to achieve a B grade (pass) when

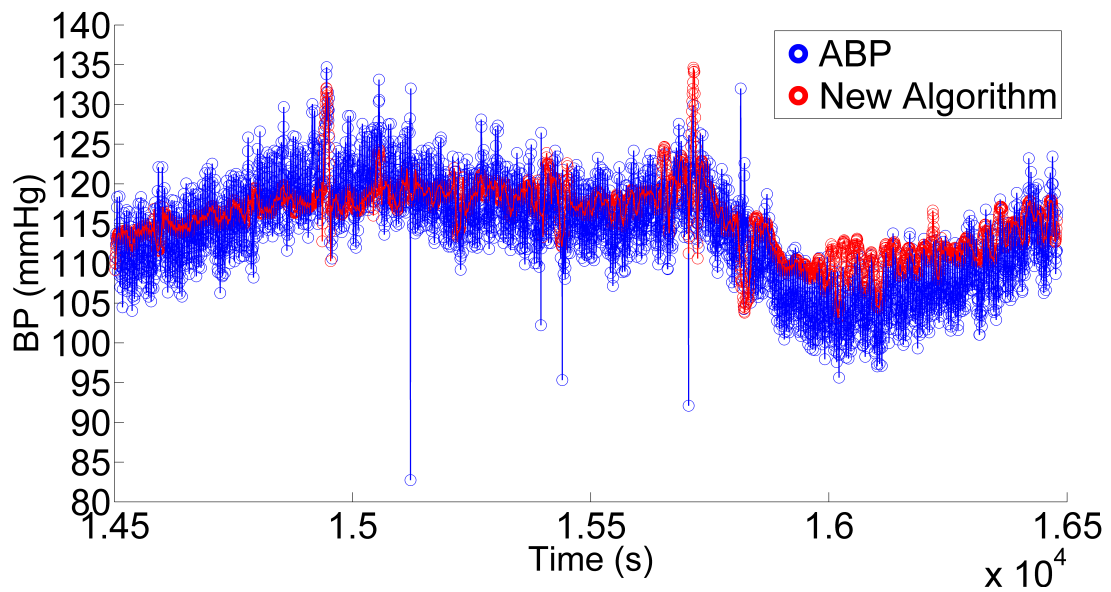


Figure 5.11: An example of the tracking ability of the new algorithm over 30 minutes. In this figure the estimation is being compared to the raw Systolic Arterial BP, rather than the ABP filtered signal

using a 12 minute calibration interval when the BHS standard was applied. It was not possible to apply a longer calibration interval when using this calibration interval, because only 9 points from each test were available and it was felt that this may not be statistically valid. When the AAMI standard was applied, the algorithm passed when using a 2 minute calibration interval, at which point the standard deviation exceeded the 8mmHg required to pass. However, for the remaining tests, the standard deviation of all the tests together never exceeded 9.33 mmHg, an improvement to that seen in both Chen's and Poon's algorithms. Table 5.6 shows the mean and standard deviation of each patient over 2 minute intervals, in a similar approach to that previously shown for Poon and Chen and shows the AAMI ratings of each individual patient. Although the new algorithm suits some patients extremely well, there are others where the algorithm consistently fails the AAMI standard by a significant amount. Referring back to Table 4.4, where Poon's algorithm was investigated on the same dataset, it can be seen that Patients 1 and 4 fail both algorithms by a significant amount across all calibration intervals.

It had been previously noted in section 5.3.5, that there were a number of tests and patients that were noted to have average results that were greater than the other patients tested i.e the outliers that were discussed previously. Patient 1 was one of the notable patients here, having a mean PTT of about 500 ms. Unfortunately, the specifics of this patient are unavailable, but this PTT is approximately twice

the normal and so may not be well suited to a PTT tracking algorithm and this is reflected by the fact that the algorithm performs poorly when either standard is applied. It is interesting to note that Poon's algorithm also performed poorly when it was applied to Patient 1 which adds weight to this statement.

The majority of tests where the algorithm doesn't do well stems from a poor initial estimation. However, even in these situations, the algorithm tracks very well over the entire test, as can be seen in Figure 5.12. It is unclear why this poor estimation only exists in some cases, despite numerous tests, but if it were possible to improve this initial estimation, possibly by a short initial calibration, a marked improvement would be observed in the results.

Patient 4 is an example of this feature, but compared to Patient 1 the mean values are well inside the normal distribution, and has no discernible differences when compared to the other patients. In Figure 5.12 one of Patient 4's tests is used as an example of a poor initial estimation but the test itself, and the values derived from it, exhibit no obvious problems.

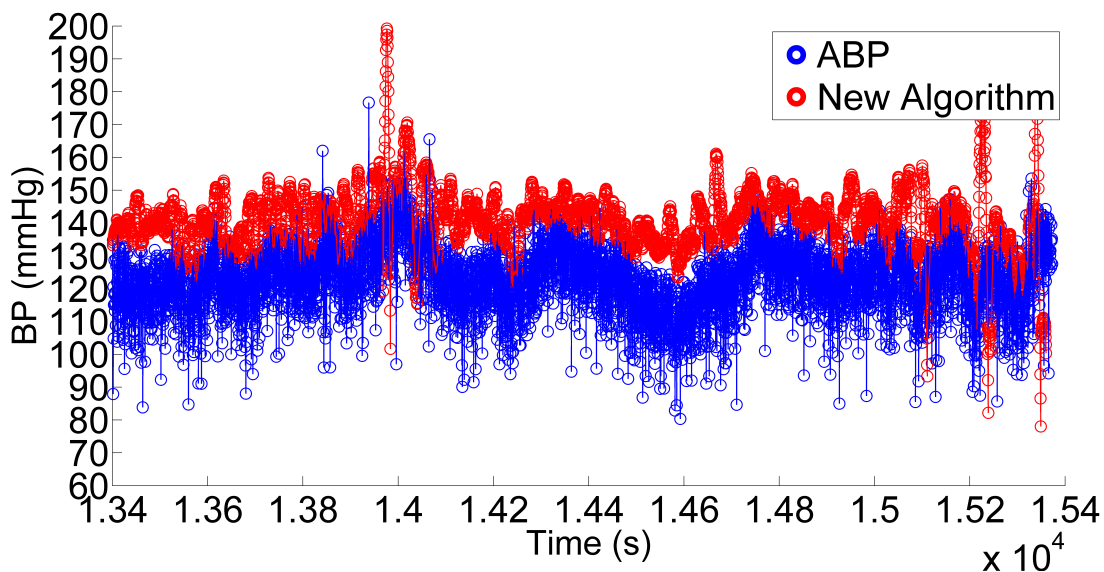


Figure 5.12: A typical example of a poor initial estimation of the new algorithm meaning a poor overall estimation of BP throughout the 30 minute duration of a test. Despite the poor initial estimation, the tracking remains accurate throughout. Again the estimation is being compared to the raw ABP rather than the filtered one.

One other patient, Patient 2, gave some interesting results. Throughout each test, it was found that the new algorithm predicted almost the exact opposite of the ABP. This was found to be the case for each test and only occurred for the tests from Patient 2. Examining the contributions from the SV and PTT, the

origin appears to be from the SV. Since this peculiarity did not appear in Poon's prediction, this would further strengthen this view. It should also be noted that the mean SV throughout Patient 2's tests is abnormally high and this may be the reason why this feature is not observed in any other test.

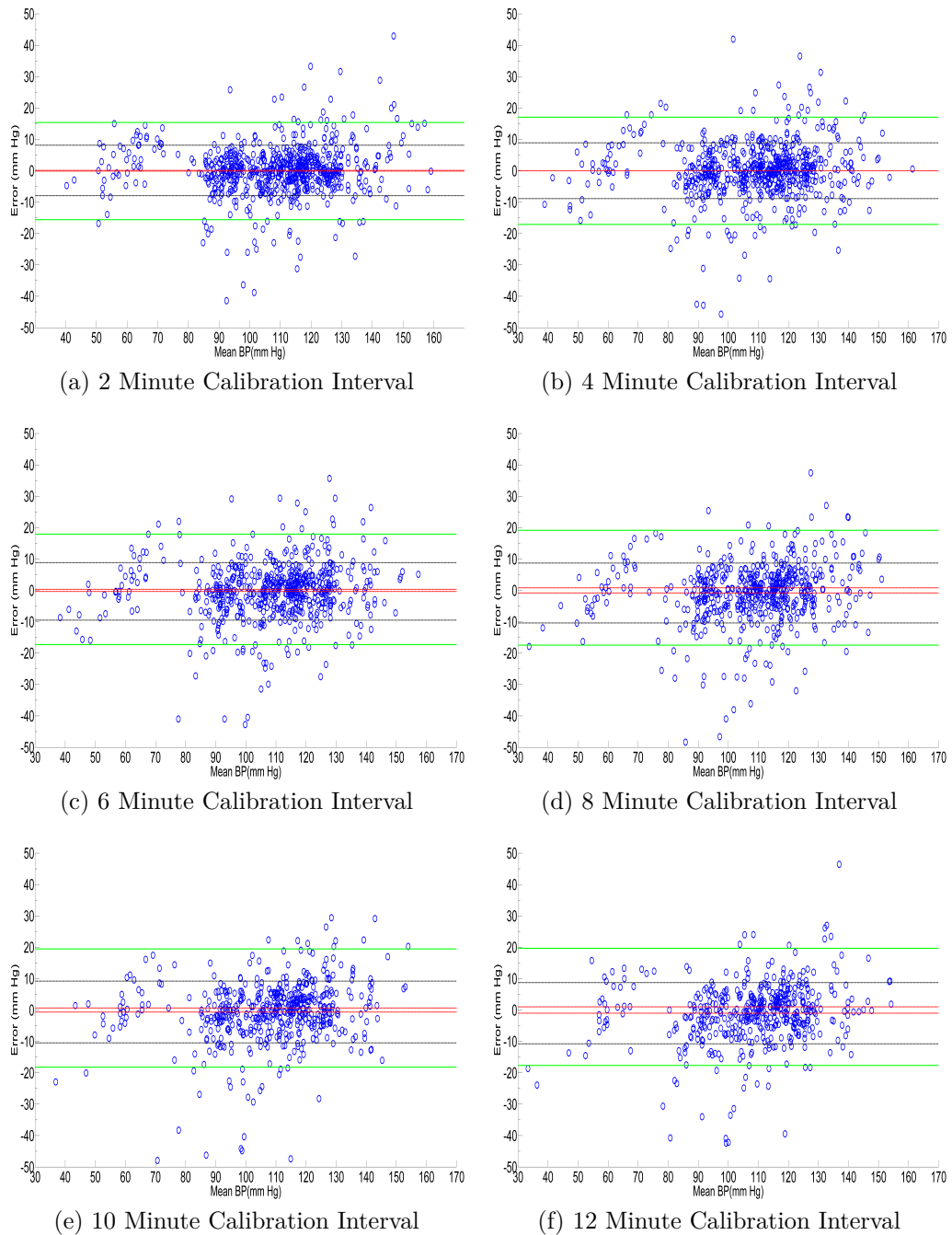


Figure 5.13: The Bland Altman graphs for the new algorithm accumulated across 13 individuals for the six intervals (a – f).

The Bland Altman graphs, shown in Figure 5.13 are an extension of both of the standards used to a certain degree. Each Bland Altman graph shows the mean

Table 5.6: A summary of the results overall and from each volunteer. Each result represents the mean error \pm the standard deviation of error between the Estimated BP, given by the PTT method, and Measured BP given by the ABP

<i>Volunteer</i>	<i>2 Minute Interval</i>	<i>4 Minute Interval</i>	<i>6 Minute Interval</i>	<i>8 Minute Interval</i>	<i>10 Minute Interval</i>	<i>12 Minute Interval</i>
pat 1	0.46 \pm 10.81	-0.29 \pm 11.09	1.71 \pm 13.72	4.39 \pm 10.55	1.17 \pm 11.36	-0.50 \pm 8.00
pat 2	1.90 \pm 12.01	2.91 \pm 14.16	3.70 \pm 15.06	4.74 \pm 16.70	5.25 \pm 17.40	7.05 \pm 16.30
pat 3	2.54 \pm 7.89	2.70 \pm 10.25	1.55 \pm 7.17	2.48 \pm 11.80	3.32 \pm 12.07	1.20 \pm 10.25
pat 4	-2.56 \pm 13.20	-2.43 \pm 11.79	-1.00 \pm 10.87	-1.34 \pm 10.16	-1.86 \pm 12.97	-1.19 \pm 13.98
pat 5	0.60 \pm 3.78	0.40 \pm 4.06	0.04 \pm 3.85	-0.15 \pm 3.92	-0.41 \pm 4.30	-0.24 \pm 4.21
pat 6	0.29 \pm 7.27	0.00 \pm 6.46	0.16 \pm 6.49	0.90 \pm 9.26	-0.25 \pm 7.34	1.92 \pm 7.65
pat 7	-0.85 \pm 8.94	-0.72 \pm 9.57	0.06 \pm 9.77	0.03 \pm 8.55	-0.60 \pm 7.43	1.30 \pm 8.03
pat 8	0.80 \pm 3.03	1.07 \pm 3.68	1.25 \pm 4.17	1.57 \pm 4.67	2.32 \pm 4.03	2.97 \pm 4.74
pat 9	-0.35 \pm 7.08	0.49 \pm 11.12	0.96 \pm 11.73	1.99 \pm 12.21	1.30 \pm 11.18	-0.11 \pm 10.90
pat 10	-3.29 \pm 7.26	-3.14 \pm 9.05	-2.63 \pm 9.43	-1.63 \pm 8.98	-1.29 \pm 8.73	-0.53 \pm 10.07
pat 11	-0.73 \pm 5.84	-0.78 \pm 6.12	-0.51 \pm 6.69	-0.35 \pm 6.64	0.18 \pm 6.68	-0.34 \pm 6.84
pat 12	-1.30 \pm 7.15	-1.04 \pm 8.36	-1.38 \pm 8.44	-1.30 \pm 9.63	0.97 \pm 10.10	-0.32 \pm 8.60
pat 13	1.25 \pm 8.29	1.23 \pm 8.90	1.42 \pm 10.13	-0.84 \pm 9.34	1.75 \pm 11.55	1.18 \pm 11.59
pat 14	0.26 \pm 5.16	-0.08 \pm 6.61	0.04 \pm 7.52	0.69 \pm 7.39	-0.59 \pm 6.58	0.12 \pm 8.76
pat 15	-0.67 \pm 3.58	-0.39 \pm 4.33	-0.29 \pm 4.33	0.12 \pm 5.80	0.57 \pm 6.09	2.18 \pm 8.81
All	0.11 \pm 8.04	0.02 \pm 8.88	-0.32 \pm 9.16	-0.84 \pm 9.54	-0.64 \pm 9.84	-1.01 \pm 9.77

and standard deviation and the AAMI standard is apparent. Examining the Bland Altman graphs more carefully can also provide an indication of the BHS standard, because it is most desirable to have an error less than ± 5 mmHg and all points less than ± 15 mmHg with the exception of a few outliers. Comparing the Bland Altman graphs of Figure 5.13 to Table 5.7, show that the vast majority of points are less than ± 15 mmHg and quite a large cluster are also with ± 5 mmHg. This is emphasised by examining the BHS results of the individual patients in Table 5.7. Again, Patients 1 and 4 perform poorly throughout, but many patients also achieve an *A* or *B* rating throughout giving an overall improvement over Poon's results discussed in Chapter 4.

As discussed in Section 5.4.1, the value of this new algorithm is not always immediately apparent due to the high variability of the Systolic Arterial BP. For this reason, it can be useful to filter this signal and then compare the new algorithm to the filtered signal. Figure 5.14 shows two examples where, although the estimation looks reasonable at first, when the prediction is compared to the filtered signal, the quality of the prediction becomes much more apparent.

5.4.4 Relative Performance

Although the previous section provides some insight into the value of the new algorithm, it is only when it is compared to the algorithms suggested by Chen

5.4 Derivation and Evaluation of a New Algorithm Based on Physiological Parameters

Table 5.7: A summary of the results of the newly developed algorithm from the perspective of the BHS standard.

Volunteer	2 Minute Interval				4 Minute Interval				6 Minute Interval			
	5 mmHg	10 mmHg	15 mmHg	Grade	5 mmHg	10 mmHg	15 mmHg	Grade	5 mmHg	10 mmHg	15 mmHg	Grade
pat 1	47.92%	77.08%	83.33%	C	57.78%	75.56%	82.22%	C	57.14%	69.05%	80.95%	C
pat 2	54.17%	81.25%	87.50%	C	51.11%	68.89%	80.00%	C	38.10%	64.29%	73.81%	D
pat 3	85.42%	85.42%	89.58%	C	84.44%	86.67%	88.89%	C	88.10%	88.10%	90.48%	A
pat 4	29.17%	54.17%	72.92%	D	35.56%	55.56%	80.0%	D	30.95%	69.05%	83.33%	D
pat 5	79.17%	97.92%	100%	A	77.78%	100%	100%	A	80.95%	97.62%	100%	A
pat 6	56.25%	91.67%	93.75%	B	62.22%	88.89%	95.56%	A	54.76%	90.48%	97.62%	B
pat 7	66.67%	85.42%	91.67%	B	53.33%	68.89%	84.44%	C	40.48%	71.43%	85.71%	B
pat 8	83.33%	100%	100%	A	80.00	100%	100%	A	73.81%	97.62%	100%	A
pat 9	63.64%	90.91%	93.94%	A	33.33%	83.33%	93.33%	D	48.15%	74.07%	77.78%	C
pat 10	39.58%	77.08%	95.83%	D	42.22%	66.67%	88.89%	A	40.48%	69.05%	85.71%	B
pat 11	83.33%	97.92%	97.92%	B	71.11%	91.11%	97.78%	B	73.81%	88.10%	97.62%	D
pat 12	54.17%	83.33%	93.75%	D	51.11%	82.22%	91.11%	C	38.10%	78.57%	95.24%	D
pat 13	43.75%	75.00%	93.75%	A	44.44%	77.78%	88.89%	A	33.33%	66.67%	85.71%	A
pat 14	68.75%	95.83%	100%	A	57.78	88.89%	95.56%	A	59.52%	85.71%	92.86%	A
pat 15	85.42%	100%	100%	D	71.11%	100%	100%	C	73.81%	100%	100%	C
All	62.70%	86.10%	92.91%	A	58.79%	82.27%	91.06%	B	55.61%	80.81%	90.08%	B

Volunteer	8 Minute Interval				10 Minute Interval				12 Minute Interval			
	5 mmHg	10 mmHg	15 mmHg	Grade	5 mmHg	10 mmHg	15 mmHg	Grade	5 mmHg	10 mmHg	15 mmHg	Grade
pat 1	71.79%	76.92 %	79.49%	C	50.00 %	80.56%	83.33%	C	66.67%	78.79%	96.97 %	A
pat 2	25.64%	56.41%	76.92%	D	27.78 %	58.33%	69.44%	D	33.33%	45.45%	75.76%	D
pat 3	74.36%	84.62%	84.62%	C	75.00 %	83.33%	83.33%	C	63.64%	87.88%	90.91%	A
pat 4	38.46%	61.54%	89.74%	D	19.44 %	55.56%	80.56%	C	33.33%	63.64%	81.82%	D
pat 5	76.92%	100%	100%	A	75.00 %	100%	100%	A	72.73%	100%	100%	A
pat 6	43.59%	71.79%	89.74%	C	55.56 %	80.56%	97.22%	B	54.55%	81.82%	93.94%	B
pat 7	41.03%	82.05%	92.31%	C	50.00 %	80.56%	91.67%	B	45.45%	81.82%	90.91%	B
pat 8	76.92%	94.87%	100%	A	69.44 %	97.22%	100%	A	69.70%	96.97%	96.97%	A
pat 9	50.00%	70.83%	79.17%	C	42.86 %	71.43%	90.48%	A	50.00%	61.11%	94.44%	B
pat 10	43.59%	71.79%	84.62%	A	52.78 %	77.78%	88.89%	C	39.39%	57.58%	90.91%	C
pat 11	74.36%	84.62%	97.44%	C	69.44 %	88.89%	94.44%	C	60.61%	87.88%	94.44%	C
pat 12	46.15%	79.49%	89.74%	C	41.67 %	66.67%	91.67%	D	51.52%	81.82%	90.91%	D
pat 13	33.33%	71.79%	89.74%	B	47.22 %	69.44%	88.89%	B	36.36%	63.64%	81.82%	B
pat 14	56.41%	89.74%	97.44%	A	55.56%	91.67%	97.22%	B	51.52%	90.91%	97.22%	B
pat 15	61.54%	92.31%	100%	C	58.33 %	91.67%	97.22%	C	51.52%	90.91%	96.97%	D
All	54.39%	79.47%	90.35%	B	52.95 %	79.81%	90.29%	B	52.08%	78.54%	91.25%	B

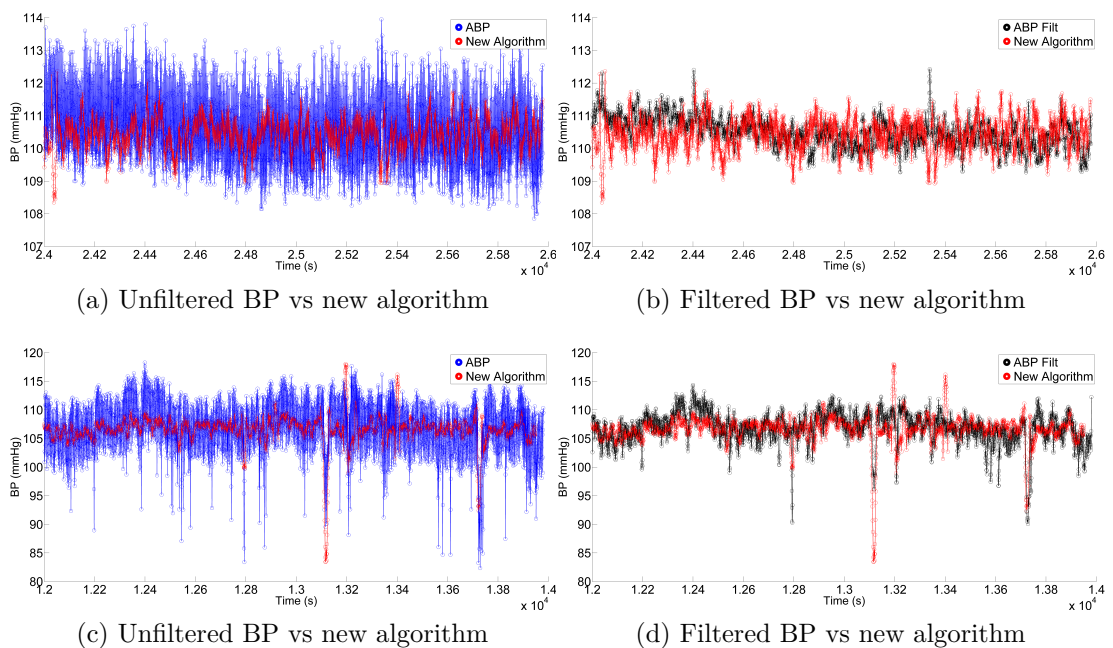


Figure 5.14: By filtering the Systolic ABP, the true value of the new algorithm becomes much more apparent

and Poon that the real value becomes evident. As has been well documented at this stage, Chen's estimation is always poor over any extended period of time, because the shape seems to be the same, regardless of what actually happens to the BP over the duration of the tests. This is shown in Figure 5.15 and this exemplifies a poor filter choice, because it not only clearly changes the PTT values, but also the shape of the signal. Comparatively, it can be easily seen that Poon's prediction and the new algorithm far exceed predictions from Chen's algorithm, especially over longer periods of time.

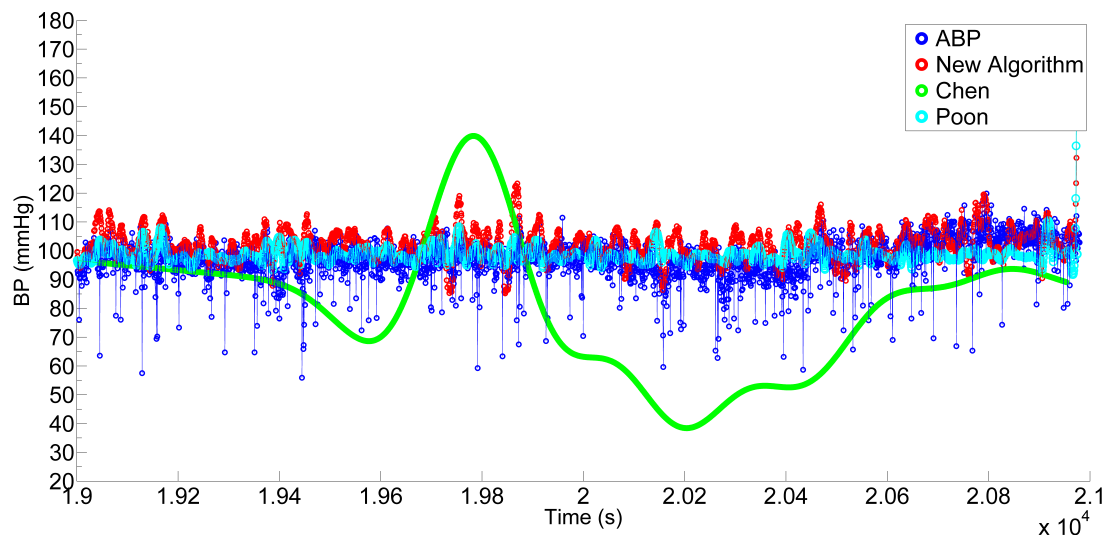


Figure 5.15: This figure shows Chen's prediction, compared to the new algorithm and Poon's prediction. Again the use of an improper filter as designed by Chen is apparent, with the prediction bearing no resemblance to actual changes to the BP

As previously examined in Chapter 4, Poon's prediction is known to provide results within the BHS standard at 2 minutes but fails thereafter. Accordingly, Poon's estimation provides some very good predictions of BP and this can be seen in Figure 5.16, where both Poon's algorithm and the new algorithm perform quite well. As has been previously noted, Poon's algorithm does not often react significantly to changes in BP to ensure a low error within the standards. However, as can be seen in Figure 5.17, the new algorithm has improved on this shortcoming and is capable of tracking BP more accurately than Poon's.

The new algorithm sometimes suffers from the same criticism as Poon where it doesn't react to large changes in BP, and this is exemplified in Figure 5.18a. In these cases, neither Chen's nor Poon's algorithms were capable of tracking these large changes and the new algorithm does track the subsequent changes in BP quite well. The occurrences of this behaviour are also significantly fewer than

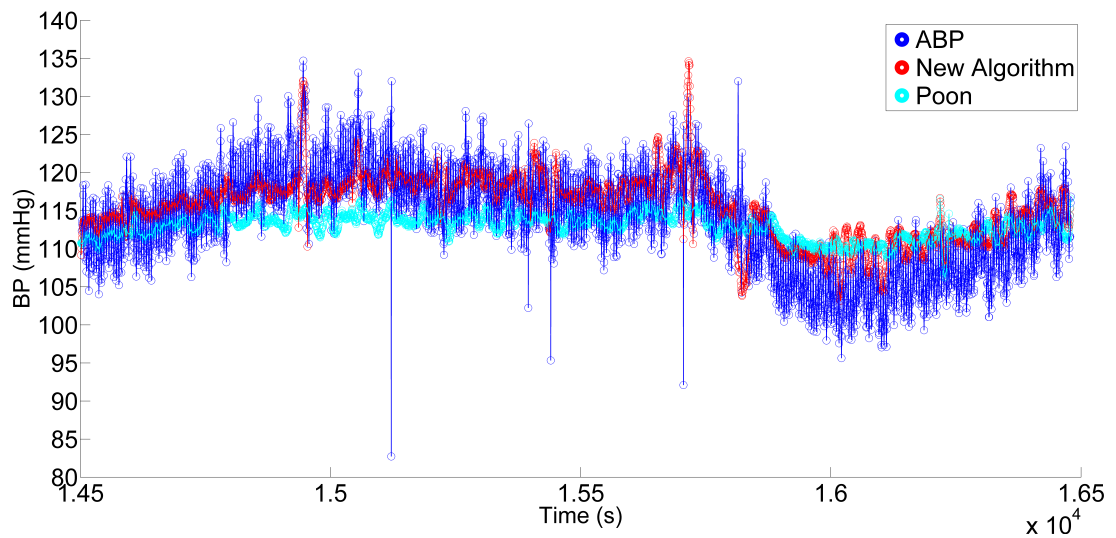


Figure 5.16: This figure shows Poon’s prediction, compared to the new algorithm. Here both algorithms perform quite well, tracking BP and providing a low error throughout.

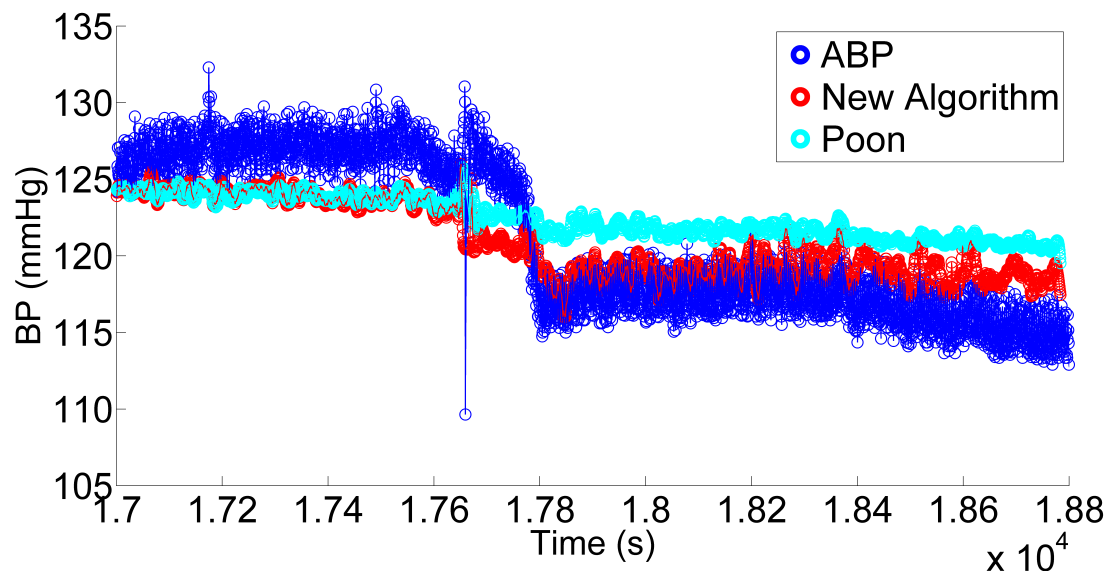
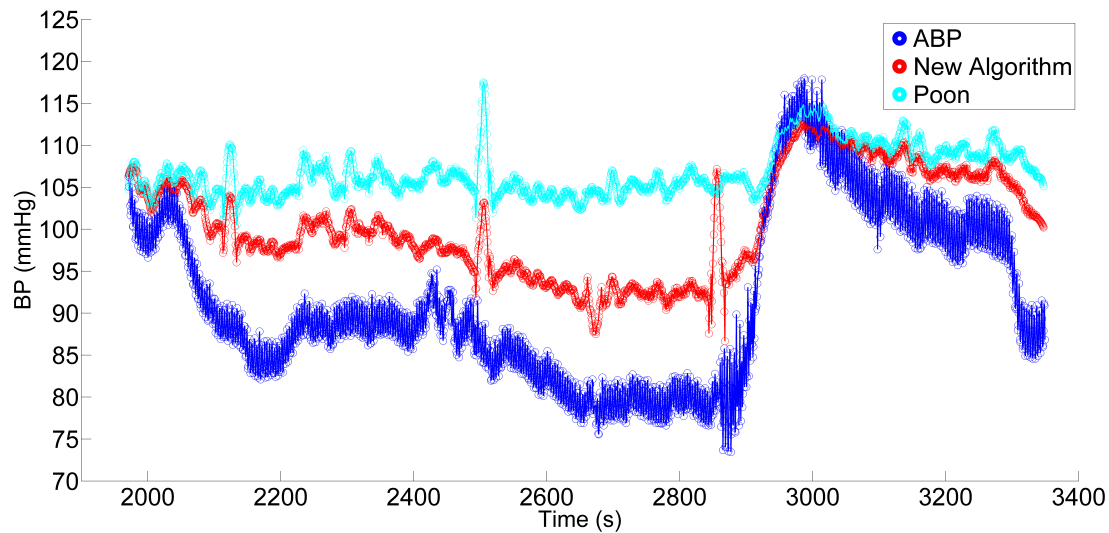
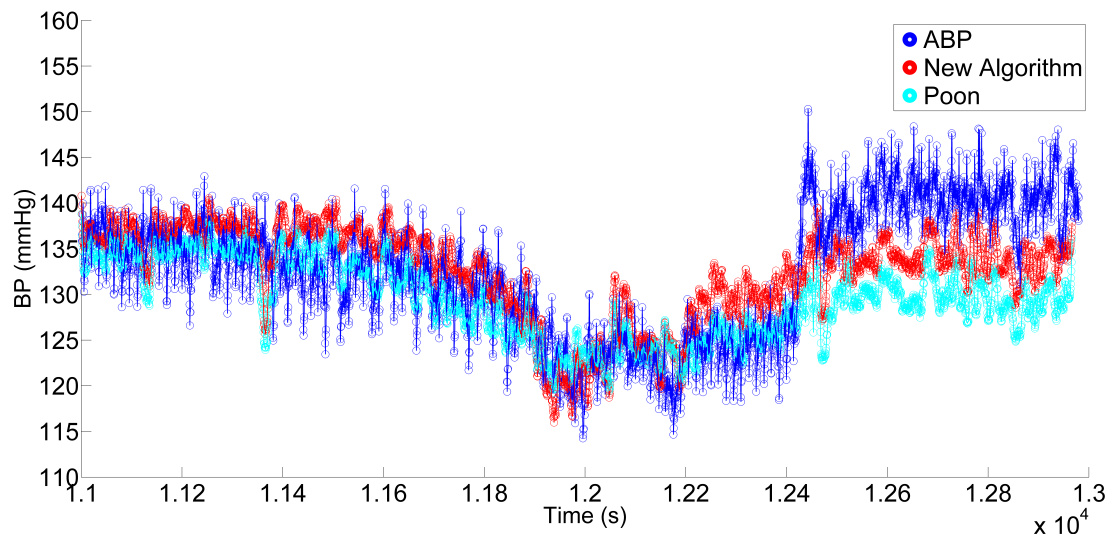


Figure 5.17: The biggest criticism of Poon’s algorithm previously is that it frequently did not react enough to changes in BP. This is apparent in this figure but unlike Poon’s prediction the new algorithm is capable of tracking changes such as these

5. DERIVING A NOVEL BLOOD PRESSURE TRACKING ALGORITHM



(a) Looking at this figure shows that although the new algorithm doesn't react enough to the change in BP, it is a significant improvement over Poon's estimation



(b) Although the new algorithm has an acceptable error in this test after the large change in BP, it is on the limit of the acceptable error. Poon's estimation doesn't react enough again and so an improvement between the two is clear

Figure 5.18: One of the main criticisms of Poon's algorithm was that it did not react adequately to actual changes in BP. On occasion the new algorithm is susceptible to the same criticism, but to a far lesser extent than Poon's algorithm.

the other algorithms but it does still exist, as is apparent in Figure 5.18b. In the tests where this type of large change in BP has been noted, the details of the patient are usually unavailable and therefore it is not possible to identify why these sudden changes occurred. Given the nature of the patients under test, it is quite possible that these reactions are not naturally occurring and could be due to measurement artifacts or a reaction to drugs or surgery. These may also be legitimate, naturally occurring changes in BP but without further information this cannot be verified.

5.5 An Investigation of the Algorithm as Part of a Wearable System

Throughout this thesis, it has been suggested that an Impedance Cardiograph could potentially be used to measure SV. In the later chapters it has also been suggested that when an Impedance Cardiograph is combined with a PTT measurement system and a BP cuff, it would be possible to measure BP on a continuous basis and by non-invasive means. In an attempt to verify these hypotheses an ICG was acquired and a number of tests were done to verify that firstly, it is practical to measure SV using an ICG and secondly, when all three systems were combined a continuous BP measurement was possible for the duration that had been found in the PhysioNet Tests.

Although it would have been most desirable to perform these tests on sick or elderly patients, it was not practical to do so. Instead three subjects that had been used in the tests in section 3.10 were sought to repeat those tests using the new system. In line with all the tests that have been performed throughout the thesis, each subject was tested three times, each test lasting 30 minutes. BP was measured using the Omron M6 oscillometric monitor at two minute intervals. ECG was measured continuously using the PHALs board and PPG was measured continuously using the Tyndall developed system. SV was measured continuously using the Bio-Pac MP36 [168] and the SS31L non-invasive cardiac output sensor [169].

The Bio-Pac system measures Z and ΔZ continuously for the duration of the tests. These signals were then post-processed using Matlab to extract the various parameters required to calculate SV. Three points need to be extracted from the ΔZ signal to calculate SV: the C Point, the B point and the X Point [147]. The

C Point is the maximum of the ΔZ signal during a heart beat, the equivalent of an R wave in an ECG signal. The B Point is the point prior to the C Point which initialises the upstroke of the signal. The X point is the minimum point after the C Point. The difference between the X Point and the B Point gives the Left Ventricle Ejection Time (LVET).

In general, it was found that it was relatively easy to extract the C Point considering it was so prominent in the signal. However, the extraction of the B and X Points were found to be much more difficult. Figure 5.19 shows a typical ΔZ recording and highlights many of the possible locations where each the B or X point could have been erroneously identified and the correct location on each beat. This type of signal is not unusual and these alternative possible B and X point locations have been previously noted by Sherwood [131].

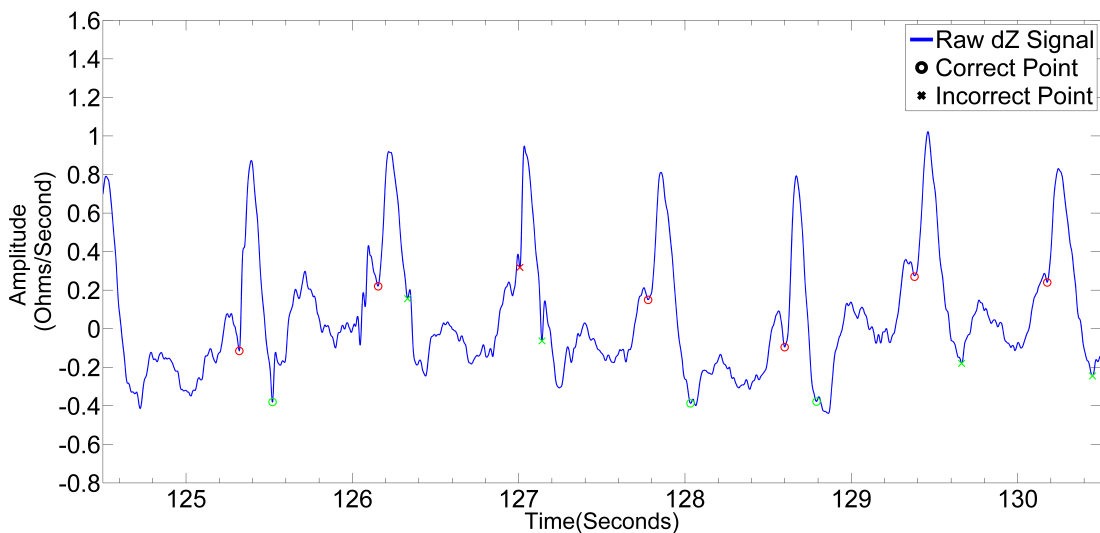


Figure 5.19: Examining the ΔZ signal it is easy to see that identifying the correct location (represented by circles) for each the B (in red) and X points (in green) from a continuous signal is quite difficult and that there are many alternative locations which could be misinterpreted (shown in by crosses) as being a B or X point.

A number of different methods were investigated to extract these points including the use of Continuous Wavelet Transforms [170, 171] and higher order differentiations. However, the solution to extracting these points was found via the use of Ensemble Averaging [172] and the use of a 4th order differentiation of the signal. Using the ECG R waves as a reference, the ΔZ signal is divided into sections defined by R-R intervals. A mean or average ΔZ signal is then formed by taking one minute's worth of R-R interval based segments and averaging each point of the signal across the one minute (usually 60-70) worth of beats as noted by Riese

[173]. An example of the resulting waveform is shown in Figure 5.20.

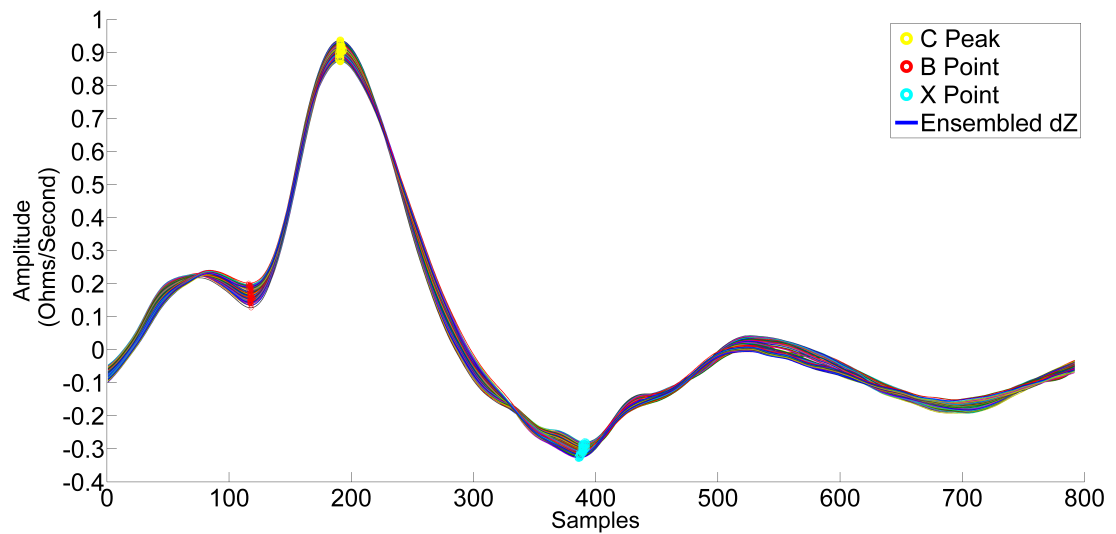


Figure 5.20: The Ensemble Averaged ΔZ signal, showing the B, C and X points

Using the ensemble averaged ΔZ signal, it becomes much easier to identify the C and X points. The C point is defined as the largest peak in the window. The X point is then defined as the lowest point after the C point. However, it is much more difficult to identify the B point. In some cases, the B point could be identified as the first minimum peak prior to the C Point. However, a feature of the ensemble averaging has been noted as a flattening of the signal and this was most prominent around the B point. An alternative and reliable method to identify the B point was found by taking the fourth derivative of the signal and searching for the first peak that occurred prior to the C Point, as shown in Figure 5.21.

Once a successful and reliable method had been found to identify each of the characteristic points, testing of the algorithm could begin on real patients and the results can be seen in Tables 5.8 and 5.9 showing the results from the BHS and AAMI standards respectively. Examining the last row and overall results of the BHS results in Table 5.9 it can be seen that the new algorithm passes the standard for the 2, 4, 6, 8 and 12 minutes intervals. The algorithm is outside the BHS standard at the 10 minute interval by 0.1%. In terms of the AAMI standard, the algorithm is inside the standard for the 2, 4, 6 and 8 minute intervals, while each of the remaining intervals are outside the standard, even though it is only by a marginal amount.

On closer examination of these results, it can be seen that the results from Volunteer 3 were significantly worse than either of the other two volunteers. In an

5. DERIVING A NOVEL BLOOD PRESSURE TRACKING ALGORITHM

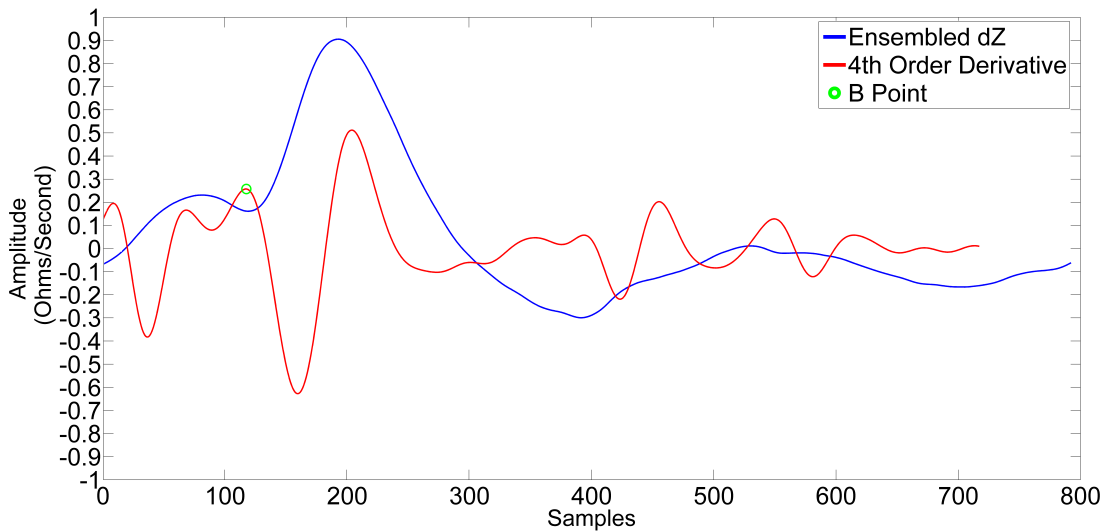


Figure 5.21: Although it is quite easy to identify the C and X Points via thresholding, identification of the B point was much more difficult and required using the 4th derivative of the signal.

Table 5.8: A summary of the results overall and from each volunteer, presented in the form of the AAMI standard. Each result represents the mean error \pm the standard deviation of error between the Estimated BP, given by the new algorithm, and the measured BP given by the cuff measurement

<i>Volunteer</i>	<i>2 Minute Interval</i>	<i>4 Minute Interval</i>	<i>6 Minute Interval</i>	<i>8 Minute Interval</i>	<i>10 Minute Interval</i>	<i>12 Minute Interval</i>
Volunteer 1	0.50 \pm 4.50	-1.26 \pm 4.06	-1.46 \pm 4.74	-1.75 \pm 4.50	-0.97 \pm 5.01	-0.77 \pm 5.05
Volunteer 2	2.74 \pm 5.65	2.72 \pm 6.06	2.91 \pm 7.20	3.51 \pm 6.28	3.39 \pm 6.58	3.29 \pm 6.78
Volunteer 3	1.17 \pm 9.65	0.27 \pm 9.61	-0.44 \pm 9.57	-0.46 \pm 10.87	-0.46 \pm 11.15	-1.96 \pm 10.60
All	1.13 \pm 7.07	0.56 \pm 7.23	0.30 \pm 7.58	0.45 \pm 8.00	0.64 \pm 8.22	0.17 \pm 8.23

Table 5.9: A summary of the results of the newly developed algorithm from the perspective of the BHS standard, using data recorded from the ICG.

<i>Volunteer</i>	<i>2 Minute Interval</i>				<i>4 Minute Interval</i>				<i>6 Minute Interval</i>			
	5 mmHg	10 mmHg	15 mmHg	Grade	5 mmHg	10 mmHg	15 mmHg	Grade	5 mmHg	10 mmHg	15 mmHg	Grade
Volunteer 1	73.33%	97.78%	100%	A	80.95%	97.62%	100%	A	74.36%	92.31%	100%	A
Volunteer 2	62.22%	84.44%	97.78%	B	61.90%	83.33%	92.86%	A	48.72%	79.49%	97.44%	C
Volunteer 3	42.22%	57.78%	86.67%	D	35.71%	71.43%	88.10%	D	38.46%	71.79%	87.18%	D
All	59.26%	80.00%	94.81%	B	59.52%	84.13%	93.65%	B	55.56%	80.34%	94.02%	B

<i>Volunteer</i>	<i>8 Minute Interval</i>				<i>10 Minute Interval</i>				<i>12 Minute Interval</i>			
	5 mmHg	10 mmHg	15 mmHg	Grade	5 mmHg	10 mmHg	15 mmHg	Grade	5 mmHg	10 mmHg	15 mmHg	Grade
Volunteer 1	63.89%	97.22%	100%	A	69.70%	96.97%	100%	A	66.67%	90.00%	100%	A
Volunteer 2	50.00%	86.11%	88.89%	B	48.48%	84.85%	93.34%	C	53.33%	83.33%	96.67%	B
Volunteer 3	33.33%	63.89%	83.33%	D	45.45%	57.58%	75.76%	D	43.33%	70.00%	86.67%	C
All	50.00%	82.41%	91.67%	B	54.55%	79.80%	89.90%	C	53.33%	78.89%	94.44%	B

Table 5.10: A summary of the results overall and from each volunteer, presented in the form of the AAMI standard. Each result represents the mean error \pm the standard deviation of error between the estimated BP, given by the new algorithm, and the measured BP given by the cuff measurement

<i>Volunteer</i>	<i>2 Minute Interval</i>	<i>4 Minute Interval</i>	<i>6 Minute Interval</i>	<i>8 Minute Interval</i>	<i>10 Minute Interval</i>	<i>12 Minute Interval</i>
Volunteer 1	0.50 \pm 4.50	-1.26 \pm 4.06	-1.46 \pm 4.74	-1.75 \pm 4.50	-0.97 \pm 5.01	-0.77 \pm 5.05
Volunteer 2	2.74 \pm 5.65	2.72 \pm 6.06	2.91 \pm 7.20	3.51 \pm 6.28	3.39 \pm 6.58	3.29 \pm 6.78
Volunteer 3	1.56 \pm 8.31	1.27 \pm 8.47	0.99 \pm 7.80	1.07 \pm 8.70	0.68 \pm 9.35	-0.15 \pm 9.01
All	1.27 \pm 6.45	0.91 \pm 6.61	0.81 \pm 6.89	0.95 \pm 6.99	1.03 \pm 7.36	0.79 \pm 7.28

attempt to understand why these results were so bad, a more comprehensive examination of the results of Volunteer 3 was completed. Although the signals recorded from this volunteer were acceptable, when the volunteer was questioned, a possible reason for the poor results was identified. During the first of the three tests carried out on Volunteer 3, it appears that the volunteer was able to see the results of the BPs and Pulse rate from the cuff measurements. Throughout the test, it emerged that the volunteer was performing “deep breath exercises” in an attempt to lower either their BP or pulse rate. The volunteer said that they would begin the deep breath exercises leading up to a cuff measurement and stop immediately afterwards. Examining the results of this first test, it was observed that the results recorded from it were worse than the other two tests.

It was therefore decided to test this volunteer once more, this time ensuring that they could not see the results from the BP monitor and with an assurance from them that they would not practice their deep breath exercise during the measurements. The results from this test are shown in Table 5.10 and Table 5.11 and show a significant improvement over the initial tests. In Table 5.10, it can now be seen that when all the results are accumulated, the results are within the AAMI standard at every interval. In a similar fashion, in Table 5.11, the accumulated results are within the BHS standard at every interval.

Once again, each of these tables highlights and reiterates results that have been seen throughout the testing of various algorithms. The first point is that no matter what the algorithm, some people are more suited to certain algorithms than others. As previously outlined, in both Table 5.11 and Table 5.10, Volunteer 1 seems to be very suited to the algorithm where as Volunteer 3 consistently exhibits much poorer results, while Volunteer 2 lies somewhere in between these two extremes. The second point is that a large number of volunteers are required to get a good picture of the value of an algorithm since one extreme set of results

Table 5.11: A summary of the results of the newly developed algorithm from the perspective of the BHS standard, using data recorded from the ICG and the re-test of Volunteer 3.

Volunteer	2 Minute Interval				4 Minute Interval				6 Minute Interval			
	5 mmHg	10 mmHg	15 mmHg	Grade	5 mmHg	10 mmHg	15 mmHg	Grade	5 mmHg	10 mmHg	15 mmHg	Grade
Volunteer 1	73.33%	97.78%	100%	A	80.95%	97.62%	100%	A	74.36%	92.31%	100%	A
Volunteer 2	62.22%	84.44%	97.78%	B	61.90%	83.33%	92.86%	A	48.72%	79.49%	97.44%	C
Volunteer 3	46.67%	71.11%	93.33%	C	35.71%	80.95%	92.86%	C	43.59%	84.62%	94.87%	C
All	60.74%	84.44%	97.78%	B	59.52%	87.30%	96.30%	B	55.56%	85.47%	97.44%	B

Volunteer	8 Minute Interval				10 Minute Interval				12 Minute Interval			
	5 mmHg	10 mmHg	15 mmHg	Grade	5 mmHg	10 mmHg	15 mmHg	Grade	5 mmHg	10 mmHg	15 mmHg	Grade
Volunteer 1	63.89%	97.22%	100%	A	69.70%	96.97%	100%	A	66.67%	90.00%	100%	A
Volunteer 2	50.00%	86.11%	88.89%	B	48.48%	84.85%	93.34%	C	53.33%	83.33%	96.67%	B
Volunteer 3	50.00%	77.78%	91.67%	B	57.78%	69.70%	84.85%	D	50.00%	80.00%	93.33%	B
All	54.63%	87.96%	96.30%	B	58.59%	83.84%	92.93%	B	56.67%	84.44%	96.67%	B

from either Volunteer 1 or Volunteer 3 can significantly skew the results, as has been exhibited by the need for a retest of Volunteer 3.

This test has established that the algorithm that has been developed can not only be used on data that has been measured invasively i.e. via the PhysioNet database, but can accurately predict and track BP using non-invasive measurements. It is clear that to be fully validated, a much larger number of volunteers would be required, but this test has validated the concept that by using the algorithm, an ICG, a PTT system and a cuff monitor, BP can now be measured continuously and non-invasively simply by taking one cuff measurement every 12 minutes. Not only does this double the calibration interval of the previously investigated algorithms, but it makes the algorithm and system practical for both users and clinicians and provides a potential breakthrough in BP measurement.

5.6 Summary

This chapter presented the key focus for this thesis, namely deriving a new algorithm that would improve existing algorithms for the calculation of BP using a PTT based method by including other parameters such as HR and SV.

The first step of this process was to identify the key parameters that had the most potential to improve the algorithms. Using methods such as including correlations and Draftsman graphs, it was possible to confirm that both SV and PTT had strong correlations to BP and should be the key parameters in any calculation. Initially, HR was also included in the investigation, despite having poor or mixed correlations with BP. This was especially highlighted when semblance analysis was included. Using semblance analysis, it also became much easier to identify

some combinations of parameters that could help provide a solution.

Once the key parameters had been established and some other combinations of these parameters were also determined, the process of deriving an algorithm began by investigating the use of Multiple Linear Regression for a solution. The β values derived by the MLR process were derived from the continuous beat to beat independent variables. During the initial tests of the various equations, it was established that using HR was having a detrimental effect on the algorithms and it was omitted from subsequent versions. Another problem that was identified was that there was a large variability in the PTT, SV and respective β values that were being derived and this was causing large offsets and errors among the estimations.

Therefore, the next evolution of the MLR equations examined the use of categorisation to compensate for the large differences that were observed across the datasets. By categorising SV and PTT according to their values and the β values that had been derived for each variable, many of the large offsets and errors were eliminated depending on which combination of parameters was being investigated. However, some offsets still existed and under further examination it became evident that the PTT and SV contributions were interlinked and so both values had to be taken into consideration when categorising the data.

The next algorithm took a ratio of PTT:SV and used the results of this ratio, along with the β values to categorise the data. It was also established that the β_0 value that was being used in the derivation could be omitted. This yielded much better results and the algorithm is now able to perform for 10 minutes without needing calibration. However, upon review, it was found that although categorisation of data can be used if a strong justification exists, the categorisation process for this process was limited and not easily justifiable. The other main concern was that although it gave good results, the algorithm had no obvious physiological meaning or derivation. In an attempt to fulfil this self imposed restriction, alternative methods and derivations were examined. From examining the correlations, the semblance analysis and each of the MLR algorithms that had been derived, it was clear that the primary components of any new algorithm should be both PTT and SV. For this reason, a further investigation was undertaken to develop a new, physiological based, algorithm that would incorporate these parameters.

Since the MLR equations that only used SV and PTT had proven to perform so well, these parameters became the focus of a more rigorous investigation. Since

Moens-Korteweg is used as a basis for nearly all PTT based algorithms, this was chosen as the basic equation that described the system and it was decided that SV should be incorporated into an algorithm derived from this equation. Another equation, the Bramwell - Hill equation, which is also frequently used in PTT algorithms has a volume component and this was also used as part of the basis of the new algorithm. Finally, after an investigation into fluid dynamics, physiological and cardiological relationships, the key component, the Poiseuille equation, was incorporated into the derivation and a new algorithm was created.

This new algorithm was evaluated using both the BHS and AAMI standard. Although the algorithm failed the AAMI standard at every calibration interval other than two minutes due to an excessive standard deviation, this excess was never greater than 1.3 mmHg, an improvement when compared to Chen and Poon. Unlike the AAMI standard, when the BHS standard was applied, the new algorithm passed at every calibration interval that was examined, up to a maximum of 12 minutes. This is twice the previously recorded best from Chen and Poon, although Chen's shortcoming has been previously identified and discussed. It has also been noted that the algorithm suited some patients better than others and it is interesting to note that the two patients who provided the worst results are those who also gave poor results when Poon was applied. For one of these patients, it had been noted that their PTT is quite high at 500 ms and so may not be suited for this type of algorithm. However, for the second patient, their mean values are not remarkable and so it is unclear why they consistently performed so poorly.

The biggest limitation to further testing was due to the lack of datasets that had continuous good quality data for greater than half an hour. As previously noted, in 9 tests the algorithm was capable of tracking changes over 45 minutes, without the need for recalibration, but since there were so few of these tests it was not possible to do a complete statistical analysis of these occasions. The next chapter discusses acquiring data for longer periods of time so a complete analysis of long term tracking of blood pressure by this new algorithm can be done.

Although the results of the new algorithm were really good, the algorithm had only been tested using data that had been gathered clinically and invasively using the PhysioNet database. Although it had been suggested throughout the thesis, there was no indication that the algorithm could be implemented in a practical system. To test this concept, an Impedance Cardiograph was purchased and together with the PTT system that had been previously used, the Omron M6

BP monitor and the new algorithm three volunteers were tested using the same procedure as before. The results of these tests were as good as had been found by using the PhysioNet database. Furthermore, this validates that the algorithm can be implemented in a practical system and has validated the conceptual system which had been previously suggested. By implementing this system it is now possible to track BP continuously and non-invasively, with high accuracy when a 12 minute calibration interval is used. Although further testing will be required as will be discussed in Chapter 6, this new algorithm and system provides a significant and important improvement, not only over existing PTT equations, but to the area of BP monitoring in general.

Chapter 6

Discussion, Conclusions and Future Work

6.1 Summary

Initially, it had been envisaged that this project would create a new BP monitoring system that would allow continuous BP to be monitored using a non-invasive technique. This system would be unobtrusive, wearable and comfortable for the user, while being accurate and reliable. During the literature review described in Chapter 2, a number of systems that were identified suited certain requirements of this project, but none completely satisfied all of them. After the PTT method had been identified as a suitable candidate, it became clear that it could potentially satisfy all the requirements. It also became evident, from examining this method, that the key to the project would not necessarily be the creation of the system but the development of the algorithm that would facilitate the measurement and monitoring functions.

The first step of the project was to identify the state of the art algorithms and to test their performance with calculations of PTT from ECG and PPG in an unbiased manner. During the literature review, it was established that many tests of the algorithms were only performed over very short periods of time (usually less than a minute) and their value was unclear. Other algorithms, such as Chen's had been tested over longer periods of time, and their accuracy had been established but the interval between measurements that required calibration was not stated. Two of these algorithms were thus chosen to test the hypothesis of the PTT method, namely Chen's and Poon's algorithms. The test was performed on 15

young, healthy individuals, with each individual being tested three times and each test lasting 30 minutes. A PTT system was built for this test and an Omron M6 BP monitor was used for calibrating and benchmarking the system. Each algorithm was tested to determine which could monitor and track BP changes the most accurately and which would provide the longest calibration interval. After analysing the results, it became clear that although Chen's algorithm provided a much longer calibration interval of 6 minutes, it was virtually useless at tracking BP changes due to the presence of a filter used in its design. Although Poon's algorithm failed even when a two minute calibration interval was used, it did provide some tracking of BP and if some improvements could be made to it, it was predicted that it would perform much better.

Overall, this set of tests established that neither of the PTT algorithms that were tested could be used in any practical implementation and that a significant improvement was necessary. After examining the results of others, it was noted that a number of authors had suggested that an improvement could only be made by including more cardiac parameters to develop the necessary algorithm. Parameters suggested included pre-ejection period, HR and SV [90, 149, 150].

Two methods of obtaining this data were identified: the PhysioNet Resource, a large database of physiological signals that had been recorded from patients in a hospital; and the use of an Impedance Cardiograph system that could be used to record new data in real life experiments.

The PhysioNet Resource contains many databases of physiological signals and some of these databases contained records from patients where SV, HR, ECG and PPG signals were being monitored directly. The benefit of using this database was that many of the signals, especially the BP, was an invasive beat to beat measurement and was much more accurate than the cuff measurements taken to date. On examination it was found that only 15 records existed that contained all the necessary signals of SV, ECG, PPG and ABP.

The alternative was to measure these parameters by using an ICG, one of the only methods by which the parameters could be measured by a non-invasive technique. However, it was also found that very little information was available about ICGs, despite the many investigations into their use in the past. A measurement using ICGs is covered by Medicare in the USA and this led to a number of ICG products being manufactured. However, most of these were found to be quite expensive and in the same price range of other medical systems, such as ECG bedside monitors, used in hospitals. Therefore, if an ICG system were to be used, it would need to

be designed and developed.

After some consideration, it was realised that since it was possible to acquire these parameters from the PhysioNet Resource, this acquisition method was preferable since the key to the project was to develop an algorithm and not an ICG system.

To test its value, the algorithms identified in Chapter 3 were retested based on the signals taken from the PhysioNet database such as ABP, ECG and PPG. The outcomes of these tests showed that using Chen's algorithm gave a similar result to that found in Chapter 3, but that using Poon's algorithm gave an improved result due to the use of the continuous invasive ABP measurements instead of the use of intermittent BP cuff measurements. In this test Poon's algorithm was able to track BP for up to 2 minutes without needing a recalibration. Although this is a significant improvement over the previous results, the calibration interval still remains too low to be of practical use. However, the value of the database had been established by this result and an approach that looked to incorporate the SV and HR parameters into an equation was undertaken.

Although a number of these parameters had been identified from various papers, it was not clear how strongly the parameters related to BP or how much value could be gained from using them. The first step in the process of designing the algorithm was to establish how strongly each parameter was related to BP and whether it should be present in a new algorithm. The use of correlations and Draftsman Charts were used to examine these parameters, but semblance analysis was found to be the most useful technique because it enables comparisons of time varying data streams. Using semblance analysis, a number of combinations were identified which showed a strong relationship to BP and that could be useful in a new algorithm.

The first method that was used to create a new algorithm was the use of Multiple Linear Regression. When this technique was used, the beat to beat continuous independent variables were used to derive the β values. The β values were then averaged and applied to the same dataset. During the development of the first MLR based algorithm i.e. *Algorithm 1-x*, it was noted that HR was having a detrimental affect on the outcome of the algorithms and it was subsequently omitted when the MLR tests were rerun giving *Algorithm 2-x*. While investigating *Algorithm 2-x*, the variance between patients became more prominent and the dominating influence of the algorithm. Therefore, the equations derived from this approach were found to be ineffective and an algorithm that was universally applicable was not found and would not be found unless a fundamental change

was applied. *Algorithm 3-x* used a categorisation process where PTT and SV along with their respective β values were grouped into different categories and β values were only applied to appropriate PTT values and SV values and most of the large offsets that had been found in *Algorithm 2-x* were eliminated. Although *Algorithm 3-x* brought a significant improvement, it was thought that the algorithm could be improved by taking both SV and PTT into account when generating and applying β values. Therefore in *Algorithm 4-x* the ratio of PTT:SV was examined and β values were categorised using this ratio. This process yielded further improved results, and when this algorithm was tested it was found that a 10 minute calibration interval could be achieved.

Although *Algorithm 4-x* was a significant improvement, not only over other MLR equations but also over Chen and Poon's algorithms. However, it had no obvious physiological basis or justification. For this reason it was decided that an alternative method should be investigated, using existing PTT algorithms as a foundation and using the lessons that had been learned from the MLR process, fluid dynamics, physical relations and equations as well as physiological and cardiological relationships. After a detailed investigation of these relationships, a new algorithm was derived from a combination of the Bramwell Hill equation, the Moens Korteweg equation and the Poiseuille equation. When this algorithm was tested, it was found that not only did it track BP changes very well, and that it was universally applicable but it also passed the BHS standard even when a 12 minute calibration interval was used. This is a calibration interval 100% and 600% greater than Chen's and Poon's algorithms, respectively. It is also suspected that a longer calibration interval may be possible but due to limitations of the database, it was neither possible to test larger calibration intervals nor to have more statistically significant results.

6.2 Discussion and Conclusions

The original goal of this project was to develop an algorithm that could be used as part of a new BP monitoring system that would monitor BP continuously and non-invasively while being unobtrusive and comfortable to the user, something which no current system provides. The algorithm that has been developed uses PTT and SV to continuously monitor BP, along with intermittent BP measurement by other means. It has been shown that the PTT satisfies all the requirements of a continuous and wearable system and that by using an ICG to

measure SV, this system would also satisfy these requirements and therefore the goal of the project has been successfully achieved.

This new algorithm is valid when using a 12 minute calibration interval, a 100% improvement over existing approaches and it is suspected that a longer calibration interval is possible. However, due to the lack of continuous data for periods greater than half an hour, it is not possible to test this theory using the PhysioNet databases, since there would not be enough data to make statistically valid conclusions. Even if it is found that 12 minutes is the limitation of this new algorithm, this is a significant improvement over the current algorithms and brings the method into the realm of being practically useful.

One of the primary methods that is used by cardiologists for “*in home*” monitoring and diagnosis of patients is the use of an oscillometric BP monitor that inflates once every 15 minutes over a 24 hour period. As has been highlighted throughout this thesis, the use of intermittent points to diagnose or assess a signal can be fraught with difficulty and it is highly recommended that such situations be avoided. If this new algorithm could be extended to have a calibration interval of 15 minutes, and if it could be incorporated into the existing system that is given to these patients, a cardiologist could then potentially have 24 hour continuous monitoring of BP. Even if the algorithm is ultimately found to only be accurate using a 12 minute calibration interval, this would only mean one extra measurement every hour for the patient to achieve continuous BP measurements.

Throughout this thesis, SBP has been the main focal point of all analysis and discussion. However, in a clinical setting, both SBP and DBP are used in tandem. The decision to focus on SBP comes from the fact that SBP is generally considered to be more important, as it provides a much greater predictor of risk and indicator of cardiovascular health [174, 78, 175]. More specifically, isolated systolic hypertension (hypertension where only the SBP is raised, while the DBP remains at a normal level) predicts risk better than isolated diastolic hypertension [176]. Epidemiologically, isolated systolic hypertension is the most common form of hypertension and is present in approximately two thirds of hypertensive individuals older than 60 years of age [177]. It was therefore felt that the ability to track SBP on a continuous basis would provide far more vital information, in far more cases. The deployment of this algorithm, which allows the beat to beat tracking of SBP, could allow the early identification of CVD and to track and monitor hypertensive patients with elevated SBPs.

Although not as important, the ability to track DBP would also be highly useful

and beneficial. An initial evaluation of the newly developed algorithms to track DBP has taken place using the PhysioNet database. These results show that the algorithm is capable of tracking DBP, again using a 12 minute calibration interval. However, these results also showed that the algorithm failed the BHS standard when either an 8 or 10 minute calibration interval was used. The source of this failure, in both cases, were due to the algorithm failing to have sufficient datapoints less than 15 mmHg i.e. at both of these interval, less than 90% of the points were less than 15 mmHg. Although the level of failure at both intervals was marginal, 0.7% and 0.1% respectively, it is a cause of concern and indicates that more volunteers/patients should be evaluated to confirm these findings. It may also be the case that more work may be needed to adapt the algorithm for DBP, or that a specific algorithm for DBP should be developed, similar to that of Poon, who had two different algorithms; one for SBP and one for DBP. The first step, in either case, should be the testing of more patients/volunteers, ideally via a clinical trial.

It is also interesting to note the failure of both the new algorithm and Poon's algorithm over certain calibration intervals when the AAMI standard is used. When both of these algorithms were analysed, no outliers were removed from either test to ensure complete analysis. Examining the Bland Altman graphs for Poon's test in Chapter 4, a drift and expansion of the data points from the zero error point (and even the 5mmHg error) can be observed as the calibration interval increases and the reason for the failure of the AAMI standard becomes more obvious than when the Bland Altman graphs for the new algorithm in Chapter 5 are examined. In these graphs the cluster of data points around the zero mark (and inside the 5mmHg error marks) does not seem to degrade as significantly. The number of outliers seems to increase a little as the calibration interval increases and certainly the numerical value of these outliers also seems to increase. Examining the associated AAMI table and even the BHS table, it is clear that there are a number of patients whose results perform poorly throughout. The details of these Patients 1 and 4 are unknown, although the large PTT of *Patient 1* could indicate that the algorithm may be unsuitable for them.

Another patient who performs poorly throughout is *Patient 14* whose specifics are stated to be post - op cardiac bypass graft. Whether this patient should have been excluded from the evaluation or not is questionable. However, examining each of the three tests of this patient reveal that the new algorithm performs very well in two of the tests and for the one that failed a large offset is apparent due to a poor initial estimation.

The major problem of using the PhysioNet database is highlighted by these three patients. Due to the limited availability of all the required signals, it was necessary that all patients where the signals were found had to be used. In the case of *Patient 14*, it could be argued that this type of patient should not be included when evaluating a new technique but their inclusion is probably of more value than their exclusion. In the case of Patients 1 and 4, it is quite possible that they should be excluded given how poorly they performed for both Poon and the new algorithms. However, without knowing their specifics, they must be included unless it was found they had abnormal signals. It is also quite possible that some of the patients that were tested were on BP altering drugs and were also not suitable for testing, but again given the limited knowledge and limited availability of data every one of the patients had to be included.

In many ways, the value of the new algorithm can be appreciated because of the test subjects that were used. It is more than likely that it is these types of people on which the algorithm would be used, rather than fit, healthy individuals. However, in order for it to be properly evaluated, the ailments and specific treatment regimes of each person under test must be fully known and a wide variety of people such as those found in the database should be evaluated.

The use and assessment of the MLR equations that were used to develop a new algorithm in this work, has emphasised the range of people and parameter values that were available in the PhysioNet database. If any BP monitors are to be evaluated, a range, such as those used in the PhysioNet database, should be mandatory. The ESH standard goes some way to enforce this, saying that the subjects used should have low, medium and high systolic and diastolic BPs in order to pass the standard. It may also be appropriate to not only examine people and categorise people (and their measurements) using a large range of BPs, but also to examine other cardiovascular parameters that have an influence on their health, such as PTT and SV.

If a large range of people is not used to evaluate BP monitors, it is possible that these monitors may pass standards they would otherwise fail. An example of this has been noted in relation to Poon's algorithm in section 3.10.2, where it was noted that the algorithm seems to be quite accurate between 100 and 130 mmHg. Had the evaluation of Poon's algorithm been limited to this range, it is possible that it would have passed the standard at every calibration interval. However, because the algorithm was evaluated using people with a much larger range, its limitations were also identified.

Although the ESH standard was not used to evaluate any algorithms in this work, due to the various concerns outlined in Appendix A, it is worth some discussion. Aside from the concerns outlined in Appendix A, it would not have been possible to implement the ESH standard completely in this work since there were not enough patients available in the PhysioNet database with the required parameters nor were there (proportionally) enough patients from each of the required ranges of BP. The ages and health of the patients that were used satisfy the requirements of the standard, although more BP readings would have been required by independent, blind observers. Since the ESH standard uses a similar grading system of the BHS standard, it is anticipated that the new algorithm would pass the ESH standard. To further emphasise this, by analysing the Bland Altman graphs in section 5.4.3, it can be seen that there are no apparent trends in the graphs that suggest the use of more patients, with either higher or lower BP ranges, would have caused a fail if the standard had been applied.

The final test, where the algorithm was implemented using a practical system and tested using volunteers, is an important validation of the work described in this thesis. Although this test was a preliminary one to establish the value of the ICG and the new algorithm, it has validated the concept of the system and the algorithm. However, even in this test, the need for a much larger study can be observed. One other factor that may influence the results, which is not immediately apparent, is the impact of using the non-invasive, non-continuous BP monitor as a reference. Since BP readings are not observable between the two minute intervals, the tracking ability of the algorithm in between these intervals is unknown whereas in section 5.4 using the ABP, the tracking ability was observable. The danger of using a non-continuous BP monitor has been established in Section 4.5.4 where the value of Poon's algorithm became more apparent when it was compared to ABP, rather than when it had been compared to the non-continuous measurement in Section 3.10 and consequently was within the BHS standard at the two minute interval when compared to ABP. Therefore, it is also possible that a further improvement could be observed if it were possible to compare the new algorithm to ABP, something which has been suggested by the EHS standard, but that would require a clinical trial.

The results of this test reflect those that had been established in section 5.4, where a 12 minute calibration interval was achieved using the PhysioNet database. However, the results of this test are even more significant as they show that it is possible to implement this system using non-invasive methods. This means that it is now possible to measure BP on a continuous basis, by non-invasive methods

over calibration intervals that are practical from the perspective of both clinicians and users. Although, this appears to only provide a 100% improvement to the calibration interval for the PTT algorithms such as Chen and Poon, the practical implications are much more momentous, providing a breakthrough in the area of BP monitoring. Up until this point, to measure BP on a continuous basis required either a catheter or a continuously inflating/inflated cuff i.e. via tonometers or the Peñáz method. Using this system though, an inflation is required only once every 12 minutes providing even less discomfort for the user but with the same accuracy and reliability for the clinician. An extra bonus of this system is that with the inclusion of the ICG and PPG sensor, it would be possible to incorporate this suggested system into the existing 24 hour BP monitors that are currently used by clinicians, the only difference being that a cuff measurement is required every 12 minutes instead of 15 minutes. This is also a very important feature, as it allows the new system to be used by clinicians without any risk, since the cuff measurement will also be recorded, but could provide far more information since every BP movement will also be recorded in the intervals.

6.3 Future Work

The next step for this project would be to confirm the findings of this thesis in a clinical trial. This would establish the limitations of the new algorithm. Any such test should be performed in a trial where ABP can be monitored as the benchmarking tool on patients with known physiological parameters. During this trial, the use of a pre-ejection period could be explored, because it has previously been found to have a significant impact on PTT methods and by accounting for it in this algorithm, a further improvement should be noted. It would also be desirable, as part of this trial, to use an ICG to monitor all of the signals of interest, as it can measure each of them on a continuous basis and its use as part of a non-invasive BP monitor could be evaluated.

As previously mentioned, the specifics of each person being tested should be known prior to any test but a wide a variety of people should be tested where possible. To ensure a proper evaluation, a large number of people, in excess of 85, should also be tested in accordance with the AAMI and BHS standards. The International protocol for BP measurements should also be used as a basis for evaluating the algorithm. However, the use of ABP would complicate these tests somewhat because all were designed for testing intermittent measurements such

as those used by a cuff.

As has been already established the PTT system and ICG systems would suit the requirements for a wearable and continuous BP monitoring system. It would also be possible to reduce the size of each system significantly. In Qu's design [178], an ECG is part of the ICG design eliminating the need for two different boards, and the ICG patches can be used to detect the ECG waveform, further reducing any potential discomfort for the patient. Another improvement could be made by incorporating the PPG sensor into a ring type device, as has been done by Shaltis [86]. Both sensors could also use a Body Sensor Network to communicate with each other or a base station as long as timing issues can be resolved. One further step, which was envisaged when developing the ECG and ICG boards, would be to use a mobile phone as a base station for these sensors via Bluetooth. The phone could then process all the raw data captured from each sensor, store the data or forward it to a GP or cardiologist on request and the other sensors could be integrated into a t-shirt similar to the concept drawing shown in Figure 6.1. Other smart vests have been previously developed [179, 180, 181], primarily for the area of AAL, and the development of such a shirt would allow the system to be implemented in a variety of different settings be it for AAL or other home monitoring systems and could allow the integration of other sensors for a complete health monitor.

This project has provided a new algorithm which has been shown to exceed the calibration intervals of two of the state of the art algorithms by 100% for calculation of blood pressure. However, the ramifications of this system are far greater, allowing BP to be measured on a continuous and non-invasive basis with even less discomfort to the patient than has been previously possible. It may perhaps even be possible to further improve the algorithm by taking pre-ejection period into account and using ABP as a reference. By using an ICG system as outlined in this section, along with a ring type PPG sensor, it would be possible to create a wearable BP monitoring system that could integrate with a person's phone to provide a non-invasive, unobtrusive, wearable and continuous BP monitor, something which does not currently exist.



Figure 6.1: A conceptual image of a t-shirt that incorporates both the ECG and ICG systems via patches built into the shirt. A BP cuff could also be incorporated into the arm and a ring photoplethysmograph sensor could also be included.

Appendices

Appendix A

The Use of the Poiseuille Equation in the New Algorithm

It is well documented that there are a number of assumptions that are necessary so that the Poiseuille Equation can be used, namely where

- The fluid is incompressible and Newtonian
- The flow is laminar through the pipe
- There is no acceleration of fluid in the pipe

For the most part, it is recognised that blood is a non-Newtonian fluid. However, it has been found that blood behaves as a Newtonian fluid only at high shear stress rates $\frac{\delta v}{\delta y} \geq 100s^{-1}$ [182]. In large arteries [183], the shear rate is well above this limit and so the blood flow through this artery can be deemed to be a Newtonian fluid.

The primary problem with using the Poiseuille equation in large arteries, is that the blood flow is pulsatile. Therefore, a modification of the Poiseuille equation is necessary to account for this difference. This alternative equation is known as Womersely's equation [166].

The derivation of this equation begins with the Navier Stokes Equation [184] and is outlined in Gabe's paper [167]. From this paper, if an idealized model of an artery as a long, straight, cylindrical, rigid tube of radius R, containing a Newtonian viscous liquid is assumed, the Navier Stokes equation can be simplified to

$$\frac{\delta w}{\delta t} = -\frac{1}{\rho} \frac{\delta p}{\delta z} + v \left(\frac{\delta^2 w}{\delta r^2} + \frac{1}{r} \frac{\delta w}{\delta r} \right) \quad (\text{A.1})$$

where w is the velocity [m/s] along the tube at radius r [m], z is the distance along the tube [m], ρ the density [kg/m³] and v the kinematic viscosity of the liquid [kg/sm]. If the pressure gradient along the tube is $P \cos(\omega t - \phi)$, it has been shown by Womersely that the volume flow Q along the tube is

$$Q = P \times \frac{\pi R^4}{\mu} \times \frac{M'_{10}(\alpha)}{\alpha^2} \times \sin[\omega t - \phi + \epsilon'_{10}(\alpha)] \quad (\text{A.2})$$

where μ is the coefficient of viscosity, α is a non-dimensional parameter $R\sqrt{\frac{\omega}{\nu}}$, where $\omega = 2\pi \times \text{frequency}$ and $M'_{10}(\alpha)$ and $\epsilon_{10}(\alpha)$ are functions of α tabulated by Womersely for $\alpha = 0$ to 10 . It should be noted that this equation is per unit length.

Comparing A.2 to Poiseuille's equation A.3, a clear relationship is evident.

$$Q = \Delta P \times \frac{\pi r^4}{8\mu K} \quad (\text{A.3})$$

Therefore, the primary difference between both equations is due to the complex relationship derived by Womersely, that defines the actual resistance to flow through the artery.

However, in the algorithm that has been derived, the value of the resistance is not critical or used because it is removed during the differentiation, and so for the sake of simplicity, the Poiseuille equation was used as a more convenient replacement.

Appendix B

An Examination of the European Society of Hypertension Standard for Blood Pressure Monitoring

B.1 The Specifics of the Standard

The European Society of Hypertension (ESH) International Protocol for validation of BP measuring devices [18, 185] is the most complex of the three standards for blood pressure monitoring and uses lessons and shortcomings learned from the BHS and AAMI standards. The aim when creating this standard was to make it more practical for smaller companies to be able to validate their devices because both the BHS and AAMI standards require a large data set to be tested with a large variance of BP across all the subjects, thus making any new device very expensive to validate.

The ESH standard is very detailed on how the validation should be carried out. It requires four people to be part of the validation team: two observers, one supervisor (typically a nurse) and one expert (typically a doctor). The validation itself uses a categorisation system similar to the BHS standard to evaluate the device over two stages. The first stage requires fifteen subjects, with at least five male and five female and the second requires an additional eighteen subjects, at least ten male and ten female. Each subject should be at least 25 years of age. The subjects should also have a wide range of Blood Pressures. In the initial round of 15 subjects, 5 subjects should have a systolic blood pressures in the range as outlined in Table B.1. In the second test, 11 subjects are required to

Table B.1: The ranges of Blood Pressure of the subjects that are required for the ESH Testing Procedure

	<i>SBP</i>	<i>DBP</i>
Low	<90 90-129	<40 40-79
Medium	130-160	80-100
High	161-180 >180	101-130 >130

have blood pressures in each of these ranges.

The procedure for the measurement is as follows. The subject is initially introduced to the validation team and allowed to rest for fifteen minutes prior to any measurements being recorded. The following measurements are then recorded:

BPA

Observers 1 and 2 take a measurement with the mercury standard which is used to categorize the subject

BPB

Observer 3 takes a blood pressure measurement with the test device. The result from this measurement is not included in the results, but if a successful measurement is not possible after three attempts, the subject is excused.

BP1

Observers 1 and 2 take a measurement using the mercury standard

BP2

The supervisor takes a measurement with the test device

BP3

Observers 1 and 2 take a measurement using the mercury standard

BP4

The supervisor takes a measurement with the test device

BP5

Observers 1 and 2 take a measurement using the mercury standard

BP6

The supervisor takes a measurement with the test device

BP7

Observers 1 and 2 take a measurement using the mercury standard

In a similar method to the BHS standard, the differences (errors) are classified into one of three ranges within 5mmHg, within 10mmHg or within 15mmHg. To test the accuracy, only measurements BP1 to BP7 are used. The mean of each pair of observer measurements is calculated, this is denoted as observer measurement BP1, BP3, BP5 and BP7. Each test device measurement is flanked by two of these measurements and one of these must be selected as the comparative measurement.

The following procedure is then followed:

1. The absolute differences of $BP2 - BP1$, $BP2 - BP3$, $BP4 - BP5$, $BP4 - BP3$, $BP6 - BP5$, $BP6 - BP7$ are calculated.
2. These are paired according to device reading
3. If the values in the pairs are unequal, the observer measurement corresponding to the smaller measurement is used
4. If the values in a pair are equal, the first of the two pairs is used

When this has been completed there are three device readings for SBP and three device readings for DBP. This further means that there are 99 measurements in the first phase of testing outlined in Table B.2. In this round there are 33 subjects in total meaning a total of 99 results. There are two criteria for the device to pass this round. The device must satisfy two of the criteria in the first row of Table B.2 **and** all of the criteria from the second row of Table B.2. At this stage the mean and standard deviation of the differences should be recorded.

Table B.2: A summary of the results required to pass phase 1 of the ESH Testing Procedure

<i>Measurements</i>	<i>Within 5 mmHg</i>	<i>Within 10 mmHg</i>	<i>Within 15 mmHg</i>
Two of	73	87	96
All of	65	81	93

If the device passes the first phase, it must pass one final test outlined in Table B.3. This table analyses data in a per subject basis. It states that at least 22 of the 33 subjects must have at least 2 of their 3 comparisons within 5 mmHg. At most, three of the subjects can have all three of their comparisons over 5 mmHg apart. If a device passes both the first and second phases of testing, it can be said to have achieved a pass from the ESH standard.

Table B.3: A summary of the results required to pass phase 2 of the ESH Testing Procedure

<i>Measurements</i>	<i>2/3 within 5 mmHg</i>	<i>0/3 within 5 mmHg</i>
At least	≥ 22	
At most		≤ 3

B.2 The Exclusion of the ESH standard in the Evaluation of this Work

There are many reasons why it would have been preferable if this standard could have been implemented in this work. The primary reason is that it is the most complete and detailed of all the standards since it is based on the lessons learned from both the AAMI and BHS standard.

However, there are many compelling reasons why the standard should not have been used. The most simple and easiest to explain is that in one of the appendices of the ESH standard, it states that any device that measures beat to beat blood pressure should be tested and its results compared to those from an arterial catheter, something which has been previously stated in this thesis.

Another reason for not using this standard is the amount of resources that are necessary to implement the tests required for the standard i.e. the number of observers, supervisors and experts that would be required. A much larger restriction was also found due to the subjects that are required since all the subjects used in this work were volunteers and colleagues. Although the age requirements of the standard would not have been a restriction, the primary concern was in getting access to the wide range of blood pressures that would be required, especially in the category of very high blood pressure.

The final reason for not implementing this standard was that the tests outlined in the ESH standard did not fit with any of the tests that were required to evaluate the devices under test. The vast majority of PTT based algorithms that have been published attempt to pass the standards after long calibration intervals. In the AAMI standard, it is quite easy to compare the differences of many measurements at a specific calibration interval and check if the results are within a certain mean and standard deviation. In a similar manner, it is possible to test these differences and add them to the accumulated ranges specified in the BHS standard. In this test seven measurements would be required at every calibration interval, making it impractical.

Appendix C

Design of an Impedance Cardiograph

Examining the literature, it was found that there were not many designs available for ICGs. However, many papers discussed the principles and basic concepts of the technique [186, 187, 188]. From this literature it was clear that there were two main components of the system: the current injection and the impedance measurement. However, beyond this basic information not much else was available. It was found that only two papers and one book outlined the hardware and components in any detail: Qu [178], Fortin [145] and Prutchi [189]. Qu's paper was first published in 1986 and gave very specific circuit information, but some of the components were found to be obsolete. Fortin's paper was much more recent on the other hand, being published in 2006. However, it provided less specific information, describing its components using block diagrams and text rather than circuit diagrams. Prutchi's book was published in 2005 and provided a high level of detail and good descriptions of each component. However, it also shared a common problem among all three sources: each circuit was powered from the mains, whereas the application for this work was for a wearable system that would be powered by batteries. To be more specific, many of the IC's in each of the designs were powered from $\pm 15V$ whereas a typical wearable system would rarely exceed $\pm 5V$. However, it was felt that by combining the technology outlined in Fortin's paper along with the specifics from Qu's paper and Prutchi's book, a good compromise could be achieved along with full functionality. This appendix will describe the resulting design and is divided into two main sections: the "current injection hardware" section and the "impedance measurement hardware" section.

C.1 Current Injection Hardware

Figure C.1 shows a block diagram of the components required for the current injection hardware. These consist of current generation block, where the current that is to be injected is generated, a DC safety circuit, which ensures no DC current is injected into the user and a precision rectifier, PI controller and two summing amplifiers (represented by two plus signs) which provide a feedback loop that monitors the leads for stray currents.

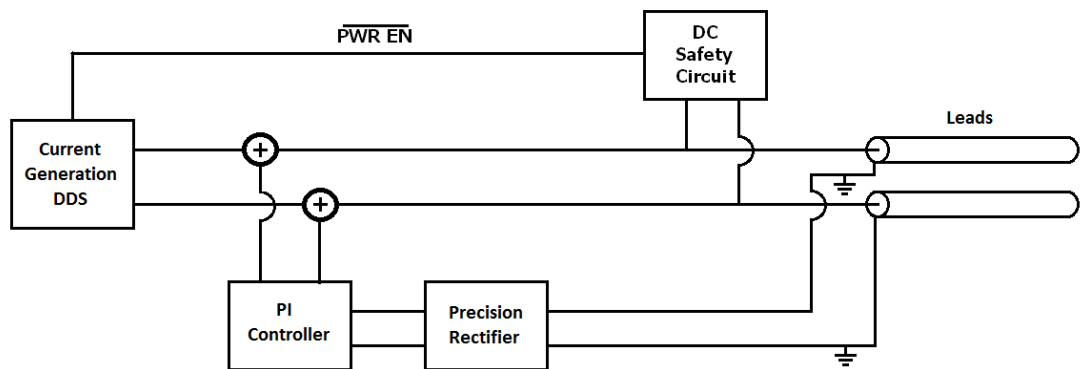


Figure C.1: A Block Diagram describing the implemented Current Injection System.

From reading the basic specifications of the current injection hardware from every source in the literature identified in the previous sections, it was evident that an oscillator was needed to generate the 100kHz sine wave that was required. Numerous different oscillators were simulated, designed and built in the course of this work, but only two basic configurations were finally considered: the Quadrature Oscillator and the Wein Bridge Oscillator.

Examining the simulations of the circuits with practical capacitor and resistor values and various implementations it was found that the circuit shown in Figure C.2, a modified Wein Bridge Oscillator, provided the best sine wave at the desired frequency of 100kHz.

Qu [178] and Prutchi [189] also used a type of Wein Bridge oscillator in their design, but took advantage of the dual power supply, which means a reduction of the component count due to the bipolar swing of the oscillator provided by the dual power supply. In other words, by using a dual power supply it is much easier for a sine wave to be generated that oscillates around 0V, whereas if the circuit does not contain a positive and negative supply, extra components are required to force the oscillation around 0V. Fortin, on the other hand, used a Direct Digital

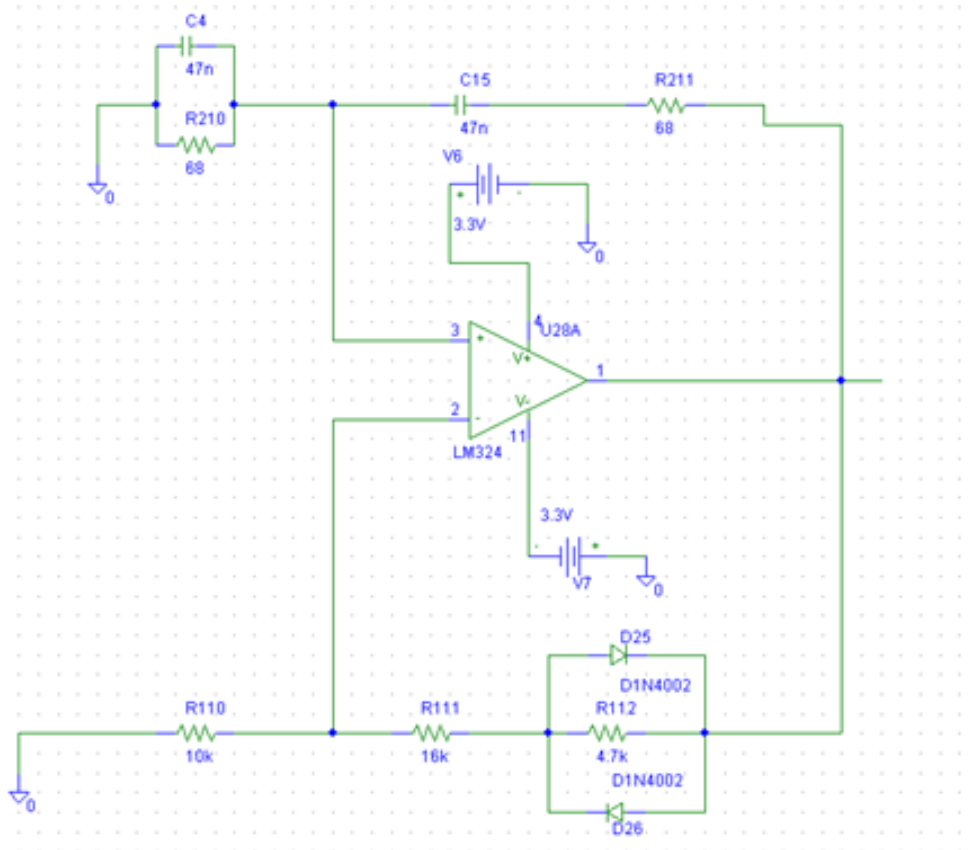


Figure C.2: A PSPICE circuit diagram of the modified Wein Bridge Oscillator developed during this work.

Synthesis (DDS) chip, which is an IC capable of generating precise sine waves via programming, usually used for modulation and demodulation of communication signals. The advantage of using this kind of device is that both the frequency and amplitude could (in theory) be changed simply by reprogramming the chip via the 3-wire SPI. Given that this design was using a combination of sources for design and that there was an understandable concern about injecting current into the body, it was felt that a circuit which could easily adjust the amplitude of the current and its frequency would be best rather than either of Wein Bridge Oscillators that would require different components if either the amplitude or frequency were to be adjusted.

An AD9834 DDS chip [190] was chosen as the basis for the current injection circuit. A 75 MHz oscillator was paired with the DDS chip to provide the required clock signal. The current was controlled by two parameters, the resistors R_{SET} placed on both of the output pins I_{OUT} and I_{OUTB} and the voltage on the input pin FS ADJUST. Although FS ADJUST is nominally set to 1.15 V, by using a DAC on its input, it is possible to have greater control over the input voltage and

therefore the output current. A 12 bit DAC, the AD5620 [191], was used in this application as recommended by the application note CN-0156 [192], because it was also programmable using a 3-wire SPI.

In Fortin's circuit diagram, a feedback loop is present which monitors the leads that are connected to the subject in case of stray voltages, which could potentially harm them. If a stray signal is detected, it is fed into a precision rectifier and Proportional + Integral (PI) controller before being subtracted from the original current "input" signal going to the body. The precision rectifier was included in case some of the modulated signal was present on the ground signal, which the rectifier would remove. The PI controller would then examine the stray signal and provide an output that would compensate this offset.

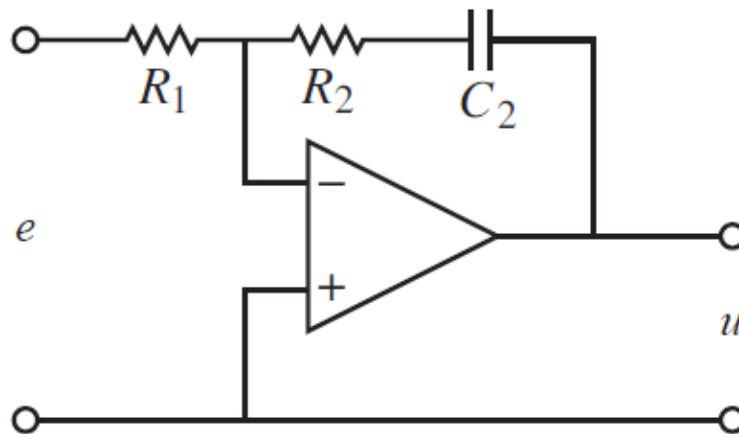


Figure C.3: The standard configuration Proportional + Integral Controller used in the feedback loop of the current injection system [193].

While the current was injected, it was constantly being monitored for DC components by a safety circuit. The safety circuit was comprised of a transimpedance amplifier, a comparator with a low reference voltage and a D flip flop with set and reset as shown in the Figure C.4. If a DC current was detected and exceeded the reference, set by resistors R155 and R156, the flip flop would toggle and send a reset to the rest of the system that would disable the current injection immediately.

C.2 Impedance Measurement Hardware

When an instrumentation amplifier is used along with a synchronous detector/demodulator, the result is a lock in amplifier. A lock in amplifier [194] is basically

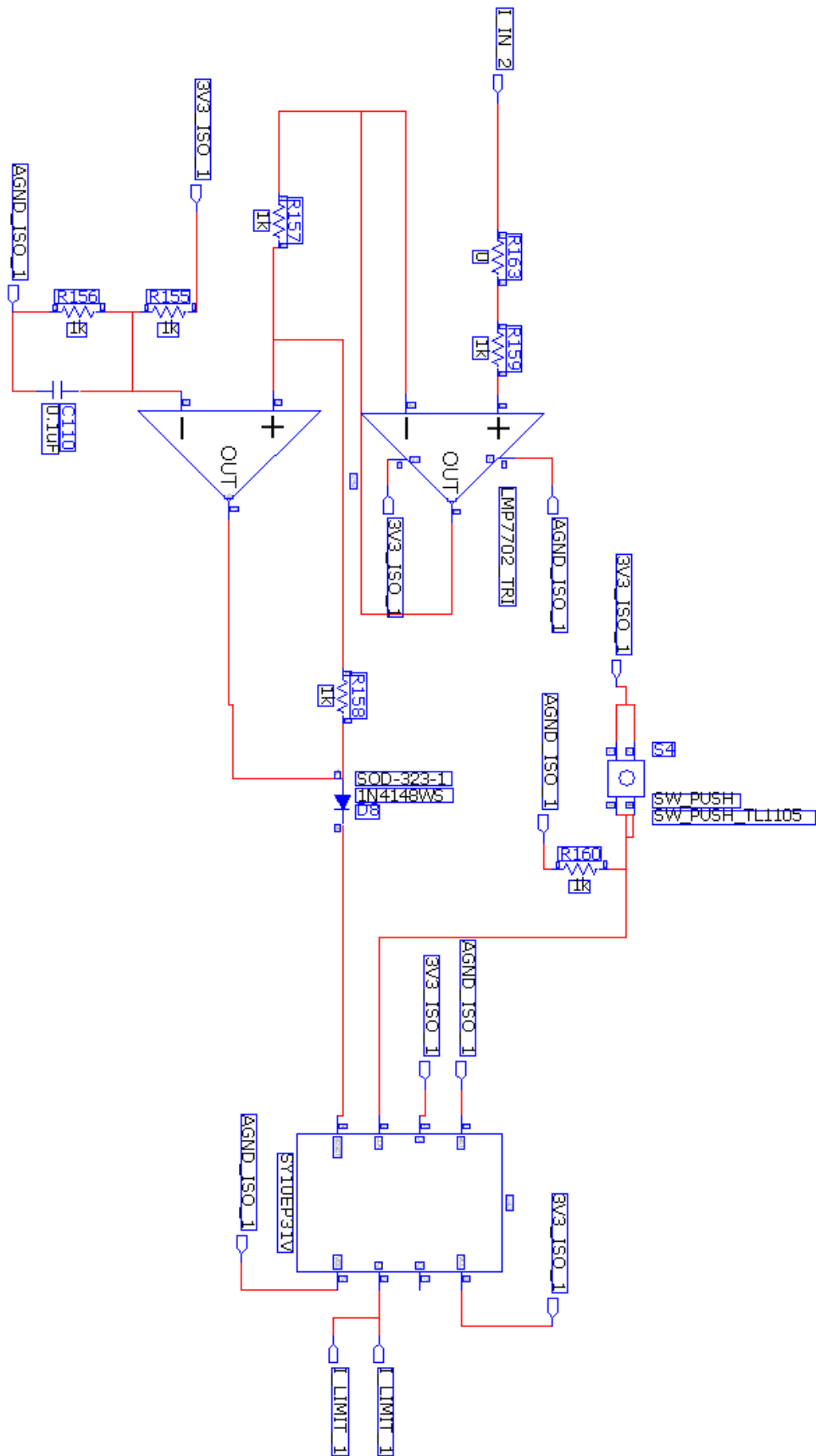


Figure C.4: The safety circuit of the ICG which ensures no DC current is injected into the body.

a synchronous demodulator followed by a narrow band, low pass filter. This allows very small signals to be detected in the presence of large amounts of uncorrelated noise when the frequency and phase of the desired signal are known [189]. The demodulator used in this design is the AD630 [195]. This is the recommended demodulator in Prutchi's design. When being used as a demodulator, the AD630 needs a reference signal that is 90° out of phase with the original input signal. This reference signal is provided by using a second DDS chip, whose amplitude is controlled by the same DAC as described earlier. This signal is then buffered and phase shifted, as described by Prutchi's design. A potentiometer is used in the phase shifting circuit to (manually) adjust the phase shift as per Prutchi's design. Again, this is a relatively standard configuration for an adjustable phase shifting circuit, [196].

Differential and common mode offset are also provided as part of the AD630 circuitry. Both of these parameters can be adjusted using potentiometers. The output of the AD630 is then filtered using a low pass filter with cutoff frequency of 0.72Hz. This LPF design is taken from Qu's schematic. The resulting signal is known as the Basal Impedance i.e. Z_0 . Impedance Cardiographs are very sensitive to motion artifacts and baseline drift due to respiration. These artifacts can cause saturation in the ICG system which could result in the loss of data for up to 10 seconds. It is therefore desirable to incorporate an automatic adjustment unit which is capable of accounting for these artifacts if they occur. There are several ways to do this, such as the successive approximation register (SAR) based method, as described by Qu but the components used in this method were found to be obsolete. However, it was found that this type of motion artefact removal can now easily be performed using a microcontroller and it was therefore omitted from the design.

The final stage of the impedance measurement unit is the calculation of dZ/dt from the ΔZ signal. This is done using a practical differentiator, as can be seen in application note 31 from National Semiconductor [197].

C.2.1 Other Design Features

As mentioned in C.2, a microcontroller was also included in this design. The microcontroller was responsible for controlling the DACs, which controlled the amplitude of the DDS signals for both the current injection and demodulation process. It was also responsible for reprogramming the DDS ICs, and the motion

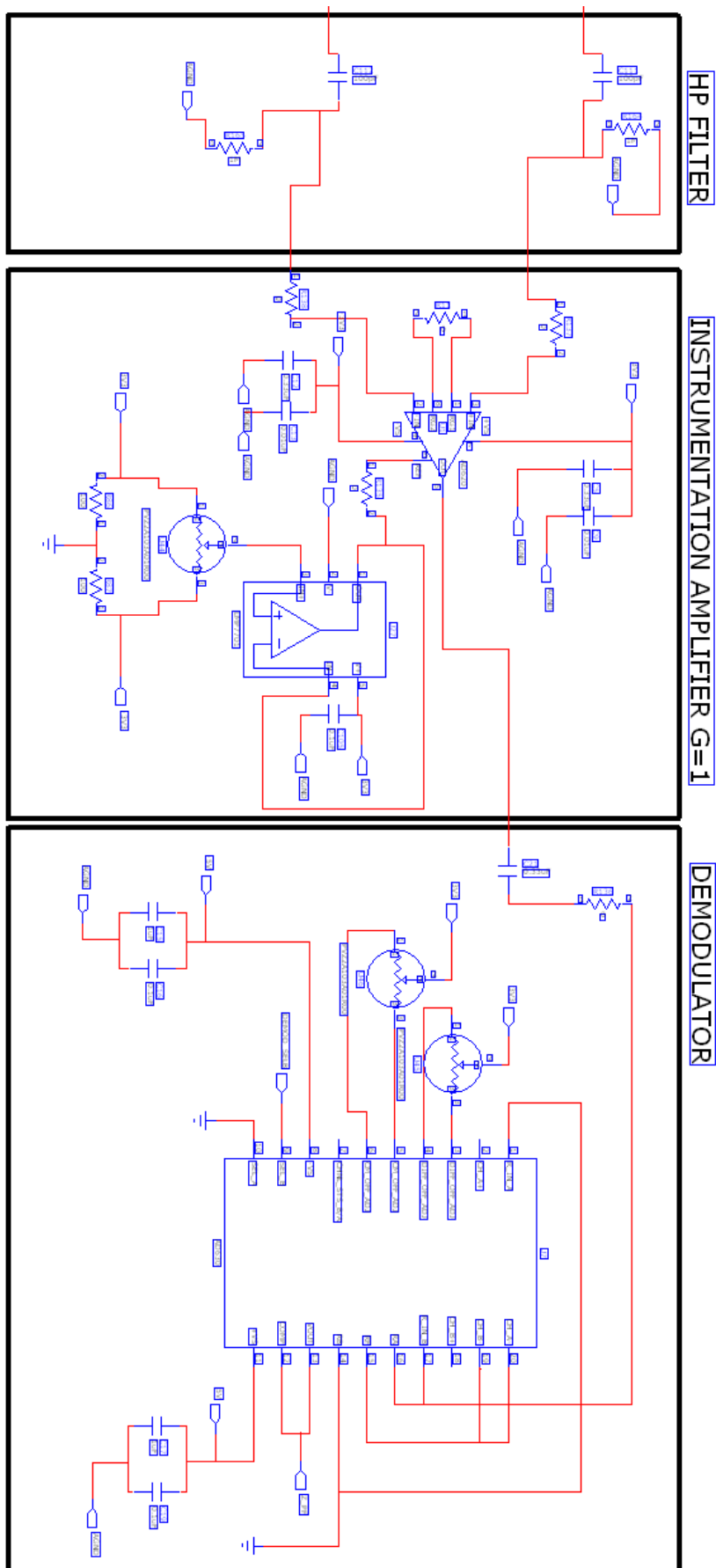


Figure C.5: The high pass filters and lock in amplifier, which consists of an instrumentation amplifier and demodulator, implemented in this project

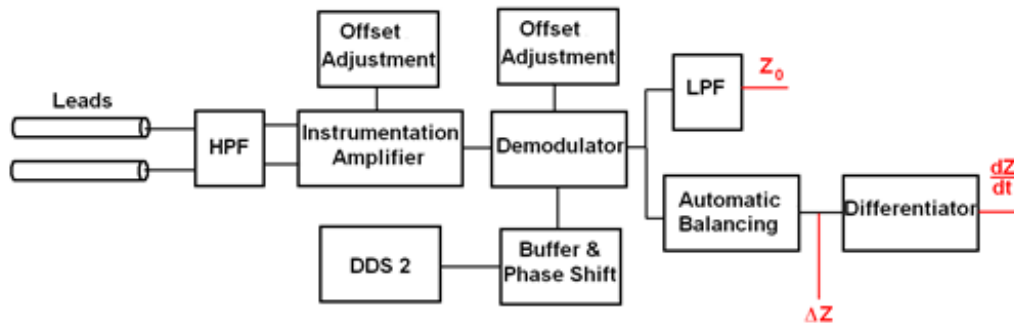


Figure C.6: A Block Diagram describing the implemented Impedance Measurement System.

artefact reduction necessary for all ICGs. Since an ADC (that was capable of sampling at 250 Kbit/s) would also be required to transmit the results of the ICG to a PC, choosing a microcontroller that had one incorporated would have been advantageous. Furthermore, the communication of the data to another source also required a microcontroller to translate the analogue or digital signal.

With all these considerations in mind, the microcontroller that was chosen was the Atmel Mega 1281 [105]. The most significant advantage of this microcontroller was that it had already been used in the design of the PHALs board and so most of the code written for that application could also be used in this one. By including this microcontroller, all other Tyndall motes could be attached as necessary at a later stage, e.g. for Zigbee communications or signal processing via an FPGA.

It was also decided that a Bluetooth module and an SD card would be included in the design, to allow for live and/or local recording respectively and to ensure compatibility in a Body Area Network (BAN). Both of these features were copied from the PHAL design where they had already been tested extensively. Unlike the PHAL design however, no battery charging circuitry was included in the design so that a subject under test would never be connected to a mains supply, regardless of the safety features included in the design.

Appendix D

Protocol for Recording Data from Volunteers

Each of the tests described in this thesis follow essentially the same protocol when volunteers are being tested. These procedures are based around the recommendations outlined by Pickering [6] for taking BP measurements from patients. The number of patients required, their genders and the ratio of genders was decided after consulting with the clinical advisor for this project, Dr. Carl Vaughan. No ethical approval was sought since none of the tests were invasive procedures.

D.1 Round 1 Testing

The procedure outlined below was followed for the first round of testing.

- Each subject was asked to refrain from ingesting anything for half an hour prior to the test
- Once each subject arrived at the laboratory, they were seated for at least 5 minutes before any data was recorded
- The Pulse Oximeter was placed on the middle finger of the left hand
- The BP cuff was placed on the upper left arm, 2-3 cm above the bend in the elbow
- The ECG electrodes were placed in the regular 3 electrode positions seen in Figure 3.12 a)

- Each volunteer was seated in an upright position, feet flat on the floor and elbow (and arm) resting comfortably on the desk
- A BP measurement was taken every 5 minutes
- ECG and Pulse Oximeter data was recorded continuously over 15 minutes, from which the PTT was later derived using Matlab [122]

Notes:

- [1] Volunteers were sought from colleagues within Tyndall. No restrictions with regard to health or age were imposed on the volunteers but all volunteers that were tested were other students. The reason for this selection was that it was felt that students had more availability and could be more flexible than staff for initial and subsequent testing. Since all volunteers were students, this meant that all volunteers were relatively young, the youngest being 22 years old and the oldest being 32 years old, and all volunteers were relatively healthy.
- [2] Each volunteer was asked to refrain from eating or drinking prior to the test, but they were also asked not to smoke as it may have adversely affected the results.
- [3] Each volunteer was asked to remain seated for at least 5 minutes prior to the test. This was to eliminate any elevated BP readings that may have occurred due to exercise. If the volunteer seemed out of breath or if it seemed that they had rushed to the laboratory, this rest period was extended until they had recovered. A few BP readings were also taken during this period, to allow the volunteer to get used to the feeling of the BP cuff. This allowed the volunteer to relax and potentially identify white coat hypertension. If there was either a very high initial BP reading or if there was a major change in BP between the first and subsequent readings of BP, this initial testing duration was extended until the BP was relatively consistent. This reduced the chances of nervousness affecting the reading or of white coat hypertension.
- [4] As previously mentioned in section 3.7.2.1, each volunteer was asked to refrain from wearing nail polish during the testing as it had been noted that it would distort the signal. Each volunteer was also asked not to move their hand or finger during the test, to eliminate motion artifacts as much as possible.
- [5] It was found that one volunteer had a very poor ECG signal, using the electrode positions shown in Figure 3.12 a). After consulting the clinical

advisor to the project, he suggested moving the electrodes to the positions shown in Figure 3.12 b) for this volunteer only.

- [6] Each volunteer was seated for the duration of the test. They were asked not to slouch but to find a comfortable position that they could hold throughout the test. It was also important that they kept their elbow and arm flat on the desk and to have both in a natural position relative to the rest of the body, essentially meaning that their lower arm was *almost* at 90° to their upper arm, but in a slightly more relaxed position.

D.2 Round 2 Testing

A number of problems were identified when the data from the first round of testing was analysed. The most important of these, from the perspective of the testing procedure was that when the cuff inflated, the data from the Pulse Oximeter disappeared (unsurprisingly). To ensure continuous data was being recorded the Pulse Oximeter was then moved to the right hand. Another important change was that the original BP monitor was replaced by a more expensive, clinically validated one, the Omron M6 [26]. Other changes were also necessary to improve the signal quality and the peak detection of the algorithms in Matlab, but these did not have an impact on the procedure.

For the most part all other procedures that had been followed were found to be adequate and so were kept in place. The following points were then added to the procedure in an attempt to improve the overall testing procedure:

- A preliminary test of each volunteer was introduced, typically lasting less than two minutes
- Each test was recorded the hours of 2.30pm and 4.00pm, in a quiet room at a comfortable temperature
- Both the PHALs board and Pulse Oximeter were packaged so nothing could interfere with the circuit or adversely affect the signal
- The Pulse Oximeter was placed on the middle finger of the right hand
- ECG and Pulse Oximeter data was recorded continuously over 30 minutes, from which the PTT was later derived

Notes:

- [1] A preliminary test of every volunteer prior to every test they provided was introduced. Initially, this was to ensure that any ECG abnormalities which would lead to errors in the peak detection algorithm could be identified. However, it was found that this became useful to ensure the signal quality was sufficient and for example none of the wires of the ECG were loose or that the person had mistakenly worn nail polish. Also, during the initial test, one of the volunteers had a panic attack during the BP measurements and had to be subsequently omitted from the tests. Therefore, it was found by performing this initial test, white coat hypertension could be avoided.
- [2] Each test was recorded was recorded at some time between 2.30pm and 4.00pm, depending on the availability of the volunteer.
- [3] Packaging the two sensors ensured that the wires coming from both were rigid and held in place and could not be accidentally moved or come loose during the test.

D.3 Round 3 Testing

By the time the second round of testing had taken place, the procedure for testing volunteers was satisfactory and was capable of producing high quality and reproducible results. For the third round of testing, two changes were made. The first of these was to increase the number of volunteers and the second was to increase the frequency of BP measurements:

- The number of volunteers was increased to fifteen
- A BP measurement was taken every 2 minutes

Notes:

- [1] Originally the number of volunteers was increased to ten; however, on submitting the results to the *Journal of Human Hypertension*, the reviewers requested the number to be increased to fifteen. These fifteen consisted of five females and ten males.
- [2] By measuring the BP every two minutes, a more exact calibration interval could be extracted from the data. The figure of two minutes was chosen because although one BP measurement typically took about 45 seconds, on occasion a second inflation was required by the BP monitor for an accurate

D. PROTOCOL FOR RECORDING DATA FROM VOLUNTEERS

reading. Although these were infrequent, extending the calibration interval to two minutes ensured a reading could be taken at every interval.

References

- [1] An Phríomh-Offig Staidrimh/(Central Statistics Office. Vital Statistics: Fourth Quarter and Yearly Summary, 2013.
- [2] P. Holejsovska, Z. Peroutka, and J. Cengery. Non-Invasive Monitoring of the Human Blood Pressure. In *Computer-Based Medical Systems, 2003. Proceedings. 16th IEEE Symposium*, pages 301–306, 2003.
- [3] B. Belhassen. A 1 Per 1,000 Mortality Rate After Catheter Ablation of Atrial Fibrillation : An Acceptable Risk? *Journal of the American College of Cardiology*, 53(19):1804–1806, 2009.
- [4] R. Leca and V. Groza. Why Are We Still Measuring Blood Pressure by Ear? In *Instrumentation and Measurement Technology Conference Proceedings, 2008. IMTC 2008. IEEE*, pages 309–313, 2008.
- [5] D. Shapiro, L. D. Jamner, J. D. Lane, K. C. Light, M. Myrtek, Y. Sawada, and A. Steptoe. Blood Pressure Publication Guidelines. *Psychophysiology*, 33(1):1–12, 1996.
- [6] T. G. Pickering, J. E. Hall, L. J. Appel, B. E. Falkner, J. Graves, M. N. Hill, D. W. Jones, T. Kurtz, S. G. Sheps, and E. J. Roccella. Recommendations for Blood Pressure Measurement in Humans and Experimental Animals: Part 1: Blood Pressure Measurement in Humans: A Statement for Professionals From the Subcommittee of Professional and Public Education of the American Heart Association Council on High Blood Pressure Research. *Circulation*, 111(5):697–716, 2005.
- [7] I. R. F. Yan, C. C. Y. Poon, and Y. T. Zhang. A Protocol Design for Evaluation of Wearable Cuff-less Blood Pressure Measuring Devices. In *Engineering in Medicine and Biology Society, 2009. EMBC 2009. Annual International Conference of the IEEE*, pages 7045–7047, 2009.
- [8] E. O’Brien, R. Asmar, L. Beilin, Y. Imai, J. M. Mallion, G. Mancia, T. Mengden, M. Myers, P. Padfield, P. Palatini, G. Parati, T. Pickering, J. Redon, J. Staessen, G. Stergiou, P. Verdecchia, and on behalf of the European Society of Hypertension Working Group on Blood Pressure Monitoring. European Society of Hypertension Recommendations for Conventional, Ambulatory and Home Blood Pressure Measurement. *Journal of Hypertension*, 21(5):821–848, 2003.

- [9] United Nations. Dept. of Economic and Social Affairs. Population Division. *World Population Aging, 1950-2050*. United Nations, 2002.
- [10] Braun (GmbH) Blood Pressure Monitors. FAQ: "What is Systolic and Diastolic Pressure?", <http://www.braunbloodpressuremonitors.com/heart-health/frequently-asked-blood-pressure-monitor-questions/> 2010.
- [11] J. Malmivuo and R. Plonsey. *Bioelectromagnetism: Principles and Applications of Bioelectric and Biomagnetic Fields*. Oxford University Press, 1995.
- [12] K. Quigley G. Berntson and D. Lozano. Cardiovascular Psychophysiology . In Gary G. Berntson John T. Cacioppo, Louis G. Tassinary, editor, *Handbook Of Psychophysiology*, pages 182–210. Cambridge University Press, 3rd edition edition, 2007.
- [13] L. W. Wilkins. *ECG Interpretation Made Incredibly Easy*. Incredibly Easy! Series. Lippincott Williams & Wilkins, 2005.
- [14] W. Chen, T. Kobayashi, S. Ichikawa, Y. Takeuchi, and T. Togawa. Continuous Estimation of Systolic Blood Pressure Using the Pulse Arrival Time and Intermittent Calibration. *Medical and Biological Engineering and Computing*, 38(5):569–574, 2000.
- [15] C. C. Y. Poon and Y. T. Zhang. Cuff-less and Noninvasive Measurements of Arterial Blood Pressure by Pulse Transit Time. *2005 27th Annual International Conference of the IEEE Engineering in Medicine and Biology Society, Vols 1-7*, pages 5877–5880, 2005.
- [16] Association for the Advancement of Medical Instrumentation. ANSI/AAMI SP10:2002 Manual, Electronic or Automated Sphygmomanometers. Technical report, 2002.
- [17] E. O'Brien, J. Petrie, W.A. Littler, M. de Swiet, P. L. Padfield, D. Altman, M. Bland, A. Coats, and N. and others Atkins. The British Hypertension Society Protocol for the Evaluation of Blood Pressure Measuring Devices. *Journal of Hypertension*, 11(Suppl 2):S43–S62, 1993.
- [18] E. O'Brien, T. Pickering, R. Asmar, M. Myers, G. Parati, J. Staessen, Th. Mengden, Y. Imai, B. Waeber, P. Palatini, et al. Working Group on Blood Pressure Monitoring of the European Society of Hypertension International Protocol for Validation of Blood Pressure Measuring Devices in Adults. *Blood pressure monitoring*, 7(1):3–17, 2002.
- [19] E. Peter, S. Wilhelm, K. D. Müller-Glaser, and N. Lutter. Noninvasive and Nonocclusive Determination of Blood Pressure Using Laser Doppler flowmetry. In *BiOS'99 International Biomedical Optics Symposium*, pages 188–196. International Society for Optics and Photonics, 1999.
- [20] E. Nicpon Marieb and K. Hoehn. *Human Anatomy & Physiology*. Pearson Education, 2007.

- [21] H. Sorvoja and R. Myllylä. Noninvasive Blood Pressure Measurement Methods. *Molecular and Quantum Acoustics*, Vol 27:pp. 239–264, 2006.
- [22] G. Beevers, G. Y. H. Lip, and E. O’Brien. ABC of Hypertension: Blood Pressure Measurement Part II: Conventional Sphygmomanometry: Technique of Auscultatory Blood Pressure Measurement. *BMJ: British Medical Journal*, 322(7293):1043, 2001.
- [23] R. Winn, J. R. Hildebrandt, and J. Hildebrandt. Semiautomatic Blood Pressure Monitor Utilizing an Electronic Sphygmomanometer. *Journal of Applied Physiology*, 43(2):379–381, 1977.
- [24] P. R. Fleming. *A Short History Of Cardiology*. Rodopi Bv Editions, 1997.
- [25] dabl Educational Trust. *Blood Pressure Monitors - Validation, Papers and Reviews*. <http://www.dablededucational.org/>.
- [26] OMRON Healthcare Europe. *Omron M6 Comfort*. <http://www.omron-healthcare.com/eu/en/our-products/blood-pressure-monitoring/m6-comfort>.
- [27] R. S. Mackay, E. Marg, and R. Oechsli. Automatic Tonometer with Exact Theory: Various Biological Applications. *Science*, 131(3414):pp. 1668–1669, 1960.
- [28] J. J. Wand, S. H. Liu, C. I. Chern, and J. H. Hsiseh. Development of an Arterial Applanation Tonometer for Detecting Arterial Blood Pressure and Volume. *Biomedical Engineering: Applications, Basis and Communications*, 16(06):322–330, 2004.
- [29] G. Drzewiecki, B. Solanki, J. J. Wang, and J. K-J Li. Noninvasive Determination of Arterial Pressure and Volume Using Tonometry [Electric Impedance Plethysmography]. In *ELECTRO '96. Professional Program. Proceedings.*, pages 61–63, 1996.
- [30] R. Dueck, O. Goedje, and P. Clopton. Noninvasive Continuous Beat-to-Beat Radial Artery Pressure via TL-200 Applanation Tonometry. *Journal of Clinical Monitoring and Computing*, 26(2):75–83, 2012.
- [31] K. G. Belani, J. J. Buckley, and M. O. Poliac. Accuracy of Radial Artery Blood Pressure Determination with the Vasotrac. *Canadian Journal of Anesthesia*, 46(5):488–496, 1999.
- [32] O. Kemmotsu, M. Ueda, H. Otsuka, T. Yamamura, A. Okamura, T. Ishikawa, D. C. Winter, and J. S. Eckerle. Blood Pressure Measurement by Arterial Tonometry in Controlled Hypotension. *Anesthesia & Analgesia*, 73(1):54–58, 1991.
- [33] D. Nair, S. Tan, H. Gan, S. Lim, J. Tan, M. Zhu, H. Gao, N. Chua, W. Peh, and K. Mak. The Use of Ambulatory Tonometric Radial Arterial Wave Capture to Measure Ambulatory Blood Pressure: The Validation of a Novel Wrist-Bound Device in Adults, 2007.

- [34] B. M. Weiss, D. R. Spahn, H. Rahmig, R. Rohling, and T. Pasch. Radial Artery Tonometry: Moderately Accurate but Unpredictable Technique of Continuous Non-Invasive Arterial Pressure Measurement. *Br J Anaesth*, 76(3):405–11, 1996.
- [35] H. W. Shirer. Blood Pressure Measuring Methods. *IRE Transactions on Biomedical Electronics*, BME9(2):116–125, 1962.
- [36] K. Yamakoshi, H. Shimazu, and T. Togawa. Indirect Measurement of Instantaneous Arterial Blood-Pressure in the Human Finger by the Vascular Unloading Technique. *IEEE Transactions on Biomedical Engineering*, 27(3):150–155, 1980.
- [37] J. Penaz. Photo-Electric Measurement of Blood Pressure, Volume and Flow in the Finger. *Digest Tenth International Conference, Dresden*, 104, 1973.
- [38] G. Parati, R. Casadei, A. Groppelli, M. Dirienzo, and G. Mancia. Comparison of Finger and Intra-Arterial Blood Pressure Monitoring at Rest and During Laboratory Testing. *Hypertension*, 13(6):647–655, 1989.
- [39] P. Sleight. Ambulatory Blood Pressure Monitoring. *Hypertension*, 7(2):163–164, 1985.
- [40] T. Kurki, N. T. Smith, N. Head, H. Dec-Silver, and A. Quinn. Noninvasive Continuous Blood Pressure Measurement from the Finger: Optimal Measurement Conditions and Factors Affecting Reliability. *Journal of Clinical Monitoring and Computing*, 3(1):6–13, 1987.
- [41] B. P. M. Imholz, W. Wieling, G. A. van Montfrans, and K. H. Wesseling. Fifteen Years Experience with Finger Arterial Pressure Monitoring: Assessment of the Technology. *Cardiovascular Research*, 38(3):605–616, 1998.
- [42] R. Maestri, G. D. Pinna, E. Robbi, S. Capomolla, and M. T. La Rovere. Noninvasive Measurement of Blood Pressure Variability: Accuracy of the Finometer Monitor and Comparison with the Finapres Device. *Physiological Measurement*, 26(6):1125, 2005.
- [43] B. P. Imholz, G. J. Langewouters, G. A. van Montfrans, G. Parati, J. van Goudoever, K. H. Wesseling, W. Wieling, and G. Mancia. Feasibility of Ambulatory, Continuous 24-Hour Finger Arterial Pressure Recording. *Hypertension*, 21(1):65–73, 1993.
- [44] NASA. *Expedition 5, International Space Station (ISS), Hardware Information*. NASA, 1999. [http : //lsda.jsc.nasa.gov/scripts/hardware/hardw.aspx?hardware;d = 664](http://lsda.jsc.nasa.gov/scripts/hardware/hardw.aspx?hardware;d=664).
- [45] G. J. Langewouters, J. J. Settels, R. Roelandt, and K. H. Wesseling. Why use Finapres or Portapres Rather than Intraarterial or Intermittent on-Invasive Techniques of Blood Pressure Measurement? *Journal of Medical Engineering & Technology*, 22(1):37–43, 1998.
- [46] J. R. Martina, B. E. Westerhof, J. van Goudoever, E. M. F. H. de Beaumont,

- Y. S. Truijen, J. and Kim, R. V. Immink, D. A. Jöbsis, M. W. Hollmann, J. R. Lahpor, B. A. J. M. de Mol, and J. J. van Lieshout. Noninvasive Continuous Arterial Blood Pressure Monitoring with Nexfin. *Anesthesiology*, 116(5), 2012.
- [47] R. Maggi, V. Viscardi, T. Furukawa, and M. Brignole. Non-Invasive Continuous Blood Pressure Monitoring of Tachycardic Episodes during Interventional Electrophysiology. *Europace*, 12(11):1616–1622, 2010.
- [48] M. O. Fischer, R. Avram, I. Cârjaliu, M. Massetti, J. L. Gérard, J. L. Hanouz, and J. L. Fellahi. Non-Invasive Continuous Arterial Pressure and Cardiac Index Monitoring with Nexfin after Cardiac Surgery. *British journal of anaesthesia*, 109(4):514–521, 2012.
- [49] D. W. E. Schattenkerk, J. J. van Lieshout, A. H. van den Meiracker, K. R. Wesseling, S. Blanc, W. Wieling, G. A. van Montfrans, J. J. Settels, K. H. Wesseling, and B. E. Westerhof. Nexfin Noninvasive Continuous Blood Pressure Validated Against Riva-Rocci/Korotkoff. *American Journal of Hypertension*, 22(4):378–383, 2009.
- [50] R. P. Garnier, A. G. E. van der Spoel, R. Sibarani-Ponsen, D. G. Markhorst, and C. Boer. Level of Agreement Between Nexfin Non-Invasive Arterial Pressure with Invasive Arterial Pressure Measurements in Children. *British Journal of Anaesthesia*, 2012.
- [51] J. Akkermans, M. Diepeveen, W. Ganzevoort, G. A. van Montfrans, B. E. Westerhof, and H. Wolf. Continuous Non-Invasive Blood Pressure Monitoring, a Validation Study of Nexfin in a Pregnant Population. *Hypertension in Pregnancy*, 28(2):230 – 242, 2009.
- [52] N. Tatara, H. Koizumi, S. Mino, S. Hayashida, K. Aihara, J. Shimada, Y. Uenishi, and O. Tochikubo. A Novel Blood Pressure Monitoring Device for Ubiquitous Healthcare Services. In *Engineering in Medicine and Biology Society, 2007. EMBS 2007. 29th Annual International Conference of the IEEE*, pages 5754–5757, 2007.
- [53] A. Hennig and A. Patzak. Continuous Blood Pressure Measurement Using Pulse Transit Time. *Somnologie - Schlafforschung und Schlafmedizin*, 17(2):104–110, 2013.
- [54] F. S. Cattivelli and H. Garudadri. Noninvasive Cuffless Estimation of Blood Pressure from Pulse Arrival Time and Heart Rate with Adaptive Calibration. volume 0, pages 114–119, 2009.
- [55] L. A. Geddes, M. H. Voelz, C. F. Babbs, J. D. Bourland, and W. A. Tacker. Pulse Transit Time as an Indicator of Arterial Blood Pressure. *Psychophysiology*, 18(1):71 – 74, 1981.
- [56] Y. Yoon, J. Cho, and G. Yoon. Non-Constrained Blood Pressure Monitoring Using ECG and PPG for Personal Healthcare. *Journal of Medical Systems*, 33(4):261–266, 2009.

- [57] C. Ahlstrom, A. Johansson, F. Uhlin, T. Länne, and P. Ask. Noninvasive Investigation of Blood Pressure Changes Using the Pulse Wave Transit Time: A Novel Approach in the Monitoring of Hemodialysis Patients. *Journal of Artificial Organs*, 8(3):192–197, 2005.
- [58] P. Fung, G. Dumont, C. Ries, C. Mott, and M. Ansermino. Continuous Noninvasive Blood Pressure Measurement by Pulse Transit Time. In *Engineering in Medicine and Biology Society, 2004. IEMBS '04. 26th Annual International Conference of the IEEE*, volume 1, pages 738–741, Sept 2004.
- [59] X. F. Teng and Y. T. Zhang. Continuous and Noninvasive Estimation of Arterial Blood Pressure Using a Photoplethysmographic Approach. *Proceedings of the 25th Annual International Conference of the IEEE Engineering in Medicine and Biology Society, Vols 1-4*, 25:3153–3156, 2003.
- [60] Y. H. Lin, P. C. I. Ko, H. Y. Wang, T. C. Lu, Y. Y. Chen, I. C. Jan, G. J. Jan, and N. K. Chou. Estimation of Beat-to-Beat Systolic Blood Pressure Using Pulse Arrive Time and Pulse Width Derived from the Photoplethysmogram. In *Engineering in Medicine and Biology Society, 2004. IEMBS '04. 26th Annual International Conference of the IEEE*, volume 2, pages 3456–3458, 2004.
- [61] M. Masé, W. Mattei, R. Cucino, L. Faes, and G. Nollo. Feasibility of Cuff-Free Measurement of Systolic and Diastolic Arterial Blood Pressure. *Journal of Electrocardiology*, 44(2):201 – 207, 2011.
- [62] A. M. Hassan, M. K. Mashor, A. K. Mohd, and M. Saad. Non-invasive Continuous Blood Pressure Monitoring Based on PWTT. *Journal of Advanced Computer Science and Technology Research*, 1(2), 2011.
- [63] B. C. Choi, H. J. Lee, Y. Ye, S, D. K. Jung, G. R. Kim, K. N. Kim, and G. R. Jeon. Evaluation of Arterial Compliance on Pulse Transit Time Using Photoplethysmography. In *Industrial Electronics Society, 2004. IECON 2004. 30th Annual Conference of IEEE*, volume 3, pages 3219–3222 Vol. 3, 2004.
- [64] R. Shriram, A. Wakankar, N. Daimiwal, and D. Ramdasi. Continuous Cuffless Blood Pressure Monitoring Based on PTT. In *Bioinformatics and Biomedical Technology (ICBBT), 2010 International Conference on*, pages 51–55. IEEE, 2010.
- [65] C. T. Phua. *Novel Method of Blood Pulse and Flow Measurement Using the Disturbance Created by Blood Flowing Through a Localized Magnetic Field*. PhD thesis, Université Paris-Est, 2012.
- [66] J. Joseph and V. Jayashankar. Magnetic Sensor for Non-Invasive Detection of Blood Pulse and Estimation of Arterial Compliance. In *Biomedical Engineering and Sciences (IECBES), 2010 IEEE EMBS Conference on*, pages 170–175, Nov 2010.
- [67] C. T. Phua and G. Lissorgues. Measurement of Blood Pressure using Mag-

- netic Method of Blood Pulse Acquisition. In *Nano/Molecular Medicine and Engineering (NANOMED), 2009 IEEE International Conference on*, pages 112–115, Oct 2009.
- [68] C. Barón et al. Balistocardiógrafo: Historia de un Instrumento Para Medir en Forma Indirecta el Desempeño del Corazón. *Rev. colomb. cardiol*, 16(1):5–10, 2009.
- [69] D. D. He, E. S. Winokur, and C. G. Sodini. A Continuous, Wearable, and Wireless Heart Monitor using Head Ballistocardiogram (bcg) and Head Electrocardiogram (ecg). In *Engineering in Medicine and Biology Society, EMBC, 2011 Annual International Conference of the IEEE*, pages 4729–4732. IEEE, 2011.
- [70] E. S. Winokur, D. D. He, and C. G. Sodini. A Wearable Vital Signs Monitor at the Ear for Continuous Heart Rate and Pulse Transit Time Measurements. In *Engineering in Medicine and Biology Society (EMBC), 2012 Annual International Conference of the IEEE*, pages 2724–2727. IEEE, 2012.
- [71] E. Pinheiro, O. Postolache, and P. Girao. Pulse Arrival Time and Ballistocardiogram Application to Blood Pressure Variability Estimation. In *Medical Measurements and Applications, 2009. MeMeA 2009. IEEE International Workshop on*, pages 132–136. IEEE, 2009.
- [72] Z. Chen, X. Yang, J. T. Teo, and S. H. Ng. Noninvasive Monitoring of Blood Pressure using Optical Ballistocardiography and Photoplethysmograph Approaches. In *Engineering in Medicine and Biology Society (EMBC), 2013 35th Annual International Conference of the IEEE*, pages 2425–2428. IEEE, 2013.
- [73] J. D. Lane, L. Greenstadt, D. Shapiro, and E. Rubinstein. Pulse Transit Time and Blood Pressure: An Intensive Analysis. *Psychophysiology*, 20(1):45–49, 1983.
- [74] C. C. Y. Poon, Zhang Yuan-Ting, G. Wong, and Poon Wai Sang. The Beat-to-Beat Relationship Between Pulse Transit Time and Systolic Blood Pressure. In *Information Technology and Applications in Biomedicine, 2008. ITAB 2008. International Conference on*, pages 342–343, 2008.
- [75] C. C. Y. Poon and Y. T. Zhang. Cuff-less and Noninvasive Measurements of Arterial Blood Pressure by Pulse Transit Time. In *Engineering in Medicine and Biology Society, 2005. IEEE-EMBS 2005. 27th Annual International Conference of the*, pages 5877–5880, 2005.
- [76] W. B. Gu, C. C. Y. Poon, and Y. T. Zhang. A Novel Parameter from PPG Dicrotic Notch for Estimation of Systolic Blood Pressure Using Pulse Transit Time. In *Medical Devices and Biosensors, 2008. ISSS-MDBS 2008. 5th International Summer School and Symposium on*, pages 86–88, 2008.
- [77] R. A. Payne, C. N. Symeonides, D. J. Webb, and S. R. J. Maxwell. Pulse

- Transit Time Measured from the ECG: An Unreliable Marker of Beat-to-Beat Blood Pressure. *J Appl Physiol*, 100:136–141, 2006.
- [78] H. D. Sesso, M. J. Stampfer, B. Rosner, C. H. Hennekens, J. M. Gaziano, J. E. Manson, and R. J. Glynn. Systolic and Diastolic Blood Pressure, Pulse Pressure, and Mean Arterial Pressure as Predictors of Cardiovascular Disease Risk in Men. *Hypertension*, 36(5):801–807, 2000.
- [79] D. B. McCombie, P. A. Shaltis, A. T. Reisner, and H. H. Asada. Adaptive Hydrostatic Blood Pressure Calibration: Development of a Wearable, Autonomous Pulse Wave Velocity Blood Pressure Monitor. In *Engineering in Medicine and Biology Society, 2007. EMBS 2007. 29th Annual International Conference of the IEEE*, pages 370–373, 2007.
- [80] P. Shaltis, A. Reisner, and H. Asada. A Hydrostatic Pressure Approach to Cuffless Blood Pressure Monitoring. In *Engineering in Medicine and Biology Society, 2004. IEMBS '04. 26th Annual International Conference of the IEEE*, volume 1, pages 2173–2176, 2004.
- [81] J. Muehlsteff, X.L. Aubert, and M. Schuett. Cuffless Estimation of Systolic Blood Pressure for Short Effort Bicycle Tests: The Prominent Role of the Pre-Ejection Period. In *Engineering in Medicine and Biology Society, 2006. EMBS '06. 28th Annual International Conference of the IEEE*, pages 5088–5092, 2006.
- [82] J. Muehlsteff, X.A. Aubert, and G. Morren. Continuous Cuff-less Blood Pressure Monitoring Based on the Pulse Arrival Time Approach: The Impact of Posture. In *Engineering in Medicine and Biology Society, 2008. EMBS 2008. 30th Annual International Conference of the IEEE*, pages 1691–1694, 2008.
- [83] J. M. Padilla, E. J. Berjano, J. Saiz, R. Rodriguez, and L. Facila. Pulse Wave Velocity and Digital Volume Pulse as Indirect Estimators of Blood Pressure: Pilot Study on Healthy Volunteers. *Cardiovascular Engineering*, 9(3):104–112, 2009.
- [84] R. Raamat, K. Jagomägi, J. Talts, and I. Mäger. Finger Beat-to-Beat Blood Pressure Responses to Successive Hand Elevations. *Medical Engineering & Physics*, 31(5):522–527, 2009.
- [85] Finapres. *Finapres Medical Systems / Portapres*. <http://http://www.finapres.com/Products/Portapres>.
- [86] P. A. Shaltis, A. Reisner, and H. H. Asada. Wearable, Cuff-less PPG-Based Blood Pressure Monitor with Novel Height Sensor. In *Engineering in Medicine and Biology Society, 2006. EMBS '06. 28th Annual International Conference of the IEEE*, pages 908–911, 2006.
- [87] L. Peter, N. Noury, and M. Cerny. A Review of Methods for Non-Invasive and Continuous Blood Pressure Monitoring: Pulse Transit Time Method is Promising? *IRBM*, 35(5):271–282, 2014.

- [88] D. Li, Y. Pan, H. Chen, S. Ye, and H. Yan. The Establishment of a Non-Invasive Continuous Blood Pressure Measure System Based on Pulse Transit Time. In *Bioinformatics and Biomedical Engineering, 2008. ICBBE 2008. The 2nd International Conference on*, pages 1624–1627, 2008.
- [89] G. Lopez, H. Ushida, K. Hidaka, M. Shuzo, J. J. Delaunay, I. Yamada, and Y. Imai. Continuous Blood Pressure Measurement in Daily Activities. In *Sensors, 2009 IEEE*, pages 827–831, 2009.
- [90] T. Ma and Y. T. Zhang. A Correlation Study on the Variabilities in Pulse Transit Time, Blood Pressure, and Heart Rate Recorded Simultaneously from Healthy Subjects. In *Engineering in Medicine and Biology Society, 2005. IEEE-EMBS 2005. 27th Annual International Conference of the*, pages 996–999, 2005.
- [91] S. J. Bellis, K. Delaney, J. Barton, and K. M. Razeeb. Development of Field Programmable Modular Wireless Sensor Network nodes for ambient systems. In *In Computer Communications, Special Issue on Wireless Sensor Networks*, 2005.
- [92] B. O’Flynn, S. Bellis, K. Delaney, J. Barton, S. C. O’Mathuna, A.M. Barroso, J. Benson, U. Roedig, and C. Sreenan. The Development of a Novel Minaturized Modular Platform for Wireless Sensor Networks. In *Information Processing in Sensor Networks, 2005. IPSN 2005. Fourth International Symposium on*, pages 370–375, April 2005.
- [93] B. O’Flynn, F. Regan, A. Lawlor, J. Wallace, J. Torres, and C. O’Mathuna. Experiences and Recommendations in Deploying a Real-Time, Water Quality Monitoring System. *Measurement Science and Technology*, 21(12):124004, 2010.
- [94] W. S. Wang, T. O’Donnell, L. Ribetto, B. O’Flynn, M. Hayes, and C. O’Mathuna. Energy Harvesting Embedded Wireless Sensor System for Building Environment Applications. In *Wireless Communication, Vehicular Technology, Information Theory and Aerospace Electronic Systems Technology, 2009. Wireless VITAE 2009. 1st International Conference on*, pages 36–41, May 2009.
- [95] M. Walsh, M. Gaffney, J. Barton, B. O’Flynn, C. O’Mathuna, A. Hickey, and J. Kellett. A Medical Study on Wireless Inertial Measurement Technology as a Tool for Identifying Patients at Risk of Death or Imminent Clinical Deterioration. In *Pervasive Computing Technologies for Healthcare (PervasiveHealth), 2011 5th International Conference on*, pages 214–217, May 2011.
- [96] K. Doughty, R. Lewis, and A. McIntosh. The Design of a Practical and Reliable Fall Detector for Community and Institutional Telecare. *J Telemed Telecare*, 6:150–154, 2000.
- [97] J. O’Donoghue, T. O’Kane, J. Gallagher, G. Courtney, A. Aftab, A. Casey, J. Torres, and P. Angove. Modified Early Warning Scorecard: The Role

- of Data/Information Quality within the Decision Making Process. *The Electronic Journal Information Systems Evaluation*, 13(3), 2011.
- [98] Analog Devices, One Technology Way, P.O. Box 9106, Norwood, MA 02062-9106, U.S.A. *AD620: Low Drift Instrumentation Amplifier*, rev. h edition.
- [99] M. Altini, S. Polito, J. Penders, N. Kim, H. and Van Helleputte, S. Kim, and F. Yazicioglu. An ECG Patch Combining a Customized Ultra-Low-Power ECG SoC with Bluetooth Low Energy for Long Term Ambulatory Monitoring, 2011.
- [100] Roving Networks, Roving Networks, Inc. 102 Cooper Court, Los Gatos, CA 95032. *RN21: Class 1 Bluetooth Module*, ds-rn21-v2 edition, March 2010.
- [101] Roving Networks, Roving Networks, Inc. 102 Cooper Court, Los Gatos, CA 95032. *RN41: Class 1 Bluetooth Module*, version 3.42r edition, November 2013.
- [102] Mitsumi. *WML-C46 Class 2 Bluetooth Module*.
- [103] Texas Instruments, Post Office Box 655303, Dallas, Texas 75265. *Texas Instruments LMX9838: Bluetooth Serial Port Module including Antenna*, rev. snosaz9e edition, January 2014.
- [104] Atmel, 2325 Orchard Parkway, San Jose, CA 95131, USA. *Atmel Mega 128: 8-bit Atmel Microcontroller with 128KBytes In-System Programmable Flash*, rev. 2549p-10/2012 edition, 2012.
- [105] Atmel, 2325 Orchard Parkway, San Jose, CA 95131, USA. *Atmel Mega 1281: 8-bit Atmel Microcontroller with 64K/128K/256K Bytes In-System Programmable Flash*, rev. 2549p-10/2012 edition, 2012.
- [106] Pe. van de Ven, A. Bourke, J. Nelson, and G. Laighin. A Wearable Wireless Platform for Fall and Mobility Monitoring. In *Proceedings of the 1st International Conference on PErvasive Technologies Related to Assistive Environments*, PETRA '08, pages 48:1–48:4, New York, NY, USA, 2008. ACM.
- [107] R. Naima and J. Canny. The Berkeley Tricorder: Ambulatory Health Monitoring. In *Wearable and Implantable Body Sensor Networks, 2009. BSN 2009. Sixth International Workshop on*, pages 53–58, June 2009.
- [108] T. H. Khan and A. W. Khan. A Portable Wireless Body Sensor Data Logger and its Application in Video Capsule Endoscopy. *Microprocessors and Microsystems*, 38(1):42 – 52, 2014.
- [109] Texas Instruments, Post Office Box 655303, Dallas, Texas 75265. *Texas Instruments MSP430: 16-Bit Ultra-Low-Power Microcontroller, 256KB Flash, 16KB RAM, 12 Bit ADC*, rev. slas612d edition, November 2013.
- [110] *Atmel ATxmega128A1U: 8/16-bit AVR Microcontroller featuring 128KB Self-Programming Flash*. 2325 Orchard Parkway, San Jose, CA 95131, USA, 8385g edition, November 2013.

- [111] N. Noury, A. Fleury, P. Rumeau, A. K. Bourke, G. O. Laighin, V. Rialle, and J. E. Lundy. Fall Detection—Principles and Methods. *Conf Proc IEEE Eng Med Biol Soc*, 2007:1663–1666, 2007.
- [112] A. K. Bourke, J. V. O’Brien, and G. M. Lyons. Evaluation of a Threshold-Based Tri-Axial Accelerometer Fall Detection Algorithm. *Gait & Posture*, 26(2):194–199, 2007. 0966-6362 doi: DOI: 10.1016/j.gaitpost.2006.09.012.
- [113] M. Gaffney, S. Coyler, M. Walsh, S. Drawer, A. Salo, B. O’Flynn, and C. S. Ó Mathúna. WIMU Instrumentation of Assassin Trainer & Skeleton Sled—Initial Data Capture. *From Beijing to London: Delivering Olympic & Elite Sport in Cross Cultural Context, March 26-27, 2012, University College Cork, Ireland*, 2012.
- [114] Analog Devices, One Technology Way, P.O. Box 9106, Norwood, MA 02062-9106, U.S.A. *ADXL345: 3-Axis, $\pm 2 g \pm 4 g \pm 8 g \pm 6 g$ Digital Accelerometer*, rev d edition, February 2013.
- [115] InvenSense, InvenSense Inc. 1197 Borregas Ave, Sunnyvale, CA 94089 U.S.A. *IDG-650 Integrated Dual-Axis Gyroscope*, ps-idg-0650b-00-05 edition, May 2010.
- [116] InvenSense, InvenSense Inc. 1197 Borregas Ave, Sunnyvale, CA 94089 U.S.A. *ISZ-650 Integrated Single-Axis Gyroscope*, ps-isz-0650b-00-02 edition, August 2009.
- [117] Honeywell, 12001 Highway 55, Plymouth, MN 55441. *HMC5843: 3-Axis Digital Compass IC*, form no. 900367 edition, June 2010.
- [118] Analog Devices, One Technology Way, P.O. Box 9106, Norwood, MA 02062-9106, U.S.A. *AD7490: 16-Channel, 1MSPS, 12-Bit ADC with Sequencer in 28-Lead TSSOP*, rev d edition, December 2012.
- [119] Microchip, 2355 West Chandler Blvd. Chandler, AZ 85224-6199. *24AA128: 128K I2C CMOS Serial EEPROM*, ds21191s edition, 2010.
- [120] J. Allen. Photoplethysmography and its Application in Clinical Physiological Measurement. *Physiological measurement*, 28(3):R1, 2007.
- [121] LabVIEW. *Build Number 11.0.0.4029*. National Instruments, 11500 Mopac Expwy, Austin, TX, 2011.
- [122] Matlab 8. *Release 2012b*. The MathWorks Inc., Natick, Massachusetts, 2012.
- [123] D. Prutchi and M. Norris. *Biopotential Amplifiers*. Wiley-Interscience, 2004.
- [124] Mathematica. *Version 8.04*. Wolfram Research, Champaign, Illinois, 2011.
- [125] T. Barill. An ECG Primer. *Nursecom Educational Technologies*, 87, 2003.
- [126] E. O’Brien. Demise of the Mercury Sphygmomanometer and the Dawning

- of a New Era in Blood Pressure Measurement. *Blood Pressure Monitoring*, 8(1):19–21, [2003].
- [127] B. M. McCarthy, B. O’Flynn, and A. Mathewson. An Investigation of Pulse Transit Time as a Non-Invasive Blood Pressure Measurement Method. *Journal of Physics: Conference Series*, 307(1):012060, 2011.
- [128] B. M. McCarthy, C. J. Vaughan, B. O’Flynn, A. Mathewson, and C. Ó Mathúna. An Examination of Calibration Intervals Required for Accurately Tracking Blood Pressure Using Pulse Transit Time Algorithms. *J Hum Hypertens*, 27(12):744–750, Dec 2013.
- [129] M. J. Bland and D. G. Altman. Statistical Methods for Assessing Agreement Between Two Methods of Clinical Measurement. *The Lancet*, 327(8476):307–310, 1986.
- [130] G. Zhang, M. Gao, D. Xu, N. B. Olivier, and R. Mukkamala. Pulse Arrival Time is Not an Adequate Surrogate for Pulse Transit Time as a Marker of Blood Pressure. *Journal of Applied Physiology*, 111(6):1681–1686, 2011.
- [131] A. Sherwood, M. T. Allen, J. Fahrenberg, R.M. Kelsey, W. R. Lovallo, and L. J. P. van Doornen. Methodological Guidelines for Impedance Cardiography. *Psychophysiology*, 27(1):1–23, 1990.
- [132] A. L. Goldberger, L. A. N. Amaral, L. Glass, J.M. Hausdorff, P. C. Ivanov, R. G. Mark, J. E. Mietus, G. B. Moody, C. K. Peng, and H. E. Stanley. PhysioBank, PhysioToolkit, and PhysioNet: Components of a New Research Resource for Complex Physiologic Signals. *Circulation*, 101(23):e215–e220, 2000.
- [133] PhysioNet Bank ATM. *Record challenge/2009/test-set-b/205a/205a, from [21:31:47.536 13/11/2018] to [21:31:57.536 13/11/2018]*. PhysioNet Resource, <http://physionet.org/cgi-bin/atm/ATM>.
- [134] J. X. Sun, A. T. Reisner, M. Saeed, and R. G. Mark. Estimating Cardiac Output from Arterial Blood Pressure Waveforms: A Critical Evaluation Using the MIMIC II Database. In *Computers in Cardiology, 2005*, pages 295–298, 2005.
- [135] PhysioNet Bank ATM. *The MIMIC Database*. PhysioNet Resource, <http://physionet.org/physiobank/database/mimicdb/>.
- [136] PhysioNet/Computing in Cardiology Challenges. *Predicting Acute Hypotensive Episodes: A Challenge from PhysioNet and Computers in Cardiology 2009*. PhysioNet Resource, <http://www.physionet.org/challenge/2009/>.
- [137] PhysioNet Bank ATM. *Record challenge/2009/test-set-b/205c/205c, from [10:53:00.000 15/11/2018] to [10:54:00.000 15/11/2018]*. PhysioNet Resource, <http://physionet.org/cgi-bin/atm/ATM>.
- [138] W. G. Kubicek, J. N. Karnegis, R. P. Patterson, D. A. Witsoe, and R. H.

- Mattson. Development and Evaluation of an Impedance Cardiac Output System. *Aerosp Med*, 37(12):1208–1212, Dec 1966.
- [139] J. M. Van De Water, T. W. Miller, R. L. Vogel, B. E. Mount, and M. L. Dalton. Impedance Cardiography. *Chest*, 123(6):2028–2033, 2003.
- [140] A. F. Connors, T. Speroff, N. V. Dawson, and et al. The Effectiveness of Right Heart Catheterization in the Initial Care of Critically Ill Patients. *JAMA*, 276(11):889–897, 1996.
- [141] L. A. H. Critchley. Impedance Cardiography The Impact of New Technology. *Anaesthesia*, 53(7):677–684, 1998.
- [142] S. N. Mohapatra. *Noninvasive Cardiovascular Monitoring of Electrical Impedance Technique*. Pitman, London, 1981.
- [143] A. E. Hoetink, T. J. C. Faes, K. R. Visser, and R. M. Heethaar. On the Flow Dependency of the Electrical Conductivity of Blood. *Biomedical Engineering, IEEE Transactions on*, 51(7):1251–1261, July 2004.
- [144] L. Y. Shyu, C. Y. Chiang, C. Liu, and W. C. Hu. Portable Impedance Cardiography System for Real-Time Noninvasive Cardiac Output Measurement. *Journal of Medical and Biological Engineering*, Vol 20(No 4):193–201, 2000.
- [145] J. Fortin, W. Habenbacher, A. Heller, A. Hacker, R. Gruellenberger, J. Innerhofer, H. Passath, C. Wagner, G. Haitchi, D. Flotzinger, R. Pacher, and P. Wach. Non-invasive Beat-to-Beat Cardiac Output Monitoring by an Improved Method of Transthoracic Bioimpedance Measurement. *Computers in Biology and Medicine*, 36(11):1185–1203, 2006.
- [146] J. Fortin, R. Grölenberger, W. Habenbacher, A. Hacker, A. Heller, H. Passath, D. Flotzinger, and P. Wach. New Aspects of Estimating Electrical Participating Volume of the Thorax for Transthoracic Impedance Cardiography. In *13th International Conference on Electrical Bioimpedance and the 8th Conference on Electrical Impedance Tomography*, volume 17 of *IFMBE Proceedings*, pages 36–39. Springer Berlin Heidelberg, 2007.
- [147] G. Cybulski. Ambulatory Impedance Cardiography. In *Ambulatory Impedance Cardiography*, volume 76 of *Lecture Notes in Electrical Engineering*, pages 39–56. Springer Berlin Heidelberg, 2011.
- [148] D. P. Bernstein. A New Stroke Volume Equation for Thoracic Electrical Bioimpedance - Theory and Rationale. *Critical Care Medicine*, 14(10):904–909, 1986.
- [149] J. E. Naschitz, R. Itzhak, N. Shaviv, I. Khorshidi, S. Sundick, H. Isseroff, M. Fields, R. M. Priselac, D. Yeshurun, and E. Sabo. Assessment of Cardiovascular Reactivity by Fractal and Recurrence Quantification Analysis of Heart Rate and Pulse Transit Time. *Journal of Human Hypertension*, 17(2):111–118, 2003.

- [150] R. P. Smith, J. Argod, J. L. Pépin, and P. A. Lévy. Pulse Transit Time: An Appraisal of Potential Clinical Applications. *Thorax*, 54(5):452–457, 1999.
- [151] B. F. J. Manly. *Multivariate Statistical Methods: A Primer*. CRC Press, 2004.
- [152] G. R. J. Cooper and D. R. Cowan. Comparing Time Series Using Wavelet-Based Semblance Analysis. *Computers & Geosciences*, 34(2):95 – 102, 2008.
- [153] J. L. Devore. *Probability and Statistics for Engineering and the Sciences*, chapter 13 Nonlinear and Multiple Regression, pages 573–597. Duxbury, fifth edition, 2000.
- [154] B. Nau. Decision 411 - Statistical Forecasting, Additional Notes on Regression Analysis. Lecture notes, Duke Universty, 2005.
- [155] J. G. Eisenhauer. Regression Through the Origin. *Teaching Statistics*, 25(3):76–80, 2003.
- [156] J. Crighton Bramwell and A. V. Hill. The Velocity of the Pulse Wave in Man. *Proceedings of the Royal Society of London. Series B, Containing Papers of a Biological Character*, 93(652):298–306, 1922.
- [157] D. J. Korteweg. Ueber die Fortpflanzungsgeschwindigkeit des Schalles in Elastischen Röhren. *Annalen der Physik*, 241(12):525–542, 1878.
- [158] P. Constantin. *Navier-Stokes Equations*. University of Chicago Press, 1988.
- [159] G. O. Brown. The History of the Darcy-Weisbach Equation for Pipe Flow Resistance. *Environmental and Water Resources History*, 38(7):34–43, 2002.
- [160] B. Le Méhauté. The Bernoulli Equation. In *An Introduction to Hydrodynamics and Water Waves*, pages 101–115. Springer, 1976.
- [161] D. Dowson. A Generalized Reynolds Equation for Fluid-Film Lubrication. *International Journal of Mechanical Sciences*, 4(2):159–170, 1962.
- [162] R. W. Schafer. What is a Savitzky-Golay Filter?[lecture notes]. *Signal Processing Magazine, IEEE*, 28(4):111–117, 2011.
- [163] A. Karagiannis and P. Constantinou. Noise-Assisted Data Processing With Empirical Mode Decomposition in Biomedical Signals. *Information Technology in Biomedicine, IEEE Transactions on*, 15(1):11–18, Jan 2011.
- [164] K. Pandia, S. Ravindran, R. Cole, G. Kovacs, and L. Giovangrandi. Motion Artifact Cancellation to Obtain Heart Sounds from a Single Chest-Worn Accelerometer. In *Acoustics Speech and Signal Processing (ICASSP), 2010 IEEE International Conference on*, pages 590–593, March 2010.
- [165] B. Pirofsky. The Determination of Blood Viscosity in Man by a Method Based on Poiseuille’s Law. *Journal of Clinical Investigation*, 32(4):292, 1953.

- [166] J. R. Womersley. Method for the Calculation of Velocity, Rate of Flow and Viscous Drag in Arteries When the Pressure Gradient is Known. *The Journal of Physiology*, 127(3):553–563, 1955.
- [167] I. T. Gabe. Arterial Blood Flow by Analogue Solution of the Navier-Stokes Equation. *Physics in Medicine and Biology*, 10(2):271, 1965.
- [168] BioPac Systems Incorporated. *MP36R: A 4-Channel Data Acquisition and Analysis System*. <http://www.biopac.com/data-acquisition-analysis-system-mp36r-system-windows>.
- [169] BioPac Systems Incorporated. *SS31L: A Non-Invasive Cardiac Output Sensor*. <http://www.biopac.com/noninvasive-cardiac-output-sensor-bsl>.
- [170] T. Sebastian, P. C. Pandey, S. M. M. Naidu, and V. K. Pandey. Wavelet Based Denoising for Suppression of Respiratory and Motion Artifacts in Impedance Cardiography. In *Computing in Cardiology, 2011*, pages 501–504, Sept 2011.
- [171] V. K. Pandey and P. C. Pandey. Wavelet Based Cancellation of Respiratory Artifacts in Impedance Cardiography. In *Digital Signal Processing, 2007 15th International Conference on*, pages 191–194, July 2007.
- [172] O. Makarova and J. Vedru. Ensemble-Averaged Waveform of Foucault Cardiogram. In *Proc. Conf. Biomedical Engineering, Kaunas, Okt. 19-20*, pages 117–120, 2000.
- [173] H. Riese, P. F. C. Groot, M. van den Berg, N. H. M. Kupper, E. H. B. Magnee, E. J. Rohaan, T. G. M. Vrijkotte, G. Willemsen, and E. J. C. de Geus. Large-Scale Ensemble Averaging of Ambulatory Impedance Cardiograms. *Behavior Research Methods, Instruments, & Computers*, 35(3):467–477, 2003.
- [174] W. B. Kannel, T. Gordon, and M. J. Schwartz. Systolic Versus Diastolic Blood Pressure and Risk of Coronary Heart Disease: The Framingham Study. *The American Journal of Cardiology*, 27(4):335–346, 1971.
- [175] A. V. Chobanian, G. L. Bakris, H. R. Black, and et al. The Seventh Report of the Joint National Committee on Prevention, Detection, Evaluation, and Treatment of High Blood Pressure: The JNC 7 Report. *JAMA*, 289(19):2560–2571, 2003.
- [176] T. E. Strandberg and K. Pitkala. What is the Most Important Component of Blood Pressure: Systolic, Diastolic or Pulse Pressure? *Current Opinion in Nephrology and Hypertension*, 12(3):293–297, 2003.
- [177] J. L. Izzo, D. Levy, and H. R. Black. Importance of Systolic Blood Pressure in Older Americans. *Hypertension*, 35(5):1021–1024, 2000.
- [178] M. Qu, Y. Zhang, J. G. Webster, and W. J. Tompkins. Motion Artifact from Spot and Band Electrodes During Impedance Cardiography. *Biomedical Engineering, IEEE Transactions on*, BME-33(11):1029–1036, 1986.

- [179] P. S. Pandian, K. Mohanavelu, K. P. Safeer, T. M. Kotresh, D. T. Shakunthala, P. Gopal, and V. C. Padaki. Smart Vest: Wearable Multi-Parameter Remote Physiological Monitoring System. *Medical engineering & physics*, 30(4):466–477, 2008.
- [180] M. Di Rienzo, F. Rizzo, G. Parati, G. Brambilla, M. Ferratini, and P. Castiglioni. MagIC System: A New Textile-Based Wearable Device for Biological Signal Monitoring. Applicability in Daily Life and Clinical Setting. In *Engineering in Medicine and Biology Society, 2005. IEEE-EMBS 2005. 27th Annual International Conference of the*, pages 7167–7169. IEEE, 2005.
- [181] A. K. Bourke, P. W. van de Ven, A. E. Chaya, G. M. O’Laighin, and J. Nelson. The Design and Development of a Long-Term Fall Detection System Incorporated into a Custom Vest for the Elderly. In *Conference proceedings: Annual International Conference of the IEEE Engineering in Medicine and Biology Society. IEEE Engineering in Medicine and Biology Society. Conference*, volume 2008, pages 2836–2839, 2007.
- [182] W. W. Nichols and M. F. O’Rourke. *McDonald’s Blood Flow in Arteries: Theoretical, Experimental and Clinical Principles*. A Hodder Arnold Publication. Hodder Arnold, 2005.
- [183] A. P. G. Hoeks, S. K. Samijo, P. J. Brands, and R. S. Reneman. Noninvasive Determination of Shear-Rate Distribution Across the Arterial Lumen. *Hypertension*, 26(1):26–33, 1995.
- [184] T. Sochi. One-Dimensional Navier-Stokes Finite Element Flow Model. *arXiv preprint arXiv:1304.2320*, 2013.
- [185] E. O’Brien, N. Atkins, G. Stergiou, G. Karpettas, N. and Parati, R. Asmar, J. and Mengden T. Imai, Y. and Wang, and A. et al. Shennan. European Society of Hypertension International Protocol Revision 2010 for the Validation of Blood Pressure Measuring Devices in Adults. *Blood pressure monitoring*, 15(1):23–38, 2010.
- [186] R. P. Patterson. Fundamentals of Impedance Cardiography. *Engineering in Medicine and Biology Magazine, IEEE*, 8(1):35–38, March 1989.
- [187] P. Stevanovic, R. Scepanovic, D. Radovanovic, D. Bajec, R. Perunovic, D. Stojanovic, and D. Stevanovic. Thoracic Electrical Bioimpedance Theory and Clinical Possibilities in Perioperative Medicine. *Signa Vitae*, 3(Suppl. 1):22–27, 2008.
- [188] J. Vedru. Electrical Impedance Methods for the Measurement of Stroke Volume in Man: State of Art. *Acta et Comm. Univ. Tartuensis*, 974:110–129, 1994.
- [189] D. Prutchi and M. Norris. *Impedance Technique*, chapter 8, pages 393–400. Wiley-Interscience, 2004.
- [190] Analog Devices, One Technology Way, P.O. Box 9106, Norwood, MA 02062-

- 9106, U.S.A. *AD9834:20 mW Power, 2.3 V to 5.5 V, 75 MHz Complete DDS*, rev. c edition.
- [191] Analog Devices, One Technology Way, P.O. Box 9106, Norwood, MA 02062-9106, U.S.A. *AD5620:Single, 12-/14-/16-Bit nanoDAC with 5 ppm/ °C On-Chip Reference in SOT-23*, rev. g edition.
- [192] Analog Devices, One Technology Way, P.O. Box 9106, Norwood, MA 02062-9106, U.S.A. *Circuit Note CN-0156: Amplitude Control Circuit for AD9834 Waveform Generator (DDS)*, rev. a edition.
- [193] K. J. Aström and R. M. Murray. *Feedback Systems: An Introduction for Scientists and Engineers*. Princeton University Press, 2010.
- [194] M. L. Meade. *Lock-in Amplifiers: Principles and Applications*, volume 1. Meade, M., 1983.
- [195] Analog Devices, One Technology Way, P.O. Box 9106, Norwood, MA 02062-9106, U.S.A. *AD630: Balanced Modulator/Demodulator*, rev. e edition, June 2004.
- [196] Maxim-IC. *Application Note 184 Digitally-Controlled Phase Shift Using the DS1669*, February 2002.
- [197] National Semiconductor. *Application Note 31: Op Amp Circuit Collection*, September 2002.